THE
PHYSICAL REVIEW
A journal of experimental and theoretical physics established by E. L. Nichols in 1893

SECOND SERIES, VOL. 70, NOS. 1 AND 2 JULY 1 AND 15, 1946

The Slowing Down of Low Energy Neutrons in Water. II. Determination of Photo-Neutron Energies

R. D. O'NEAL
University of Illinois, Urbana, Illinois
(Received June 13, 1942)*

A new method for determining neutron energies which should be particularly useful below 500 kev has been developed and applied. The method consists in slowing down the neutrons from the source in water and measuring the distribution of D group neutrons. The arrangement is calibrated with neutron sources of known energy. The energies of the photo-neutrons emitted from Y(100*d*)+Be and Sb(60*d*)+Be have been determined and found to be 220±20 kev and 100±20 kev respectively. This is in agreement with previous measurements by other methods. This method has the advantage of great simplicity and should be applicable to neutron energies below 100 kev, which cannot be studied by other known methods.

INTRODUCTION

PHOTO-NEUTRON energies above 100 kev have been determined by measuring the energy of recoil protons in a hydrogen-filled ionization chamber.[1,2] However, it is not possible to use this method for photo-neutrons of energy less than about 100 kev, since the amplifier noise level and the γ-ray background obscure the measurement of such low energy recoil protons. It is desirable, therefore, to have a method which could be employed for energies below as well as above 100 kev. As is well known, the distribution of C neutrons and also group neutrons in water varies with neutron energy since the number of collisions necessary to reduce the neutron energy to some particular value increases with initial energy. A theoretical deduction of the distribution curve for a given energy is not exact enough to be used for the inverse problem of determining the energy from a measured curve. An empirical calibration is therefore necessary.

As was shown in a previous report,[3] the distribution curves for resonance neutrons (D, I groups) fall off much more rapidly than the C neutron curve. One might therefore expect that the curves for resonance neutrons will vary more sensitively with the initial energy than will the C neutron curves which are spread out by the diffusion of the C neutrons.

APPARATUS AND PROCEDURE

The apparatus used is quite simple. The photo-neutron sources were placed in a soft glass tube centrally in a tank of water 100 cm long and 60 cm wide which was filled to a depth of 60 cm. Six different photo-neutron sources were used: 100 mC Ra+Be; 100 mC Ra+D_2O; 8 mC

* This paper was received for publication on the date indicated but was voluntarily withheld from publication until the end of the war.
[1] G. Scharff-Goldhaber, Phys. Rev. **59**, 937A (1941).
[2] G. S. Klaiber and G. Scharff-Goldhaber, Baltimore meeting (1942).
[3] M. Goldhaber and R. D. O'Neal, Phys. Rev. **60**, 834L (1941).

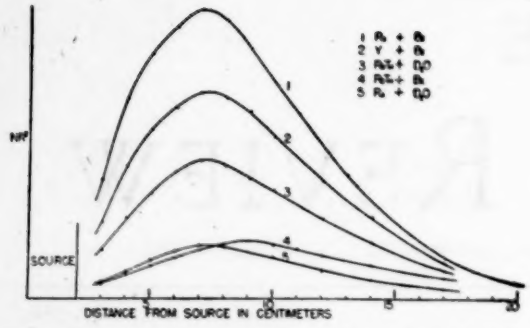

FIG. 1. C neutron distribution in water. Ordinates = activation × square of distance from center of source. Curve 2 drawn to $\frac{1}{2}$ and curve 1 drawn to $\frac{1}{4}$ scale of ordinates for curves 3, 4, and 5.

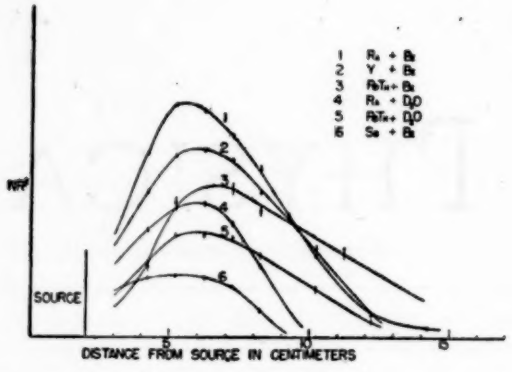

FIG. 2. D neutron distribution in water. Ordinates = activation × square of distance from center of source. Curve 1 is drawn to $\frac{1}{4}$ and curve 2 to $\frac{1}{2}$ the scale of ordinates for curves 3, 4, 5, and 6. Vertical lines give probable errors.

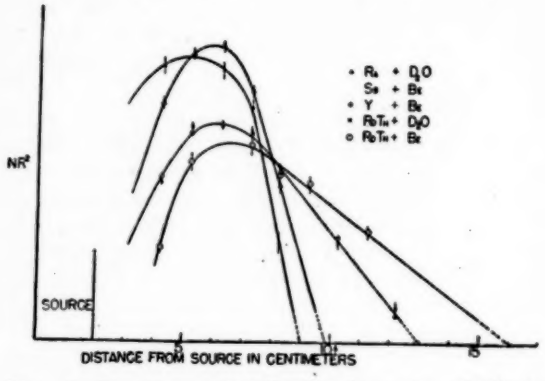

FIG. 3. D neutron distribution in water. Ordinates = activation × square of distance from source. The units of the ordinates are chosen so that each curve includes the same area. Vertical lines give probable errors.

RdTh+Be; 8 mC RdTh+D_2O; 35 mC Y(100*d*)+Be; and 2.5 mC Sb(60*d*)+Be. The γ-ray sources were of somewhat different sizes, but were all cylindrical and from 1 to 2.5 cm long. The beryllium block was 7 cm long and 3 cm in diameter and had a hole along the axis 4.5 cm long and 1 cm in diameter. It weighed 85 g. Forty-five grams of D_2O were contained in a soft glass vessel of outer diameter 3.5 cm and 5.5 cm high. The γ-ray source was placed in a recess at the center of this cylinder 4 cm long and 0.4 cm in diameter.

Thin indium foils placed in water-tight aluminum containers were used for detecting the slow neutrons. The 54-minute β-activity of these foils (corrected for infinite bombardment time and to initial activity) was measured by wrapping them around a thin-wall Geiger counter in a standard position. The group neutron activity of indium was measured by placing the foils in a water-tight cadmium container of thickness 0.17 cm. The indium foil during bombardment was folded into a target of dimensions 4.5 cm by 2 cm. Lead iodide was used as a detector for the iodine group neutrons. The sample used was the same size as the indium sample.

RESULTS

C Neutron Curves

In Fig. 1 are shown the distribution curves for C neutrons. In these curves N is the difference in the induced activity of the indium foil without and with cadmium surrounding it. The distance is measured from the center of the source. One might use either of two criteria for measuring the initial energy of the neutrons—(1) position of maxima or (2) falling-off or decay of the curve. It may readily be seen that the maxima do vary with energy; i.e., RdTh+Be (900-kev neutrons) has a maximum about 1.5 cm farther out than RdTh+D_2O (220-kev neutrons) while the maximum for the latter agrees very well with that for Y(100*d*)+Be, and the maximum for Ra+Be is in still closer (strongest γ-ray gives rise to 120 kev neutrons). However, as can be seen from these curves, and easier still by normalizing them, the slow neutron curves do not offer a very sensitive method for determining energies.

D Neutron Curves

While the C neutron curves may be measured rather easily and rapidly, the group neutron curves are more tedious to measure, since the

activities here are roughly only 1/10 the activities one gets for C neutrons. The curves as measured are shown in Fig. 2 and these curves normalized to equal area are shown in Fig. 3. It may be seen that both the maxima and especially the manner in which these curves fall off are rather sensitive functions of the initial neutron energy. One may extrapolate the very nearly straight line portion of the curve to the axis (actually it must fall off approximately exponentially) and use this "apparent intercept" as a criterion of neutron energy. This has been done and we have 3 calibration points as shown in Table I. As can be seen from Fig. 2 and Fig. 3, the distribution of the neutrons from RdTh+Be has not been so accurately measured. There are two reasons for this—(1) the source is so weak that counting at distances far from the source is very difficult and (2) fewer data were taken in this case since this energy region can be better investigated by the recoil proton method.

In Table I the neutron energies are calculated from the γ-ray energies on the basis of 1.62 as the binding energy for beryllium[4,5] and 2.17 as the binding energy for the deuteron.[4] If one were interested in the exact neutron distribution instead of the "apparent intercepts" one might prefer to use the root-mean-square of the distance that neutrons travel in getting from source to detector instead of the measured distance from the center of the source. This can easily be done when one knows the dimensions of the source and detector. This, of course changes the shape of the curve somewhat, but adds little to the use of the curves as criteria of initial neutron energy.

TABLE I. Neutron energies from Fig. 3.

Source	γ-ray energy (Mev)	Neutron energy* (Mev)	Apparent intercept (cm)	Neutron energy from Fig. 3 (kev)
RdTh+D_2O	2.62	220	13.0	Standard
Y(100d)+Be	1.87,[a] 1.89,[b] 1.92[c]	220, 240, 270	13.0	220±20
Ra+D_2O	2.42	120	9.8	Standard
Sb(60d)+Be	1.75,[d] 1.72,[e] 1.82[f]	115, 90, 180	9.0	100±20
RdTh+Be	2.62	900	16.0	Standard

* Calculated from γ-ray energy or taken from previous work.
[a] See reference 1.
[b] See reference 6.
[c] See reference 7.
[d] See reference 2.
[e] E. B. Hales and E. B. Jordan, private communication. Determined from difference in end-points of β-ray spectra. 2.43±0.07 Mev—0.71 ±0.03 Mev gives 1.72±0.07 Mev.
[f] A. C. G. Mitchell, L. M. Langer, and P. W. McDaniel, Phys. Rev. 57, 1107 (1940).

TABLE II. Neutron energies from Ra+Be.

Gamma energy of radium (Mev)	Relative[a] intensity	Neutron energy (Kev)
1.62	0.54	0
1.69	0.40	60
1.75	2.42	120
1.82	0.41	180
2.09	0.37	420
2.20	1.0	510
2.42	0.5	710

[a] A. I. Alichanow, Comptes Rendus Acad. Sci. U.S.S.R. 20, 429 (1938).

One may see from the curves that the "apparent intercepts" for RdTh+D_2O and Y(100d) +Be are not distinguishable from one another. This is in excellent agreement with the measurements[1] of the energy of the recoil protons for these two and the energy of the γ-ray of yttrium that one deduces from these measurements is in good agreement with independent measurements of the γ-ray energy.[6,7] Small discrepancies might be accounted for by a slight error in the values used for the binding energies of beryllium and the deuteron.

As is seen in Table II the Ra+Be source is not homogeneous, its main intensity being around 100 kev. One sees in Fig. 2 how the higher energy neutrons push the curve out.

There is no indication in the curve for Ra +D_2O of neutrons by the 2.20 Mev γ-ray. This may be caused by the small cross section for photo-disintegration of the deuteron near the threshold. The neutrons from Ra+D_2O are probably mainly caused by the 2.42 Mev γ-ray line, but one should not exclude the possibility that a small contribution is made by very weak high energy γ-ray lines. The measurement of this curve was made more difficult by the neutrons from the radium source itself. However, this was an exceptionally good source as the neutron activity of the γ-ray source itself was less than 1 percent of the neutron activity when surrounded by the beryllium block. This activity and its different distribution had to be taken into account in all measurements with radium

[4] F. E. Myers and L. C. Van Atta, Phys. Rev. 61, 19 (1942).
[5] L. S. Skaggs, Phys. Rev. 56, 24 (1939).
[6] J. R. Downing, M. Deutsch, and A. Roberts, Phys. Rev. 60, 470L (1941).
[7] J. R. Richardson, Phys. Rev. 60, 188 (1941).

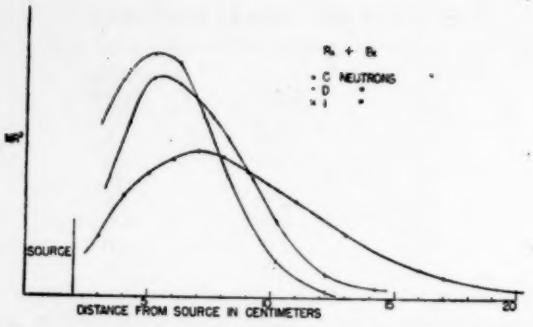

FIG. 4. Ordinates = activation × square of distance from center of source. The units of the ordinates are chosen so that each curve includes the same area.

and the "apparent intercept" of this curve has been determined rather accurately. From this "apparent intercept," that of RdTh+D_2O, and the fact that zero energy neutrons must have an "apparent intercept" near zero, the initial energy of the neutrons from Sb+Be was deduced to be 100 kev with an estimated error of about 20 kev. This is in essential agreement with the energy determination by the proton recoil method.

Comparison of Curves

Previously a comparison has been made[3] between the C, D, and I curves for the initially low energy monokinetic neutrons from a Y(100*d*) +Be source. This comparison brought out the important fact that, unlike the case for neutrons of high initial energy, there was no region at some distance from the source where the two curves decayed at the same rate, but that here at some distance from the source the ratio of group neutrons to C neutrons decreased and so at fairly large distances from the source there are principally C neutrons left.

In Fig. 4 is shown a comparison of the C, D, and I curves for the most commonly used source, Ra-γ-Be. Conclusions similar to those above may be drawn from this comparison, but the presence of the higher energy neutrons makes these conclusions less obvious here.

The accuracy of these measurements and the ease with which they can be carried out can of course be increased by using stronger sources. For convenient measurements of neutron energies of approximately 100 kev, a source of at least 5 millicuries strength should be used if beryllium is being disintegrated and one of at least 10 millicuries if deuterium is being disintegrated.

ACKNOWLEDGMENT

I wish to express appreciation to Professor M. Goldhaber for suggesting this problem and for his constructive criticism throughout. I would also like to thank the Graduate School of the University of Illinois for a grant which made this work possible. Thanks are due Dr. M. Kamen and Professor E. O. Lawrence for the artificial radioactive sources which have been used in this work and which they generously sent to Professor M. Goldhaber.

High Energy Neutron-Proton Scattering and the Meson Theory of Nuclear Forces with Strong Coupling*

J. LEITE LOPES**
*Palmer Physical Laboratory, Princeton University, Princeton, New Jersey****

(Received January 28, 1946)

In the first part of this paper the anisotropy of the elastic scattering of 14-Mev neutrons by protons is investigated in the meson field theory of nuclear forces with the scheme proposed by Møller and Rosenfeld in the strong coupling limit and in the symmetrical form. In the second Born's approximation, the virtual isobars decrease the ratio R of the differential cross sections in the backward and perpendicular directions (in the center of mass system), and R decreases with the isobar energy. R is still larger than 1; nevertheless, our results suggest the possibility that the combined effects of the virtual isobars and the tensor force might give a forward scattering in agreement with Amaldi's experiments. In the second part, the cross section of the inelastic scattering of 100–200-Mev neutrons by protons with production of isobars is evaluated in the Møller-Rosenfeld, pseudoscalar and Schwinger theories. The ratio of the total inelastic cross section and the elastic one is of the order of 0.03, for 100-Mev neutrons and for an isobar energy equal to 45 Mev. An experiment to detect the isobars would be important for a check of the fundamental ideas of the strong coupling formalism.

INTRODUCTION

IN this paper we investigate the two following problems: (1) the anisotropy of the elastic scattering of 14-Mev neutrons by protons in the symmetrical meson field theory of nuclear forces in the form proposed by Møller and Rosenfeld[1]; (2) the total cross section of the inelastic scattering of 100–200 Mev neutrons by protons with production of isobars, in the Møller-Rosenfeld, pseudoscalar[2] and Schwinger[3] forms of the meson theory, both problems in the limiting case of a strong coupling[4] between the meson field and the nucleons.

The angular distribution of the elastic scattering of high energy neutrons by protons was studied experimentally by Amaldi, Bocciarelli, Trabacchi, and Ferretti[5] and they found a preferentially forward scattering for neutrons of energies 12.5, 13.5, and 14 Mev. Their results are in contradiction with the assumption of an exchange force between the nucleons[6] and so cannot be explained by the meson theory in the symmetrical form[7] and in the weak coupling limit, as was shown by Hulthén[8] and Jauch.[9]

This is essentially due to the fact that in a theory which assumes a charge-exchange force between nucleons, the potential of states with an even angular momentum has a sign opposite to that of the potential of states with an odd angular momentum.[10] As the P-waves are the most important for determining the anisotropy of the scattering of 14-Mev neutrons by protons, the repulsive P-potential is essentially responsible for the theoretical discrepancies.

Recently, Fierz and Wentzel[11] showed that in

* This paper contains the essential results of a thesis submitted to the Faculty of Princeton University for the degree of Doctor of Philosophy.

** Exchange Fellow of the U. S. Department of State.

*** Now at the Faculdade Nacional de Filosofia, University of Brazil, Rio de Janeiro, Brazil.

[1] C. Møller and L. Rosenfeld, Kgl. Danske Vid. Sels. Math.-Fys. Medd. **17**, No. 8 (1940).

[2] N. Kemmer, Proc. Roy. Soc. **166A**, 127 (1938).

[3] J. Schwinger, Phys. Rev. **61**, 387 (1942).

[4] G. Wentzel, Helv. Phys. Acta **13**, 269 (1940); **14**, 633 (1941); **16**, 222, 551 (1943); J. R. Oppenheimer and J. Schwinger, Phys. Rev. **60**, 150 (1941); W. Pauli and S.M. Dancoff, Phys. Rev. **62**, 85 (1942); R. Serber and S. M. Dancoff, Phys. Rev. **63**, 143 (1943); W. Pauli and S. Kusaka, Phys. Rev. **63**, 400 (1943).

[5] E. Amaldi *et. al.*, Naturwiss. **30**, 582 (1942).

[6] G. Wick, Zeits. f. Physik **84**, 799 (1933).

[7] The neutral meson theory (H. A. Bethe, Phys. Rev. **57**, 260, 390 (1940)) gives a satisfactory angular distribution for the scattering, as would be expected, since in this theory there is no charge exchange between the nucleons. This theory, however, does not take into account charged mesons, which were observed in the cosmic radiation, gives no saturation for the nuclear forces, and spoils the explanation of the β-decay, which was already given by Yukawa by assuming charged mesons alone. The theory in the symmetrical form, which considers both neutral and charged mesons in a symmetrical way, is the only one which satisfies the above requirements and accounts for the equality of the forces between like and unlike particles in corresponding states.

[8] L. Hulthén, Arkiv. f. Mat. Astr. Fysik **29A**, No. 33 (1943); **30A**, No. 9 (1943); **31A**, No. 15 (1944); also B. Ferretti, Ricerca Scient. **12**, 843,993 (1941).

[9] J. M. Jauch, Phys. Rev. **67**, 125 (1945).

[10] Cf. W. Pauli, "Meson theory of nuclear forces," Lectures at the Massachusetts Institute of Technology, 1944, p. 43.

[11] M. Fierz and G. Wentzel, Helv. Phys. Acta **17**, 215 (1944).

the meson theory with strong coupling the P-potential changes its sign for small distances of the interacting nucleons and for certain values of the isobar energy. And they already pointed out that such a behavior of the potential energy in the strong coupling theory might well give an anisotropy for the high energy neutron-proton scattering in agreement with Amaldi's experiments.

In the first part of this paper we investigate this possibility. We shall study the anisotropy of 14-Mev neutrons scattered by protons in the Møller-Rosenfeld theory in the strong coupling limit (and in the symmetrical form) and in the second Born's approximation. The use of this approximation is justified as far as the energy of the particles is concerned. It is not yet clear whether Born's collision method is good for the present problem, since the coupling constants, in rising powers of which we develop the wave function, are bounded from below in the strong coupling theory. The coupling constants that we chose, however, are still less than 1 and the convergence of the above development is assured in the Møller-Rosenfeld theory even if we replace the source function by the δ-function. As the first Born's approximation gives a cross section which essentially coincides with the one calculated in the weak coupling limit theory, we have treated the problem in the second approximation. It is only from this approximation on that the virtual excited states (isobars) of the nucleons make a contribution to the scattering cross section. Our task was to investigate whether this contribution is such as to decrease the value of R computed[12] with the first approximation and to see the dependence of R on the isobar energy. Our calculations lead to an affirmative conclusion and show that R decreases with the isobar energy. We believe that this result will remain if one treats the problem with a better approximation method.

In the second part of this paper we evaluate the cross section of the inelastic scattering of very high energy neutrons by protons with production of isobars. This problem has a great interest for the following reasons: if the strong coupling theory is basically true one should be able to detect experimentally the excited states of the nucleons. The fact that such excited particles have not yet been observed might be due to the high value of the isobar energy—energy of excitation of a nucleon into a higher spin and charge state—as compared to the experimentally available energies in the laboratory up to now. An estimation of the order of magnitude of the isobar energy can be obtained from the value of this energy which gives a satisfactory angular distribution of 14-Mev neutrons elastically scattered by protons. The results presented in Table I indicate that a rather too low value of the isobar energy would be expected for an agreement of the Møller-Rosenfeld theory with the Amaldi's experiments, if such an agreement is attained at all. This is highly improbable since a value of the isobar energy of the order of 5 Mev would give rise to an inelastic scattering of 14-Mev neutrons which has not been observed. One possibility, of course, is that the lifetime of such isobars might be very small so that the excited particles would fall down to their ground state before detection. Even so, one would expect to detect the slower unexcited particles as well as the remaining energy which would be carried out by electrons and neutrinos or by γ-rays.

On the other hand, the tensor force, which does not occur in the Møller-Rosenfeld potential, was shown by Jauch[9] to decrease appreciably the ratio R as compared to the value obtained with the Møller-Rosenfeld theory, both cases in weak coupling approximation. One may therefore expect that the combined effects of the tensor force and the isobar states of the nucleons will give a value for R in agreement with experiment and for a reasonably high isobar energy. In a paper just published, Wentzel[13] indicates that the isobar energy must be of the order of 45 Mev, if the tensor force is taken into account. This is the value that we used in our calculations.* Such isobar energy would require nucleons with a

[12] $R=\sigma(\pi)/\sigma(\pi/2)$ is the ratio of the differential cross sections in the backward and perpendicular directions in the center of mass system.

[13] G. Wentzel, Helv. Phys. Acta 18, 430 (1945).

* I am indebted to Professor Pauli and Professor Jauch for communicating Wentzel's results to me in advance of their publication. Wentzel (reference 13) was able to show that the strong coupling theory with a tensor force (Schwinger's mixture) gives a value for R in agreement with Amaldi's experiments. This result shows the importance of the tensor force for the scattering problem (besides its quadrupole moment effect) and, together with the present calculations (Part I), is a decisive argument against the original Møller-Rosenfeld formalism.

minimum energy of the order of 100 Mev—in the laboratory system—for the effect to be detected experimentally.

PART I. THE ANISOTROPY OF THE SCATTERING OF 14-MEV NEUTRONS BY PROTONS IN THE MØLLER-ROSENFELD THEORY IN THE SYMMETRICAL FORM AND IN THE STRONG COUPLING LIMIT

1. The Wave Equation of the Two-Body Problem

The Hamiltonian of two nucleons in the symmetrical theory with strong coupling has the following form:*

$$H=\frac{1}{2M}(\Delta_I+\Delta_{II})+\frac{\epsilon}{2}\sum_{k=1}^{3}(d_{Ik}^2+d_{IIk}^2)+V. \quad (1)$$

The first and third terms are the usual kinetic and potential operators; the second term is the isobar energy of the two nucleons, where ϵ is a constant depending on the extension of the source and on the coupling constants, and the d's are the operators of the spin of the particles. The spin d_k and the isotopic spin h_k have the eigenvalues:

$$\sum_{k=1}^{3} d_k^2=\sum_{k=1}^{3} h_k^2=j(j+1); \quad j=\tfrac{1}{2}, \tfrac{3}{2}, \cdots$$

$$d_3=m; \quad h_3=n,$$

$$j\geqslant m, n\geqslant -j$$

and $n+\frac{1}{2}$ represents the nucleon charge in e-units.

In the Møller-Rosenfeld theory the potential energy of two nucleons I and II is:

$$V=\Omega W(r); \quad \Omega=\sum_\alpha(\mathbf{e}_\alpha^I\cdot\mathbf{e}_\alpha^{II});$$
$$W(r)=(f\mu)^2e^{-\mu r}/r, \quad (2)$$
$$r\equiv|\mathbf{x}|=|\mathbf{x}_I-\mathbf{x}_{II}|$$

where f is the coupling constant of the meson fields with the nucleons and μ is the meson mass; the matrix $e_{\alpha i}$ satisfies the commutation rules:

$$[d_1, e_{i2}]=[e_{i1}, d_2]=ie_{i3},$$
$$[h_1, e_{2\alpha}]=[e_{1\alpha}, h_2]=ie_{3\alpha},$$

and corresponds to the matrix $\tau_\alpha\sigma_i$ of the weak coupling theory.

The expression (2) for the potential operator holds only for distances r considerably larger than the source size a. It gives reasonable nuclear forces only if we assume that a is small compared to the forces range μ^{-1}:

$$a\mu\ll 1.$$

Besides this inequality, another condition has to be fulfilled in the present theory, namely:

$$(f\mu)^2\gg(a\mu)^2$$

which defines the strong coupling approximation.[4]

Because of the occurrence of the term Ω in (2) the spin of each nucleon does not commute with the Hamiltonian (1). It is therefore more convenient to replace the set of quantum numbers $j_I, m_I, n_I; j_{II}, m_{II}, n_{II}$ of two nucleons by the equivalent set $J, M, K, N; j_I, j_{II}$, where J, M, K, N are the total spin and isotopic spin quantum numbers:

$$\left.\begin{aligned}&\textstyle\sum_k (d_k^I+d_k^{II})^2=J(J+1),\\ &\textstyle\sum_k (h_k^I+h_k^{II})^2=K(K+1),\\ &d_3^I+d_3^{II}=M; \quad h_3^I+h_3^{II}=N,\end{aligned}\right\} \quad (3)$$

$$|j_I-j_{II}|\leqslant J, K\leqslant j_I+j_{II} \quad (4)$$

which are integrals of motion.

Eliminating the motion of the center of mass and the spin-isotopic spin wave functions, the equation of two nucleons can be written in the following form:

$$\{\Delta/M+E-E_j\}F(j_I, j_{II}; \mathbf{x})$$
$$=W(r)\sum_{j_I'j_{II}'}(j_I, j_{II}; J, M, K, N|\Omega|j_I', j_{II}';$$
$$J, M, K, N)F(j_I', j_{II}'; \mathbf{x}), \quad (5)$$

where F is the wave function and:[14]

$$E_j=\tfrac{1}{2}\epsilon\{(j_I+\tfrac{1}{2})^2+(j_{II}+\tfrac{1}{2})^2-2\}. \quad (6)$$

$(j_I, j_{II}; J, M, K, N|\Omega|j_I', j_{II}'; J, M, K, N)$ is the matrix of Ω with respect to the adopted set of quantum numbers. This matrix, which was calculated by Fierz[15] in a recent paper, is diagonal with respect to the quantum numbers J, M, K, N and obeys the selection rule:

$$\Delta j_A=\pm 1; \quad A=I, II. \quad (7)$$

2. The Cross Section in the Second Born's approximation

In order to solve Eq. (5) by successive approximations, we develop the function F in a series of powers of the coupling constant $(f\mu)^2$; assuming

* In the system of units in which $\hbar=c=1$.

[14] The isobar energy in this form vanishes for the ground state $j_I=j_{II}=\frac{1}{2}$ of the nucleons.

[15] M. Fierz, Helv. Phys. Acta 17, 181 (1944).

these powers already included in the functions f_n we obtain from:

$$F(j_I, j_{II}; \mathbf{x}) = \sum_n f_n(j_I, j_{II}; \mathbf{x})$$

the sequence of equations:

$$\left\{\frac{\Delta}{M}+E-E_j\right\} f_n(j_I, j_{II}; \mathbf{x}) = W(r) \sum_{j_I' j_{II}'} (j_I j_{II}|\Omega|j_I', j_{II}') \times f_{n-1}(j_I', j_{II}'; \mathbf{x}) \quad (8)$$

where, for abbreviation, we have omitted the indices J, M, K, N of the matrix. These equations refer, of course, to a given set of values of these indices.

For our purpose, it is more convenient to work in momentum space and use Dirac's theory of scattering.[16] Let $\varphi_n(j_I, j_{II}; \mathbf{k})$ and $(\mathbf{k}|W|\mathbf{k}')$ be the transformed functions of f_n and $MW(r)$ in this space. The Eqs. (8) will go over to:

$$\{k^2_{j_I j_{II}} - k^2\} \varphi_n(j_I, j_{II}; \mathbf{k}) = \sum_{j_I' j_{II}'} (j_I j_{II}|\Omega|j_I' j_{II}') \times \int (\mathbf{k}|W|\mathbf{k}') \varphi_{n-1}(j_I' j_{II}'; \mathbf{k}') d^3k', \quad (9)$$

$$k^2_{j_I j_{II}} = M(E-E_j).$$

Born's approximation consists in taking a plane wave as the zeroth approximation. The normalized plane waves which obey the Pauli principle are, in configuration space:

$$u_a \cos(\mathbf{k}\cdot\mathbf{x}) \quad \text{and} \quad u_s \sin(\mathbf{k}\cdot\mathbf{x}), \quad (10)$$

where u_a and u_s are functions, respectively, antisymmetric and symmetric in the spin and isotopic spin variables. In the elastic scattering problem the only possible values of J and K are 0 and 1. The spin-isotopic spin wave function will be antisymmetric for the states $J=1$, $K=0$ and $J=0$, $K=1$, while it will be symmetric for $J=K=0$ and $J=K=1$; thus the functions (10) give the following plane waves in momentum space:

for $J=1$, $K=0$ and $J=0$, $K=1$:

$$\frac{(2\pi)^{\frac{1}{2}}}{2}\{\delta(\mathbf{k}-\mathbf{k}_0)+\delta(\mathbf{k}+\mathbf{k}_0)\},$$

for $J=1$, $K=1$, and $J=0$, $K=0$:

$$\frac{(2\pi)^{\frac{1}{2}}}{2}\{\delta(\mathbf{k}-\mathbf{k}_0)-\delta(\mathbf{k}+\mathbf{k}_0)\}. \quad (11)$$

$\mathbf{k}_0$ is the wave vector of the initial state in the center of mass system.

If we impose the condition that the particles be initially in their ground state, $j_0=(\frac{1}{2}, \frac{1}{2})$, we have to multiply the functions (10) by δ_{jj_0}, where we indicate with a single letter j the pair j_I, j_{II}.

As we see from (11), each spin state is composed of four different states, a singlet ($K=0$) and the triplet states ($K=1$) in the isotopic spin variables. N, however, is an integral of motion and as we require that the two particles be a proton and a neutron in the initial and final states we can fix $N=0$ (if we remember that $N+1=$charge of the two nucleons in e-units) and disregard the two other states corresponding to $N=\pm 1$ for $K=1$.

From the plane waves (11) multiplied by δ_{jj_0} we obtain the following first approximation:

for $J=1$, $K=0$:

$$\varphi_1(j;\mathbf{k}) = \frac{(2\pi)^{\frac{1}{2}}}{2}\left[\frac{1}{k_j^2-k^2} - i\pi\delta(k_j^2-k^2)\right] \cdot (j;1,0|\Omega|j_0;1,0)[(\mathbf{k}|W|\mathbf{k}_0) + (\mathbf{k}|W|-\mathbf{k}_0)] \quad (12)$$

and analogous formulas for $J=0$, $K=1$; $J=K=1$; $J=K=0$. We have now indicated in the matrix of Ω the values of J and K. The expression which contains the δ-term in (12) corresponds to the condition of only outgoing waves in configuration space.

The second approximation will be:

for $J=1$, $K=0$:

$$\varphi_2(j;\mathbf{k}) = \frac{(2\pi)^{\frac{1}{2}}}{2}\left[\frac{1}{k_j^2-k^2} - i\pi\delta(k_j^2-k^2)\right] \cdot \sum_{j'} (j;1,0|\Omega|j';1,0)(j';1,0|\Omega|j_0;1,0) \times \left\{\int \frac{(\mathbf{k}|W|\mathbf{k}')(\mathbf{k}'|W|\mathbf{k}_0)}{k_{j'}^2-k'^2} d^3k' + \int \frac{(\mathbf{k}|W|\mathbf{k}')(\mathbf{k}'|W|-\mathbf{k}_0)}{k_{j'}^2-k'^2} d^3k'\right\}$$

and analogous expressions for the remaining states.

[16] P. A. M. Dirac, *Quantum Mechanics* (Clarendon Press, Oxford, 1935), second edition, p. 195.

Finally the differential cross section is:

$$\sigma(\vartheta)=\tfrac{1}{4}\sum_{J,M}\{\text{ampl. }\textstyle\sum_K(\varphi_1+\varphi_2)\}^2 \tag{13}$$

or

$$\sigma(\vartheta)=\tfrac{1}{4}\sigma_S(\vartheta)+\tfrac{3}{4}\sigma_{tr}(\vartheta),$$

where

$$\begin{aligned}\sigma_S(\vartheta)=4\pi^4\Big\{&[(j;0,0|\Omega|j_0;0,0)+(j;0,1|\Omega|j_0;0,1)](\mathbf{k}|W|\mathbf{k}_0)+[(j;0,1|\Omega|j_0;0,1)\\&-(j;0,0|\Omega|j_0;0,0)](\mathbf{k}|W|-\mathbf{k}_0)+\textstyle\sum_{j'}\Big([(j;0,0|\Omega|j';0,0)(j';0,0|\Omega|j_0;0,0)\\&+(j;0,1|\Omega|j';0,1)\cdot(j';0,1|\Omega|j_0;0,1)]\int\frac{(\mathbf{k}|W|\mathbf{k}')(\mathbf{k}'|W|\mathbf{k}_0)}{k_0^2-ME_{j'}-k'^2}d^3k'\\&+[(j;0,1|\Omega|j';0,1)(j';0,1|\Omega|j_0;0,1)-(j;0,0|\Omega|j';0,0)\cdot(j';0,0|\Omega|j_0;0,0)]\\&\int\frac{(\mathbf{k}|W|\mathbf{k}')(\mathbf{k}'|W|-\mathbf{k}_0)}{k_0^2-ME_{j'}-k'^2}d^3k'\Big)\Big\}^2\end{aligned} \tag{14}$$

for the ordinary spin singlet, $J=0$. An analogous expression is easily derived for $\sigma_{tr}(\vartheta)$, the cross section of the triplet states $J=1$.

The denominator which occurs in the integrals of (13) comes from the conservation of energy:

$$E=E_{j_0}+k_0^2/M,$$

where E is the total energy of the system in the final state. This relation gives, together with the definition (9) of k_j^2:

$$k_j^2=k_0^2+M(E_{j_0}-E_j),$$
$$E_{j_0}=0 \text{ for } j_0=(\tfrac{1}{2},\tfrac{1}{2}).$$

As in our problem the initial and final spins of the two nucleons must be $\frac{1}{2}$, only the matrix elements with $j=j_0=\frac{1}{2}$ will occur in the first two terms of σ_s and σ_{tr}. In the terms with integrals the following elements will be present:

$$\begin{aligned}&(\tfrac{1}{2},\tfrac{1}{2};J,K|\Omega|\tfrac{1}{2},\tfrac{1}{2};J,K)\\&\quad\times(\tfrac{1}{2},\tfrac{1}{2};J,K|\Omega|\tfrac{1}{2},\tfrac{1}{2};J,K),\end{aligned} \tag{15}$$

$$\left.\begin{aligned}&(\tfrac{1}{2},\tfrac{1}{2};J,K|\Omega|\tfrac{1}{2},\tfrac{3}{2};J,K)\\&\quad\times(\tfrac{1}{2},\tfrac{3}{2};J,K|\Omega|\tfrac{1}{2},\tfrac{1}{2};J,K),\\&(\tfrac{1}{2},\tfrac{1}{2};J,K|\Omega|\tfrac{3}{2},\tfrac{1}{2};J,K)\\&\quad\times(\tfrac{3}{2},\tfrac{1}{2};J,K|\Omega|\tfrac{1}{2},\tfrac{1}{2};J,K),\end{aligned}\right\} \tag{16}$$

$$\begin{aligned}&(\tfrac{1}{2},\tfrac{1}{2};J,K|\Omega|\tfrac{3}{2},\tfrac{3}{2};J,K)\\&\quad\times(\tfrac{3}{2},\tfrac{3}{2};J,K|\Omega|\tfrac{1}{2},\tfrac{1}{2};J,K).\end{aligned} \tag{17}$$

Terms with values of j_I, j_{II}, higher than $\frac{3}{2}$ are excluded in the second approximation because of the selection rule (7) and the elastic condition. The elements (16) and (17) represent the contribution of the virtual isobars to the cross section in that approximation. Furthermore, the indices j_I, j_{II} of the matrix Ω must obey the vector model inequalities (4). These exclude the two terms (16) from the singlet cross section ($J=0$) as well as from the terms with $K=0$.

The final expression of the cross section is easily obtained by means of Fierz's formulas[15] for the matrix Ω and of the momentum transformed of the Yukawa potential:

$$(\mathbf{k}|W|\mathbf{k}')=\frac{g^2}{\mu^2+(\mathbf{k}'-\mathbf{k})^2};\quad g^2=\frac{(f\mu)^2M}{2\pi^2}.$$

3. Numerical Results and Conclusions

The integrals which occur in the cross section can be reduced to a simpler form, suitable for numerical evaluation; we shall not give here the details of this reduction.[17] The evaluation of these integrals leads to two different expressions for the cross section according to whether we have:

$$k_0^2<ME_j, \tag{18}$$

or:

$$k_0^2>ME_j. \tag{19}$$

In this work we evaluated the ratio $R=\sigma(\pi)/\sigma(\pi/2)$ only for the condition (18). This inequality means physically that the kinetic energy of the bombarding particles must be less than the isobar energy and this leads to only elastic scattering. The inequality (19) would imply inelastic scattering, the outgoing nucleon or the scatterer or both being able to make a transition into an

[17] Cf. J. Leite Lopes, Ph.D. Thesis, Princeton University, 1945; also J. Leite Lopes, An. Acad. Bras. Ci. (to be published).

TABLE I. Angular distribution of the scattering of 14-Mev neutrons by protons in the symmetrical Møller-Rosenfeld theory with strong coupling (second Born approximation). $R=8.04$ for $(f\mu)^2=0.59$ in the first Born approximation; the theory does not include longitudinal mesons.

E_i (in Mev)	R $(f\mu)^2=0.375$	$(f\mu)^2=0.46$	$(f\mu)^2=0.59$
9	5.73	5.25	4.85
15	5.81	5.65	5.13
30	6.71	6.56	6.01

excited state at the cost of the kinetic energy (initial). The problem of inelastic scattering will be considered in the second part of this paper.

The inequality (18) imposes an additional condition upon the second order terms of the cross section (13): it excludes the terms with the intermediate values $\frac{1}{2}$, $\frac{1}{2}$ of j_I and j_{II} (reality of the kinetic energy of the incident neutrons).

The numerical evaluation of $\sigma(\vartheta)$ was made for $\vartheta=\pi$ and $\vartheta=\pi/2$ with the following data: $E_0=14$ Mev (in the laboratory system); $\mu=177m$, where m is the electron rest mass. The ratio R depends on ϵ, the isobar energy constant and on the coupling constant. We give the results in Table I. The numerical evaluation of the integrals was made by taking a sum of the integrands over five equidistant points in the interval (0, 1). The values of $(f\mu)^2$ that we chose are those given by Pauli and Kusaka,[4] Jauch and Hu,[18] and Hulthén.[8] Hulthén's coupling constant is perhaps the most reliable for our problem since he determined it with the Møller-Rosenfeld scheme.

One sees from Table I that the ratio R decreases with the isobar energy. This is in agreement with Fierz and Wentzel finding that the potential energy of the P-waves becomes attractive for values of ϵ less than about 30 Mev. A comparison of the values of R given in the table with the value of R calculated in the first Born's approximation, namely $R=8.04$,* shows that the virtual isobars make a contribution to R in the direction of decreasing the backward anisotropy of the scattering. As to the values of R themselves, they depend, of course, on the approximation used and on the rough evaluation of the integral terms of the cross section. Since the Born's approximation underestimates the S-waves we expect the exact values of R to be smaller than those given in Table I. On the other hand, as was already pointed out in the Introduction, a possibility which the results of our calculations suggests is that the combined effects of the tensor force and of the isobars give a result in final agreement with the experimental angular distribution (see reference 13).

We must also have in mind that in the Møller and Rosenfeld theory here investigated, only one coupling constant of the vector field was taken into account, namely that of the transverse mesons. For the sake of simplicity, the vector theory so far studied in the strong coupling limit excludes the interaction of the nucleons with the longitudinal mesons. This results in the fact that the mixed theory in second Born's approximation disposes of two constants, the isobar energy and the coupling constant $(f\mu)^2$. With regard to the values of R the theory is thus equivalent to the same theory in weak coupling limit and in first approximation, which also disposes of two constants, the longitudinal and transverse mesons coupling constants. We do not know yet the effect, in strong coupling limit, of the longitudinal mesons on the anisotropy of the neutron-proton scattering.

PART II. INELASTIC SCATTERING OF HIGH ENERGY NEUTRONS BY PROTONS WITH PRODUCTION OF ISOBARS

4. Introduction

In the preceding part of this paper, it was shown that the virtual excited states of the nucleons give a contribution to the cross section of the elastic scattering of high energy neutrons by protons in such a way as to decrease the backward anisotropy which is obtained with the weak coupling theory in the symmetrical form. This result is of interest because it suggests that the wrong angular distribution given by the thus far investigated meson theories in the symmetrical form is due not only to the exchange character of the potential operator but also to the weak coupling approximation. Or, in other words, in the theory with strong coupling the symmetrical form may be maintained, as it is desirable for the saturation requirements of the nuclear forces, and the observed anisotropy of the

[18] J. M. Jauch and N. Hu, Phys. Rev. 65, 289 (1944).

* This value of R is obtained with only the interaction nucleons-transverse mesons. If one includes longitudinal mesons one gets $R=4.8$.

neutron-proton scattering may be attributed to the virtual excited states of the nucleons. If this is so, a question which immediately arises is whether it is possible to detect experimentally the nucleons in an excited state.* If the theory predicts the excitation of heavy particles in a certain range of energy then, at least in principle, an experiment to detect the isobars would furnish a crucial test for the strong coupling assumptions. If one could thus decide between the two alternative approximations—the weak and the strong coupling approximations—a new light would certainly be shed on the nature of the nuclear particles.

In this part, we evaluate, for a certain range of energy of the bombarding particles, the cross section of the inelastic scattering of neutrons by protons, with excitation of one of the particles into a higher spin and charge state. In a paper just published by Wentzel,[13] it is shown that one obtains a reasonable forward elastic scattering in a strong coupling theory with a tensor force, for values of the isobar energy of the order of 45 Mev. This is the value that we assumed in this section. We limited our evaluation of the inelastic cross section to the first Born approximation. This is probably not too bad an approximation within the high energy region to which we restricted ourselves. The computations were also made for the three main forms of the meson field theory, namely the Møller-Rosenfeld, the pseudoscalar, and the Schwinger theories. The ratio of the inelastic to the elastic cross section is found to be of the order of 3 percent for 100-Mev bombarding neutrons.

5. Inelastic Cross Section in the Møller-Rosenfeld Theory

From (13), Section 2, we obtain the differential cross section in the first approximation by simply cancelling the second-order terms. In the inelastic problem and in this approximation the dependence of σ_{inel} on the isobar energy E_j arises from the energy equation:

$$k^2/M+E_j=k_0^2/M.$$

The process which we investigate is the following: two particles collide against each other, each having an initial spin $\frac{1}{2}$; after collision one of the nucleons is left with spin $\frac{3}{2}$: transition $\frac{1}{2}, \frac{1}{2}\rightarrow\frac{1}{2}, \frac{3}{2}$. From the vector model inequalities (4) we see that the nucleons cannot be in a singlet state $J=0$, $K=0$.

Fierz's formulas[15] for the matrix Ω give:

$$(\tfrac{1}{2}, \tfrac{1}{2}; 1, 1|\Omega|\tfrac{1}{2}, \tfrac{3}{2}; 1, 1)=4\sqrt{2}/9$$

and the differential cross section has the following form:

$$\sigma_{\text{in}}{}^{MR}(\vartheta)=\frac{32}{27}\frac{k}{k_0}(f\mu)^4M^2\frac{k^2k_0{}^2\cos^2\vartheta}{\{(\mu^2+k^2+k_0{}^2)^2-4k^2k_0{}^2\cos^2\vartheta\}^2}.$$

The total cross section is:

$$\sigma_{\text{in}}{}^{MR}=2\pi\int_0^\pi\sigma_{\text{in}}{}^{MR}(\vartheta)\sin\vartheta d\vartheta$$

$$=\frac{4\pi}{27}(f\mu)^4M^2\frac{1}{k_0{}^2}\left\{\frac{4kk_0}{(\mu^2+k^2+k_0{}^2)^2-4k^2k_0{}^2}-\frac{1}{\mu^2+k^2+k_0{}^2}\log\frac{\mu^2+(k+k_0)^2}{\mu^2+(k-k_0)^2}\right\}.$$

6. Inelastic Cross Section in the Pseudoscalar Theory

In this theory, the component M of the total ordinary spin of two nucleons is not a constant of motion. The cross section is accordingly:

$$\sigma(\vartheta)=\tfrac{1}{4}\sum_{J,M,M_0}\{\textstyle\sum_K \text{ampl. } \varphi_1\}^2. \qquad (13')$$

*A question which is intimately connected with the observation of these excited states is the lifetime of such states and the possible processes of unexcitation or disintegration. A nucleon with spin $\frac{3}{2}$ can have any one of the following charges (degeneracy in the symmetrical theory): $(n+\frac{1}{2})e=-e$, 0, e, $2e$. For a nucleon with spin $j=\frac{3}{2}$ and charge 0 or e, Jauch, in recent calculations, has found a lifetime of the order of 10^{-13} sec. for a transition into the ground state ($j=\frac{1}{2}$) with emission of γ-rays. A nucleon which has undergone such intermediate processes of excitation and emission of photons will have a final kinetic energy much smaller than the initial one and this can be easily detected in a cloud-chamber picture. A nucleon with excited charge $-e$ or $2e$ would probably undergo β-decay.

Using the matrix elements given in Appendix I we obtain:

$$\sigma_{\text{in}}{}^{P}(\vartheta)=\frac{1}{81}f^4\frac{k}{k_0}M^2\left\{\frac{12k^2k_0{}^2\kappa^4\cos^2\vartheta}{\{(\kappa^2+k^2+k_0{}^2)^2-4k^2k_0{}^2\cos^2\vartheta\}^2}+\frac{k^2k_0{}^2\sin^2\vartheta}{(\kappa^2+k^2+k_0{}^2)^2-4k^2k_0{}^2\cos^2\vartheta}\right\}.$$

The tensor force singularities cancel out in first Born's approximation.

The total cross section is:

$$\sigma_{\text{in}}{}^{P}=\frac{\pi}{162}\frac{f^4M^2}{k_0{}^2}\left\{\frac{12kk_0\kappa^4}{(\kappa^2+k^2+k_0{}^2)^2-4k^2k_0{}^2}-\frac{6\kappa^4+(\kappa^2+k^2+k_0{}^2)^2-4k^2k_0{}^2}{2(\kappa^2+k^2+k_0{}^2)}\log\frac{\kappa^2+(k+k_0)^2}{\kappa^2+(k-k_0)^2}+8kk_0\right\}.$$

7. Inelastic Cross Section in the Schwinger Theory

The differential cross section in Schwinger's theory is obtained in the same way as in the pseudoscalar case. With the help of the matrices given in Appendix II we find:

$$\begin{aligned}\sigma_{\text{in}}{}^{S}(\vartheta)=\frac{1}{324}f^4M^2\frac{k}{k_0}\Bigg\{&3(\mu^2-\kappa^2)^2\left[\frac{(\mathbf{k}-\mathbf{k}_0)^2}{[\kappa^2+(\mathbf{k}-\mathbf{k}_0)^2][\mu^2+(\mathbf{k}-\mathbf{k}_0)^2]}-\frac{(\mathbf{k}+\mathbf{k}_0)^2}{[\kappa^2+(\mathbf{k}+\mathbf{k}_0)^2][\mu^2+(\mathbf{k}+\mathbf{k}_0)^2]}\right]^2\\&+4(\mu^2-\kappa^2)^2\frac{|\mathbf{k}\times\mathbf{k}_0|^2}{[\kappa^2+(\mathbf{k}-\mathbf{k}_0)^2][\mu^2+(\mathbf{k}-\mathbf{k}_0)^2][\kappa^2+(\mathbf{k}+\mathbf{k}_0)^2][\mu^2+(\mathbf{k}+\mathbf{k}_0)^2]}\\&+8\Bigg[\frac{3\mu^4[(k+k_0)^2-(\mathbf{k}-\mathbf{k}_0)^2]}{[\mu^2+(\mathbf{k}-\mathbf{k}_0)^2][\mu^2+(\mathbf{k}+\mathbf{k}_0)^2]}-\frac{2\mu^2(\mu^2-\kappa^2)[(\mathbf{k}+\mathbf{k}_0)^2-(\mathbf{k}-\mathbf{k}_0)^2]}{[\mu^2+(\mathbf{k}-\mathbf{k}_0)^2][\mu^2+(k+k_0)^2]}\\&\times\left(\frac{(\mathbf{k}-\mathbf{k}_0)^2}{[\kappa^2+(\mathbf{k}-\mathbf{k}_0)^2][\mu^2+(\mathbf{k}-\mathbf{k}_0)^2]}-\frac{(\mathbf{k}+\mathbf{k}_0)^2}{[\kappa^2+(\mathbf{k}+\mathbf{k}_0)^2][\mu^2+(\mathbf{k}+\mathbf{k}_0)^2]}\right)\Bigg]\Bigg\}.\end{aligned}$$

The total cross section is easily obtained from this formula and has a long expression which we do not need to write here.

8. Differential Cross Section of the Elastic Scattering

Møller-Rosenfeld theory:

$$\sigma_S(\vartheta)=\frac{M^2(f\mu)^4}{9}\left\{\frac{1}{\mu^2+4k_0{}^2\sin^2(\vartheta/2)}-\frac{2}{\mu^2+4k_0{}^2\cos^2(\vartheta/2)}\right\}^2$$

$$\sigma_{\text{tr}}(\vartheta)=\frac{M^2(f\mu)^4}{81}\left\{\frac{1}{\mu^2+4k_0{}^2\sin^2(\vartheta/2)}+\frac{2}{\mu^2+4k_0{}^2\cos^2(\vartheta/2)}\right\}^2.$$

Pseudoscalar theory:*

$$\sigma_S(\vartheta)=\frac{M^2(f\kappa)^4}{81}\left\{\frac{1}{\kappa^2+4k_0{}^2\sin^2(\vartheta/2)}-\frac{2}{\kappa^2+4k_0{}^2\cos^2(\vartheta/2)}\right\}^2,$$

$$\begin{aligned}\sigma_{\text{tr}}(\vartheta)=\frac{M^2}{81}f^4\Bigg\{48\Bigg[&\frac{k_0{}^2\sin^2(\vartheta/2)}{\kappa^2+4k_0{}^2\sin^2(\vartheta/2)}+\frac{2k_0{}^2\cos^2(\vartheta/2)}{\kappa^2+4k_0{}^2\cos^2(\vartheta/2)}\Bigg]^2-8\Bigg[\frac{k_0{}^2\sin^2(\vartheta/2)}{\kappa^2+4k_0{}^2\sin^2(\vartheta/2)}\\&+\frac{2k_0{}^2\cos^2(\vartheta/2)}{\kappa^2+4k_0{}^2\cos^2(\vartheta/2)}+\frac{8k_0{}^4\sin^2\vartheta}{(\kappa^2+4k_0{}^2\sin^2(\vartheta/2))(\kappa^2+4k_0{}^2\cos^2(\vartheta/2))}\Bigg]+3\Bigg\}.\end{aligned}$$

* The formula given by Hulthén (Arkiv. Mat. Astr. Fysik **31A**, No. 15 (1944)) for the triplet cross section in the pseudoscalar theory and in first Born's approximation is not correct. The above formula was derived in the well-known way from potential (20) or (21) of Appendix I. The tensor force is responsible for the occurrence of k_0 in the numerator of the triplet cross section and this makes the total cross section larger than the one given by the Møller-Rosenfeld theory; the constant term of the triplet cross section is due to the δ-term of (20).

9. Numerical Results and Conclusions

In Table II the numerical values of the total cross section of the inelastic scattering are given in each theory. E_0 is the energy of the bombarding neutrons in the laboratory system and the value assumed for the isobar energy was 45 Mev. The coupling constant was taken equal to 0.375, as given by Pauli and Kusaka.[4] It is seen that the tensor force increases considerably the cross section, its effect being smaller, as would be expected, in the Schwinger theory than in the pseudoscalar theory. The total elastic cross section (which is easily obtained from the formulas given in Section 8 by integration over the angles) is of the order of $0.06\cdot10^{-24}$ cm² for 100-Mev particles and Møller-Rosenfeld potential while it is of the order of $0.4\cdot10^{-24}$ cm² for the pseudoscalar theory and the same energy. A comparison between these values and those of the inelastic cross section shows that the ratio σ_{in}/σ_{el} is of the order of 0.03 for the M.R. theory and of the order of 0.05 for the pseudoscalar theory. This ratio is probably inside the experimental range and gives a test for the theory as soon as 100-Mev heavy particles are available in the laboratory.

TABLE II. Cross section of the inelastic scattering of neutrons by protons with production of isobars.

E_0 (in Mev)	σ_{in} (in cm²) Møller-Rosenfeld	Pseudosc.	Schwinger
100	$0.18\cdot10^{-26}$	$0.26\cdot10^{-25}$	$0.9\cdot10^{-26}$
110	$0.32\cdot10^{-26}$	$0.32\cdot10^{-25}$	$1.1\cdot10^{-26}$
150	$0.81\cdot10^{-26}$	$0.58\cdot10^{-25}$	$2.6\cdot10^{-26}$
180	$0.88\cdot10^{-26}$	$0.64\cdot10^{-25}$	
	$\mu=177m$	$\kappa=177m$	$\kappa=177m$; $\mu=2\kappa$

In conclusion, I wish to express my gratitude to Professor W. Pauli and Professor J. M. Jauch for the suggestion of this problem and many valuable discussions.

APPENDIX I. THE POTENTIAL MATRIX IN THE PSEUDOSCALAR THEORY

In the pseudoscalar theory with strong coupling the potential energy of two nucleons I and II is (in the small source assumption):

$$V=f^2\sum_\alpha\left\{(\mathbf{e}_\alpha{}^I\cdot\boldsymbol{\nabla})(\mathbf{e}_\alpha{}^{II}\cdot\boldsymbol{\nabla})\frac{e^{-\kappa r}}{r}+\frac{4\pi}{3}(\mathbf{e}_\alpha{}^I\cdot\mathbf{e}_\alpha{}^{II})\delta(\mathbf{x})\right\}, \tag{20}$$

where κ is the pseudoscalar meson mass.

In the current literature only the first term of V is written down but it is easily seen that this first term alone and the differentiated form of V, namely:

$$\left.\begin{aligned} V&=\frac{f^2}{3}\left\{\Omega\frac{\kappa^2}{r}e^{-\kappa r}+\Lambda\frac{1}{r^3}(3+3\kappa r+\kappa^2r^2)e^{-\kappa r}\right\},\\ \Omega&=\textstyle\sum_\alpha(\mathbf{e}_\alpha{}^I\cdot\mathbf{e}_\alpha{}^{II}),\\ \Lambda&=\sum_\alpha\left\{\frac{3}{r^2}(\mathbf{e}_\alpha{}^I\cdot\mathbf{x})(\mathbf{e}_\alpha{}^{II}\cdot\mathbf{x})-(\mathbf{e}_\alpha{}^I\cdot\mathbf{e}_\alpha{}^{II})\right\}, \end{aligned}\right\} \tag{21}$$

do not give the same transformed in momentum space. This is essentially due to the small source assumption which substitutes for the potential energy:

$$V=-f^2\textstyle\sum_\alpha\sum_{ij}e_{\alpha i}{}^Ie_{\alpha j}{}^{II}J_{ij}$$

$$J_{ij}=-\int\int U^I(x)U^{II}(x')\frac{\partial^2}{\partial x_i\partial x_j}\frac{e^{-\kappa R}}{R}d^3xd^3x';\quad R=|\mathbf{x}-\mathbf{x}'|$$

its value for point sources.* The first term of (20) thus obtained gives rise to (21) and to an additional δ-term, analogous to the right-hand side of Yukawa's equation:

$$\{-\nabla^2+\kappa^2\}X=4\pi\delta(\mathbf{x})$$

for point sources. If this singular term is subtracted from the potential energy—because it gives no

* $U^A(x)$ is the source function of nucleon A; for a point-nucleon $U(x)=\delta(x)$. See Pauli and Dancoff, reference 4.

finite binding energy for the deuteron nor any scattering cross section*—we get (21) and (20), whose momentum transformed is:

$$(\mathbf{k}|\,V|\mathbf{k}') = -G^2\left\{\frac{\Gamma}{\kappa^2+\mathbf{K}^2}-\frac{\Omega}{3}\right\},$$

$$G^2=f^2/2\pi^2; \quad \mathbf{K}=\mathbf{k}'-\mathbf{k}; \quad \Gamma=\sum_\alpha (\mathbf{e}_\alpha{}^I\cdot\mathbf{K})(\mathbf{e}_\alpha{}^{II}\cdot\mathbf{K}).$$

Because of the occurrence of the tensor force Λ or Γ in the potential operator, the component M of the total (ordinary) spin is not an integral of motion. The potential matrix has the form:

$$(J, M, K, N; j_I, j_{II}; \mathbf{k}|\,V|J, M', K, N; j_I', j_{II}'; \mathbf{k}')$$
$$= -G^2\left\{\frac{1}{\kappa^2+\mathbf{K}^2}(J, M, K, N; j_I, j_{II}; \mathbf{k}|\,\Gamma|J, M', K, N; j_I', j_{II}'; \mathbf{k}')\right.$$
$$\left.-\tfrac{1}{3}(J, M, K, N; j_Ij_{II}; \mathbf{k}|\,\Omega|J, M', K, N; j_I', j_{II}'; \mathbf{k}')\right\}.$$

The matrix of Ω was already calculated by Fierz and the computation of the matrix of Γ is straightforward if we use Fierz's formulas for the $e_{\alpha i}$'s.[15] The calculation is a little long and we shall not give its details here as they do not involve anything new.

The final matrix elements for the excitation of only one nucleon are the following:

$$J=K=1$$

$$(1;\tfrac{1}{2},\tfrac{1}{2};\mathbf{k}|\,V|-1;\tfrac{1}{2},\tfrac{3}{2};\mathbf{k}') = G^2\frac{\sqrt{2}}{18}\frac{(K_1-iK_2)^2}{\kappa^2+\mathbf{K}^2}, \tag{A}$$

$$(1;\tfrac{1}{2},\tfrac{1}{2};\mathbf{k}|\,V|0;\tfrac{1}{2},\tfrac{3}{2};\mathbf{k}') = \frac{G^2}{9}\frac{(K_1-iK_2)K_3}{\kappa^2+\mathbf{K}^2}, \tag{B}$$

$$(\pm1;\tfrac{1}{2},\tfrac{1}{2};\mathbf{k}|\,V|\pm1;\tfrac{1}{2},\tfrac{3}{2};\mathbf{k}') = -\frac{G^2\sqrt{2}}{9}\left\{\frac{3(K_1^2+K_2^2)+2K_3^2}{2(\kappa^2+\mathbf{K}^2)}-\frac{4}{3}\right\}, \tag{C}$$

$$(0;\tfrac{1}{2},\tfrac{1}{2};\mathbf{k}|\,V|0;\tfrac{1}{2},\tfrac{3}{2};\mathbf{k}') = \frac{2G^2\sqrt{2}}{9}\left\{\frac{K_1^2+K_2^2+2K_3^2}{2(\kappa^2+\mathbf{K}^2)}-\frac{2}{3}\right\},$$

$$(-1;\tfrac{1}{2},\tfrac{1}{2};\mathbf{k}|\,V|1;\tfrac{1}{2},\tfrac{3}{2};\mathbf{k}') = \text{c.c. of (A)},$$

$$(-1;\tfrac{1}{2},\tfrac{1}{2};\mathbf{k}|\,V|0;\tfrac{1}{2},\tfrac{3}{2};\mathbf{k}') = -\text{c.c. of (B)}$$

$$(0;\tfrac{1}{2},\tfrac{1}{2};\mathbf{k}|\,V|-1;\tfrac{1}{2},\tfrac{3}{2};\mathbf{k}') = -\text{(B)},$$

$$(0;\tfrac{1}{2},\tfrac{1}{2};\mathbf{k}|\,V|1;\tfrac{1}{2},\tfrac{3}{2};\mathbf{k}') = \text{c.c. of (B)}.$$

The Eqs. (9), Section 2, are now of the form:

$$\{k_j^2-k^2\}\varphi_n(j;\mathbf{k}) = \sum_{j'}\int (M;j;\mathbf{k}|\,V|\,M_0;j';\mathbf{k}')\varphi_{n-1}(j';\mathbf{k}')d^3k',$$

where we have omitted the constant indices of the matrix and put: $j=(j_I, j_{II})$. These equations hold for a given set of values of J, K, N, M, M_0. From this equation an expression for (13′) is easily derived, as in Section 2. The term δ_{jj_0} does not multiply (11) any more.

APPENDIX II. THE POTENTIAL MATRIX IN THE SCHWINGER THEORY

The potential energy of two nucleons (small sources) in this theory is

$$V=f^2\sum_\alpha\left\{(\mathbf{e}_\alpha{}^I\cdot\nabla)(\mathbf{e}_\alpha{}^{II}\cdot\nabla)\frac{e^{-\kappa r}-e^{-\mu r}}{r}+(\mathbf{e}_\alpha{}^I\cdot\mathbf{e}_\alpha{}^{II})\mu^2\frac{e^{-\mu r}}{r}\right\}, \quad \mu>\kappa$$

which gives in momentum space

$$(\mathbf{k}|\,V|\mathbf{k}') = G^2\sum_\alpha\left\{(\mathbf{e}_\alpha{}^I\cdot\mathbf{K})(\mathbf{e}_\alpha{}^{II}\cdot\mathbf{K})\left[\frac{1}{\mu^2+\mathbf{K}^2}-\frac{1}{\kappa^2+\mathbf{K}^2}\right]+(\mathbf{e}_\alpha{}^I\cdot\mathbf{e}_\alpha{}^{II})\frac{\mu^2}{\mu^2+\mathbf{K}^2}\right\},$$

* N. Kemmer, Helv. Phys. Acta 10, 47 (1937) (for the deuteron binding energy); Professor Pauli has shown, in unpublished calculations, that a δ-potential gives no scattering cross section.

where again

$$G^2=\frac{f^2}{2\pi^2};\quad \mathbf{K}=\mathbf{k}'-\mathbf{k}.$$

The matrix

$$(J, M, K, N; j_I, j_{II}; \mathbf{k}|\, V|\, J, M', K, N; j_I', j_{II}'; \mathbf{k}')$$

is obtained in the same way as was indicated in Appendix I. The non-diagonal elements, with respect to M, are easily derived from the pseudoscalar case since the Ω-term does not contribute to these elements. The diagonal terms are

$$(\pm 1; \tfrac{1}{2}, \tfrac{1}{2}; \mathbf{k}|\, V|\, \pm 1; \tfrac{1}{2}, \tfrac{3}{2}; \mathbf{k}')=\frac{-G^2\sqrt{2}}{9}\left\{\frac{(\mu^2-\kappa^2)[3(K_1^2+K_2^2)+2K_3^2]}{2[\kappa^2+\mathbf{K}^2][\mu^2+\mathbf{K}^2]}-\frac{4\mu^2}{\mu^2+\mathbf{K}^2}\right\},$$

$$(0; \tfrac{1}{2}, \tfrac{1}{2}; \mathbf{k}|\, V|\, 0; \tfrac{1}{2}, \tfrac{3}{2}; \mathbf{k}')=-\frac{G^2\sqrt{2}}{9}\left\{\frac{(\mu^2-\kappa^2)[K_1^2+K_2^2+2K_3^2]}{[\kappa^2+\mathbf{K}^2][\mu^2+\mathbf{K}^2]}-\frac{4\mu^2}{\mu^2+K^2}\right\}.$$

PHYSICAL REVIEW VOLUME 70, NUMBERS 1 AND 2 JULY 1 AND 15, 1946

Resonance Reactions and Anomalous Scattering

EUGENE P. WIGNER
Princeton University, Princeton, New Jersey

(Received April 11, 1946)

The purpose of the present paper is to give a derivation of the resonance formula for nuclear reactions which is free from artificial assumptions. Mathematically, the method used amounts to a Taylor series development of the wave function with respect to the energy. It is assumed that the first (energy independent) term in this development is, within a region of configuration space where all particles are close together, the same, no matter in which way the compound state is formed and that this is, in that region of configuration space, already a good approximation. The second term in the development of the wave function with respect to the energy difference from the resonance energy can then be calculated very easily and this calculation is carried out in Section II for resonance scattering, in Sections III and IV for resonance reactions. It is assumed in both calculations that the colliding particles have zero orbital angular momentum around their center of mass. The third term in the same expansion is estimated for resonance scattering in Section VI and it is shown that, if there were no other resonances in the neighborhood, the effect of the third term would be negligible over a very wide energy range (several hundred kilovolt). The formulae for the cross sections, as obtained, are of greater generality than the customary ones inasmuch as they contain extra terms which could be interpreted as potential scattering and potential reaction. The existence of such terms has been noticed already by Bethe. However, as discussed in Section V, the extra terms are, particularly in the neighborhood of the resonance, much smaller than the resonance terms so that one is led back, in practice, to the ordinary resonance formulae, as given, e.g., by Bethe. In particular, the disintegration probability is, as function of energy, proportional to the velocity with which the reaction products separate if the orbital angular momentum of the separating particles vanishes. It may be worth while to remark that the resonance part of the collision matrix has a particularly simple form and is, e.g., of rank 1. The case of orbital angular momentum $1\hbar$ is discussed in Section VII. In this case, the disintegration probability of the compound state is proportional to the third power of the velocity of the separating particles so that the scattering is, at very low energies, proportional to the square of the energy. The same holds, in this case, of the "potential scattering" also. Section VII also contains an investigation of the region of validity of the formulae in case of angular momentum $1\hbar$ between the colliding particles and shows that this region will extend to the neighboring resonances.

I. INTRODUCTION

ALTHOUGH there is no experimental evidence available to corroborate the resonance formula[1] with any great accuracy, a number of reformulations of the underlying picture[2] have appeared in the literature.[3] All these formula-

[1] The first four sections of the present article are based on a report, dated April 23, 1945, which the writer prepared for the Uranium Project. He is indebted to the Army Engineers for clearing that report for publication.

[2] G. Breit and E. P. Wigner, Phys. Rev. **49**, 519, 642 (1936); N. Bohr, Nature **137**, 344 (1936).

[3] H. A. Bethe and G. Placzek, Phys. Rev. **51**, 450 (1937); F. Kalckar, J. R. Oppenheimer, and R. Serber, Phys. Rev. **52**, 273 (1937); H. A. Bethe, Rev. Mod. Phys. **9**, 71 (1937); P. L. Kapur and R. Peierls, Proc. Roy. Soc. **166**, 277 (1938); and, in particular, A. J. F. Siegert, Phys. Rev. **56**, 750 (1939).

tions endeavor to give a quantum-mechanical equivalent to the picture of the formation of a compound nucleus which disintegrates subsequently and differ from each other in the (more or less openly made) assumptions as to what constitutes a compound state. They have been discussed and critically evaluated by G. Breit.[4] The present attempt borrows more from his results and those of Siegert than from the preceding treatments although some of the underlying ideas are the same as given by Kapur and Peierls.

Because of its greater mathematical simplicity the case of the resonance scattering will be treated separately. However, the basic assumption will be the same for resonance reaction and resonance scattering: that if all the particles of the system are close to each other, thus forming a compound nucleus, it is a good approximation to assume that the wave function is (apart from a constant factor) independent of the energy within the range for which the results are expected to hold and also independent of the origin of the compound state. Thus, the wave function of the compound nucleus is the same no matter whether, for instance, it was obtained from ${}_3Li^7+{}_2He^4$ or from ${}_4Be^9+D$ or from ${}_5B^{10}+$neutron or from ${}_5B^{11}+\gamma$.

Evidently, the above assumption is very rigid and does not permit one, e.g., to treat the energy region just between two resonances. It seems to me, however, that it corresponds more accurately than any other formulation that one can easily think of to the picture of a reaction through one definite compound state. It is also evident how one has to generalize the above picture in order to treat the region between two or even more resonances but this subject will not be taken up at the present time.

In addition to the above assumption, it will be assumed that the amplitude of the compound wave function is very large compared with the amplitude of the wave function at places where the particles which form the system are not all close together. The large amplitude of the wave function corresponds to a high probability, i.e., long lifetime of the compound state. It is believed that no other special assumptions are made in the following considerations.

[4] G. Breit, Phys. Rev. **58**, 506, 1068 (1940).

To anticipate the result: the formulae which will be obtained are of a greater "generality" than the customary ones, i.e., they are less definite inasmuch as they involve more parameters. It can be shown, however, by a very simple example, that this is not the result of the insufficiency of the assumptions but that the customary formulae fail to hold even in very simple cases.

The system will always be described with a wave function in ordinary configuration space. Thus complications which may arise from the inclusion of spin variables are not solved although they are touched upon in the last section. More important, the case of light emission cannot be described by a wave function. It is difficult to believe, however, that the formulae to be obtained should not hold also for light (γ-ray) emission and absorption also. This is explicitly demonstrated in the case of resonance scattering where the corresponding process has been treated by means of Dirac's light theory.[5] On the contrary, it is to be expected that the formulae to be obtained can be further specialized in case of light quanta (i.e., some of the parameters set equal to zero) because of the special properties of these "particles": they do not interact with each other and their interaction with nuclear particles can be considered to be "weak." The expectation that the formulae to be obtained can be specialized in the case of light quanta can be confirmed in the case of resonance scattering where a detailed treatment is available. For real reactions, an extension of the present treatment on the basis of Dirac's light theory is desirable.

Mathematically, the present treatment will be the customary one: it will deal only with stationary states, with a constant flux of the incident particles coming in and a constant flux of the reaction products leaving.

II. RESONANCE SCATTERING

In this, as well as in the following sections, the plane wave which describes a collision will be considered to be decomposed into spherical waves. This decomposition, the value of which has been demonstrated by Faxen and Holtsmark, will not be carried out explicitly as it is described

[5] Cf. e.g., V. Weisskopf and E. Wigner, Zeits. f. Physik **63**, 54 (1930); F. Hoyt, Phys. Rev. **36**, 860 (1930).

in standard textbooks. It will be further assumed in this section that the first spherical wave of this decomposition, i.e., the one with zero angular momentum, is responsible for the scattering so that the scattering cross section can be found by investigating the properties of the spherical wave.

When the two particles are far from each other, the wave function has the form

$$\varphi_E = \frac{1}{(4\pi)^{\frac{1}{2}} r u}(e^{-ikr} - U_E e^{ikr})\psi(i). \qquad (1)$$

Herein r is the distance between the colliding particles, u is the square root of their velocity toward each other so that their relative energy is $E=\frac{1}{2}Mu^4$, where M is their relative mass. The first term of (1) corresponds to the incident wave, the second to the scattered wave, k is the wave number $k=Mu^2/h$. The $\psi(i)$ is the normalized, real wave function of the internal coordinates of the two colliding particles. Both waves of (1) are normalized to unit flux so that the conservation law for the number of particles demands $|U_E|=1$. The factor in the bracket of (1) can be written as $-2ie^{i\delta}\sin(kr+\delta)$ so that U_E is, in terms of the "phase shift," equal to $U_E=e^{2i\delta}$. While U_E depends on the energy E with which the particles collide, $\psi(i)$ is independent of E.

If the two particles form a compound nucleus (i.e., in that part of the configuration space which corresponds to all particles being close together), the wave function is in first approximation

$$\varphi_E = \alpha_E \Psi; \qquad (2)$$

Ψ is a normalized wave function involving all the coordinates of the system and is, according to out first assumption, within the energy range considered, independent of E. On the other hand, α_E is independent of the variables of the wave function but a function of the energy: $|\alpha_E|^2$ is of the dimension of a time and can be interpreted as the lifetime of the compound state.

We now lay a sphere around the origin of the coordinate system which corresponds to the coincidence of all particles. The radius of this sphere is as small as possible consistent with the requirement that φ shall have already the form (1) on its surface. We then write down the condition that φ_{E_1} is a state with the energy E_1

$$H\varphi_{E_1} = E_1\varphi_{E_1} \qquad (3)$$

and a similar equation for another energy

$$H\varphi_{E_2} = E_2\varphi_{E_2}. \qquad (3a)$$

In order to simplify the formulae, φ_1 and φ_2 will be written for φ_{E_1} and φ_{E_2} and a similar convention will be adopted with respect to U, and u, k so that the index 1, 2, . . . will stand to indicate the value of the variable E_1, E_2, . . . As customary, we multiply (3) with φ_2^* and the conjugate complex of (3a) with φ_1, and integrate the difference of the resulting equations over the above sphere. All terms corresponding to the interaction of the particles drop out on the left side; those corresponding to the kinetic energy can be transformed by Green's theorem so that

$$-\frac{h^2}{2M}\int(\varphi_2^* \operatorname{grad}\varphi_1 - \varphi_1 \operatorname{grad}\varphi_2^*)_n dS = (E_1-E_2)\int \varphi_1\varphi_2^* dV; \qquad (4)$$

dS denotes integrations over the surface, dV over the volume of "the sphere." The index n denotes the normal component of the vector in parentheses to the surface of integration.

This result appears to contradict our original assumption that φ is, in the region where all particles are close together, independent of the energy. If φ_1 and φ_2 were, apart from a constant, identical within the sphere considered, they would be identical also on the surface of the sphere and the left side of (4) would vanish identically. Actually, (4) corresponds to a one-order higher approximation than an energy independent wave function and can be derived in a more natural way as follows. Let us assume that we know the wave function φ for a certain energy E so that $H\varphi=E\varphi$. We then can try to find the solution of

$$H\varphi_1 = (E+\delta E)\varphi_1 \qquad (5)$$

by a perturbation method. We write $\varphi_1=\varphi+\varphi'$ and assume that φ' satisfies the equation

$$(H-E)\varphi' = \delta E\varphi \qquad (5a)$$

which is obtained from (5) by neglecting the second-order quantity $\delta E\varphi'$. Multiplying (5a) with φ^* and integrating over the above sphere, one has

$$\int \varphi^*(H-E)\varphi' dV = \delta E\int|\varphi|^2 dV. \qquad (6)$$

Since $H-E$ is a Hermitean operator, the first integral would be equal, if it could be extended over the whole space, to $\int[(H-E)\varphi]^*\varphi' dV$ which is zero and one would obtain the paradoxical result that the integral of $|\varphi|^2$ vanishes. It would then follow that (5) has no solution for $\delta E \neq 0$. In our case, the integral over $|\varphi|^2$ diverges if extended over the whole space and the neglect of the $\delta E\varphi'$ term is only justified if the sphere over which the integration is extended is relatively small. For a finite sphere, additional terms will appear if one takes $H-E$ over to the other factor, resulting from the partial integration of the operator of the kinetic energy. One has, as a result,

$$-\frac{\hbar^2}{2M}\int(\varphi^* \operatorname{grad}\varphi' - \varphi' \operatorname{grad}\varphi^*)dS = \delta E\int|\varphi|^2 dV. \quad (6a)$$

This equation will remain valid if one replaces in it φ' by $\varphi_1=\varphi+\varphi'$ and is then identical with (4). One sees that the algebra leading to (4) is only a simplified method for deriving the variation of $\operatorname{grad}\varphi/\varphi$ with energy. If one were to apply literally the condition of the independence of φ from energy, $\operatorname{grad}\varphi/\varphi$ would be independent of energy also. This would not prove to be sufficiently accurate.

Introducing (1) for the left side of (4) and neglecting, in the sense of the second assumption of the Introduction, the region where (2) does not hold on the right side, one obtains

$$-\frac{\hbar^2}{2Mu_1u_2}(e^{ik_2a}-U_2^*e^{-ik_2a})ik_1(-e^{-ik_1a}-U_1e^{ik_1a}) + \frac{\hbar^2}{2Mu_1u_2}(e^{-ik_1a}-U_1e^{ik_1a})ik_2(e^{ik_2a}+U_2^*e^{-ik_2a}) = (E_1-E_2)\alpha_1\alpha_2^*; \quad (7)$$

a is the distance of the colliding particles corresponding to the surface of the sphere in configuration space over which we carried out the integration. Derivations similar to that leading to (7) have been described so often that it was not considered worth while to go into more detail in the present case.

There is an alternative way of deriving (7) which involves, perhaps, more algebra but which shows more clearly the fundamental nature of this equation. This is based on the consideration of the wave function

$$\varphi_1\exp(-iE_1t/\hbar)+\varphi_2\exp(-iE_2t/\hbar),$$

which is a non-stationary solution of Schroedinger's time dependent equation. If one calculates the current which flows into a sphere of radius a, one finds (assuming $|U_1|=|U_2|=1$) that this is a periodic function of time and contains terms proportional to $\exp[i(E_2-E_1)t/\hbar]$ and $\exp[i(E_1-E_2)t/\hbar]$. The average value of this current vanishes, as it must. However, there is a periodically changing flow into the sphere and out of it so that the probability of r having a value below a also shows periodic fluctuations with time and contains terms proportional to the above exponentials. The probability in question is, however,

$$|\alpha_1\exp[-iE_1t/\hbar]+\alpha_2\exp[-iE_2t/\hbar]|^2 = |\alpha_1|^2+|\alpha_2|^2+\alpha_1\alpha_2^*\exp[i(E_2-E_1)t/\hbar] + \alpha_1^*\alpha_2\exp[i(E_1-E_2)t/\hbar].$$

Hence $\alpha_1\alpha_2^*$ must be equal to the time integral of the term in the current which is proportional to $\exp[i(E_2-E_1)t/\hbar]$, and this gives Eq. (7). Comparison of the coefficients of the terms proportional to $\exp[i(E_1-E_2)t/\hbar]$ in the last expression and in the integrated current gives the conjugate imaginary to (7). Equation (22) can be derived in a similar way.

If the ka in (7) can be assumed to be small, (7) becomes ($k=Mu^2/\hbar$),

$$\frac{u_1}{u_2}(1+U_1)(1-U_2^*)+\frac{u_2}{u_1}(1-U_1)(1+U_2^*) = \frac{2}{i\hbar}(E_1-E_2)\alpha_1\alpha_2^*. \quad (8)$$

If ka is not small, (8) will still be valid if one substitutes

$$\begin{aligned} U_1&=\bar{U}_1\exp(-2ik_1a);\\ U_2^*&=\bar{U}_2^*\exp(2ik_2a);\\ \alpha_1&=\bar{\alpha}_1\exp(-ik_1a);\\ \alpha_2^*&=\bar{\alpha}_2^*\exp(ik_2a). \end{aligned} \quad (8a)$$

Equation (8) holds for the barred quantities if (7) applies for the unbarred ones. However, the bar will be left off in the following. Evidently, the unbarred quantities, being defined by (1),

are independent of a while the barred quantities are not. On the other hand, Eq. (7) which holds for the unbarred quantities contains a, Eq. (8) which holds for the barred quantities, does not contain a. This somewhat paradoxical situation is partly caused by the approximate nature of these equations. For most of the present paper, the difference between the two kinds of quantities is negligible.

Incidentally, setting $E_1=E_2$ gives, because of $u_1=u_2$, $U_1=U_2$, the equation

$$U_1U_1^*=|U_1|^2=1, \tag{8b}$$

i.e., the conservation law of particles.

The reality condition can be obtained by observing that the conjugate complex of φ_E must be, apart from a constant, equal to φ_E. Since $\psi(i)$ is real, this constant is $-U_E^*$. Hence $\alpha_E^*\Psi^*=-U_E^*\alpha_E\Psi$. This shows that Ψ can be chosen to be real and that, if this is done

$$\alpha_E^*=-U_E^*\alpha_E;\ \alpha_E=-U_E\alpha_E^*. \tag{9}$$

This equation remains unchanged if one replaces the unbarred quantities, for which it is derived, by the barred ones.

Equations (8) are ∞^2 equation for the 2∞ quantities U and α. In order to solve them, one can make the substitution

$$U=\frac{1+ivS}{1-ivS},\quad vS=i\frac{1-U}{1+U}; \tag{10}$$

S will be, of course, just as U is, a function of the energy and velocity. Since the absolute value of U is 1, the S becomes real. Its physical interpretation is that, if multiplied with v, it should give the tangent of the phase shift. The dimension of hS/M is that of a length which will be closely related by (16) to the scattering radius of the colliding particles.

Since the U of (10) is a barred quantity, the S defined by it is also a barred quantity. Hence the above relation for the tangent of the phase shift is only approximate. It should be replaced by the following relation for the square of the sine of the phase shift (which is a more important quantity),

$$\sin^2\delta=\tfrac{1}{4}(2-e^{2i\delta}-e^{-2i\delta})=\tfrac{1}{4}(2-\bar{U}e^{-2ika}-\bar{U}^*e^{2ika}).$$

Substituting for $\bar{U}$ the expression (10) with barred $\bar{S}$, one has

$$\sin^2\delta=\frac{1}{4}\left[2-\frac{1+iv\bar{S}}{1-iv\bar{S}}e^{-2ika}-\frac{1-iv\bar{S}}{1+iv\bar{S}}e^{2ika}\right]$$
$$=\frac{(v\bar{S}\cos ka-\sin ka)^2}{1+v^2\bar{S}^2}. \tag{10a}$$

For small ka, one can write for this

$$\sin^2\delta=\frac{(vS)^2}{1+v^2S^2}, \tag{10b}$$

where

$$S=\bar{S}\cos ka-v^{-1}\sin ka\sim\bar{S}-Ma/\hbar. \tag{10c}$$

One can easily convince oneself that the error made by replacing the denominator of (10a) by the denominator of (10b) is small both if vS is small compared to 1 and also if it is large.

One now divides (8) by $-iu_1(1+U_1)(1+U_2^*)u_2$ to obtain with $u_1^2=v_1$; $u_2^2=v_2$

$$-S_2+S_1=\frac{2}{\hbar}(E_1-E_2)\frac{\alpha_1}{u_1(1+U_1)}\frac{\alpha_2^*}{u_2(1+U_2^*)}. \tag{11}$$

The left side of this is evidently real. It follows that the phase factor ω of

$$\frac{\alpha_1}{u_1(1+U_1)}=b_1\omega \tag{11a}$$

is independent of energy, b_1 being real. This, combined with (9), shows that $\omega=\pm i$. One can assume $\omega=i$, since the sign of b is still at our disposal. Introducing now (11a) into (11)

$$S_1-S_2=(2/\hbar)(E_1-E_2)b_1b_2. \tag{12}$$

If one writes down this equation for the pairs of energy values E_3, E_2 and E_1, E_3, instead of E_2, E_1 and adds the three equations thus obtained, the left side will vanish and one obtains

$$(E_2-E_1)b_1b_2+(E_3-E_2)b_2b_3$$
$$+(E_1-E_3)b_1b_3=0 \tag{13}$$

or

$$b_1=\frac{(E_2-E_3)b_2b_3}{E_1(b_3-b_2)+E_2b_2-E_3b_3}. \tag{13a}$$

The same equation, with the same coefficients, will be obtained if one substitutes b_4, b_5, etc. for b_1 and E_4, E_5, etc. for E_1. This shows that

$$b_1=\frac{\frac{1}{2}\hbar b}{E_1-E_0} \tag{13b}$$

in which the real b and E_0 are independent of energy. Re-introducing this into (12)

$$S_1-S_2=\tfrac{1}{2}\hbar b^2\frac{E_1-E_2}{(E_1-E_0)(E_2-E_0)}$$

$$=\tfrac{1}{2}\hbar b^2\left(-\frac{1}{E_1-E_0}+\frac{1}{E_2-E_0}\right). \quad (14)$$

Hence

$$S_1=-\frac{\tfrac{1}{2}\hbar b^2}{E_1-E_0}+S_\infty \quad (14a)$$

where again S_∞ is independent of E_1. This gives, finally, with (10)

$$U_1=\frac{(1+iv_1S_\infty)(E_1-E_0)-\tfrac{1}{2}ihb^2v_1}{(1-iv_1S_\infty)(E_1-E_0)+\tfrac{1}{2}ihb^2v_1}, \quad (15)$$

and with (11)

$$\alpha_1=\frac{hibu_1}{(1-iv_1S_\infty)(E_1-E_0)+\tfrac{1}{2}ihb^2v_1}. \quad (15a)$$

The S_1 of (14a) is, strictly speaking, a barred quantity. However, if ka is small, (10c) shows that the unbarred S differs from it only by the constant amount Ma/h which can be absorbed into the S_∞. If ka is large, its energy dependence, as well as that of v, becomes negligible. The U of (15) then becomes the ratio of two linear functions of E which retains its form even if multiplied by e^{-2ika}. One can therefore write for the scattering cross section

$$\sigma(E)=\frac{4\pi}{k^2}\sin^2\delta=\frac{\pi}{k^2}(2-U-U^*)=\frac{4\pi(hS/M)^2}{v^2S^2+1}$$

$$=\frac{4\pi h^2}{M^2}\frac{(S_\infty(E-E_0)-\tfrac{1}{2}hb^2)^2}{(S_\infty(E-E_0)-\tfrac{1}{2}hb^2)^2v^2+(E-E_0)^2}. \quad (16)$$

This goes over into the formula that one would expect

$$\sigma(E)=\frac{\pi}{k^2}\frac{\Gamma^2}{\tfrac{1}{4}\Gamma^2+(E-E_0)^2}, \quad (16a)$$

if $S_\infty=0$, $\Gamma=\hbar b^2v$. The Γ is proportional to v which is an important feature of the resonance formula. Since Γ is[5] h divided by the mean lifetime τ of the compound state, $1/b^2$ can be interpreted as the average distance $l=v\tau$ which the escaping particle could cover during the lifetime of the compound state $l=v\tau=v\hbar/\Gamma=1/b^2$. Inserting for Γ the experimentally observed neutron widths in the n,γ processes, one finds that l is usually more than a million times greater than the nuclear radius.

One may suspect, first, that the occurence of an additional constant S_∞ in (16) is caused by the inadequacy of the two assumptions made in the introduction. It can be shown, however, by means of a simple example[1] that (16) is correct and that its S_∞ does not vanish in general. Another evidence is the simple formula for the proton-neutron scattering. This is obtained from (16) by setting $b=0$ and $\frac{1}{2}M/S_\infty^2$ equal to the binding energy of the deuteron. It corresponds, therefore, to a special case of (16), which is different from (16a), showing that the latter cannot be the generally valid formula. (When comparing (16) with the simple proton-neutron scattering formula, one has to remember that M in (16) is the relative mass of proton and neutron, i.e., half the proton mass, and that E is the energy in the center of mass coordinate system, i.e., half the neutron energy in the laboratory coordinate system.)

There is a way of writing (16) which has the appearance of a resonance formula even if S_∞ does not vanish:

$$\sigma(E)=\frac{\pi}{k^2}\left\{\frac{4S_\infty^2v^2}{1+S_\infty^2v^2}\right.$$

$$\left.+\frac{\Gamma^2-4\Gamma S_\infty v(E-E_0)/(1+S_\infty^2v^2)}{\tfrac{1}{4}\Gamma^2+(E-E_0-\tfrac{1}{2}\Gamma S_\infty v)^2}\right\}, \quad (17)$$

$$\Gamma=\hbar b^2v/(1+S_\infty^2v^2). \quad (17a)$$

In (17) the first term can be called potential scattering; the second term is then the sum of the resonance scattering and of the interference between resonance scattering and potential scattering. Equation (17) may appear quite artificial. However, the general case of resonance reactions naturally leads to an Eq. (45a) of this kind. Clearly, once one admits energy or velocity dependent Γ and resonance energies, (16) can be written in numerous ways, the plain fact being that the ordinary resonance formula (in which Γ and E_0 are independent of energy) does not hold in this case.

III. RESONANCE REACTIONS WITH ZERO ANGULAR MOMENTUM

The treatment of the resonance reactions differs from the treatment of the resonance scattering mainly because it is necessary to take the different modes of disintegration into account. Strictly speaking, this is necessary also in the case of resonance scattering, and it was avoided in the above treatment only by tacitly assuming that the colliding particles had no spin and that their relative angular momentum was zero. Neither of these assumptions is justified in general although they may be valid under certain conditions; the latter assumption particularly at low velocities and for uncharged particles. It will be adopted also in the present section. However, the cases in which one can disregard the possibility of a nuclear reaction are so rare that the separate consideration of the resonance scattering which was carried out above must be regarded as largely schematic.

According to our assumptions, if the integrals of motion are given, the wave function is, apart from a constant factor, uniquely determined in the region of the configuration space in which all particles are close together. This, however, does not hold for the asymptotic behavior of the wave function, at distant parts of the configuration space. There, the wave function will in general contain both incoming and outgoing waves corresponding to the several possible modes of disintegration or reaction, e.g., both an incoming and an outgoing wave corresponding to the reactions of or into ${}_3Li^7+{}_2He^4$, ${}_4Be^9+D$, etc. These different possibilities will be distinguished by indices, j, l, etc. In order to specify a stationary state one can stipulate that it contains an incoming wave only of the variety, say, l. The corresponding wave function φ_l may be called the l wave. Its form outside a sphere in the configuration space can be written as

$$\varphi_l=\sum_j (4\pi)^{-\frac{1}{2}}(r_j u_j)^{-1}$$

$$\times(\exp(-ik_j r_j)\delta_{lj}-U_{lj}\exp(ik_j r_j))\psi_j(i_j). \quad (18)$$

In this $\psi_j(i_j)$ is the product of the real normalized wave functions of the two constituents which correspond to the jth type of disintegration, r_j is the distance between these two constituents, u_j the square root of their relative velocity, and k_j the corresponding wave number $k_j=M_j v_j/\hbar=M_j u_j^2/\hbar$ where M_j is the relative mass of the two constituents in the jth type of disintegration. The first term of the bracket corresponds to approaching particles, the δ_{lj} indicates that, in the wave φ_l, only the constituents of the type l do approach each other. The second term in the bracket corresponds to the products of the reaction or, for $j=l$, to scattered particles of the original kind. The U_{lj} are elements of the "collision matrix" introduced by J. A. Wheeler.[6] It is a set of n^2 constants if the number of possible disintegrations is n. The quantity $|U_{lj}|^2$ is the probability of a reaction, yielding the jth type of constituents, if originally the lth type of constituents are present. In (18) u_j, k_j, U_{lj} depend on the energy, $\psi_j(i_j)$ does not.

While (18) is supposed to represent φ_j outside the sphere of interaction of the particles, if all the particles are close, it will be assumed that φ_j has in first approximation the form

$$\varphi_j=\alpha_j\Psi. \quad (19)$$

As in (2), α_j is a function of energy, Ψ is the normalized wave function of the compound state and is, in first approximation, independent of energy. In order to express the energy dependence of the quantities u_j, k_j, U_{lj}, α_j, an additional index will be given to them, 1, 2, 3, . . . indicating that they are coefficients in the expressions (18) or (19) for a φ which corresponds to the values of the energy E_1, E_2, E_3, etc. The matrix $||U_{lj}||$ will also be denoted by $\mathfrak{U}$; if it occurs in the expression for φ_1 with the energy E_1 it will be denoted by $\mathfrak{U}_1$. The quantities α_j, α_l, . . . will be considered to form a vector $\mathfrak{a}$ with n components; if they occur in the expansion of φ_1 with the energy E_1, the vector will be called $\mathfrak{a}_1$, etc. In addition, a real positive diagonal matrix $\mathfrak{u}$ will be defined, its diagonal elements are the u_j, u_l, etc., which are the square roots of the relative velocities of the particles in the different modes of disintegration. The significance of the diagonal matrices $\mathfrak{u}_1$, $\mathfrak{u}_2$, . . . etc., will be clear from the preceding.

We now go over to deriving an equation which is analogous to (6). For this purpose we write

[6] J. A. Wheeler, Phys. Rev. **52**, 1107 (1937); W. Heisenberg, Zeits. f. Physik **120**, 513,-673 (1943).

down the two equations

$$H\varphi_{1m}=E_1\varphi_{1m}, \tag{20a}$$

$$H\varphi_{2l}=E_2\varphi_{2l}. \tag{20b}$$

We multiply again (20a) with φ_{2l}^*, the conjugate complex of (20b) with φ_{1j}, subtract the resulting equations and integrate over the sphere which corresponds to all the particles being close together. This gives, after a partial integration, an equation analogous to (4), except that φ_2 is replaced by φ_{2l} and φ_1 by φ_{1m}. On the left side, in the surface integral, (18) will be substituted for φ; in the volume integral (19). Again, no details of the calculation will be given since it is a repetition of a transformation which is carried out several times in any book on quantum mechanics. One obtains

$$\sum_j -(\hbar^2/2M_j u_{1j}u_{2j})(\exp(ik_{2j}a_j)\delta_{lj}-U_{2lj}^*\exp(-ik_{2j}a_j))ik_{1j}(-\exp(-ik_{1j}a_j)\delta_{mj}-U_{1mj}\exp(ik_{1j}a_j))$$
$$+\sum_j(\hbar^2/2M_j u_{1j}u_{2j})(\exp(-ik_{1j}a_j)\delta_{mj}-U_{1mj}\exp(ik_{1j}a_j))ik_{2j}(\exp(ik_{2j}a_j)\delta_{lj}+U_{2lj}^*\exp(-ik_{2j}a_j))$$
$$=(E_1-E_2)\alpha_{1m}\alpha_{2l}^*. \tag{21}$$

In deriving (21) it is necessary to observe that terms with $\psi_j(i_j)$ and $\psi_{j'}(i_{j'})$ are orthogonal on the surface of the sphere if $j\neq j'$ because some of the particles, which are close in the term of ψ_j, are separated into different constituents in the term with $\psi_{j'}$ so that the integral over the product of ψ_j and $\psi_{j'}$ vanishes. This reduces the double sum which should be on the left side of (21) to a single sum and in fact eliminates any integrals from it since the integral of $|\psi_j(i_j)|^2$ is 1. In (21), a_j is the distance between the jth constituents on the surface of the sphere.

If we again assume, as we did in the case of resonance scattering, that the ka are small and introduce $k_j=M_j u_j^2/\hbar$, (21) can be written in the form

$$\sum_j hi(\delta_{mj}+U_{1mj})u_{1j}u_{2j}^{-1}(\delta_{lj}-U_{2lj}^*)$$
$$+hi(\delta_{mj}-U_{1mj})u_{1j}^{-1}u_{2j}(\delta_{lj}+U_{2lj}^*)$$
$$=2(E_1-E_2)\alpha_{1m}\alpha_{2l}^*. \tag{22}$$

This can be written with the notation explained above in the matrix form

$$hi(1+\mathfrak{U}_1)\mathfrak{u}_1\mathfrak{u}_2^{-1}(1-\mathfrak{U}_2^\dagger)$$
$$+hi(1-\mathfrak{U}_1)\mathfrak{u}_1^{-1}\mathfrak{u}_2(1+\mathfrak{U}_2^\dagger)$$
$$=2(E_1-E_2)\mathfrak{A}_{12}, \tag{23}$$

where

$$(\mathfrak{A}_{12})_{ml}=\alpha_{1m}\alpha_{2l}^* \quad\text{and}\quad \mathfrak{1}_{ml}=\delta_{ml}; \tag{23a}$$

(23) is the generalization of (8) for resonance reactions. It will serve as a basis for most of the remainder of this work. It embodies the second approximation for the change of the wave function of the compound nucleus with energy. In the first approximation, this wave function was independent of energy. The relation of the second approximation to the first one was explained more fully through Eqs. (5) to (6a).

Setting $E_1=E_2$, it follows that $\mathfrak{u}_1=\mathfrak{u}_2$, $\mathfrak{U}_1=\mathfrak{U}_2$; and we have

$$(1+\mathfrak{U}_1)(1-\mathfrak{U}_1^\dagger)+(1-\mathfrak{U}_1)(1+\mathfrak{U}_1^\dagger)$$
$$=2-2\mathfrak{U}_1\mathfrak{U}_1^\dagger=0, \tag{24}$$

i.e., that the $\mathfrak{U}$ are unitary. This can be derived in the same way even if the assumptions in the introduction are not made. It corresponds to the conservation law for the number of systems[6] and has the same role which $U=1$ had in the case of resonance scattering.

If (18), (19) represent a solution, this also holds for their conjugate imaginary. In this conjugate imaginary, the second term in the bracket of (18) represents the incoming waves. Hence the conjugate imaginary is equal to

$$\varphi_l^*=-\sum_j U_{lj}^*\varphi_j. \tag{25}$$

Since the incoming waves of the right side of (25) are the same as on the left side, the two sides must be equal. It then follows, first, that the outgoing wave corresponding to the mth constituent is also the same

$$(4\pi)^{-\frac{1}{2}}(r_m u_m)^{-1}\exp(ik_m r_m)\delta_{ml}$$
$$=-\sum_j U_{lj}^*(4\pi)^{-\frac{1}{2}}(r_m u_m)^{-1}U_{jm}\exp(ik_m r_m)$$

or that

$$\delta_{ml}=\sum_j U_{lj}^*U_{jm};\quad \mathfrak{U}^*\mathfrak{U}=1. \tag{26}$$

This, together with $\mathfrak{U}\mathfrak{U}^\dagger=\mathfrak{U}^\dagger\mathfrak{U}=1$ of (24b)

shows that $\mathfrak{U}^*=\mathfrak{U}$ or $\mathfrak{U}=\mathfrak{U}'$, i.e., that $\mathfrak{U}$ is symmetric. This is again known[6] to hold independently of the assumptions made in the introduction.

It follows from (25) also that the wave functions of both sides of (25) are the same in the region of the configuration space where all particles are close together. This gives, with (19)

$$\alpha_l^*\Psi^*=-\sum_j U_{lj}^*\alpha_j\Psi. \tag{27}$$

It follows from (27), first, that Ψ^* is, apart from a constant factor, equal to Ψ so that it can be made real by multiplication with a constant of unit absolute value. Since such a constant was left free when Ψ was defined, we can assume that Ψ is real and write instead of (27)

$$\alpha_l^*=-\sum_j U_{lj}^*\alpha_j;\quad \alpha_l=-\sum_j U_{lj}\alpha_j^*. \tag{27a}$$

In the matrix-vector notation explained above this reads

$$\boldsymbol{\alpha}_1^*=-\mathfrak{U}_1^*\boldsymbol{\alpha}_1;\quad \boldsymbol{\alpha}_1=-\mathfrak{U}_1\boldsymbol{\alpha}_1^*; \tag{27b}$$

(27b) is the generalization of (9) for resonance reactions and will play a role similar to that of (9).

The above derivations were abbreviated but it is believed that further details would make them more cumbersome without elucidating the situation very much more.

IV. SOLUTION OF EQUATIONS (23), (27b)

We introduce a quantity similar to the S of (10) by the equations

$$\mathfrak{U}_1=\frac{1+i\mathfrak{u}_1\mathfrak{S}_1\mathfrak{u}_1}{1-i\mathfrak{u}_1\mathfrak{S}_1\mathfrak{u}_1};\quad \mathfrak{u}_1\mathfrak{S}_1\mathfrak{u}_1=i\frac{1-\mathfrak{U}_1}{1+\mathfrak{U}_1}. \tag{28}$$

The $\mathfrak{S}$ are now matrices just as the $\mathfrak{U}$ are and have the same number of rows and columns as the latter. Each row and column corresponds to a particular mode of disintegration of the compound nucleus. The $\mathfrak{u}$ are diagonal matrices, the diagonal elements, which are functions of energy, are the square roots of the velocities with which the particles collide. The $\mathfrak{S}$ are symmetric because the $\mathfrak{U}$ are, and they are hermitian because the $\mathfrak{U}$ are unitary. They are, therefore, real, symmetric matrices

$$\mathfrak{S}_1=\mathfrak{S}_1^*=\mathfrak{S}_1'=\mathfrak{S}_1^\dagger. \tag{28a}$$

Introducing (28) into (23) and multiplying the resulting equation with $\mathfrak{u}_1^{-1}(1-i\mathfrak{u}_1\mathfrak{S}_1\mathfrak{u}_1)$ from the left, $(1+i\mathfrak{u}_2\mathfrak{S}_2\mathfrak{u}_2)\mathfrak{u}_2^{-1}$ from the right, one obtains

$$-\mathfrak{S}_2+\mathfrak{S}_1=(2\hbar)^{-1}(E_1-E_2)\mathfrak{u}_1^{-1}(1-i\mathfrak{u}_1\mathfrak{S}_1\mathfrak{u}_1)\mathfrak{A}_{12}(1+i\mathfrak{u}_2\mathfrak{S}_2\mathfrak{u}_2)\mathfrak{u}_2^{-1}=2\hbar^{-1}(E_1-E_2)\mathfrak{B}_{12}. \tag{29}$$

The last part of (29) is the definition of $\mathfrak{B}_{12}$. One obtains for the matrix elements of $\mathfrak{B}_{12}$ in a straightforward way with the help of (23a)

$$(\mathfrak{B}_{12})_{ml}=\beta_{1m}\beta_{2l}^*, \tag{27a}$$

where

$$\beta_{1m}=\tfrac{1}{2}\sum u_{1m}^{-1}(1-i\mathfrak{u}_1\mathfrak{S}_1\mathfrak{u}_1)_{mk}\alpha_{1k}$$

so that the vector $\boldsymbol{\beta}$ is defined by

$$\boldsymbol{\beta}_1=\tfrac{1}{2}\mathfrak{u}_1^{-1}(1-i\mathfrak{u}_1\mathfrak{S}_1\mathfrak{u}_1)\boldsymbol{\alpha}_1. \tag{29b}$$

It follows from (29) that $\mathfrak{B}_{12}$ must be real and symmetric. It is a consequence of the former property (i.e., that all $\beta_{1m}\beta_{2l}^*$ are real) that the phase factor of all the β_{1m} is the same, independent of m and the energy E_1 to which they refer. It follows from the symmetry of $\mathfrak{B}$ that $\beta_{1m}\beta_{2l}^*=\beta_{1l}\beta_{2m}^*$ or $\beta_{1m}/\beta_{1l}=\beta_{2m}^*/\beta_{2l}^*$. This is equivalent with the statement that all vectors $\boldsymbol{\beta}$ are multiples of a common vector

$$\boldsymbol{\beta}_1=b_1\omega\boldsymbol{\beta}\ (b_1 \text{ real}), \tag{30}$$

where b_1 is a real number, depending on energy, while the number ω and the vector $\boldsymbol{\beta}$ are independent of energy. ω has the absolute value 1, the $\boldsymbol{\beta}$ is real and we can assume it to be normalized

$$(\boldsymbol{\beta},\boldsymbol{\beta})=\sum\beta_j^2=1\ (\boldsymbol{\beta}\text{ real}). \tag{30a}$$

Equation (27b) also can be written in terms of $\mathfrak{S}$

$$(1+i\mathfrak{u}_1\mathfrak{S}_1\mathfrak{u}_1)\boldsymbol{\alpha}_1^*=-(1-i\mathfrak{u}_1\mathfrak{S}_1\mathfrak{u}_1)\boldsymbol{\alpha}_1; \tag{31}$$

comparing this with (29b) one obtains $\mathfrak{u}_1\boldsymbol{\beta}_1^*=-\mathfrak{u}_1\boldsymbol{\beta}_1$ or with (30) that $\omega=\pm i$. One can assume $\omega=i$ since the sign of the vector $\boldsymbol{\beta}$ remained undetermined so far. Uniting these equations, we can write

$$\boldsymbol{\alpha}_1=2ib_1(1-i\mathfrak{u}_1\mathfrak{S}_1\mathfrak{u}_1)^{-1}\mathfrak{u}_1\boldsymbol{\beta} \tag{32}$$

and[7]

$$\mathfrak{B}_{12}=b_1b_2\mathfrak{B};\ \mathfrak{B}_{ml}=\beta_m\beta_l;\ \mathfrak{B}=\mathfrak{B}^2=\mathfrak{B}^3=\cdots. \tag{32a}$$

[7] The mathematicians call matrices which are equal to their powers idempotents. $\mathfrak{A}$ and, later, $\mathfrak{B}$ are idempotents of rank 1. $\mathfrak{A}$ (and $\mathfrak{B}$) transform every vector into a vector of a definite direction which is, in the case of $\mathfrak{A}$, the direc-

This last result enables one to determine the $\mathfrak{S}$. One sees from (29) that $\mathfrak{S}_1$ must have the form

$$\mathfrak{S}_1=\mathfrak{S}_\infty-c_1\mathfrak{B}, \tag{32b}$$

where c_1 is a so far unknown real function of E_1 while the real symmetric matrix $\mathfrak{S}_\infty$ is independent from E_1.

Introducing now (32b) into (29), one obtains

$$-c_1+c_2=2\hbar^{-1}(E_1-E_2)b_1b_2. \tag{33}$$

If one writes down this equation for the pairs E_2, E_3 and E_3, E_1 instead of E_1, E_2 and adds the three resulting equations, the c's drop out and one obtains

$$[(E_1-E_2)b_2+(E_3-E_1)b_3]b_1=(E_3-E_2)b_2b_3.$$

This shows in the same way as was explained after (13) that $1/b_1$ is a linear function of the energy E_1 so that one can write

$$b_1=\frac{\frac{1}{2}\hbar b}{(E_1-E_0)} \quad (b, E_0 \text{ real}). \tag{34}$$

This gives with (33)

$$-c_1+c_2=\tfrac{1}{2}\hbar b^2\frac{(E_1-E_2)}{(E_1-E_0)(E_2-E_0)}$$

$$=\tfrac{1}{2}\hbar b^2\left(-\frac{1}{E_1-E_0}+\frac{1}{E_2-E_0}\right); \tag{35}$$

from this we have

$$c_1=\frac{\frac{1}{2}\hbar b^2}{E_1-E_0}+c_\infty. \tag{35a}$$

One can redefine S_∞ of (32b) by decreasing it by $c_\infty\mathfrak{B}$. As a result, the last term in (32b) will also have to be decreased by $c_\infty\mathfrak{B}$ or c_1 by c_∞. One sees that $c_\infty=0$ can be written without loss of generality. As a result, we have

$$\mathfrak{S}_1=\mathfrak{S}_\infty-\frac{\frac{1}{2}\hbar b^2}{E_1-E_0}\mathfrak{B} \tag{36}$$

so that the matrix $\mathfrak{S}_\infty$ which was introduced in (32b) merely as an energy independent matrix, becomes equal to $\mathfrak{S}_1$ for $E_1=\infty$. Equation (32) and (34) now give

$$\alpha_1=\frac{i\hbar b}{E_1-E_0}(1-i\mathfrak{u}_1\mathfrak{S}_1\mathfrak{u}_1)^{-1}\mathfrak{u}_1\beta. \tag{37}$$

In these, E_0 and b are arbitrary real numbers, β an arbitrary real vector of length 1, $\mathfrak{S}_\infty$ an arbitrary real symmetric matrix and

$$\mathfrak{B}_{jl}=\beta_j\beta_l;\ \mathfrak{B}=\mathfrak{B}^2=\mathfrak{B}^3=\cdots. \tag{36a}$$

All these quantities are independent of energy. For $\mathfrak{U}$ one has

$$\begin{aligned}\mathfrak{U}&=(1+i\mathfrak{u}_1\mathfrak{S}_\infty\mathfrak{u}_1-\tfrac{1}{2}i\hbar b^2(E_1-E_0)^{-1}\mathfrak{u}_1\mathfrak{B}\mathfrak{u}_1)\\&\quad\times(1-i\mathfrak{u}_1\mathfrak{S}_\infty\mathfrak{u}_1+\tfrac{1}{2}i\hbar b^2(E_1-E_0)^{-1}\mathfrak{u}_1\mathfrak{B}\mathfrak{u}_1)^{-1}\\&=[(1+i\mathfrak{u}_1\mathfrak{S}_\infty\mathfrak{u}_1)(E_1-E_0)-\tfrac{1}{2}i\hbar b^2\mathfrak{u}_1\mathfrak{B}\mathfrak{u}_1]\\&\quad\times[(1-i\mathfrak{u}_1\mathfrak{S}_\infty\mathfrak{u}_1)(E_1-E_0)\\&\qquad+\tfrac{1}{2}i\hbar b^2\mathfrak{u}_1\mathfrak{B}\mathfrak{u}_1]^{-1}.\end{aligned} \tag{38}$$

One can easily verify that the $\mathfrak{U}$ given by (38), together with the α given by (37) and (36), actually satisfy (24) and (27b). The reader will recognize that the derivation of this section, and indeed the result (38), is very closely patterned on the derivation of the similar formula (15) for resonance scattering. The only difference, as far as the result is concerned, is first that $\mathfrak{S}_\infty$ of (38) is an arbitrary real symmetric matrix rather than an arbitrary real number and, second, that the b^2 of (15) is replaced by $b^2\mathfrak{B}$ where $\mathfrak{B}$ is the matrix defined in (36a). In spite of these apparently minor differences, the calculation of the scattering and reaction cross sections from (38) (or (36)) in their general form is less immediate than the calculation of the former was from (15). Indeed, even the transformation of (38) into a form more suggestive of the resonance formula

$$\mathfrak{U}=\frac{1+i\mathfrak{u}\mathfrak{S}_\infty\mathfrak{u}}{1-i\mathfrak{u}\mathfrak{S}_\infty\mathfrak{u}}-\frac{i\hbar b^2}{E-E_0+\frac{1}{2}i\lambda}(1-i\mathfrak{u}\mathfrak{S}_\infty\mathfrak{u})^{-1}\times\mathfrak{u}\mathfrak{B}\mathfrak{u}(1-i\mathfrak{u}\mathfrak{S}_\infty\mathfrak{u})^{-1}, \tag{39}$$

$$\lambda=\hbar b^2\sum_{jl}\beta_j\mathfrak{u}_j(1-i\mathfrak{u}\mathfrak{S}_\infty\mathfrak{u})^{-1}_{jl}\mathfrak{u}_l\beta_l, \tag{39a}$$

$$\alpha=\frac{i\hbar b}{E-E_0+\frac{1}{2}i\lambda}(1-i\mathfrak{u}\mathfrak{S}_\infty\mathfrak{u})^{-1}\mathfrak{u}\beta, \tag{39b}$$

tion of the vector α. Hence, for every vector $\mathfrak{v}$, the $\mathfrak{A}\mathfrak{v}$ is a constant times α. The length of $\mathfrak{A}\mathfrak{v}$ (and of $\mathfrak{B}\mathfrak{v}$) depends only on the component of $\mathfrak{v}$ in a definite direction which is the direction of α in case of the matrix A. It is evident from this that $\mathfrak{A}\mathfrak{R}\mathfrak{A}$ is, for any matrix $\mathfrak{R}$, a multiple of $\mathfrak{A}$ since it has both the above properties of $\mathfrak{A}$. These remarks are designed to give a better understanding to some of the calculations carried out in the text and the appendix.

is quite cumbersome and will be given only in the appendix.

V. PARTICULAR CASES OF THE COLLISION MATRIX (38) FOR ZERO ANGULAR MOMENTUM

Although (38) is the most general $\mathfrak{U}$ compatible with (23) and (27b), it can be argued that it does not satisfy all conditions set forth in the introduction. It is seen that it goes over, for very large $E-E_0$, into $(1-i\mathfrak{u}\mathfrak{S}_\infty\mathfrak{u})(1+i\mathfrak{u}\mathfrak{S}_\infty\mathfrak{u})^{-1}$ while, according to (37), α goes to zero at the same time. This last fact shows that any reaction or scattering, if present, does not go through the intermediate state if $E-E_0$ is large since in this case the coefficient of Ψ in (19) tends to zero. One can add, therefore, to (23), (27b) the further condition that either $\mathfrak{U}=1$ for $E-E_0$ large, or that $\mathfrak{U}$ become a diagonal matrix in this case. In the former case, which will be taken up first, one stipulates that both reaction and scattering go through the intermediate state Ψ; in the latter case one assumes only that any actual reaction has to go through the intermediate state. It follows from the first, more stringent assumption that $(1+i\mathfrak{u}\mathfrak{S}_\infty\mathfrak{u})(1-i\mathfrak{u}\mathfrak{S}_\infty\mathfrak{u})^{-1}=1$, i.e., $\mathfrak{S}_\infty=0$. The matrix $\mathfrak{U}-1$ then becomes

$$\mathfrak{U}-1=-\frac{ihb^2}{E-E_0+\frac{1}{2}i\lambda}\mathfrak{u}\mathfrak{B}\mathfrak{u}, \tag{40}$$

$$\lambda=hb^2\sum_j v_j\beta_j^2. \tag{40a}$$

The cross section for the transition from the state j to the state l is

$$\sigma_{jl}=\frac{\pi}{k_j^2}|(\mathfrak{U}-1)_{jl}|^2=\frac{\pi}{k_j^2}\frac{h^2b^4(u_j\beta_j\beta_l u_l)^2}{(E-E_0)^2+\frac{1}{4}\lambda^2},$$

$$\sigma_{jl}=\frac{\pi}{k_j^2}\frac{\Gamma_j\Gamma_l}{\frac{1}{4}\Gamma^2+(E-E_0)^2}, \tag{41}$$

where

$$\Gamma_j=hb^2\beta_j^2v_j,\quad \Gamma=\lambda=\sum_j\Gamma_j. \tag{41a}$$

One sees that the more rigorous restriction leads to the ordinary resonance formula just as the similar restriction specialized (16) to (16a). It is worth while to note that Γ_j is again proportional to the velocity with which the constituents of the jth type of particle collide before or separate after the reaction.

It may be remembered that the $1/v$ law of the slow neutron capture is a consequence of this: the $1/k^2$ factor gives proportionality with v^{-2} which multiplied with the Γ_{neutron} gives v^{-1}. Under the more stringent assumption which we consider now, (41) is valid also for scattering and one sees that the scattering cross section should go to zero for large $E-E_0$, i.e., (41) gives only what is usually considered to be the anomalous scattering cross section, but does not give the normal scattering.

The second restriction, the consequences of which one may be interested in, is that the first term of (39) be a diagonal matrix. In this case, $\mathfrak{S}_\infty$ also must be diagonal, its diagonal elements—which must be real—will be denoted by s_j. One obtains from (39)

$$(\mathfrak{U}-1)_{jl}=\frac{2is_jv_j}{1-is_jv_j}\delta_{jl}-\frac{ihb^2}{E-E_0+\frac{1}{2}i\lambda}\times(1-is_jv_j)^{-1}u_j\beta_j\beta_lu_l(1-is_lv_l)^{-1}, \tag{42}$$

$$\lambda=hb^2\sum_j\frac{\beta_j^2v_j}{1-is_jv_j}. \tag{42a}$$

It appears natural to separate real and imaginary parts of λ

$$\lambda=\Gamma+2i\Delta, \tag{43}$$

$$\Gamma=hb^2\sum\frac{\beta_j^2v_j}{1+s_j^2v_j^2};\quad \Delta=\tfrac{1}{2}hb^2\sum\frac{\beta_j^2s_jv_j^2}{1+s_j^2v_j^2}. \tag{43a}$$

Let us first consider the case of nuclear reaction, i.e., $j\neq l$. The first term of (42) then vanishes and we have for the effective cross section of the reaction yielding the particles l from a collision of particles j with the relative velocity v_j and total energy E:

$$\sigma_{jl}=\frac{\pi}{k_j^2}|(\mathfrak{U}-1)_{jl}|^2=\frac{\pi}{k_j^2}\frac{\Gamma_j\Gamma_l}{\frac{1}{4}\Gamma^2+(E-E_0-\Delta)^2};\quad (j\neq l), \tag{44}$$

where now

$$\Gamma_j=\frac{hb^2\beta_j^2v_j}{1+s_j^2v_j^2};\quad \Gamma=\sum_j\Gamma_j. \tag{44a}$$

Equations (44) differ in two ways from Eqs. (41): first, there is an energy shift Δ present in the former, the shift being velocity dependent.

It will appear, however, in the last paragraph of this section that, at least for reactions involving only uncharged particles, Δ is very small even if compared with Γ if v_j corresponds to less than about a million volts. If, on the other hand, v_j corresponds to a high energy, the corresponding term in Δ becomes energy independent so that the occurrence of Δ in the denominator of (44) is without much practical significance. The second difference between (44) and (41) is the definition of Γ_j, the dependence of which on energy became more complicated. However, virtually the same remarks apply as before: if v_j corresponds to a low energy, $v_j s_j \ll 1$, at least for uncharged particles. If the energy corresponding to the jth type of reaction is large, v_j changes so little within the resonance region that $1+s_j^2 v_j^2$ becomes practically independent of energy. As a result, the second, more general, assumption leads in practice to the same energy dependence of the cross section of resonance reactions as the first assumption.

For the scattering cross section, on the other hand, one has after a brief calculation

$$\sigma_{jj}=\frac{\pi}{k_j^2}|(\mathfrak{U}-1)_{jj}|^2=\frac{\pi v_j^2}{k_j^2(1+s_j^2v_j^2)^2}\left|2s_j(1-is_jv_j)-\frac{\hbar b^2\beta_j^2}{E-E_0-\Delta+\frac{1}{2}i\Gamma}\right|^2. \tag{45}$$

Expanding the square, this becomes with (43) and (44a)

$$\sigma_{jj}=\frac{4\pi s_j^2v_j^2}{k_j^2(1+s_j^2v_j^2)}+\frac{\pi}{k_j^2}\frac{\Gamma_j^2}{\frac{1}{4}\Gamma^2+(E-E_0-\Delta)^2}-\frac{4\pi s_j\Gamma_j v_j}{k_j^2(1+s_j^2v_j^2)}\frac{E-E_0-\Delta+\frac{1}{2}s_j\Gamma v_j}{\frac{1}{4}\Gamma^2+(E-E_0-\Delta)^2}. \tag{46}$$

The terms in the first two lines are the squares of the two terms in (45) between the absolute sign.[8] They correspond to ordinary and resonance scattering, respectively. The last term of (46) is the cross product of the two terms between the absolute sign. It corresponds to the interference between ordinary and resonance scattering. One sees from (45) or (46) that the scattering cross section remains finite for $v=0$.

It may be worth while to give a more visualizable interpretation of the quantities occurring in the equations of this section than is provided by the equations themselves and also to give expressions for them in more conventional units.

If one expresses the energy E in electron volts, π/k^2 becomes $(0.65\times10^{-18}/E)$ cm^2 for a particle of the mass of the neutron.

The quantities β_j are dimensionless, as evident from (30a), since the sum of their squares is 1. They serve in our formalism only to subdivide the total level width Γ into partial widths (cf. (41a) and (44a)). In the usual n,γ processes, the β_{neutron} is practically 1 while $\beta_{\text{radiation}}$ is very small, in spite of the $\Gamma_{\text{radiation}}$ being much greater than Γ_{neutron}, because the ratio of the neutron velocity to light velocity is much greater than the ratio of the corresponding Γ. The interpretation of b has been given before: $1/b^2\beta_j^2$ is the average distance which a particle of velocity v_j could cover during the partial lifetime of the compound nucleus for the j type of disintegration. This partial lifetime is defined as the reciprocal disintegration constant of the compound nucleus for the j type of disintegration. It is usual to express Γ_j in electron volts and write for it $\Gamma_j=aE_j^{\frac{1}{2}}$, where E_j is again expressed in electron volts. The $1/b^2\beta_j^2$ then becomes $1/b^2\beta_j^2=3.2\times10^3\ (M_{\text{neutron}}/M_j)^{\frac{1}{2}}a^{-1}(e^2/mc^2)$. Since a is usually less than 10^{-3} for slow neutron processes, one sees that $1/b^2$ is, at least in the case of the n,γ process, more than a million times greater than the electronic radius or the nuclear radius. The $\Gamma_{\text{radiation}}$ is usually of the order of 0.1 ev. As a result, $\beta_{\text{radiation}}$ is, in the slow neutron processes, of the order of one tenth.

The s are the diagonal elements of the matrix $\mathfrak{S}_\infty$ which determines the normal scattering. The dimension of the s is a reciprocal velocity, which is also the dimension of the matrix elements of all S. If we express the normal cross section σ_j for a collision in cm^2, $s_j=\pm13.4\times10^{12}(M_j/M_{\text{neutron}})\sigma_j^{\frac{1}{2}}/c$. Since σ_j is usually a few times 10^{-24} cm^2, $|s_j|$ for particles is of the order of $25/c$. The $s_{\text{radiation}}=0$ because the normal nuclear scattering of γ rays is negligible. It follows that,

[8] H. A. Bethe, Rev. Mod. Phys. 9, §55, 71 (1937) already derived this formula (p. 152) except that the ambiguity of the sign in (45), caused by the ambiguity of the sign of s, has been overlooked.

unless the energy E_j is very high, $s_j v_j \ll 1$, and then from (43a) that $\Delta \ll \Gamma$.

VI. REGION OF VALIDITY OF RESONANCE EQUATIONS

The basis for the equations for resonance scattering was (7) and it will be remembered that this appeared as a second approximation, obtained by replacing φ_1 and φ_2^* in the right side of (4) by $\alpha_1\Psi$ and $\alpha_2^*\Psi$, respectively. Since, as pointed out after (4), φ_1 and φ_2^* cannot be accurately equal to these expressions, one may wonder whether their use for the right side of (4) is justifiable.

Let us assume that, as the energy increases, the phase of U goes through -1 at E_0. Then $U_0 = -1$ holds accurately and we can denote by Ψ the exact expression for φ for $E = E_0$ inside the sphere of radius a defined in Section II. For all other values of the energy, φ will not be exactly a multiple of Ψ but will be, inside the sphere of radius a,

$$\varphi_1 = \alpha_1\Psi + \gamma_1\Psi_1, \tag{47}$$

where Ψ_1 is orthogonal to Ψ and is assumed to be normalized

$$(\Psi_1, \Psi_1) = 1, \ (\Psi_1, \Psi) = 0. \tag{47a}$$

For $E = E_0$, the second term of (47) vanishes, i.e., $\gamma_0 = 0$; α_0 is real because of (9).

Equation (8) now reads for the barred quantities defined in (8a)

$$\frac{u_1}{u_2}(1+U_1)(1-U_2^*) + \frac{u_2}{u_1}(1-U_1)(1+U_2^*) = \frac{2}{ih}(E_1 - E_2)(\alpha_1\alpha_2^* + \gamma_{12}), \tag{48}$$

where

$$\gamma_{12} = \gamma_1\gamma_2^*(\Psi_2, \Psi_1). \tag{48a}$$

If we express the U again by the S by means of (10) this becomes

$$S_1 - S_2 = \frac{E_1 - E_2}{2\hbar u_1 u_2}(1 - iv_1S_1) \times (\alpha_1\alpha_2^* + \gamma_{12})(1 + iv_2S_2). \tag{48b}$$

Since $\gamma_0 = 0$, also $\gamma_{10} = 0$ and one sees from (10) that $S_0 = \infty$. Setting $E_2 = E_0$ in (48b) and equating the coefficients of S_0 on both sides of (48b) gives

$$\alpha_1 = \frac{2ihu_1}{\alpha_0 u_0(1 - iv_1S_1)(E_1 - E_0)}. \tag{49}$$

Re-introducing this and a similar expression for α_2 into (48b) yields

$$S_1 - S_2 = \frac{2\hbar}{\alpha_0^2 v_0}\left(-\frac{1}{E_1 - E_0} + \frac{1}{E_2 - E_0}\right) + \frac{E_1 - E_2}{2\hbar u_1 u_2}(1 - iv_1S_1)\gamma_{12}(1 + iv_2S_2). \tag{50}$$

We can introduce $b^2 = 4/\alpha_0^2 v_0$ in this and obtain

$$S_1 + \frac{\frac{1}{2}\hbar b^2}{E_1 - E_0} = S_2 + \frac{\frac{1}{2}\hbar b^2}{E_2 - E_0} + \frac{E_1 - E_2}{2\hbar}(1 - iv_1S_1)\frac{\gamma_{12}}{u_1 u_2}(1 + iv_2S_2). \tag{50a}$$

It is seen from this equation that the left side would be independent of energy if the last term could be neglected. No approximations were used in Eqs. (47)–(50a). As could have been anticipated, the accuracy of (14) depends on the possibility to neglect γ_{12} or $\gamma_1\gamma_2^*$.

The fact that φ cannot be accurately a multiple of Ψ, i.e., that $\gamma_1 \neq 0$, can be best seen from the fact that the logarithmic derivative of the asymptotic expression (1) for φ is not independent of energy. Since the result obtained in Section II gives at least an approximate expression for φ outside the sphere, one can see what the deviation of the value and gradient of this approximate expression is from the value and gradient of $\alpha\Psi$ which are also given in that section. If the difference between the values of φ and $\alpha\Psi$, as calculated in Section II, has the value δ_1, and if the difference between their derivatives is δ_1', one can assume that γ_1^2 is of the order of magnitude

$$|\gamma_1|^2 \sim (4\pi a^3/3)(\delta_1^2 + a^2\delta_1'^2). \tag{51}$$

This assumes that the discrepancy between the outside and inside solutions obtained in Section II does not get magnified toward the inside of the sphere. It is very likely that such a magnification would occur only in the neighborhood of another resonance.

When calculating δ_1, it is well to remember that the quantities obtained in Section II are

barred quantities from which the unbarred quantities must be first obtained by the Eqs. (8a). One has, therefore,

$$\delta_1=\bar{\alpha}_1\exp(-ik_1a)\Psi(a)$$
$$-\frac{\exp(-ik_1a)-\bar{U}_1\exp(-2ik_1a)\exp(ik_1a)}{(4\pi)^{\frac{1}{2}}u_1a}$$
$$=\exp(-ik_1a)\left(\bar{\alpha}_1\Psi(a)-\frac{1-\bar{U}_1}{(4\pi)^{\frac{1}{2}}u_1a}\right). \quad (52)$$

This is, because of (15), (15a) equal to

$$\frac{i\hbar bu_1\Psi(a)+(2iu_1S_\infty(E_1-E_0)-i\hbar b^2u_1)(4\pi)^{-\frac{1}{2}}a^{-1}}{(1-iv_1S_\infty)(E_1-E_0)+\frac{1}{2}i\hbar b^2v_1}.$$

Since, however, Ψ(a) is accurate for $E_1=E_0$, it must be true that $\Psi(a)=b(4\pi)^{-\frac{1}{2}}a^{-1}$ and we have

$$\delta_1=\frac{\exp(-ik_1a)}{(4\pi)^{\frac{1}{2}}au_1}$$
$$\times\frac{2iv_1S_\infty(E_1-E_0)}{(1-iv_1S_\infty)(E_1-E_0)+\frac{1}{2}i\hbar b^2v_1}. \quad (52a)$$

It is worth noticing that the solution obtained in Section II gives no discontinuity in φ if $S_\infty=0$.

One can calculate δ_1' in a similar way and obtain

$$a\delta_1'=\frac{\exp(-ik_1a)}{(4\pi)^{\frac{1}{2}}au_1}$$
$$\times\frac{(2ik_1a-2iv_1S_\infty)(E_1-E_0)}{(1-iv_1S_\infty)(E_1-E_0)+\frac{1}{2}i\hbar b^2v_1}. \quad (52b)$$

These equations enable us to estimate the last term of (50a). It appears to be an overestimate to write for this term

$$\frac{E_1-E_2}{2\hbar u_1u_2}(1-iv_1S_1)\gamma_1\gamma_2^*(1+iv_2S_2)$$
$$\leq\frac{|E_1-E_2|}{2\hbar u_1u_2}\frac{4\pi}{3}a^3|(1-iv_1S_1)(\delta_1+a\delta_1')$$
$$\times(\delta_2+a\delta_2')(1+iv_2S_2)|$$
$$=\frac{|E_1-E_2|}{2\hbar u_1u_2}\frac{4\pi}{3}a^3\frac{|2ik_1a||2ik_2a|}{4\pi a^2u_1u_2}$$
$$=\frac{2(E_1-E_2)a}{3\hbar v_1v_2}k_1k_2a^2. \quad (53)$$

Strictly speaking $|\delta_1|+a|\delta_1'|$ and $|\delta_2|+a|\delta_2'|$ should stand in the second line of (53) which gives the result obtained in (53) only if $k_1a>v_1S_\infty$. Otherwise, the last term of (50a) can be estimated to be

$$\frac{2(E_1-E_2)a}{3\hbar}S_\infty^2. \quad (53a)$$

In general, the correction term of (50a) will be of the order of the larger of (53) and (53a). One sees at any rate that $S_2+\frac{1}{2}\hbar b^2(E_2-E_0)^{-1}$ must converge to a finite value as E_2 converges to E_0 and this value can be denoted by S_∞ if we keep in mind that this may not be the value of S for infinite energy. One then sees that (14a) holds with an error the order of magnitude of which is given by the greater of two expressions

$$\frac{2(E_1-E_0)a}{3\hbar}\left(\frac{M^2a^2}{\hbar^2}\text{ or }S_\infty^2\right); \quad (54)$$

$hk=Mv$ has been used in the first expression. Actually, if one assumes a to be of the order of a nuclear radius, the two expressions of (54) become about equal, except if S_∞ is exceptionally small. The order of magnitude of S_∞ is taken to be $25/c$, following the estimates given at the end of the last section.

The expression of (54) has to be small compared with (14a) if our approximations are to be valid. This will be the case unless $E-E_0$ is very large. However, in order that (54) be larger than S_∞, the $E-E_0$ must be either larger than $\hbar^3S_\infty/M^2a^3$ which is, for $a=e^2/mc^2$, equal to $137^3\times1840^{-2}S_\infty mc^2$. This is several million electron volts and larger than $\hbar/S_\infty a\sim137\,mc^2/S_\infty c$. This latter expression is also of the order of a couple of million electron volts unless S_∞ and the normal scattering cross section is unreasonably large. This shows that one must be far indeed from the resonance before the approximations break down.

The other region in which (54) is larger than (14a) lies around $E=E_0+\frac{1}{2}\hbar b^2/S_\infty$ where (14a) vanishes. The range within which (54) is larger than (14a) has the extension of $\Delta E=\hbar b^4a/S_\infty$ if the first expression of (54) is the larger one. ΔE is in this case $ab^2\sim10^{-6}$ times smaller than its distance from E_0. This case can be disregarded. On the other hand, if the second of the expressions of (54) holds, the width of the region in

which (14a) is invalid is $b^4a^3M^2/\hbar S_\infty^3$ and the ratio of this width to the distance of the region from E_0 becomes $M^2a^3b^2/\hbar^2S_\infty^2 \sim 180ab^2/(S_\infty c)^2$. Ordinarily, this is of the same order as ab^2 but can be much larger if S_∞ is very small, i.e., if the ordinary scattering cross section is anomalously low. However, even in this case, there is little danger that the region of invalidity of (14a) assumes any importance as long as ab^2 remains of the order of 10^{-6}.

The above discussion appears to show that the validity of the resonance formula extends over a region of the order of a million electron volts—that is a much wider region than expected. One must remember, however, that the discussion was based on the assumption that the discontinuity of the solution used in Section II gives a fair measure for the deviation of the actual wave function from the wave function used there, even inside the sphere of radius a on the surface of which the discontinuity occurs. This is certainly not true in the neighborhood of another resonance and, in fact, the validity of the formulae of the preceding sections will be limited in most cases by the occurrence of other resonances. The above calculated limitation would apply only if there were no resonances other than the one considered within the limits calculated. It is true also that the above consideration applies only to the developments of Section II, i.e., when one has to deal only with resonance scattering. However, a similar consideration can be carried out also on the basis of the calculations of Section IV and the result is substantially the same inasmuch as the calculated limits of the validity of the equations are only inconsequentially narrower. The real limit of validity will be, also in this case, the occurrence of other resonances unless there is a substantial probability for non-resonance reactions all over the resonance regions.

VII. HIGHER SPIN AND ANGULAR MOMENTA

This subject will not be taken up here in full generality but only two special cases considered. In the first of these, the relative angular momentum of the two colliding particles still remains zero but the particles themselves have spins J_1 and J_2, respectively. If the compound state has a spin J_0, the reaction will be possible only if the spins J_1 and J_2 are combined in such a way that their resultant be J_0. From the $(2J_1+1)(2J_2+1)$ states of the separated particles one can make $2J_0+1$ linear combinations with a total angular momentum J_0. Since the original $(2J_1+1)(2J_2+1)$ states are all equally probable, this holds also for their linear combinations which can be obtained, as in the present case, by an orthogonal transformation. Hence the *a priori* probability that the system be in a state which can lead to a reaction is

$$f=\frac{2J_0+1}{(2J_1+1)(2J_2+1)} \tag{55}$$

and the reaction cross sections of Section V must be multiplied by this factor. J_1 and J_2 are the spins of the colliding particles in the original system which is denoted by j throughout Section VI. In order to calculate the scattering cross section, one must average over the scattering cross sections for the different total angular momenta of the whole system. This gives

$$\sigma=(2J_1+1)^{-1}(2J_2+1)^{-1}\sum_{J=|J_1-J_2|}^{J_1+J_2}(2J+1)\sigma_J. \tag{56}$$

In this, all the σ_J will be normal scattering cross sections, only for the term corresponding to $J=J_0$ will (45) or (46) have to be applied.

In the second case to be considered, the spins of the colliding particles vanish but they have an orbital momentum in the collision. This momentum is equal to the spin of the compound state. The equation for the resonance scattering can be derived in this case very much in the same way as it was derived in Section II for angular momentum zero. The only difference is that the asymptotic form of the wave function is, instead of (1), in case of angular momentum $1\hbar$ (this is the only case which will be taken up)

$$=\left(\frac{3}{4\pi}\right)^{\frac{1}{2}}\frac{x}{ru}\left[\left(\frac{i}{r}+\frac{1}{kr^2}\right)e^{-ikr}+U\left(\frac{i}{r}-\frac{1}{kr^2}\right)e^{ikr}\right]\psi(i). \tag{57}$$

The $U=e^{2i\delta}$ again determines the scattering by means of the phase shift. The equation analogous

to (8) or (48) now is

$$\frac{u_1}{u_2}(1-\bar U_1)(1+\bar U_2{}^*)+\frac{u_2}{u_1}(1+\bar U_1)(1-\bar U_2)$$
$$+\frac{ih}{Ma}\left(\frac{u_1}{u_2{}^3}-\frac{u_2}{u_1{}^3}\right)(1-\bar U_1)(1-\bar U_2{}^*)$$
$$=\frac{2}{ih}(E_1-E_2)(\bar\alpha_1\bar\alpha_2{}^*+\bar\gamma_{12}). \quad (58)$$

The $\bar U_1=U_1\exp(2ik_1a)$; $\bar\alpha_1=\alpha_1\exp(ik_1a)$; $\bar\gamma_{12}$ $\gamma_{12}\exp[i(k_1-k_2)a]$ but the bar will be left off these quantities henceforth. The important difference between (58) and (8) or (48) is the last term on the left side which becomes infinite if a, that is the radius of the sphere in configuration space over which we integrate, goes to zero. The reason for this apparently anomalous behavior is that the irregular solution of the equation $\Delta\psi=-k^2\psi$ is not square integrable for angular momentum $1\hbar$ while both solutions are integrable for angular momentum 0. Similar terms appear in the solutions for all higher angular momenta. The γ_{12} is introduced for (58) in the same way as for (48): it vanishes if either E_1 or E_2 are equal to a definite energy E_0 for which $U_0=-1$. It will be assumed here that there is such an energy. Equation (9), which remains valid in this case, then shows that α_0 is real.

One can introduce again by (10) the real quantity $vS=i(1-U)/(1+U)$ instead of the U. In terms of these, (58) reads

$$v_1{}^2S_1-v_2{}^2S_2-(\hbar/Ma)(v_1{}^2-v_2{}^2)S_1S_2$$
$$=(2\hbar)^{-1}(E_1-E_2)(1-iv_1S_1)u_1$$
$$\times(\alpha_1\alpha_2{}^*+\gamma_{12})u_2(1+iv_2S_2). \quad (59)$$

If one substitutes E_0 for E_2, the γ_{12} will vanish and α_0 becomes real. Since S_0 is infinite, its coefficients on both sides of (59) must be equal. This gives for

$$\alpha_1=\frac{2ihu_0}{E_0\alpha_0u_1}\frac{E_0+(\hbar/Ma)(E_1-E_0)S_1}{(E_1-E_0)(1-iv_1S_1)}. \quad (60)$$

The velocities v were expressed by the corresponding energies in (60). One can now substitute this α_1, and a similar expression for α_2, into (59). Again expressing the velocities in terms of the energies

$$E_1S_1-E_2S_2-(\hbar/Ma)(E_1-E_2)S_1S_2$$
$$=\frac{2(E_1-E_2)\hbar}{E_0v_0\alpha_0{}^2}\frac{[E_0+(\hbar/Ma)(E_1-E_0)S_1][E_0+(\hbar/Ma)(E_2-E_0)S_2]}{(E_1-E_0)(E_2-E_0)}$$
$$+(M/4\hbar)(E_1-E_2)(1-iv_1S_1)u_1\gamma_{12}u_2(1+iv_2S_2). \quad (60a)$$

Neglecting γ_{12}, for the time being, this equation can be written after division by the square brackets and multiplication by E_0 as

$$\frac{E_1S_1}{E_0+(\hbar/Ma)(E_1-E_0)S_1}-\frac{E_2S_2}{E_0+(\hbar/Ma)(E_2-E_0)S_2}$$
$$=\frac{2\hbar}{v_0\alpha_0{}^2}\left(\frac{1}{E_0-E_1}-\frac{1}{E_0-E_2}\right). \quad (60b)$$

This shows that the difference of the first terms of both sides is a constant B independent of the energy E_1. Hence one can express S_1 in terms of $Bv_0\alpha_0{}^2$ and E_0. In order to simplify the formulae one can introduce $F=E_0+2\hbar/Bv_0\alpha_0{}^2$ and $E_0'=F(1-Ma/\hbar B)^{-1}$ and obtain

$$S_1=\frac{Ma}{\hbar}\frac{E_0E_0'}{F}\frac{F-E_1}{(E_0-E_1)(E_0'-E_1)} \quad (61)$$

and

$$\alpha_1=\frac{2iE_1}{u_1F}\frac{[(E_0-F)(F-E_0')E_0E_0'a]^{\frac12}}{(E_0-E_1)(E_0'-E_1)(1-iv_1S_1)}; \quad (61a)$$

(61) appears to correspond to two resonances: one at E_0 and another at E_0'. The S becomes infinite for both these values of energy and the cross section therefore appears to assume its maximum possible value of $12\pi/k^2$. The E_0, E_0', F are arbitrary constants, except that the quantity under the square root sign of (61a) must be positive.

The S given by (61) is in most cases smaller than the S calculated in Section II. It is more important, therefore, to make the correction indicated in that section (10c), i.e., to subtract

$Ma/\hbar$ from it. This then gives

$$S_1=\bar{S}_1-\frac{Ma}{\hbar}=\frac{Ma}{\hbar}\frac{E_1(FE_0+FE_0'-FE_1-E_0E_0')}{F(E_0-E_1)(E_0'-E_1)}$$

$$=\frac{Ma(F-E_0)E_0'}{\hbar F(E_0'-E_1)}\frac{E_1}{E_0-E_1}+\frac{Ma}{\hbar}\frac{E_1}{E_0'-E_1}. \quad (61b)$$

If the domain in which (61) is valid is much smaller than $E_0'-E_0$—and the discussion of the validity of (61) will necessitate restriction of E_1 to such a domain—$E_0'-E_1$ can be considered to be a constant. Hence S_1 can be written in a form very similar to (14a)

$$S_1=\frac{-\frac{1}{2}\hbar c^2E_1}{E_1-E_0}+CE_1. \quad (61c)$$

The only difference is the factor E_1 which occurs in both terms of S_1. The first of these has the effect that, if one writes the cross section in the form of a resonance formula, the width Γ becomes proportional to the third rather than the first power of the velocity. The effect of the factor E_1 in the second term is to render the total scattering zero for $E_1=0$. One has, in fact, for $E\sim 0$

$$\sigma(E)\sim 12\pi a^2E^2\left(\frac{1}{E_0}+\frac{1}{E_0'}-\frac{1}{F}\right)^2 \quad (62)$$

so that the cross section due to the wave with angular momentum $1\hbar$ is proportional to E^2 at $E\sim 0$. Of course, there is always a cross section present from the spherical wave with zero angular momentum.

Above $E=0$, the cross section increases and reaches the theoretical maximum at E_0. The half-width of the absorption line can be obtained by calculating the distance at which vS becomes 1. The full half-width Γ_0 is twice this distance and is equal to

$$\Gamma_0=2ak\frac{F-E_0}{F}\frac{E_0'}{E_0'-E_0}E_0, \quad (63)$$

if all the differences occurring in (63) are large compared with Γ_0. This will be true in general if ak is small, i.e., the energy E_0 not excessively large. In the neighborhood of E_0 the cross section will follow the usual resonance form. As the energy increases further, the cross section drops and becomes zero at F. It then increases again and (61) would indicate that it reaches the theoretical limit again at E_0'. It will be shown, however, that (61) ceases to be valid somewhere midway between E_0 and E_0'.

The above discussion applies if $0<E_0<F<E_0'$. In addition to this, the following arrangements are possible, $0<E_0'<F<E_0$, in which case (61) ceases to be valid at low energies. The same holds true in general if $E_0'<0<E_0<F$ and if $F<E_0'<0<E_0$. This last case appears somewhat unlikely. It is possible, finally, that $E_0<0$ which is usually called a virtual resonance. The discussion of all these cases is very similar to the one above.

Before going into the discussion of the validity of (61), it appears worth while to calculate the ratio of the square integral $|\alpha|^2$ of the wave function inside the sphere with radius a, to the value which this square integral would assume if the wave function were as large inside this sphere as it is on its surface. Evidently, this ratio is very large if we have a real resonance. The first quantity is $|\alpha|^2$ and is given by (61a). The second one is the volume of the sphere multiplied by the square of the coefficient of $\psi(i)$ in (57) for $r=a$. In this last expression x^2/r^2 can be replaced by $\frac{1}{3}$. One has, therefore, for this ratio

$$\frac{3|\alpha_1|^2v_1}{a^3|i(1+\bar{U}_1)/a+(1-\bar{U}_1)/ka^2|^2}$$

$$=\frac{3(E_0-F)(F-E_0')E_0E_0'}{4(FE_1-FE_0-FE_0'+E_0E_0')^2}. \quad (64)$$

For a real resonance, this should be large at least for $E_1=E_0$. This means that

$$\frac{E_0}{E_0'}\frac{E_0'-F}{F-E_0}\gg 1 \quad (64a)$$

is certainly a necessary condition for a real resonance. Hence either E_0' must be very small or F must be very close to E_0.

It will be seen below that (61) may be valid over a considerable region even if neither of these conditions is fulfilled. The reason for this is that the centrifugal potential *outside a* acts as a barrier and assures a long lifetime for the compound nucleus even if there is no proper reson-

ance inside a. In this case, the lifetime of the compound nucleus is essentially given by this barrier and the width of the level will be of the order $2akE_0$. If either of the above conditions for a real resonance is satisfied, the lifetime of the compound nucleus will be considerably increased and the width of the level a good deal smaller than $2akE_0$—as is seen from (63).

As a last point, we discuss the validity of (61) and (61a), i.e., try to take the γ_{12} of (58) into account. The definition of γ_{12} is the same as in the preceding section (48a) and the calculation will be similar also. It hinges on the calculation of γ_1 and γ_2 which are defined by (47) and estimated in (51). In the latter formula, we shall take into account only the first term of the bracket, involving the discontinuity δ_1 of the value of the wave function at a. This is

$$\delta_1 e^{ika} = \alpha_1 \Psi(a, i) - \left(\frac{3}{4\pi}\right)^{\frac{1}{2}} \frac{\cos\vartheta}{u_1} \times \left[\frac{i}{a}(1+U_1) + \frac{1}{ka^2}(1-U_1)\right]\psi(i). \quad (65)$$

In this, $\cos\vartheta$ has been written for x/r and the α_1 and U_1 are the barred quantities, given by (61), (61a). It follows that the exponentials occurring in (57) give a common factor just as in (52). This factor was brought to the left side of (65). The variables of Ψ were replaced by i, the internal coordinates of the reacting particles, and by the distance between these which is a where the discontinuity occurs.

Since we assume that there is no discontinuity in the wave function at $E_1 = E_0$, (65) must vanish at that point. This condition determines $\Psi(a, i)$ and greatly simplifies the expression for

$$\delta_1 e^{ika} = \left(\frac{3}{4\pi}\right)^{\frac{1}{2}} \frac{2i\cos\vartheta}{u_1 a} \frac{E_1}{(E_0' - E_1)(1 - iv_1 S_1)}. \quad (65a)$$

We can now estimate $(1-iv_1S_1)\gamma_{12}(1+iv_2S_2)$ easily to be

$$|(1-iv_1S_1)\gamma_{12}(1+iv_2S_2)| = \frac{4\pi}{3}a^2 |(1-iv_1S_1)\delta_1\delta_2^*(1+iv_2S_2)| \sim \frac{4a}{u_1u_2} \frac{E_1E_2}{(E_0'-E_0)(E_0'-E_2)}. \quad (66)$$

However, unless we have a real resonance as discussed above, this estimate is less safe than the corresponding estimate given in the preceding section because there is reason to believe that the error at the surface of the sphere becomes greatly magnified inside the sphere. This is made plausible already by the form of the asymptotic form of the wave function (57) which increases as r^{-2} toward the inside of the sphere.

The above estimate can be substituted into (60a). At the same time $S_1+\epsilon_1$ and $S_2+\epsilon_2$ will be written for S_1 and S_2, respectively, where S_1 and S_2 are the values of S given by (61), and ϵ_1 and ϵ_2 indicate the amount by which this expression is in error. Neglecting then terms in which the product of ϵ_1 and ϵ_2 occurs, (60a) gives

$$\frac{E_1-E_0'}{E_2-E_0'}E_2\epsilon_1 - \frac{E_2-E_0'}{E_1-E_0'}E_1\epsilon_2 \sim \frac{Ma}{\hbar} \frac{(E_1-E_2)E_1E_2}{(E_1-E_0')(E_2-E_0')}. \quad (66a)$$

Since for $E=E_0$ the equations are accurately satisfied, ϵ_2 will vanish for $E_2=E_0$. Hence

$$\epsilon_1 \sim \frac{Ma}{\hbar} \frac{(E_1-E_0)E_1}{(E_1-E_0')^2}. \quad (67)$$

A comparison of (67) and (61) shows that (61) is certainly grossly inaccurate if E_1 is as close or even closer to E_0' as it is to E_0. It also appears that (61) is inaccurate if E_1 is in the neighborhood of F. This is, however, only apparent and a similar phenomenon to that observed after (54): it only shows that the position of zero scattering may be slightly displaced from the position indicated in (61). However, the first limitation is real and shows that (61) is not valid in the neighborhood of the second resonance and, in fact, becomes invalid at best halfway in between E_0 and E_0'.

On the other hand, for $E_1 \sim 0$ the ϵ_1 becomes so small that the cross section given in (62) remains valid unless F is very close to E_0. This shows that Eqs. (61) have a validity quite comparable to that of the similar equations for zero relative angular momentum of the colliding particles.

APPENDIX

In order to prove Eqs. (39) of the text it is necessary to prove first that every expression $\mathfrak{B}\mathfrak{C}\mathfrak{B}$, where $\mathfrak{C}$ is an arbitrary matrix, is a multiple of $\mathfrak{B}$. This is a consequence of (36a), or, as the mathematicians express it, that $\mathfrak{B}$ is an idempotent of rank 1. We have, in fact

$$(\mathfrak{B}\mathfrak{C}\mathfrak{B})_{kl}=\sum_{jm}\beta_k\beta_j C_{jm}\beta_m\beta_l=(\sum_{jm}\beta_j C_{jm}\beta_m)B_{kl}. \quad \text{(A1)}$$

We now can go over to verifying (39). Equation (28) and (32b) give for $\mathfrak{U}$

$$\begin{aligned}\mathfrak{U}&=\frac{1+i\mathfrak{u}\mathfrak{S}\mathfrak{u}}{1-i\mathfrak{u}\mathfrak{S}\mathfrak{u}}=(1+i\mathfrak{u}\mathfrak{S}_\infty\mathfrak{u}-ic\mathfrak{u}\mathfrak{B}\mathfrak{u})(1-i\mathfrak{u}\mathfrak{S}_\infty\mathfrak{u}+ic\mathfrak{u}\mathfrak{B}\mathfrak{u})^{-1}\\&=[1+i\mathfrak{u}\mathfrak{S}_\infty\mathfrak{u}-ic\mathfrak{u}\mathfrak{B}\mathfrak{u}][(1-i\mathfrak{u}\mathfrak{S}_\infty\mathfrak{u})\\&\quad\times(1+ic(1-i\mathfrak{u}\mathfrak{S}_\infty\mathfrak{u})^{-1}\mathfrak{u}\mathfrak{B}\mathfrak{u})]^{-1} \quad \text{(A2)}\\&=[1+i\mathfrak{u}\mathfrak{S}_\infty\mathfrak{u}-ic\mathfrak{u}\mathfrak{B}\mathfrak{u}][1+ic(1-i\mathfrak{u}\mathfrak{S}_\infty\mathfrak{u})^{-1}\mathfrak{u}\mathfrak{B}\mathfrak{u}]^{-1}\\&\quad\times(1-i\mathfrak{u}\mathfrak{S}_\infty\mathfrak{u})^{-1}.\end{aligned}$$

For the first factor of this we shall try to write

$$1+i\mathfrak{u}\mathfrak{S}_\infty\mathfrak{u}-ic\mathfrak{u}\mathfrak{B}\mathfrak{u}=[1+i\mathfrak{u}\mathfrak{S}_\infty\mathfrak{u}-\mu(1-i\mathfrak{u}\mathfrak{S}_\infty\mathfrak{u})^{-1}\mathfrak{u}\mathfrak{B}\mathfrak{u}]\times[1+ic(1-i\mathfrak{u}\mathfrak{S}_\infty\mathfrak{u})^{-1}\mathfrak{u}\mathfrak{B}\mathfrak{u}]. \quad \text{(A3)}$$

If this proves to be possible, the product of the first two factors of (A2) will be equal to the first factor on the right side of (A3). We can substitute, by (A1), for the product of the last two terms on the right side of (A3) $-ic\mu\gamma(1-i\mathfrak{u}\mathfrak{S}_\infty\mathfrak{u})^{-1}\mathfrak{u}\mathfrak{B}\mathfrak{u}$ with

$$\gamma=\sum_{jm}\beta_j(\mathfrak{u}(1-i\mathfrak{u}\mathfrak{S}_\infty\mathfrak{u})^{-1}\mathfrak{u})_{jm}\beta_m. \quad \text{(A4)}$$

The right side of (A3) then gives

$$1+i\mathfrak{u}\mathfrak{S}_\infty\mathfrak{u}+(-\mu+2ic-ic\mu\gamma)(1-i\mathfrak{u}\mathfrak{S}_\infty\mathfrak{u})^{-1}\mathfrak{u}\mathfrak{B}\mathfrak{u}+ic(-1+i\mathfrak{u}\mathfrak{S}_\infty\mathfrak{u})(1-i\mathfrak{u}\mathfrak{S}_\infty\mathfrak{u})^{-1}\mathfrak{u}\mathfrak{B}\mathfrak{u}.$$

This is equal to the left side of (A3) if

$$-\mu+2ic-ic\mu\gamma=0 \quad \text{(A5)}$$

or, with (35a) and $c_\infty=0$

$$\mu=\frac{2ic}{1+ic\gamma}=\frac{i\hbar b^2}{E-E_0+\frac{1}{2}i\hbar b^2\gamma}. \quad \text{(A6)}$$

With this μ, (A3) becomes an identity. Equation (A2) therefore gives

$$\mathfrak{U}=(1+i\mathfrak{u}\mathfrak{S}_\infty\mathfrak{u}-\mu(1-i\mathfrak{u}\mathfrak{S}_\infty\mathfrak{u})^{-1}\mathfrak{u}\mathfrak{B}\mathfrak{u})(1-i\mathfrak{u}\mathfrak{S}_\infty\mathfrak{u})^{-1}$$

$$\mathfrak{U}=\frac{1+i\mathfrak{u}\mathfrak{S}_\infty\mathfrak{u}}{1-i\mathfrak{u}\mathfrak{S}_\infty\mathfrak{u}}-\mu(1-i\mathfrak{u}\mathfrak{S}_\infty\mathfrak{u})^{-1}\mathfrak{u}\mathfrak{B}\mathfrak{u}(1-i\mathfrak{u}\mathfrak{S}_\infty\mathfrak{u})^{-1}. \quad \text{(A7)}$$

This is indeed equivalent to (39). The λ of (39a) is $\hbar b^2\gamma$.

PHYSICAL REVIEW VOLUME 70, NUMBERS 1 AND 2 JULY 1 AND 15, 1946

The Temperature Dependence of Secondary Electron Emission from Oxide-Coated Cathodes*

MARTIN A. POMERANTZ
Bartol Research Foundation of the Franklin Institute, Swarthmore, Pennsylvania

(Received January 19, 1946)

The secondary electron emission from alkaline-earth oxide-coated cathodes has been investigated under both continuous and pulsed bombardment. Experiments have been performed with three types of apparatus. Yield *vs.* energy data reveal values of δ of 4–7 at room temperature, with a more or less flat maximum at approximately 1000 volts primary energy. The yield increases with temperature in an exponential manner, and plots of log $\Delta\delta$ (i.e., $\delta_K{}^\circ - \delta_{200^\circ K}$) *vs.* $1/T$ give straight lines. Values of Q_1 between 0.9–1.5 ev are generally indicated, and from extrapolation of these curves, yields exceeding 100 at 850°C are deduced. The secondary emission depends upon the degree of activation, and increases with enhancement of the thermionic emission characteristics. Short time effects such as growth or decay of secondary current after the onset of primary bombardment or persistence after the cessation of bombardment have not been observed, and values of yield obtained by pulsed methods are in accord with those obtained under d.c. conditions. Tail phenomena reported by J. B. Johnson and interpreted as "enhanced thermionic emission" from oxide-coated cathodes become manifest only under experimental conditions characterized by certain space-charge effects, and have been effectively simulated by bombarding a tantalum target adjacent to an electron-emitting tungsten filament. Various measurements of the energy distribution of secondary electrons as a function of primary voltage and temperature have been obtained. It was observed that the average energy of the secondary electrons decreases with temperature at a rate which more than compensates for the increase in the number of secondaries emitted per incident primary. The mechanism of the observed dependence of yield upon temperature is not well understood. Various alternative explanations are discussed and, in the light of the present state of our knowledge, regarded as untenable.

I. INTRODUCTION

MEASUREMENTS of the secondary electron emission from BaSr oxide-coated cathodes at room temperature have been reported by several investigators.[1] The first suc-

* This work was done in whole under Contract No. OEMsr-358 between The Franklin Institute of the State of Pennsylvania and the Office of Scientific Research and Development, which assumes no responsibility for the accuracy of the statements contained herein.

[1] K. Sixtus, Ann. d. Physik **3**, 1017 (1929); M. Zeigler,

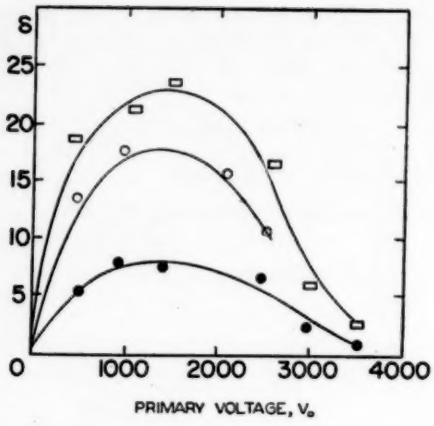

FIG. 1. Secondary electron yield, δ, as a function of primary energy V_p, for an oxide-coated cathode at different temperatures. Tube SE 13. Closed circle, room temperature; open circle, 615°C; open square, 660°C.

cessful attempt to study the phenomenon at elevated temperatures was made by Morgulis and Nagorsky,[2] who observed a fivefold increase in the yield at 850°K.

Because of recent developments associated with the attainment of high pulsed thermionic emissions from oxide-coated emitters,[3] it was of interest to examine simultaneously both thermionic and secondary emission characteristics of cathodes prepared under conditions whereby the physical-chemical state of the system requisite for copious pulsed thermionic emission is realized. It was also important to determine whether the secondary emission available in pulses of short duration differs from that under steady-state conditions, as in the case of thermionic emission.

II. APPARATUS AND RESULTS

A. Experimental Tubes

Experiments have been performed with three types of apparatus to be described in detail elsewhere:[4]

(1) *Beam tube* was a demountable continuously-pumped arrangement comprising a more or less standard system of electron gun, collector, and target mounted on removable grinds.

(2) *S.E. tube* permitted simultaneous study of both thermionic and secondary emission properties of oxide-coated cathodes. A movable mounting was provided whereby the specimen cathode could be shifted from its position as target in the secondary electron measuring system into a Kovar-cup anode for diode operation and thermionic emission tests. S.E. tubes were sealed-off after processing.

(3) *Spec. S.E. tube* incorporated special features for the study of transient phenomena. Both pulsed and d.c. measurements were obtained with this apparatus.

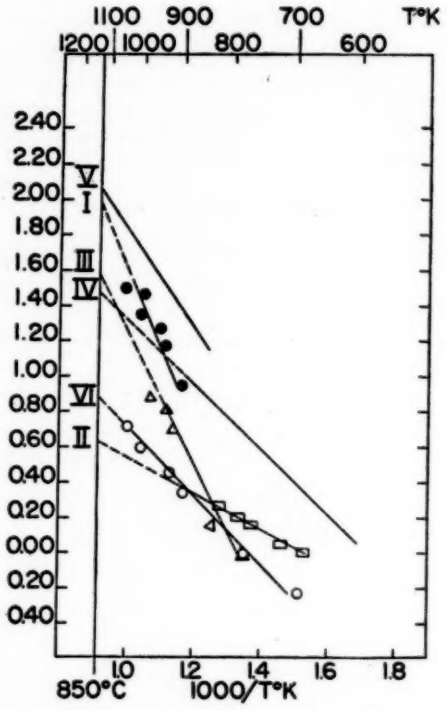

FIG. 2. Typical curves of log $\Delta\delta$ *vs.* $1000/T$°K. (See Eq. (1)). I, closed circle, SE 13: $Q_1=1.4$; II, open square, SE 3 (badly poisoned screen cathode): $Q_1=0.36$; III, open triangle, beam tube: $Q_1=1.4$; IV, Morgulis and Nagorsky, reference 2, $Q_1=0.73$; V, W. E. Danforth, reference 7, electrical conductivity of oxide-cathode coating: $Q_1=1.1$; VI, open circle, Spec. SE 2: $Q_1=0.75$.

B. Steady-State Experiments

1. Yield vs. Energy

At room temperature, δ attains a maximum value generally in the range 4–7, at a primary energy of approximately 1000 volts. Figure 1 is

Physica **3**, 307 (1936); H. Bruining and J. H. DeBoer, Physica **6**, 823 (1939).

[2] N. Morgulis and A. Nagorsky, Tech. Phys. U.S.S.R. **5**, 848 (1938).

[3] M. A. Pomerantz, Proc. I.R.E., in process of publication.

[4] M. A. Pomerantz, J. Frank. Inst., in process of publication.

a typical curve of yield *vs.* primary energy at room temperature, as well as at two higher temperatures.

2. *Yield vs. Temperature*

It is evident that the yield increases with temperature, confirming the earlier results of Morgulis and Nagorsky. Furthermore, if the so-called "anomalous" yield, i.e., the difference between the yield at T°K and that at room temperature, is plotted logarithmically as a function of the reciprocal of the absolute temperature, a straight line is obtained. The dependence is thus of an exponential character, and is represented by the equation

$$\Delta\delta = A \exp(-Q_1/2kT). \quad (1)$$

In Fig. 2, typical data obtained in various experiments are plotted in this manner. Because of technical difficulties arising from space-charge effects when thermionic emission from the target becomes excessive, the attainment of reliable measurements at normal cathode operating temperatures (850°C) is precluded. It is consequently necessary to extrapolate data obtained at lower temperatures, a procedure which is justified by available evidence.[4]

Table I summarizes some pertinent data obtained with a representative group of S.E. tubes during the optimum phase of the life history of oxide-coated cathodes. The following constitute the essential features:

(a) The yield from a well-activated oxide-coated cathode increases with temperature in an exponential manner and may substantially exceed 100 at 850°C;

(b) In general, the slopes of the curves are of the same magnitude, having Q_1 values of approximately 0.9–1.5 ev.

3. *Yield vs. Degree of Activation*

As a consequence of improved activation techniques, the yields observed have exceeded those reported by others.[1,2] In general, as the degree of activation is improved, the capacity for both thermionic and secondary emission are enhanced, although no quantitative correlation between secondary yield and pulsed thermionic emission has been established. Life test studies have also revealed a qualitative correlation between thermionic and secondary emission characteristics (see Table II).

TABLE I. Typical secondary emission yield data for oxide-coated cathodes.

Tube No.	Type of coating	Max. yield δ_{max}, at room temperature	Max. extrapolated yield, δ_{max}, at 850°	Pulsed thermionic emission characteristics of cathode: Pulse width = 1 μsec. Rec. freq. = 60 p.p.s.
1	C-51-2 sprayed on grade A Ni	6.7	115	18 amp./cm², emission-limited
5	C-51-2 sprayed on grade A Ni	6.8	110	20 amp./cm², space-charge limited to sparking
9	C-51-2 sprayed on grade A Ni	4.7	Not obs.	27 amp./cm, s.c.l. to sparking
12	C-51-2 sprayed on grade A Ni	3.9	124	20 amp./cm², s.c.l. to sparking
13	Bowie #1 sprayed on Wise #1 Ni	5.7	136	20 amp./cm², s.c.l.
14	50% MgO, 50% C-51-2 sprayed on grade A Ni	5.8	106	20 amp./cm², s.c.l.
6	C-51-2 painted on 60×60 Ni screen	3.2	54	13 amp./cm², emission limited
3	C-51-2 painted on 60×60 Ni screen	2.7	7	1.7 amp./cm² Badly poisoned by diffusion pump oil owing to power failure during bakeout

C-51-2 is here used to designate a certain commercial Ba-Sr-carbonate coating with an organic binder. Coating densities were generally approximately 10–12 mg/cm².

TABLE II. Life history of an oxide-coated cathode.

Run No.	Pulsed thermionic emission—characteristic of cathode: pulse width = 1 μsec. recur. freq. = 60 p.p.s.	δ	Secondary emission Temp. C°	Aging run
1	Flat at 2 amp./cm²			
2		5.3	Room temp.	
		55	850°C	
3				17 hr. = 13.5 amp./cm² peaks at end of run: pulse width = 0.9 μsec. rec. freq. = 400 p.p.s.
4	14 amp./cm²			
5		6.4	Room temp.	
6				55 hr. additional, total = 72 hours
7	20 amp./cm² s.c.l.			
8		5.8	Room temp.	
		106	850°	
9				49 hr. additional, total = 121 hours
10	20 amp./cm² s.c.l.			
11		5.8	Room temp.	
		86	850°	
12				67 hr. additional, total = 188 hours
13	14 amp./cm² emission limited			
14		4.2	Room temp.	Lead burned out
		54	850°	

Runs with SE No. 14 are numbered in chronological order.

C. Pulsed Measurements

As a possible explanation of the mechanism responsible for the aforementioned high yields it had been proposed that thin-film field emission,[5] or a modification thereof, might be operative. However, this hypothesis appeared to be inconsistent with available theoretical and experimental data. For example, one fundamental argument against invoking the Malter effect for explaining the high yield from oxide-coated cathodes involves the temperature dependence of the electrical conductivity of this impurity semiconductor. Although it is well known that the resistivity *decreases* with temperature, Malter had demonstrated that in the case of his special films illumination of the surface *reduced* both the high yield and the decay period as a consequence of the lowering of the resistivity by photo-conductivity. Actually, the secondary electron emission from an oxide-coated cathode *increases* with temperature. Nevertheless, in view of the controversial nature of this matter, a direct search for short time effects was undertaken.

Two different experimental arrangements were utilized for the pulsed observations. In the earlier work, measurements with S.E. tubes were extended to times of the order of 10^{-4} sec., whereas the Spec. S.E. tubes were designed for observations in which the primary beam would remain on for intervals in the microsecond range.

In the initial investigations, there was no evidence of growth or decay of the secondary electron emission following application of the bombarding beam, nor was there any indication of persistence and decay of emission following the interruption of the primary beam, with a time constant as low as 10^{-4} sec.

Experiments later performed by J. B. Johnson[6] yielded results which he has ascribed to a new type of electron-emission from oxide-coated thermionic cathodes. This phenomenon manifested itself as an electron current from the target gradually increasing microseconds after the onset of primary bombardment, and a more slowly decreasing current persisting after the abrupt cessation of the bombardment. The effect was described by Johnson as "enhanced thermionic emission excited by electron bombardment." It presumably varied with temperature in about the same way as the steady emission, thus roughly following Richardson's law. It increased with bombardment voltage and current density, and might exceed the steady thermionic current in value. Calculations reveal that the surface temperature rise of the target caused by the bombardment is far too small to explain the increased emission. It was asserted that the effect no doubt explains the exponential rise with temperature previously reported for the yield from oxide-coated cathodes. Johnson concludes from his data that when he subtracts "enhanced thermionic emission" from the total electron current, the secondary emission does not increase with temperature.

The practical importance of ascertaining the magnitude of the secondary emission available in microsecond pulses, as well as the significant theoretical implications of the results of Johnson, stimulated the present attempt to extend the measurements to the 10^{-6} sec. range. The experimental arrangement whereby this has been accomplished will be described in detail in reference 4. Steady-state and pulsed data could be obtained practically simultaneously.

Cathode-ray tube observations revealed that the pulsed secondary emission increases with temperature, just as in the case of d.c. measurements. Furthermore, the yields measured when the primary beam was applied in the form of rectangular microsecond pulses were in good agreement with practically simultaneously-measured steady-state yields at all temperatures from room temperature up to the maximum temperature at which reliable data were available (see Sec. II, B, 2).

When the cathode is heated above some critical temperature, an increase in the amplitude of the secondary emission pulse and a tail (the origin of which will become apparent presently), persisting after the cessation of the primary pulse, begins to appear. It is this phenomenon which Johnson has interpreted as "enhanced thermionic emission." During the present experiments, however, it was observed that the nature of this tail depends quite markedly upon the position of the bombarding beam, which could

[5] L. Malter, Phys. Rev. **50**, 48 (1936).
[6] J. B. Johnson, Phys. Rev. **66**, 352 (1944).

be caused to scan the surface of the target. This observation was consistent with the expectation that the tail might arise as a consequence of certain instrumental considerations which could be sensitive to the geometry.

The experimental tubes incorporated a feature whereby the target cathode could be moved out of the path of the bombarding beam away from the collector electrode, thereby exposing to the beam a tantalum target with an adjacent helical tungsten filament. It was discovered that upon heating this filament to temperatures at which thermionic emission sets in, an increase in amplitude and a tail on the secondary emission pulse from the tantalum target begins to appear. Its characteristics are similar to those manifested with an oxide-coated cathode as target, and it is particularly significant that *the tail observed with tantalum occurs when the d.c. thermionic emission from the filament is of the same magnitude as that emitted by the oxide-coated cathode targets when the latter manifest tail effects*. This experiment effectively simulates the Johnson effect.

The tail heretofore identified as being attributable to "enhanced thermionic emission" consequently is presumed to arise from purely extraneous causes associated with the presence in the target-collector region of an excessive electronic space-charge. Previously, it had been observed with S.E. tubes that for high target cathode temperatures under d.c. conditions the glass envelope becomes charged, and peculiar growth and decay of currents to the collector occur when the beam is turned on and off, or when the glass is touched. The changes in some instances were of the same magnitude as the initial steady currents. Additional complicated effects of this nature might arise in some instances under conditions of poor vacuum, because of neutralization of some space-charge by positive ion emission from the target produced by bombardment, for example. In fact, any transient disturbance which alters the net d.c. current from target to collector by only an extremely small amount with an appropriate time-constant would result in the appearance of a tail on the target current pulse. In a typical actual case, a rapid variation of microamperes in the steady current to the collector of several milliamperes has been shown to cause the appearance of the tail.

Furthermore, it should be emphasized that the tail phenomenon appears only at those temperatures at which in any event reliable secondary emission measurements are precluded by the considerations already discussed in Section II, B, 2, and hence has not affected the conclusions based upon d.c. measurements. In fact, significant increases in δ already occur prior to the onset of detectable thermionic emission from the target cathode. Therefore, regardless of the exact nature of the effect which causes the short time fluctuation in the steady current from target to collector, the phenomenon must be considered as being not pertinent in discussions regarding the true secondary emission from an oxide-coated cathode. On the contrary, it depends critically upon certain experimental factors including the geometrical disposition of components of the experimental tube, and is a property to be associated with space-charge considerations rather than with the target itself.

III. FACTORS PERTINENT TO THEORY

A. Effect of Coating Resistance

A possible explanation for the increase of yield with temperature might be sought in the electrical conductivity characteristics of the oxide-coated cathode. If the resistance is sufficiently high to cause an appreciable fall of potential in the coating at room temperature, it would be expected that the decrease in resistivity with increase in temperature might enhance the apparent yield. There are several reasons for considering this improbable in the present experiments:

(1) The absence of time effects upon bombardment of targets at room temperature, particularly with microsecond pulses, indicates that the influence of coating resistance is negligible. For high resistances, variations of the secondary current with a time constant RC, where C is the capacitance of the target coating and R its resistance, would be expected to arise.

(2) The resistivity of coatings of this type, prepared according to approximately similar techniques, have been measured by W. E. Danforth[7] using cathodes containing embedded

[7] W. E. Danforth, OSRD Report, Contract OEMsr-358, Bartol Research Foundation, October 1945, to be published shortly.

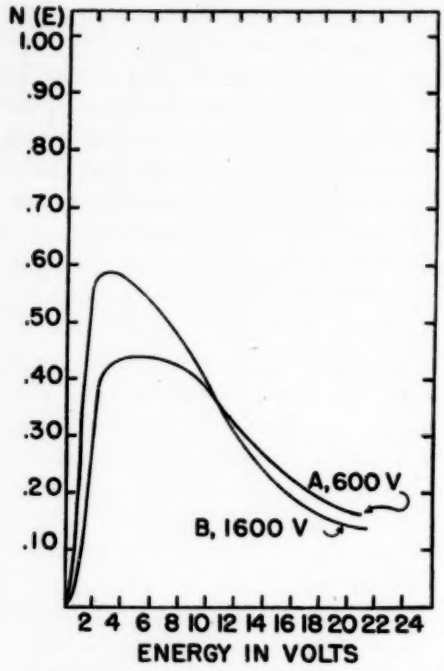

FIG. 3. Energy distribution curves for two primary energies at room temperature. *A*—primary voltage $V_p = 600$ v; *B*—primary voltage $V_p = 1600$ v.

probes. Danforth observed resistances ranging from 50,000 ohms to perhaps as high as 10 megohms occasionally. For the electron currents here involved, the effect of this resistance is negligible. However, it is not difficult to conceive of situations involving cathodes less active than those used here, where the resistance might be considerably higher than the aforementioned upper limit, thereby introducing pulsed effects.

B. Resolution of Dilemma Regarding Conservation of Energy

Difficulty in accounting for the high yields, particularly extrapolated values of 100 secondaries per primary, became apparent in the early stages of the investigation. It seemed impossible to reconcile the observed data with the principle of conservation of energy, if it was assumed that the average energy of the secondaries was even several volts. Consideration of competing processes, preferred directions, solid angles, etc., led to the conclusion that apparently an excessive fraction of the primary energy was manifesting itself as observable secondaries. Studies were therefore undertaken to determine the energy distribution of secondary electrons under various conditions. Where experimental data are comparable, the results are at least in qualitative agreement with those reported by Morgulis and Nagorsky.[2]

The Spec. S.E. tube was particularly well adapted to this phase of the investigation. The measurements were obtained by applying retarding potentials V_c to the collector, and observing the current I_s from the bombarded target to the collector. This provides data for plotting an integral distribution. For any negative value of V_c, the current I_s to the collector is given by:

$$I_s = \int_{V_c^-}^{\infty} N(E)dE, \tag{2}$$

where $N(E)dE$ represents the number of secondaries in the interval dE at E. Differentiation with respect to the lower limit gives the differential energy distribution, or the original function:

$$N(E) = -dI_s/dV_c^-. \tag{3}$$

Secondaries emerging from the target surface into the vacuum in all directions are included in these measurements.

1. Energy Distribution as a Function of Primary Energy

The energy distributions derived from curves of I_s *vs.* V_c^- at two primary voltages, with the cathode at room temperature, appear in Fig. 3. Increasing the bombarding energy results in a shift of the maximum and average energies to lower values. This increase with V_p in the number of slow electrons may be attributed to the greater depth of penetration of primaries, and the subsequent additional energy losses suffered by secondaries which, on the average, must traverse a longer path before emerging from the surface. A change in collision cross section with energy might also be responsible for a shift.

2. Energy Distribution as a Function of Temperature

The energy distributions at room temperature and at two elevated temperatures, for a fixed primary voltage, appear in Fig. 4. It is evident

that a considerable change occurs, with a marked shift of the maximum toward lower energies as the temperature is raised. It seems unlikely that the magnitude of this effect is consistent with that expected solely by virtue of the increased amplitude in the thermal vibrations of the lattice and the resulting small additional energy loss per interaction. The difference might be accounted for by the production of tertiaries by the secondary electrons, a process which could also be invoked to account for the increased yields.

The shift in the energy distributions cannot be explained as an experimental consequence of the variation of coating conductivity with temperature. The I_sR_T drop in the target, even at room temperature, was negligible in the present instance. Furthermore, thermionic emission has not been involved in any of the curves, inasmuch as it was still negligibly small compared with secondary emission at the highest temperature cited.

3. *Total Emergent Energies*

The previously mentioned difficulty regarding the conservation of energy is obviated by the decrease in average secondary energy associated with the increase in the yield. The average value of the secondary-electron energy, V_{av}, is obtained from the energy distribution curves of Fig. 4. The mean emergent energy per incident primary is equal to $V_{av}\delta$, and the data summarized in Table III indicate that this total emitted energy at first increases only slightly, if at all, and thereafter even decreases as the temperature is raised.

The yield from the target used in this experiment was lower than those obtained in previous measurements with S.E. tubes. It is therefore necessary to assume that for more active emitters

TABLE III. Total emergent secondary energy per incident primary.

Temperature, C°	Yield, δ	Mean energy of secondary electron, V_{av}	Mean secondary energy in ev, per 1600 volt primary, $V_{av}\delta$
Room temp.	2.0	11.7	23.4
470	3.1	8.5	26.3
615	5.3	3.7	19.6

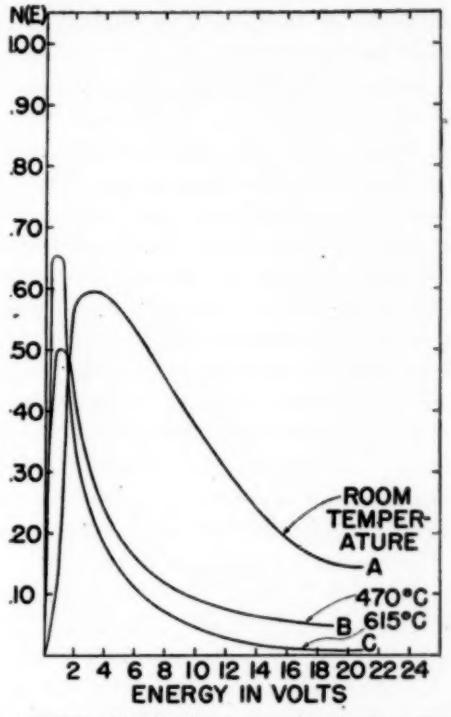

FIG. 4. Energy distribution curves for three temperatures at a constant primary energy $V_p = 1600$ volts. The shapes, but not the relative amplitudes, may be compared. *A*—room temperature; *B*—470°C; *C*—615°C.

the average secondary energies are even lower than those indicated above. This is tantamount to predicting that the secondary electron energy distribution might vary as a function of the degree of activation of the oxide-coated cathode target. An attempt was made to improve the emitting properties of the target by a treatment involving pulsed aging as a thermionic cathode in the diode position. Unfortunately, only a small but distinct enhancement in emission was thus induced, and although the resulting energy distribution displayed a change exceeding the experimental uncertainty, this effect cannot yet be regarded as having been conclusively established. Further experiments embracing cathodes of widely varying activity should be performed.

C. Mechanism for Temperature Dependence of Yield

The mechanism whereby the secondary electron emission from oxide-coated cathodes increases with temperature is not well understood. An obvious explanation for the additional second-

ary currents at temperatures higher than the threshold for thermionic emission was sought in terms of local temperature rise of the target surface owing to electron bombardment. Calculations based upon the experimental conditions indicate that this hypothesis is precluded. Johnson[6] has also pointed out that this is far too small to explain the effect. Finally, the increases in yield observed prior to the onset of thermionic emission could not be accounted for in this way.

The similarity between the functional relationship here and in the case of the electrical conductivity (Eq. (1)) appears to be significant. (See Fig. 2, Curve IV). This result might be understood as follows: In general, secondary emission depends directly upon the number of electrons available in the conduction band. In the alkaline-earth oxides, as in other semiconductors, the number of valence electrons is just sufficient to fill an energy band, so that if no excitation occurs, as is the case for low temperatures, no electrons are available for conduction. With increase of temperature, however, thermal excitation to higher-lying bands (conduction bands) occurs. It is these electrons which are responsible for the electronic conductivity of semiconductors at higher temperatures, and which it might be assumed are also available for secondary emission. Quantitatively, the yield *vs.* temperature dependence would then result from the fact that the electronic population in the conduction band is proportional to the Boltzmann factor $\exp[-Q_1/2kT]$ where Q_1 represents the excitation energy,[8] i.e., the energy difference between bands. Thus, provided the work function does not vary sensitively with temperature, and the physical characteristics of the system are preserved as the temperature increases, the yield-dependence upon temperature is given by the corresponding density of conduction electrons.

Theoretical difficulties exist, however. As Fröhlich[9] has pointed out, the laws of conservation of energy and momentum render it improbable that a free (conduction) electron would emerge in the direction from which the primary electron has entered. Thus, only bound electrons are available for secondary emission in the required direction. Furthermore, the number of free electrons in a semiconductor, even at high temperatures, is much smaller than in the case of metals. In any event, it is low compared with the number of bound electrons, which must constitute the main source of secondary emission at lower temperatures. These theoretical difficulties appear to be of a fundamental nature, and probably will be resolved only by the formulation of a new model for the process of secondary emission from an impurity semiconductor of this type.

[8] Actually the alkaline-earth oxides are impurity semiconductors, the impurity taking the form of free metal (Ba, Ca, or Sr) atoms scattered throughout the oxide. The free atoms provide discrete energy levels which are localized in the forbidden energy region between the filled and conduction bands. The electrons from impurity levels, therefore, require a smaller excitation energy and Q_1 should be identified with this energy required to excite electrons from the impurity level to the conduction band.

IV. ACKNOWLEDGMENTS

It is a pleasure to acknowledge valuable assistance rendered by Daniel L. Goldwater during several phases of these investigations. The Cathode Research Group of M.I.T. Radiation Laboratory, with which a valued close collaboration was maintained throughout the course of this project, supplied cathode targets of various descriptions for the present experiments. In the latter connection, appreciation is expressed particularly to E. A. Coomes, J. G. Buck, and A. Fineman.

[9] H. Fröhlich, *Elektronentheorie der Metalle* (1936), p. 91.

PHYSICAL REVIEW VOLUME 70, NUMBERS 1 AND 2 JULY 1 AND 15, 1946

The Magnetic Moments of H^3 and He^3*

R. G. SACHS
Metallurgical Laboratory, University of Chicago, Chicago, Illinois
AND
JULIAN SCHWINGER
Department of Physics, Harvard University, Cambridge, Massachusetts

A measurement of the magnetic moments of the nuclei H^3 and He^3 would yield information concerning the deviations from L-S coupling in these nuclei. It is shown that the sum of the moments of the two nuclei can be directly related to the amount of admixture of the ^2P, ^4P, and ^4D eigenfunctions with the ^2S function. Thus the measurement of both moments would lead to direct information concerning the contributions of these functions to the ground state of the two nuclei. The individual moments depend to some extent on the detailed properties of the wave functions, but if only the ^2S and ^4D functions contribute appreciably to the ground state, and if particularly simple forms of these functions are assumed, the moment of each nucleus is shown to be expressible in terms of the amount of admixture of the two functions. If then the amount of ^4D function is taken to be 4 percent on the basis of an estimate by Gerjuoy and Schwinger, the moments of H^3 and He^3 are found to be 2.71 and -1.86 nuclear magnetons, respectively.

1. INTRODUCTION

THE existence of the quadrupole moment of the deuteron indicates that the neutron-proton interaction must involve an interaction of tensor type in order that the ground state of the deuteron contain the required mixture of S and D eigenfunctions.[1] Evidence for a similar deviation from L-S coupling in heavier nuclei is found in the marked decrease of the magnetic moments of the odd-odd nuclei with increasing atomic weight.[2] Some of the consequences of assuming that the tensor interaction acts between the particles in H^3 to the same degree as in the deuteron have been obtained by Gerjuoy and Schwinger.[3] They carried out a variation calculation with results indicating that in the ground state the probability for the system to be in a $^4D_{\frac{1}{2}}$ state is about 4 percent, while the system is to be otherwise found in the $^2S_{\frac{1}{2}}$ state. In general it might be expected that $^2P_{\frac{1}{2}}$ and $^4P_{\frac{1}{2}}$ functions would also be mixed in but their contribution was assumed to be small since they would appear in second order only if the tensor interaction were treated as a perturbation.

Unfortunately, the computation led to a binding energy that was only a fraction of the observed energy, so that the above conclusions concerning the character of the wave function cannot be considered to be very reliable. A somewhat more hopeful method of obtaining information concerning the relative contributions of states of different orbital and spin angular momenta to the ground state of a nucleus is to determine its magnetic moment, since this moment depends in a very sensitive way on just such contributions. In general, it would also be useful to determine the quadrupole and higher moments for this purpose but these moments vanish for nuclei, such as H^3 and He^3, which have a total angular momentum of $\frac{1}{2}$.

An exact calculation of the moments of the nuclei cannot at present be carried out because the results contain integrals which depend on the detailed properties of the wave functions which are, of course, not known. However, in the approximation that the neutron-neutron and proton-proton interactions are identical, the sum of the moments of H^3 and He^3 is independent of the detailed behavior of the wave functions. This will be shown in Section 2. As a consequence of this result, measurements of the moments of both nuclei could be combined to give very useful information concerning the relative contributions of the various possible terms to the ground states of the nuclei.

The moments of the individual nuclei can be expressed in simple terms if the wave function is

* This work was completed when the authors were at Purdue University. The results were reported at the Baltimore Meeting of the American Physical Society, May 1–2, 1942 (Phys. Rev. **61**, 732 (1942)).

[1] W. Rarita and J. Schwinger, Phys. Rev. **59**, 436 and 556 (1941).

[2] S. Millman and P. Kusch, Phys. Rev. **60**, 91 (1941).

[3] E. Gerjuoy and J. Schwinger, Phys. Rev. **61**, 138 (1942).

assumed to contain only ^2S and ^4D components, and if certain simplifying assumptions, roughly equivalent to those made by Gerjuoy and Schwinger,[3] are made concerning the functions representing these states. The moments are calculated under these conditions in Section 3.

2. THE SUM OF THE MOMENTS OF H^3 AND He^3

In order to bring out the symmetry of the two nuclei with respect to the interchange of neutrons and protons it is desirable to introduce a notation which has this symmetry. Therefore, we label the variables referring to the neutrons in H^3 and to the protons in He^3 with the indices 1, 2, and we label the variables referring to the other particle in each of the nuclei with the index 3. Then the magnetic moments of the nuclei are given in units of the nuclear magneton by

$$\mu_H=\langle L_3^z+2\mu_n(S_1^z+S_2^z)+2\mu_p S_3^z\rangle_{Av}, \quad (1)$$

and

$$\mu_{He}=\langle L_1^z+L_2^z+2\mu_p(S_1^z+S_2^z)+2\mu_n S_3^z\rangle_{Av}, \quad (2)$$

where L_i^z is the z-component of the orbital angular moment of the ith particle, S_i^z is the z-component of the spin of that particle, and μ_n, μ_p are the magnetic moments of neutron and proton. The average is to be taken over the wave function of that ground state of the nucleus for which the z-component of the total angular momentum has its maximum value, $\frac{1}{2}$.

If the difference between neutron-neutron and proton-proton forces is neglected, the wave functions of the two nuclei are identical so the averages indicated in both Eq. (1) and in Eq. (2) involve the same wave function. Then the sum, $\mu=\mu_H+\mu_{He}$, of the moments of the two nuclei is

$$\mu=\langle L^z+2(\mu_n+\mu_p)S^z\rangle_{Av}, \quad (3)$$

where $L^z=L_1^z+L_2^z+L_3^z$ and $S^z=S_1^z+S_2^z+S_3^z$ are the z-components of the total orbital and spin angular momenta, respectively. The average here is to be taken over the common wave function of the two nuclei.

Since $L^z+S^z=J^z$, the z-component of the total angular momentum, S^z can be eliminated from Eq. (3) to give

$$\mu=\mu_n+\mu_p-2(\mu_n+\mu_p-\tfrac{1}{2})\langle L^z\rangle_{Av}, \quad (4)$$

in a state for which the projection of the total angular momentum on the z axis has its maximum value, $\frac{1}{2}$. The average in Eq. (4) can be simplified by means of the usual vector addition rule

$$\langle L^z\rangle_{Av}=J^z\langle J(J+1)+\mathbf{L}^2-\mathbf{S}^2\rangle_{Av}/2J(J+1). \quad (5)$$

Thus

$$\mu=\mu_n+\mu_p-2(\mu_n+\mu_p-\tfrac{1}{2})\langle\tfrac{3}{4}+\mathbf{L}^2-\mathbf{S}^2\rangle_{Av}/3. \quad (6)$$

Now the ground state of each of the nuclei is made up of a combination of ^2S, ^2P, ^4P, and ^4D eigenfunctions and for each of these functions, $\mathbf{L}^2=L(L+1)$ and $\mathbf{S}^2=S(S+1)$. The average value of $\mathbf{L}^2-\mathbf{S}^2$ is therefore obtained by multiplying $L(L+1)-S(S+1)$ by the amount of admixture of the corresponding state, and adding. If, for simplicity, the amount of admixture is designated by the term symbol for the state, Eq. (6) becomes

$$\mu=\mu_n+\mu_p-2(\mu_n+\mu_p-\tfrac{1}{2})(3\,^4D-\,^4P+2\,^2P)/3. \quad (7)$$

Equation (7) would be most useful for obtaining an estimate of the relative contributions to the ground state of either nucleus of the states other than the ^2S state from measurements of the two magnetic moments. In the absence of such measurements, we give the value of the sum of the moments which is obtained from the results of Gerjuoy and Schwinger.[3] They found $^4D=0.04$, $^2P=\,^4P=0$. With these values, the sum of the moments is 0.849, if the moments of the neutron and proton are taken to be $^2-1.911$ and 2.790. This is to be compared to the value $\mu_n+\mu_p=0.879$ which would be expected if L-S coupling held rigorously in these nuclei.

A result similar to Eq. (7) applies to the sum of the moments of any pair of nuclei which can be obtained from each other by the interchange of protons and neutrons.

3. THE MAGNETIC MOMENTS OF H^3 AND He^3

In order to calculate the moments of H^3 and He^3, it is necessary to make some simplifying assumptions concerning the wave function of the ground state. Following Gerjuoy and Schwinger,[2] it is assumed that this function contains only ^2S and ^4D eigenfunctions and that these eigenfunctions are of a particularly simple form. The ^2S function will be taken to be that function which is antisymmetric for interchange of the spins of the two like particles. No detailed statement

concerning the spatial dependence will be required. There are four possible types of ^4D eigenfunction, of which a particularly simple one was chosen by Gerjuoy and Schwinger. The spin dependent part of this function was symmetrical in the variables $\boldsymbol{\rho}$ and $\mathbf{r}$ where

$$\boldsymbol{\rho}=\mathbf{r}_1-\mathbf{r}_2,$$
$$\mathbf{r}=\mathbf{r}_3-(\mathbf{r}_1+\mathbf{r}_2)/2. \quad (8)$$

For the calculation of the moments it is only this symmetry property that is needed. As long as the spin dependent factor in the ^4D function is either symmetric or antisymmetric in $\mathbf{r}$ and $\boldsymbol{\rho}$, it will be found that the moment is independent of the detailed spatial form of the function. Thus the functions used here are more general than those used by Gerjuoy and Schwinger, but they are not perfectly general since there is no *a priori* reason against the appearance of a combination of the symmetric and antisymmetric types of function. Nevertheless, it is felt that the simple results which will be obtained on the assumption that only one or the other type of function occurs may be useful as an indication of the magnitude of the influence of the ^4D state on the magnetic moment.

The averages indicated in Eqs. (1) and (2) contain no cross terms between the ^2S and ^4D eigenfunctions since these functions are orthogonal separately in space and spin. Therefore Eq. (1) becomes

$$\mu_H={}^2S\langle L_3^z+2\mu_n(S_1^z+S_2^z)+2\mu_pS_3^z\rangle_S$$
$$+{}^4D\langle L_3^z+2\mu_n(S_1^z+S_2^z)+2\mu_pS_3^z\rangle_D, \quad (9)$$

where the coefficients ^2S and ^4D are, as before, the squares of the amplitudes of these functions and $\langle\rangle_S$ and $\langle\rangle_D$ indicate averages over the ^2S and ^4D wave functions, respectively. Considering first the ^2S term, the orbital angular momentum makes no contribution since the S state has spherical symmetry. Of the spin terms, only the spin of the proton contributes since the assumed ^2S function is antisymmetric in the neutron spins, as stated in the beginning of the section. The value of the first term in Eq. (9) is therefore $^2S\mu_p$.

Since the three spins are parallel in the ^4D state, the expectation values of the three spins are equal. Thus

$$\langle S_1^z\rangle_D=\langle S_2^z\rangle_D=\langle S_3^z\rangle_D=\langle S^z\rangle_D/3.$$

By means of the usual vector addition rule it is found that $\langle S^z\rangle_D=-\frac{1}{2}$, so Eq. (9) becomes

$$\mu_H={}^2S\mu_p-{}^4D(2\mu_n+\mu_p)/3+{}^4D\langle L_3^z\rangle_D. \quad (10)$$

In order to evaluate the last term, it is necessary to make use of the particular symmetry properties of the ^4D function which have been assumed. In terms of the variables $\mathbf{r}_1$, $\mathbf{r}_2$, $\mathbf{r}_3$, and $\mathbf{R}=(\mathbf{r}_1+\mathbf{r}_2+\mathbf{r}_3)/3$, the orbital angular momentum operators are $\mathbf{L}_1=[(\mathbf{r}_1-\mathbf{R})\times\nabla_1 i/j]$, etc. Expressed in terms of the variables $\mathbf{r}$ and $\boldsymbol{\rho}$ given in Eq. (8), these operators satisfy the following relations:

$$\mathbf{L}_3=2(\mathbf{r}\times\nabla_r i/j)/3 \quad (11)$$

$$\mathbf{L}=\mathbf{L}_1+\mathbf{L}_2+\mathbf{L}_3=(\mathbf{r}\times\nabla_r i/j)+(\boldsymbol{\rho}\times\nabla_\rho i/j). \quad (12)$$

Because of the assumed symmetry of the ^4D function in $\mathbf{r}$ and $\boldsymbol{\rho}$, the average values of the two terms in Eq. (12) are equal.[4] Therefore $\langle\mathbf{r}\times\nabla_r i/j\rangle_D=\frac{1}{2}\langle\mathbf{L}\rangle_D$. It follows from Eq. (11) that

$$\langle L_3^z\rangle_D=\tfrac{1}{3}\langle L^z\rangle_D=\tfrac{1}{3}, \quad (13)$$

according to Eq. (5). Inserting this result in Eq. (10) and making use of the normalization condition $^2S+{}^4D=1$, we find

$$\mu_H=\mu_p-2{}^4D(\mu_n+2\mu_p-\tfrac{1}{2})/3. \quad (14)$$

The magnetic moment of He^3 can be obtained directly by subtracting μ_H from Eq. (7) with $^4P={}^2P=0$. It is

$$\mu_{He}=\mu_n-2{}^4D(2\mu_n+\mu_p-1)/3. \quad (15)$$

For L-S coupling, the magnetic moments of H^3 and He^3 would be equal to the moments of the proton and neutron, respectively. Any observed deviation from these values can be used as a measure of the amount of mixing of the ^4D state, as shown by Eqs. (14) and (15). It is to be remembered in applying these formulae that they are valid only if the contribution of P states to the ground state is negligible and, even then, only if the S and D functions have the particularly simple forms which have been assumed.

If we accept the estimate $^4D=0.04$, the magnetic moments of the nuclei are found to be $\mu_H=2.71$; $\mu_{He}=-1.86$.

[4] It is to be noted that symmetry is required only for the spin dependent factor in the function. The spherically symmetrical, space dependent factor makes no contribution to the orbital angular momentum.

PHYSICAL REVIEW VOLUME 70, NUMBERS 1 AND 2 JULY 1 AND 15, 1946

On the Theory of Ionization Yield of Radiations in Different Substances*

U. FANO
Carnegie Institution of Washington, Cold Spring Harbor, New York
(Received March 18, 1946)

The energy absorbed by a substance exposed to an ionizing radiation is used partly in ionization, partly in optical excitation. Arguments based on atomic mechanics are presented, to show that, the greater the ionization potential, the greater is the share of the absorbed energy which is actually spent in ionization. This explains why the ionization potential of a substance has little influence upon the amount of energy that must be absorbed by that substance per each pair of ions actually produced.

1. INTRODUCTION

THE over-all efficiency of a corpuscular or electromagnetic radiation in ionizing a gas is the reciprocal of the average energy spent by the radiation per ion pair produced:

$$\epsilon = V/J, \qquad (1)$$

where V is the total amount of radiation energy absorbed by a volume of gas and J is the number of ion pairs produced within this volume.

While the absorption of ionizing radiations by matter starts a complicated chain of phenomena, there are only a few comparatively simple processes that play a central rôle in the mechanism of ionization. Positive ions arise from the stripping of an electron from a molecule; this is caused most frequently by the impact of a fast charged particle against the molecule, whether the primary radiation is corpuscular or electromagnetic. The formation of positive ions with release of electrons is the essential process from the standpoint of energy balance, as negative ions are then formed with a minor release of energy when the free electrons are eventually captured by other molecules.[1]

Experimental determination[2] of ϵ for a number of gases has not yielded very consistent results; but, taken as a whole, it indicates that:

(a) ϵ is largely independent of the characteristics of the primary ionizing radiation, and of the mass, charge, and velocity of the fast charged particles (primary or secondary) whose impact is the immediate cause of the ionization.

(b) While ϵ has a different value for different gases, this value is generally of the order of magnitude of 30 ev and shows no general correlation with the ionization potential of the gas—that is, with the energy actually required to tear off an electron from a gas molecule. (For instance, ϵ is especially small for the rare gases, whereas their ionization potential is especially great.)

(c) An experiment on liquid CS_2 indicates a basic similarity between the values of ϵ in gaseous and in condensed state.[3] This result is important with respect to the action of radiations on biological materials.

Of these results, (a) has been explained theoretically, and (c) is not so unexpected as to require particular investigation at this time. On the other hand, (b) is a remarkable fact, which has important applications and which is still unexplained. Theoretical calculation of ϵ is difficult, because it requires an evaluation of the number of further ionizations produced by the electron set free in each ionization. An early estimate,[4] and a later more complete calculation,[5] using quantum-mechanical methods, gave satisfactory estimates of the order of magnitude of ϵ in general, and of its value for atomic hydrogen in particular. These theories, however, incorrectly predicted a distinct positive correlation of ϵ with the ionization potential. The present

* A preliminary report was given at a meeting of the American Physical Society, see Phys. Rev. **63**, 222 (1943).

[1] Radiation in the far ultraviolet is set apart from other ionizing radiations because it produces positive ions primarily by direct action on individual molecules. This radiation is of little practical interest, however, as it can be handled only in a vacuum; therefore it will not be considered in this paper.

[2] J. J. Thomson, *Conduction of Electricity through Gases* (1933), Vol. 2, pp. 103, 160, 237. Geiger-Scheel, *Handbuch der Physik* (1933), Vol. 22, No. 2, pp. 61, 217. W. Gerbes, Ann. d. Physik **30**, 169 (1937).

[3] F. Mohler and L. Taylor, J. Research Nat. Bur. Stand. **13**, 659 (1934).

[4] H. Bethe, Ann. d. Physik **5**, 325 (1930).

[5] E. Bagge, Ann. d. Physik **30**, 72 (1937).

paper is intended to explain this discrepancy between theory and experiment, and to show why, on the contrary, ϵ may be nearly independent of the ionization potential.

In Section 2 available theoretical data are taken as a clue to the observed behavior of ϵ. In Section 3 a discussion of earlier theories traces the cause of their shortcomings and leads to a more definite qualitative understanding of the behavior of ϵ. In Section 4 approximate expressions of ϵ are obtained in terms of optical constants. Substitution of theoretical values of these constants for H and He leads to satisfactory results; in particular, the results give a quantitative justification of the arguments used in Section 3.

2. INFORMATION OBTAINED FROM THE DISTRIBUTION OF OSCILLATOR STRENGTHS

The energy ϵ must be greater than the ionization potential I because a part of the energy absorbed by a substance is always spent for other purposes than ionization. Most of the energy thus "wasted" goes into excitation of optical levels and thus into the production of light. In order to explain how I can be especially large for a particular substance without bringing about a correspondingly large value of ϵ, it must be shown that the "wasted" energy $\epsilon-I$ is especially small in that substance.

Most of the energy of ionizing radiations is absorbed by molecules through induced dipole oscillations of their electronic charge. Lower frequency oscillations lead to excitation, those of higher frequency to ionization of the molecules. The behavior of a gas with reference to dipole oscillations is equivalent to the behavior of a mixture of different harmonic oscillators whose frequencies are the characteristic spectral absorption frequencies of the gas. All of these oscillators absorb approximately the same amount of energy under the influence of an ionizing radiation. The *proportion of oscillators* whose frequency corresponds to any particular process of energy absorption by the gas molecules is called the "oscillator strength" of that process. Therefore the sum of the oscillator strengths of all excitation processes in any substance is an index of the amount of energy spent in excitations, and may be expected to parallel the "waste" of energy incurred by radiation acting upon that substance. In the following table available theoretical information[6,7] on the oscillator strengths of excitations is compared with the value of the ionization potential, for a series of three characteristic atoms (Table I). This shows a critical inverse correlation between the total oscillator strength of excitations and the ionization potential, suggesting that the "waste" of energy $\epsilon-I$ is actually an inverse function of I. In particular, the data in the table roughly account for the small value of ϵ observed for He. This indicates that theoretical methods should be available for an improved calculation of ϵ.

3. QUALITATIVE DISCUSSION

Arguments will be presented, in the various subdivisions of this section, which lead, respectively, to the following conclusions: (a) The simple "hydrogen-like" approximation of atomic mechanics implies a detailed similarity between different atoms and thus leads to the incorrect prediction of a positive correlation between ϵ and I. (b) Bagge's calculation of ϵ involves the same type of shortcoming as the simple hydrogen-like approximation. (c) Important departures from similarity between atoms act to suppress the correlation between ϵ and I. (d) A qualitative theory of the observed behavior of ϵ follows from a type of hydrogen-like approximation which takes into account the effect of outer screening.

(a)

Bethe's calculation[4] of ϵ is based upon his own theory of the excitation and ionization of molecules by fast charged particles. This theory, which applies primarily to atomic hydrogen, is adjusted for approximate application to other

TABLE I.

Substance	H	He	Li
I(ev)	13.5	24.5	5.4
Oscillator strength of all excitations	57%	21%	88%

[6] Geiger-Scheel, *Handbuch der Physik* (1933), Vol. 24, No. 1, pp. 443, 467.
[7] J. A. Wheeler, Phys. Rev. **43**, 258 (1933).

molecules by treating each molecular electron as though it belonged to a hydrogen-like atom. In the application to He, for example, each of the two electrons is assumed to behave as though it belonged to a hydrogen-like atom of "effective atomic number" $\mathbf{Z}=1.35$. This value is so chosen that the ionization potential $I=\mathbf{Z}^2Ry$ (Ry = Rydberg's energy = 13.5 ev) will coincide with the experimental value 24.5 ev. The difference between the actual atomic number of He, $Z=2$, and the effective number $\mathbf{Z}=1.35$ is assumed to take care of the repulsion of the two atomic electrons.

A hydrogen atom and a hydrogen-like atom are thus treated as "dynamically similar" systems, in which all corresponding lengths (e.g., the atomic radii) are in a ratio of 1 to $1/\mathbf{Z}$ and all corresponding energies (e.g., the ionization potentials) are in a ratio of 1 to $\mathbf{Z}^2$. All dimensionless quantities, on the other hand, have the same value in two similar systems; such are the total oscillator strength of all excitations, the ratio of the cross sections for excitation and ionization of the atom by an impinging particle, and the ratio ϵ/I, which is the object of the present study. Bethe's theory is thus bound to yield equal values of all these quantities for all atoms and molecules; in particular, it yields a proportionality between ϵ and I. None of these results agrees with the experimental evidence. Indeed, the large difference between the theoretical values of the oscillator strengths exhibited in Section 2 shows that similarity is a characteristic of the hydrogen-like approximation which is not preserved by the more accurate methods.

(b)

Some comments may be added concerning Bagge's calculation of ϵ,[5] based on the Thomas-Fermi instead of the hydrogen-like model. Since the ionization potential given by the Thomas-Fermi model is a smooth function of the atomic number, a function which does not account for the individual properties of the elements, the theoretical ionization potential of each molecule is replaced in Bagge's calculation by the corresponding experimental value. This procedure is akin to the adjustment of the effective atomic number in the hydrogen-like approximation to yield the correct ionization potential, and therefore it leads to the same incorrect prediction, namely, a positive correlation between ϵ and I.

(c)

A comparison of the ground state and of the excited states of H and He shows a striking departure from dynamic similarity between the two atoms. The binding energies of the electron, as well as the atomic radii of H and He in excited states of equal quantum number, are very nearly equal, since the repulsion of the excited electron in He by the second electron, which remains in the ground state, offsets almost completely the greater attraction exerted by the double nuclear charge. In the ground state of He, on the contrary, the two electrons are, on the average, equally distant from the nucleus; hence their repulsion offsets only a small part of the double nuclear charge, so that the binding energy is far larger and the atomic radius far smaller than the corresponding quantities for H in the ground state.[8]

In general, the binding energy of an electron in an excited state and the radius of its orbit are smooth, slowly varying functions of the atomic number; while for outer electrons in the ground state the binding energy and the orbital radius undergo sharp variations, depending upon the number of electrons in the outermost shell of each atom. As the number of electrons in the outermost shell is increased, the binding energy of each of these electrons (i.e., the ionization potential of the atom) is increased and the radius of the whole atom in the ground state is decreased, but no correspondingly large variation is observed for the excited states.

In the hydrogen-like approximation, which preserves similarity, dimensionless quantities are independent of the ionization potential. Actually, the larger the ionization potential the larger is, in general, the ratio of the binding energy of the outermost electron in the ground state to its binding energy in the first excited state, and the

[8] A fair description of the ground state of He uses for each electron a hydrogen-like wave function with $\mathbf{Z}=27/16=1.6875$ (compare with $\mathbf{Z}=1.35$ above), while $\mathbf{Z}=1$ should be taken for the wave function of an excited or ionized p electron. The use of different values of $\mathbf{Z}$ for the ground state and for the excited states of atoms has been suggested, for example, by D. R. Bates (Roy. Astronom. Soc. M. N. **100**, 23 (1939)) with reference to the photo-ionization of different gases.

smaller the ratio of the corresponding orbital radii. It may, then, be expected that this lack of similarity should also involve variations of those other dimensionless quantities that are important in the calculation of ϵ—namely, the total oscillator strength of all excitations, the ratio of the cross sections for excitation and for ionization of a molecule by an impinging particle, and the ratio ϵ/I itself. All these quantities are of course directly related to each other. Furthermore, it seems reasonable that they should also be directly related to the ratio of the atomic radii in the ground state and in the excited states. Hence, all of them should be inversely related to the ionization potential I. This conclusion explains qualitatively why the quantity $\epsilon = I \times (\epsilon/I)$ should be little affected by variations of I.

(d)

These general arguments will now be made a little more specific by using a form of hydrogen-like approximation which takes into account the lack of similarity between different atoms. In Bethe's treatment, the repulsion exerted on one electron (k) by all other electrons of the same atom was taken into account by replacing the actual atomic number Z, which characterizes the nuclear attraction, with a lower "effective number" $\mathbf{Z} = Z - s$. The number s is called "inner screening number." It represents the average effect of offsetting—or "screening"—of the nuclear charge by that part of the electronic cloud which is nearer to the nucleus than the electron k, and thus acts to keep k away from the nucleus. Taking into account the inner screening only, it is found that the binding energy of the electron k should be $\mathbf{Z}^2 Ry$; or, more generally,

$$\text{binding energy} = \mathbf{Z}^2 Ry/n^2, \qquad (2)$$

if the electron is in a state of total quantum number n. Consideration will be given now to the "outer screening" effect due to that part of the electronic cloud which is farther away from the nucleus than the electron k. The average repulsion of this part of the cloud affects the electron k like an outer screening, i.e., like an outer electrically charged shell. Such a charged shell does not exert any electric force upon a charge in the interior of the shell, where the electron is, but establishes a negative potential difference of $-S$ volts between the interior of the shell and external points at infinite distance. The effect of this potential difference becomes apparent if one tries to remove the electron from the atom: as soon as the electron passes to the exterior of the outer screening shell the charge of this shell exerts a repulsive force and thus helps to remove the electron. This effect causes the binding energy of the electron to be reduced by the product of the potential difference S and of the electronic charge e. Hence (2) must be replaced by

$$\text{binding energy} = \mathbf{Z}^2 Ry/n^2 - eS. \qquad (2')$$

The outer screening effect upon an optical electron[9] is negligible in the case of alkali atoms. However, when there are many electrons in the outermost shell, they interact with one another partly by inner but also partly by outer screening. In this case the effect of outer screening (i.e., S) becomes comparatively large at the expense of the effect of inner screening (i.e., s); and so it happens that, as a rule, all three quantities—the ionization potential I, $\mathbf{Z} = Z - s$, and S—are directly related to each other. S varies even more sharply than I and $\mathbf{Z}$: it is more than half as large as I in the case of He, while it vanishes for H.

For qualitative purposes, the excitation or ionization of an atom or molecule may be resolved into two phases. In the first phase, an electron in the outer shell absorbs energy as if it belonged to a hydrogen-like atom with atomic number $\mathbf{Z} = Z - s$. The average energy absorbed by the electron under the impact of a charged particle is directly related to $\mathbf{Z}^2$; hence it is even greater when $\mathbf{Z}$ is related to the given binding energy I by formula (2′) than when it is related by formula (2). In the second phase, the electron uses its newly acquired energy to move farther away from the nucleus (or nuclei); energy absorptions that would only be sufficient to excite a hydrogen-like atom with atomic number $\mathbf{Z}$ may then result in ionizations, owing to the effect of outer screening which reduces the binding energy. The greater S, therefore, the greater will be the comparative frequency of ionizations.

[9] Internal electrons are infrequently affected by the impact of fast charged particles and hence are not considered in this connection.

The behavior of ϵ as a function of the atomic number can thus roughly be described as follows. Within any single row of the periodic system, the number of electrons in the outermost shell increases from left to right; and thus, as indicated above, the ionization potential I and the corresponding value of S also increase at the same time. Hence the comparative frequency of excitations decreases with increasing I in such a way as to reduce the "waste" of energy. In the transition from one row to the next along the first column of the periodic system the ionization potential decreases; but at the same time the total quantum number increases, and this in turn is known[4] to increase the "waste" of energy. The variations of ionization potential and of energy waste appear thus to be generally correlated in such a way as to minimize the variations of ϵ.

4. APPROXIMATE CALCULATION OF ϵ

It is proposed here to calculate an approximate expression for ϵ suitable for a quantitative test of the qualitative considerations presented in the previous sections. The calculation will be conducted with particular reference to H and He but may be applicable, with suitable changes, to other substances as well. One basic assumption will be carried over from Bethe's theory:[4] namely, that particles of different charge, mass, and velocity are equally efficient in producing ionizations, provided that they are capable of ionizing at all. The accuracy of this assumption will be discussed on the basis of the results to be obtained.

The total cross section σ for inelastic impacts of a charged particle against an atom will be separated into three parts: (a) σ_e refers to inelastic impacts leading to excitation only; (b) σ_{i1} refers to impacts which lead to ionization and in which the residual energy of the ejected electron is less than the ionization potential I of the atom; and (c) σ_{i2} refers to impacts which lead to ionization and in which the residual energy of the ejected electron exceeds I. The average energy lost by the impinging particle in an impact type (a) or type (b) will be indicated by E_e or E_{i1}. The electron ejected in an impact of type (c) is capable of ionizing further atoms; moreover, according to the assumption made, its kinetic energy is used to produce ionizations with the same efficiency as the energy of the impinging particles. This kinetic energy ($E_{i2}-I$ on the average) is thus merely transferred from one particle to another, which makes little difference to the over-all production of ionizations. Hence the calculation of ϵ may be carried out *as though* the kinetic energy $E_{i2}-I$ were not lost by the impinging particle; that is, as though the impinging particle lost only the energy I in any impact of type (c). The energy ϵ absorbed per ion pair produced can then be expressed thus:

$$\epsilon=(\sigma_e E_e+\sigma_{i1}E_{i1}+\sigma_{i2}I)/(\sigma_{i1}+\sigma_{i2}). \qquad (3)$$

In the case of atomic H, sufficient theoretical numerical data are available[10] for a quantitative evaluation of this result. One finds

$$\epsilon\sim 36 \text{ ev}$$

in the case of impinging electrons of 10 kv, and $\epsilon\sim 37$ ev for 100-kv electrons. Since experimental data are not available for atomic H, comparison is limited to observing that this value is near the experimental values of ϵ for most substances. It is also only 8 percent greater than Bagge's corresponding theoretical value.[5] The agreement is therefore not unsatisfactory.

In the case of substances other than H, it is not easy to apply the standard theory of inelastic impacts in sufficient detail to provide good numerical data for evaluating (3). It seems advisable, therefore, to simplify this theory in order to obtain more workable equations. Inelastic impacts of charged particles are conveniently classified according to the change of momentum (and hence the deflection) undergone by the particle. Impacts with a small momentum change are loosely identified with those in which the particle interacts with an atom while passing far outside of it ("grazing impacts"). In cases of extremely small change of momentum, the perturbation exerted by the particle on the atom consists of an electromagnetic pulse of short duration. It is therefore equivalent to the perturbation exerted by a continuous spectrum of electromagnetic radiation of uniform intensity (like a continuous x-ray spectrum), and hence it induces dipole oscillations within the atom.

[10] Geiger-Scheel, *Handbuch der Physik* (1933), Vol. 24, No. 1, pp. 517 and 519.

Dipole oscillations seldom result in the ejection of an electron having great residual energy. Impacts with large changes of momentum are loosely identified with those in which the impinging particle passes very near to an atomic electron ("head-on impacts"). The atomic electron then acts much as if it were free, and usually receives a large amount of energy. The relative probability of different types of impacts is inversely related to the change of momentum involved: grazing impacts are much more probable, head-on impacts much less probable.

First Approximation

For purposes of orientation, a drastic simplification will be made by assuming that only the extreme type of grazing impacts (involving a very small change of momentum) occurs with any considerable frequency. The circumstance that some of these impacts result in the ejection of an electron with sufficient residual energy to produce further ionizations will be disregarded; that is, the entire cross section for ionization will be taken as σ_{i1}, and it will be assumed that $\sigma_{i2}=0$.[11]

The probability of transition of an atom from the ground (0th) state to the jth excited or ionized state is then proportional to the square of the dipole matrix element $x_{j0}=\int\psi_j x\psi_0 d\tau$ associated with this transition. This matrix element will be assumed, for simplicity, to be real and will be expressed in terms of the atomic unit $a=0.53\times10^{-8}$ cm. Hence,

$$\begin{aligned}\sigma_e&=\text{const.}\sum_{ej}x_{j0}^2,\\ \sigma_{i1}&=\text{const.}\sum_{ij}x_{j0}=\text{const.}\times x_i^2,\end{aligned}\tag{4'}$$

where the first sum is over excited states, the second over ionized states. The latter is actually an integration and its value is denoted by x_i^2. Moreover,

$$\begin{aligned}\sigma_e E_e+\sigma_{i1}E_{i1}&=\text{const.}\sum_j h\nu_{j0}x_{j0}^2\\ &=\text{const.}\,h^2/8\pi^2ma^2\sum_j f_{j0}\\ &=\text{const.}\times Ry.\end{aligned}\tag{4''}$$

(As usual, ν_{j0} and f_{j0} indicate, respectively, the oscillation frequency and the oscillator strength of the transition from 0 to j; $\sum_j f_{j0}=1$, according to Thomas-Kuhn's sum rule; and $Ry=h^2/8\pi^2ma^2$ is Rydberg's energy.) The first approximation for ϵ is then

$$\epsilon_1=(\sigma_e E_e+\sigma_{i1}E_{i1})/\sigma_{i1}=Ry/x_i^2.\tag{4}$$

For atomic H, $x_i^2=0.283$ [12] and hence $\epsilon_1=48$ ev, that is about 35 percent in excess of the value obtained above. Since the frequency of excitations, and hence the "waste" of energy, are comparatively greatest in the case of grazing impacts, it was expected that (4) would yield too great a value of ϵ_1. In general, all the errors involved in the assumption made tend to increase the resulting value of ϵ_1.

In the case of He, x_i^2 has been calculated by using hydrogen-like wave functions with $\mathbf{Z}=27/16$ for the ground state and $\mathbf{Z}=1$ for the excited and ionized states.[8] (This method involves the use of one-electron wave functions that do not belong to a single orthogonal system; this means disregarding the two-electron transitions which, however, are unimportant.)[13] The result is $x_i^2=0.256$, $\epsilon_1=53$ ev. The difference between these results and the ones obtained for H appears to be very small, considering that if the single value $\mathbf{Z}=1.35$ had been used for all states the results would have been $x_i^2=0.156$, $\epsilon_1=87$ ev. The inaccuracy of our method did not seem to warrant the use of better wave functions.

Since x_i^2 is the characteristic of an atom that determines the value of ϵ_1, we should supplement the qualitative considerations of Section 3 by investigating why the difference between the values of x_i^2 for H and for He is so small. x_i^2 was therefore calculated as a function of the parameter $\mathbf{Z}$ characterizing the ground state, while $\mathbf{Z}$ for the ionized states was kept equal to 1. The results are shown in Table II. The third line shows the ratio of $x_i^2=\sum_{ij}x_{j0}^2$ to $x^2{}_{kk}=\sum_j x_{j0}^2=1/\mathbf{Z}^2$. ($x^2{}_{kk}$ is the mean value of x^2 for an electron in the ground state.) This ratio represents the proportion of all inelastic impacts that produce ionizations; and it increases from 0 to 1 as $\mathbf{Z}$ increases from 0.5 to ∞. The total fre-

[11] Actually, σ_{i2} should include about 14 percent of the cross section for ionization in the case of H, 24 percent in the case of He.

[12] Geiger-Scheel, *Handbuch der Physik* (1933), Vol. 24, No. 1, p. 442.

[13] J. P. Vinti, Phys. Rev. **42**, 632 (1932).

quency of inelastic impacts, proportional to x^2_{kn}, is steadily decreasing as $\mathbf{Z}$ increases. Therefore, the frequency of ionizations, proportional to x_i^2, shows a maximum which happens to occur at a value of $\mathbf{Z}$ intermediate between those corresponding to H and He. If a single value of $\mathbf{Z}$, determined on the basis of (2), were used for the ground state and the ionized states, the ratio would be fixed at .283, and both x_i^2 and x^2_{kn} would be inversely proportional to $\mathbf{Z}^2$, i.e., to I.

As a further supplement to the discussion at the end of Section 3, it should be noted that the average energy lost by the impinging particle in an inelastic impact is $Ry/x^2_{kn}=Ry\mathbf{Z}^2$ (cf. (4′) and (4″)), and is equal to I or $I+eS$, depending on whether $\mathbf{Z}^2$ is related to I by (2) or by (2′); note that $n=1$, in the case of He. Thus as a direct effect of the outer screening—i.e., of the energy term eS—the average energy lost in an impact becomes greater than the ionization potential; this clearly increases the comparative frequency of ionizations.

The value of $\mathbf{Z}$ to be entered in (2′), and hence the wave function to be used, can best be determined for the ground states of substances other than H and He on the basis of Slater's rules.[14] No similar rules seem to be available, however, for determining the wave functions of the ionized states.

Details of the calculation of dipole matrix elements are given in an appendix.

Second Approximation

Head-on inelastic impacts, in addition to grazing impacts, will now be taken into account; but every impact will be considered as belonging to one extreme type—i.e., as being either typically grazing or typically head-on. This approximation is still quite rough, but it yields values for the total cross sections for ionization or for excitation of H atoms that are close to those obtained by more accurate methods. Also, its results do not appear to depend critically upon the position of the boundary which must be assumed to separate grazing from head-on impacts. In this calculation it will be assumed that an impact is grazing or head-on, according to whether the change of momentum undergone by the impinging particle is smaller or greater than $(2mI)^{\frac{1}{2}}$. Furthermore, it will now be taken into account that $\sigma_{i2}\neq 0$ for grazing as well as for head-on impacts.

The cross section σ_{j0} for induced transition of an atom from the ground to the jth state is then separated into two parts, $\sigma_{j0}^{(g)}$ and $\sigma_{j0}^{(h)}$, corresponding to grazing or head-on impacts. On the basis of Born's approximation,[15] one finds approximately:

$$\sigma_{j0}^{(g)}=(kx_{j0}^2\log r)/Ry, \quad \sigma_{j0}^{(h)}=k/(h\nu_{j0})^2, \tag{5′}$$

except that $\sigma_{j0}^{(h)}$ vanishes unless the jth state is ionized. In these formulae $k=2\pi z^2e^4/mv^2$ (e and m are charge and mass of an electron, ze and v are charge and velocity of the impinging particle), and $r=2mv^2/I$; r should depend on the index j, but this has been disregarded. On the basis of the analogy with (4′), it follows easily that:

$$\begin{gathered}\sigma_e^{(g)}E_e^{(g)}=kf_e\log r, \quad \sigma_{i1}^{(g)}E_{i1}^{(g)}=kf_{i1}\log r, \quad \sigma_{i2}^{(g)}I=k(I/Ry)x_{i2}^2\log r,\\ \sigma_e^{(h)}E_e^{(h)}=0, \quad \sigma_{i1}^{(h)}E_{i1}^{(h)}=k\log 2, \quad \sigma_{i2}^{(h)}I=k/2,\\ \sigma_{i1}^{(g)}+\sigma_{i2}^{(g)}=(kx_i^2\log r)/Ry, \quad \sigma_{i1}^{(h)}+\sigma_{i2}^{(h)}=k/I,\end{gathered} \tag{5″}$$

where the meaning of the indices (g), (h), e, $i1$, $i2$ is the same as used elsewhere in this section. According to (3), (4), (5′), and (5″), the second approximation to the value of ϵ can then be written as:

$$\begin{aligned}\epsilon_2&=\frac{kf_e\log r+kf_{i1}\log r+k\log 2+k(I/Ry)x_{i2}^2\log r+k/2}{kx_i^2\log r/Ry+k/I}\\ &=Ry/x_i^2\frac{(f_e+f_{i1}+x_{i2}^2I/Ry)\log r+1.2}{\log r+Ry/x_i^2I}=\epsilon_1\frac{1-(f_{i2}-x_{i2}^2I/Ry)+1.2/\log r}{1+\epsilon_1/I\log r}.\end{aligned} \tag{5}$$

[14] J. C. Slater, Phys. Rev. **36**, 57 (1930).
[15] Geiger-Scheel, *Handbuch der Physik* (1933), Vol. 24, No. 1, pp. 493 ff.

TABLE II.

Z	0.5	1.0	1.2	1.4	1.6	1.6875	1.8	2.0	$\gg 1$
x_{i2}^2	0	0.283	0.313	0.299	0.271	0.256	0.238	0.207	$1/Z^2$
x_{i2}^2/x_{hy}^2	0	0.283	0.450	0.587	0.693	0.730	0.772	0.828	1

This formula includes two separate corrections to the first approximation: (a) The term in parentheses in the numerator of the final expression takes into account the fact that some of the electrons ejected through dipole oscillations are capable of further ionizing action. (b) The remaining part of the final expression indicates that ϵ_2 is the weighted mean of the quantity $\epsilon_1[1-(f_{i2}-x_{i2}^2 I/Ry)]$—the value of ϵ corresponding to grazing impacts only—and of the quantity $1.2I$—the value of ϵ corresponding to head-on impacts only; the "weights" of head-on and grazing impacts are in the ratio of their frequencies—namely, $\epsilon_1/I \log r$ to I. The following approximate numerical data may be used to calculate ϵ_2 in the case of 10 kv electrons impinging on H or He (relativistic corrections are required in the case of 100 kv electrons) (Table III). Correction (b) is less important for He than for H, because of the larger value of I; but at the same time the "outer screening" again becomes effective by greatly increasing the importance of correction (a).

Incidentally, formulae (4) and (5) show why ϵ is largely independent of the physical characteristics of the impinging particle. In the first approximation (grazing impacts only), the action of the particle is equivalent to the action of a continuous spectrum of electromagnetic radiation, and ϵ_1 is wholly independent of the mass, charge, and velocity of the particle. In the second approximation, the velocity of the particle determines the parameter r, which in turn affects, through a logarithmic factor only, the weight of correction (b). Formula (5) shows that this influence of the velocity is directed towards making ϵ_2 greater for faster particles. The ionizing secondary electrons (whose residual energy exceeds I) are generally not very fast, and hence they should be more efficient in ionizing than the primary particle. This consideration introduces a further corrective factor that cannot be easily calculated but must reduce ϵ to below ϵ_2. It must also be emphasized that our calculation has been based entirely on Born's approximation to the theory of inelastic impacts; this approximation is not accurate when applied to comparatively slow secondary ionizing electrons, so that any assumption as to the ionizing efficiency of secondary electrons is necessarily tentative.

The calculation shown in this section does not bring the theoretical value of ϵ for He into close agreement with its experimental value, which is less than 30 ev.[2] It indicates, however, that the effect of outer screening discussed in Section 2 is of sufficient importance to cancel the effect of the difference between the ionization potentials of H and of He. The rough simplifications introduced into the theory of inelastic impacts do not seem to have appreciably affected the result; since, in the case of 10 kv electrons impinging on H, the same result is found by using (5) as by evaluating (3) on the basis of Bethe's numerical data.

APPENDIX

The computation of dipole matrix elements, using hydrogen-like wave functions with different values of $\mathbf{Z}$ ($\mathbf{Z}_g$ and $\mathbf{Z}_e=\mathbf{Z}_g/\alpha$) for the ground state and for the excited states, can be easily carried out if the wave functions are expressed by means of the confluent hypergeometric function. The result for a $1s$ to np transition is:

$$x_{n1}^2=(1/\mathbf{Z}_e^2)(2^8/3)\alpha^3(2\alpha-1)n^7(n^2-1)$$
$$\times(n\alpha-1)^{2n-6}/(n\alpha+1)^{2n+6} \text{ atomic units.}$$

This formula was used in the computations for He with $\mathbf{Z}_e=1$, $\alpha=27/16$. The sum of the squares

TABLE III.

	H	He
f_{i2}	0.10	0.35
x_{i2}^2	0.04	0.06
I/Ry	1.0	1.81
$f_{i2}-x_{i2}^2 I/Ry$	0.06	0.24
$\log r$	8.0	7.4
ϵ_2	36 ev	38 ev

of the matrix elements for the ionized states of the p series is then given by:

$$(x^2)_{11}-\sum_2^\infty x_{n1}^2=1/\mathbf{Z}_g^2-\sum_2^\infty x_{n1}^2,$$

where the summation over n converges rapidly. The use of this formula relies on the fact that the set of p wave functions, considered as functions of the distance from the nucleus, forms a complete system.

A different method may be suggested here for calculating dipole matrix elements by means of properly adjusted hydrogen-like wave functions. For an electron in the region where the wave functions of the ground state and of the excited states overlap, the inner screening number s is likely to be nearly $Z-1$; therefore it should not be proper in this problem to use a value of $\mathbf{Z}(=Z-s)$ much different from 1. On the other hand, even with the restriction $\mathbf{Z}=1$, it is still possible to adjust the binding energies and the atomic radii for each state by introducing a suitable potential term A/r^2. Indicate, then, the ionization potential of an atom—i.e., the binding energy of an electron in the outermost shell—by $Ry/\mathbf{n}_g^2$, and the binding energy of an electron in the first excited state of a series of $Ry/\mathbf{n}_e^2$. Since the behavior of the wave functions in the interior of the atom is not very important for our purpose, it may be assumed that the radial parts of the wave functions of these states have no node. Hence the "effective total quantum number" $\mathbf{n}$ may be written in the form $l+1+1$, where l is the actual azimuthal quantum number and 1 is an additional effective azimuthal quantum number which defines the additional potential term $(h^2/8\pi^2 m)1(1+1)/r^2$. The binding energy of the $(p+1)$th term of the excited series is then $Ry/(\mathbf{n}_e+p)^2$. The square of the dipole matrix element for the transition from the ground state to this state is:

$$x_{\mathbf{n}_e+p,\,\mathbf{n}_g}{}^2=\frac{l'}{2l_g+1}\,\frac{\Gamma(2\mathbf{n}_e+p)}{p!\Gamma(2\mathbf{n}_g)}\exp\{2(\mathbf{n}_g+\mathbf{n}_e)\log 2-\log 3+2(\mathbf{n}_e+1)\log\mathbf{n}_g+2(\mathbf{n}_g+1)\log(\mathbf{n}_e+p)-2(\mathbf{n}_g+\mathbf{n}_e+2)\log(\mathbf{n}_g+\mathbf{n}_e+p)\}\left[\frac{\Gamma(\mathbf{n}_g+\mathbf{n}_e+2)}{\Gamma(2\mathbf{n}_e)}\times F\left(-p,\,\mathbf{n}_g+\mathbf{n}_e+2,\,2\mathbf{n}_e,\,\frac{2\mathbf{n}_g}{\mathbf{n}_g+\mathbf{n}_e+2}\right)\right]^2,$$

where l' is equal to l_g or to l_e, whichever is larger and where F indicates the hypergeometric function. The factor in square brackets can be also indicated by:

$$\sum_\nu\binom{p}{\nu}(\Gamma(\mathbf{n}_g+\mathbf{n}_e+2+\nu)/\Gamma(2\mathbf{n}_e+\nu))\times(-2\mathbf{n}_g/(\mathbf{n}_g+\mathbf{n}_e+p))^\nu.$$

The sum of the squares of the matrix elements for the ionized states of the series is given by:

$$(l'/(2l_g+1))(x^2)_{\mathbf{n}_g\mathbf{n}_g}-\sum_0^\infty x_{\mathbf{n}_e+p,\,\mathbf{n}_g}{}^2=(l'/(2l_g+1))\mathbf{n}_g{}^2(\mathbf{n}_g+1/2)(\mathbf{n}_g+1)/3-\sum_0^\infty x_{\mathbf{n}_e+p,\,\mathbf{n}_g}{}^2.$$

The Absorption of One-Half Centimeter Electromagnetic Waves in Oxygen*

ROBERT BERINGER
Radiation Laboratory, Massachusetts Institute of Technology, Cambridge, Massachusetts

(Received April 5, 1946)

The absorption of electromagnetic waves in the one-half cm wave-length range has been measured for O_2 and O_2-N_2 mixtures as a function of pressure. The apparatus employs a klystron oscillator, crystal-rectifier frequency-multiplier, wave guide absorption path, and crystal detector. The measured values are in agreement with the theory of Van Vleck both as regards the absolute value of the absorption (which is as great as 67 db/km at the band center for pure O_2 at a pressure of one atmosphere) and the dependence on pressure.

THE development of radiofrequency sources and techniques in the centimeter wave-length range has made possible the observation of gaseous resonance phenomena of considerable interest in molecular structure.[1] In addition there is an engineering interest in these processes since they affect the propagation of centimeter waves in gaseous media. The present paper is a part of studies concerned with the absorption of atmospheric gases in their relation to the development and use of microwave radar.

The ½ cm O_2 absorption band was investigated theoretically in 1942 by Van Vleck.[2] The magnetic dipole moment of the $^3\Sigma$ ground state of O_2 couples with electromagnetic waves to give (a) a band of resonant absorption lines in the region of 2 cm^{-1} corresponding to the rotational transitions $J \rightarrow J \pm 1$ in a large number of spin triplets thermally excited at room temperatures and (b) a non-resonant absorption band corresponding to $\Delta J = 0$, arising because the lifetime of the states against collision is of the order of the incident wave periods. The absorption coefficients of both of these contributions were calculated with a single undetermined parameter: the lifetime or line breadth[3] of the excited states ($\Delta\nu/c$ in cm^{-1}). The experiments reported here were carried out in 1944[4] to determine this line breadth.

EXPERIMENTAL APPARATUS

The experimental arrangement consisted of a source of ½-cm radiation, and absorption path into which gas mixtures could be introduced, and a detector of the transmitted radiation. Changes in the detected signal were measured to determine the absorption when gases were introduced. For the most part this apparatus was an obvious extension of techniques developed in this laboratory for somewhat longer wave-lengths.

The source of ½-cm radiation was a silicon-tungsten crystal detector operated as a generator of the second harmonic of signals produced by a 1-cm oscillator. These 1-cm signals were introduced into the crystal *via* a coaxial line and the ½-cm harmonic was extracted with a wave guide circuit. This is shown in Fig. 1. The plunger and sliding "line-stretcher" are adjustments for maximizing the radiation of ½-cm power into the wave guide. The chokes in the coaxial line prevent ½-cm signals from entering the oscillator tube. The efficiency of these harmonic generators (available ½-cm power ÷ available 1-cm power) was at most 10 percent.

The oscillator tubes were designed and built by H. V. Neher, G. A. Hobart, and C. Z. Nawrocki in this laboratory.[5] They were reflex klystrons operating with accelerator voltages in the range of 2 kv, and were similar, except for oscillation frequency, to the type A-5022A klystrons later manufactured by the Radio Corporation of America. In all, four tubes were used to cover the wave-length range 0.96 cm to 1.25 cm. The accelerator, focusing, reflector, and heater volt-

* This paper is based on work done for the Office of Scientific Research and Development under contract OEMsr-262 with Massachusetts Institute of Technology.

[1] For example, the NH_3 resonance: C. E. Cleeton and H. H. Williams, Phys. Rev. **45**, 234 (1934).

[2] Radiation Laboratory Report 43-2 (April 27, 1942) and Radiation Laboratory Report 664 (March 1, 1945).

[3] The line breadth $\Delta\nu$ sec.$^{-1}$ used here is one-half of the total line breadth at half-maximum.

[4] Radiation Laboratory Report 684 (January 26, 1945).

[5] H. V. Neher, Radiation Laboratory Report IV-8S (March 1, 1942).

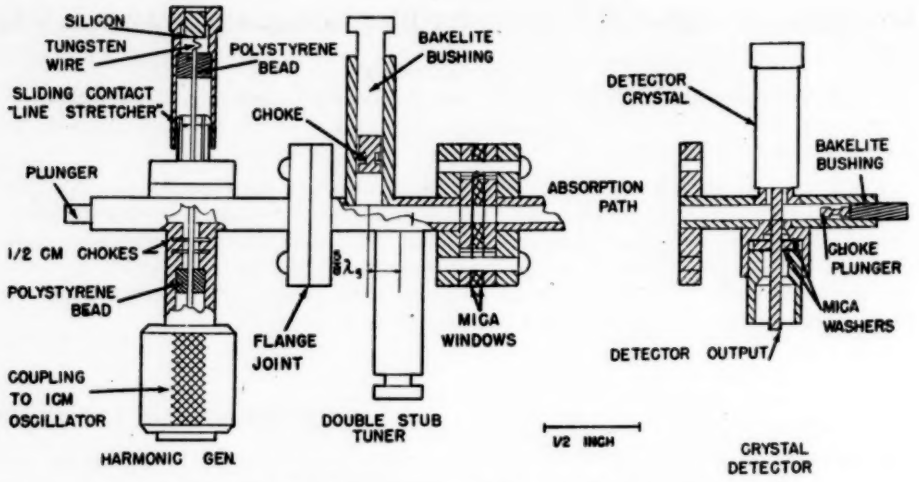

FIG. 1. Details of components of the absorption apparatus.

ages were derived from an electronically regulated power supply of conventional design. With ordinary precautions the power output from a tube (2 to 10 milliwatts) was stable to about 0.1 percent and the oscillation frequency was stable to about one part in 2000 over short (one-minute) time intervals.

The absorption path was a 6.19-meter length of rectangular, coin silver, wave guide[6] of internal dimensions 0.086 inch×0.180 inch. It was provided with a double mica window at each end (see Fig. 1). Joints were waxed. A small hole in the side of the wave guide permitted evacuation and the introduction of gas from a system including manometers, storage flasks, and a commercial fore-pump.

The detector of the transmitted radiation was a silicon-tungsten crystal in a coaxial cartridge which was mounted in a wave guide circuit provided with adjustments for maximizing the detected signal. These crystals were assembled of boron-doped silicon slabs (0.003 percent Boron), prepared by M. Fox and C. S. Pearsall[7] in this laboratory, and sharply pointed 0.0015-inch tungsten wires (electrolytically etched points, 1 min. in 10 *N* KOH at 6 volts a.c.). The wire was formed into a U shaped spring, the point brought into contact with the silicon, pressed against it with a force corresponding to a 0.001-inch spring deflection, and the unit set permanently in that position. No tapping was used.

A wave meter, consisting of a micrometer driven plunger in round wave guide (TE_{11} mode) of known diameter (0.1495 inch) was used to measure the $\frac{1}{2}$-cm wave-lengths λ. This was mounted behind the detector and tuned to successive resonances indicated by zero detector signal. These are spaced $\lambda g/2$ apart in plunger displacement, where $\lambda g=\lambda/[1-(\lambda/\lambda c)^2]^{\frac{1}{2}}$ and $\lambda c=1.706\times$(diameter) for the TE_{11} mode.[8]

The $\frac{1}{2}$-cm source was modulated with a 1000-cycle/sec. oscillator (20 percent modulation) to produce an audiofrequency detector output. This was done because the d.c. output from a crystal detector contains very much larger noise fluctuations than does the output at audiofrequencies. The 1000-cycle/sec. detected signal was amplified in a three-stage triode amplifier of conventional design followed by another ampli-

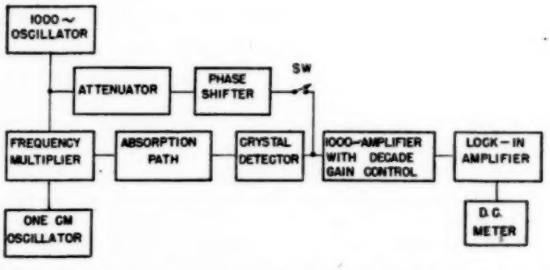

FIG. 2. Schematic diagram of the absorption apparatus.

[6] Manufactured by Horton-Angell Company, Attleboro, Massachusetts.

[7] M. Fox, C. S. Pearsall, and V. Powell, Radiation Laboratory Report 501 (December 21, 1943).

[8] S. Ramo and J. R. Whinnery, *Fields and Waves in Modern Radio* (John Wiley and Sons, Inc., New York, 1944), page 403.

fier having a coherent or "lock-in" mixer as the output stage. Such mixers are sensitive to a very narrow band of signal frequencies (about 5 cycle/sec. wide in this case), and so the noise background is reduced. The mixer output was measured with a d.c. milliammeter.

EXPERIMENTAL METHOD

The experimental arrangement is shown in Fig. 2. It operates as follows: with *SW* open the meter reading is proportional to the ½-cm power incident on the detector. Denote this reading by e. When absorbing gas is introduced, the meter reading changes by an amount Δe, proportional to the absorption and to the original incident power. Thus $\Delta e/e$ is a measure of the absorption.

In practice the deflection Δe is magnified by closing *SW* and adjusting the phase and amplitude of the 1000-cycle/sec. balancing signal for zero output reading. The amplifier gain is then raised by a known factor and Δe is magnified by this factor. The precision to which $\Delta e/e$ can be measured is determined by spontaneous fluctuations, about 0.1 percent for the apparatus described. These fluctuations were largely attributed to tube and circuit noise present because of the high gain of the amplifier system which was necessary because of the low efficiency of the harmonic generator and the large ohmic losses in the wave guide path (12 db or a factor 16 for 0.50 cm signals).

The degree to which a medium absorbs radiation is usually denoted by an absorption coefficient γ (absorption per unit length) defined by $I=I_0\exp(-\gamma x)$, where I and I_0 are the intensities (energy/sec.) of a plane wave in the medium at x and at $x=0$, respectively. The absorption coefficient can also be expressed in decibels (db) per unit length defined by $A=(10/x)\log_{10}(I_0/I)=(4.343\cdots)\gamma$. In terms of the measured quantity, $\Delta e/e$, this latter absorption coefficient is[9]

$$A=-\frac{\lambda}{\lambda g}\frac{10}{6.19(10)^{-3}}\log_{10}\left(1-\frac{\Delta e}{e}\right)\text{ db/km}, \quad (1)$$

where λ and λg are, respectively, the free space wave-length and the wave-length in the wave guide absorption path.

[9] S. Ramo and J. R. Whinnery, reference 8, p. 345.

The quantity $\Delta e/e$ was measured relative to an evacuated wave guide path as a function of the pressure and composition of the absorbing gas and as a function of the signal frequency. The coefficient A was then calculated from changes in output meter readings. Several precautions and extraneous effects must be considered for this procedure.

EXPERIMENTAL PRECAUTIONS AND EXTRANEOUS EFFECTS

In order that $\Delta e/e$ be proportional to the absorption it is necessary that the detector-amplifier system be linear in the intensity of the incident wave. That is, one desires a pure square-law detector (detector voltage proportional to incident intensity) and a linear voltage amplifier. The amplifier linearity was checked with a calibrated 1000-cycle/sec. signal generator. The detector was checked by replacing the amplifier by a low impedance d.c. current meter and comparing the $\Delta e/e$ values given by the two methods. This is a useful procedure since it is well known that the short-circuit direct current from a crystal is more nearly linear with absorbed radio-frequency power than is the open-circuit voltage. At the signal levels used no non-linearities could be found.

When a gas is introduced into a wave guide, the ohmic losses in the wave guide change because of the change in dielectric constant ϵ of the medium. This is of interest since all gas losses were measured relative to an evacuated wave guide path. If α_{vac} and α_{gas} are the ohmic attenuations in db/meter, then

$$\alpha_{gas}\cong\alpha_{vac}(1+\Delta\beta),$$

where

$$\epsilon_{gas}=1+\Delta$$

and

$$\beta\cong\frac{\left(\frac{2a}{\lambda}\right)^2}{\left(\frac{2a}{\lambda}\right)^2+2\frac{b}{a}}-\frac{1}{2}\frac{\left(\frac{2a}{\lambda}\right)^2}{\left(\frac{2a}{\lambda}\right)^2-1},$$

a and b being, respectively, the wide and narrow dimensions of the wave guide.[10]

For the present wave guide path, this effect is less than 0.04 percent for all wave-lengths and

[10] S. Ramo and J. R. Whinnery, reference 8, p. 346.

gas pressures used and so is negligible as compared with noise fluctuations.

Another extraneous effect related to the dielectric constant of the gas is the change which it produces in the phase length between the source and detector. If standing waves exist in the wave guide path, a change in this phase length produces a change in the absorbed signal and hence in the detector output. If Γ_S and Γ_D are the amplitude reflection coefficients of the source and detector, respectively, then the maximum change possible in the absorbed power corresponds to $|\Delta e/e| = 8a^2\Gamma_S\Gamma_D$, where a is the reduction in amplitude which a wave suffers in one traversal of the path because of ohmic or other losses. For the apparatus used $a^2 \cong \frac{1}{16}$, so that for $\Gamma_S = \Gamma_D \leqslant 0.05$ the maximum $|\Delta e/e| \leqslant 0.12$ percent which is considered satisfactory in relation to the noise fluctuations. These very small reflection coefficients were attained with the double stub tuners shown in Fig. 1 and the absence of the above effect was checked by introducing lossless gases (argon or N_2) into the path. Of course, in order to carry $\Delta e/e$ from a maximum to a minimum, it is necessary to change the phase length of the path by $\lambda g/4$. This is about the phase change resulting when an atmospheric pressure of O_2 is introduced.

It might be thought that adsorbed vapors on the wave guide walls would produce losses which would change upon evacuation or that mechanical deformation of the wave guide with changing pressure would change the ohmic loss and so give rise to spurious effects. However, in the experiments with argon and N_2 no apparent absorptions were observed which could not be removed by eliminating standing waves in the path.

EXPERIMENTAL RESULTS AND CONCLUSIONS

The absorption was measured as a function of pressure for dried (P_2O_5) tank O_2 and for several O_2-N_2 mixtures at several wave-lengths in the $\frac{1}{2}$-cm range. A typical set of data are shown in Fig. 3.

It was found that the absorption per O_2 molecule was a function only of the wave-length and the *total pressure*. This indicates that O_2-O_2 and O_2-N_2 collisions are equally effective in determining the line breadth. However, the absorption per molecule at a given wave-length has a complex pressure dependence because of the large number of overlapping absorption lines, which are not resolved at atmospheric pressure.

In the center of the band (data at 0.48, 0.50

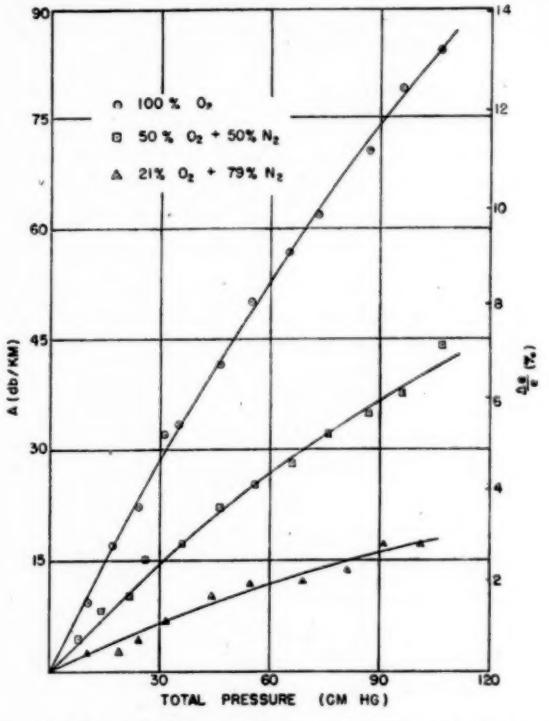

FIG. 3. Observed attenuation as a function of total gas pressure at $\lambda = 0.481 \pm 0.002$ cm and 22°C.

TABLE I. "Best fit" data at a total pressure of 76 cm Hg.

λ(cm)	Gas % by partial pressure	Temp. °C	A(db/km)	db/km in O_2	db/km in air
0.540±0.002	O_2	30	23.1	23.1	4.85
0.540±0.002	75% O_2+25% N_2	27	17.9	23.9	5.01
0.540±0.002	50% O_2+50% N_2	27	11.7	23.4	4.91
0.540±0.002	20% O_2+80% N_2	27	4.7	23.5	4.93
0.481±0.002	O_2	22	64.5	64.5	13.6
0.481±0.002	50% O_2+50% N_2	22	32.3	64.6	13.6
0.481±0.002	21% O_2+79% N_2	22	13.9	66.5	14.0
0.583±0.002	O_2	24	2.4	2.4	0.51
0.500+0.002	O_2	29	59.6	59.6	12.5
0.500+0.002	20% O_2+80% N_2	29	11.2	56.0	11.8
0.502±0.002	O_2	23	70.5	70.5	14.8
0.516±0.002	O_2	24	52.7	52.7	11.1
0.540±0.002	O_2	28	21.4	21.4	4.5
0.565±0.002	O_2	27	6.3	6.3	1.3
0.565±0.002	O_2	29	7.2	7.2	1.5
0.565±0.002	50% O_2+50% N_2	30	3.6	7.1	1.5
0.573±0.002	O_2	23	6.7	6.7	1.4
0.554±0.002	O_2	25	18.3	18.3	3.8
0.547±0.002	O_2	29	18.5	18.5	3.9
0.550±0.002	O_2	29	16.7	16.7	3.5
0.563±0.002	O_2	27	10.4	10.4	2.2
0.611±0.002	O_2	26	1.2	1.2	0.25

and 0.52 cm) the absorption per molecule decreases slightly with increasing pressure. At 0.54 cm the absorption per molecule is independent of the pressure. For longer wave-lengths the absorption per molecule increases with pressure, and finally approaches a linear pressure dependence in the far tails of the band (data at 0.56 cm and 0.58 cm).

The values of $\Delta e/e$ observed experimentally were reduced to db/km with Eq. (1) and plotted *vs.* total pressure as in Fig. 3 for each gas mixture and source wave-length. A smooth curve was then drawn so as to fit the plotted points. These "best fit" values of the absorption at a total pressure of 76 cm Hg are collected in the fourth column of Table I. In the fifth column these values are reduced to db/km in pure O_2 at 76 cm Hg and in the sixth column they are reduced to db/km in air (21 percent O_2) at 76 cm Hg, using the empirical result that the absorption coefficient is directly proportional to the O_2 partial pressure at constant total pressure.

The best fit values reduced to db/km in O_2 at 76 cm Hg are also shown in Fig. 4 together with Van Vleck's theoretical curves for a temperature of 27°C and several values of the line breadth parameter ($\Delta\nu/c$ in cm^{-1} for total pressure of 76 cm Hg). The best fit with these curves is seen to be in the range $0.02\ cm^{-1}<\Delta\nu/c<0.05\ cm^{-1}$.

In assessing the agreement of the data with the theory it must be remembered that there are no adjustable constants except for $\Delta\nu/c$ and that in a large part of the experimental wave-length range the absorption is very insensitive to this.

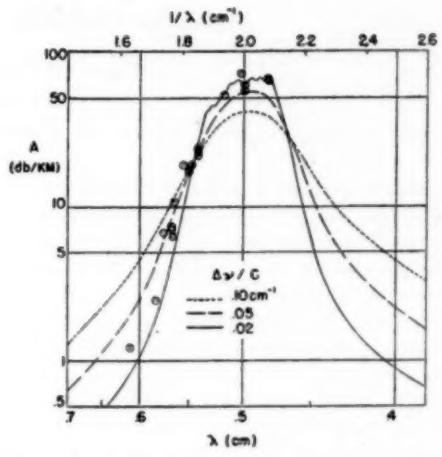

FIG. 4. "Best fit" data for pure O_2 and theoretical curves for pure O_2 at 76 cm Hg and 27°C.

Thus the agreement is in absolute terms and seems rather satisfactory.

On the other hand the accuracies of the data are not great enough to test the finer points of the theory: Whether $\Delta\nu/c$ is truly constant over the band, whether $\Delta\nu/c$ is accurately linear with total pressure, and the form and location of the individual absorption lines. Some of these points are of considerable interest and could be investigated with an improved apparatus, particularly with regard to higher intensity and greater frequency stability in the source and a more sensitive receiver. Then measurements could be made at low pressures and in the far tails of the band where these theoretical points are more easily investigated.

PHYSICAL REVIEW VOLUME 70, NUMBERS 1 AND 2 JULY 1 AND 15, 1946

The Stability of Synchrotron Orbits*

DAVID M. DENNISON AND T. H. BERLIN
Randall Laboratory of Physics, University of Michigan, Ann Arbor, Michigan

(Received April 11, 1946)

The stability of electron orbits in a synchrotron with a frequency modulated r-f has been investigated. The method consists in expanding the equations of motion and in solving them to zeroth and to first order of approximation. Attention is centered on the relatively low voltages —up to 200 Mev—and consequently the effects of radiation damping are of minor importance and may be neglected. With the correct frequency modulation, the electrons, in zeroth order, move in circular orbits with a constant radius. In first order their r and θ coordinates oscillate with the two frequencies ω_1 and ω_2 while the axial coordinate z oscillates with the frequency ω_3. It is shown that as the energy of the electrons increases, the amplitudes of the ω_1 and ω_3 motions decrease approximately as $1/E^{\frac{1}{2}}$ while the ω_2 amplitude decreases as $1/E^{\frac{1}{4}}$. Thus the electron orbits are stable. A numerical example is calculated in detail for a machine where the injection energy is $\frac{1}{2}$ Mev and the final energy 150 Mev. The accuracy of the solution is discussed and it is concluded that it will be correct to better than one percent provided the frequencies ω_1, ω_2, and ω_3 are not commensurable. In the latter case, under certain conditions, secular changes in the orbits could occur which would destroy their stability.

THE purpose of the present paper is to investigate the stability of electron orbits in a synchrotron accelerator. The type of synchrotron to be considered is similar to that described by Veksler[1] and by McMillan,[2] but contains a variation proposed by H. R. Crane; namely, the radiofrequency which furnishes the electron acceleration is to be frequency modulated in such a manner that the equilibrium electron orbits consist of circles with a constant radius.

The equations of motion for the electrons are very complex and there is little hope of finding an exact solution of them. It is, however, possible to develop the variables and to solve by the method of successive approximation. The present work carries the problem through the zeroth and first orders of approximation. It is found that, providing the injection velocity of the electrons is fairly high, say 25,000 ev or more, the orbits are definitely stable and that any oscillational motions which are initially present will be damped out as the electrons attain higher energy.

Cylindrical coordinates will be employed. The z axis is the symmetry axis of the synchrotron, r, the radius of the orbit, and θ is its azimuthal angle. The electron orbits lie in a ring shaped region defined by the coordinates $z=\pm z_0$ and $r=a\pm r_0$. Within this region the magnetic field has its greatest component in the z direction but, except in the median plane, it also possesses an r component. It is assumed that the field varies inversely as r^n and that it changes sinusoidally in time. The electron motion is to take place close to the median plane, $z=0$, and to the equilibrium orbit where $r=a$. It is therefore possible to develop

$$\frac{1}{r^n} \text{ as } \frac{1}{a^n}-\frac{n(r-a)}{a^{n+1}}+\cdots$$

and, since the calculation will not go beyond first order, to retain only the first two terms. The magnetic field has neither curl nor divergence in the region and these conditions impose relationships between the components of the field. (Strictly speaking, curl H is not zero since H is assumed to vary with the time. The extra terms, however, are proportional to $a^2\Omega^2/c^2$ and are negligibly small.) One thus obtains,

$$H_z=H_0(1-n(r-a)/a)\sin\Omega t,$$
$$H_r=-(nz/a)H_0\sin\Omega t,$$
$$H_\theta=0.$$

The electron will be subjected to two types of electric fields both of which are directed mainly in the θ, that is, in a tangential direction. The first of these is caused by the betatron effect and is equal to,

$$(\epsilon_\theta)_\beta=-\frac{1}{2\pi rc}\int_0^r\frac{\partial H_z}{\partial t}2\pi r\,dr.$$

* The work described in this paper has been supported by the Bureau of Ordnance, U.S. Navy, under contract NOrd-7924.

[1] V. Veksler, J. Phys. U.S.S.R. 9, 153 (1945).
[2] E. M. McMillan, Phys. Rev. 68, 143 (1945).

The integral may be divided into two parts, (1) the contribution from $r=0$ to $r=a$ and (2) the contribution from $r=a$ to $r=r$. The former may be designated by means of a constant coefficient, L, while the latter may be developed in powers of $(r-a)/a$ and only the terms through the first order of approximation retained.

$$(\epsilon_\theta)_\beta = -(\Omega/cr)[L+H_0a(r-a)]\cos\Omega t.$$

The second type of electric field is that caused by the radiofrequency. Let there be N gaps each with an oscillating potential of frequency ω_0 and magnitude V_0. While the accelerations occur at the gaps, it will be convenient to consider that the electric field is spread out over the entire ring. The field which the electron feels depends upon the phase of its motion relative to the phase of the radiofrequency. Thus

$$(\epsilon_\theta)_{rf} = -\frac{V_0N}{2\pi r}\sin\left(\theta-\int^t\omega_0\,dt\right).$$

The radiofrequency, ω_0, is to be made a function of the time in order that the equilibrium orbit may have the constant radius $r=a$, and for that reason it will prove convenient to express the argument of the radiofrequency as $\int^t\omega_0 dt$.

The equations of motion of an electron in an electric and magnetic field are well known and in cylindrical coordinates have the following form,

$$\frac{d}{dt}(m\dot r)-mr\dot\theta^2=\frac{e}{c}[VH]_r+e\epsilon_r, \tag{1}$$

$$\frac{d(r^2m\dot\theta)}{dt}=\frac{er}{c}[VH]_\theta+er\epsilon_\theta, \tag{2}$$

$$\frac{d}{dt}(m\dot z)=\frac{e}{c}[VH]_z+e\epsilon_z. \tag{3}$$

The velocity V and the mass m of the electron are further related,

$$m=\frac{m_0}{[1-(V^2/c^2)]^{\frac{1}{2}}}, \tag{4}$$

and

$$V^2=\dot r^2+r^2\dot\theta^2+\dot z^2. \tag{5}$$

These equations may be put in a somewhat more suitable form. Multiply Eqs. (1)–(3) by $m\dot r$, $m\dot\theta$, and $m\dot z$ and add. The result may be written,

$$\frac{1}{2}\frac{d}{dt}[m^2\dot r^2+m^2r^2\dot\theta^2+m^2\dot z^2]=em(\dot r\epsilon_r+r\dot\theta\epsilon_\theta+\dot z\epsilon_z).$$

The left-hand side of the equation is, however, from (4) and (5) equal to

$$\frac{1}{2}\frac{d}{dt}(m^2c^2-m_0^2c^2)=mc^2\dot m.$$

Thus the four equations which define r, θ, z, and m may be expressed as,

$$\frac{d}{dt}(m\dot r)-mr\dot\theta^2=\frac{e}{c}[VH]_r+e\epsilon_r, \tag{6}$$

$$c^2\frac{dm}{dt}=e(\dot r\epsilon_r+r\dot\theta\epsilon_\theta+\dot z\epsilon_z), \tag{7}$$

$$\frac{d}{dt}(m\dot z)=\frac{e}{c}[VH]_z+e\epsilon_z, \tag{8}$$

$$m^2\dot r^2+m^2r^2\dot\theta^2+m^2\dot z^2=m^2c^2-m_0^2c^2. \tag{9}$$

The magnetic and electric field components may be substituted into the above equations. It will be convenient to replace e by $-e$, corresponding to the negative electronic charge. Two simplifying assumptions will be made. (1) The growth of the magnetic field is exceedingly slow in comparison with the electronic motions and, therefore, in any study of the stability of the orbits it will be possible to replace $\sin\Omega t$ by Ωt and $\cos\Omega t$ by unity without materially changing the problem. This approximation is strictly valid only for the initial portion of the cycle but it will be shown later that it may be adapted for any portion. (2) It will appear that for reasonable values of the radiofrequency potential V_0, the phase $\int^t\omega_0 dt-\theta$ will be small and consequently $\sin(\int^t\omega_0 dt-\theta)$ will be simplified to $\int^t\omega_0 dt-\theta$. An auxiliary study has been made which apparently shows that the assumed simplification, while it may affect the motion somewhat, cannot have any essential influence upon the orbit stability.

With these simplifications and substitutions

the equations of motion (6) through (9) become,

$$m\frac{d\dot{r}}{dt}+\dot{r}\dot{m}-mr\dot{\theta}^2=-\frac{e}{c}r\dot{\theta}\left[1-\frac{n(r-a)}{a}\right]H_0\Omega t, \quad (10)$$

$$c^2\dot{m}=\frac{e\Omega\dot{\theta}}{c}[L+H_0a(r-a)]+\frac{eV_0N\dot{\theta}}{2\pi}\left(\theta-\int^t\omega_0dt\right), \quad (11)$$

$$m\frac{d\dot{z}}{dt}+\dot{m}\dot{z}=-\frac{enr\dot{\theta}z}{ca}H_0\Omega t, \quad (12)$$

$$m^2\dot{r}^2+m^2r^2\dot{\theta}^2+m^2\dot{z}^2=m^2c^2-m_0^2c^2. \quad (13)$$

It will be noted that terms arising from the radiation damping have been omitted. Two remarks may be made. (1) The most critical portion of the electron motion from the point of view of orbit stability is the initial portion and here the radiation is of negligible importance. (2) At the later times when the radiation becomes larger, it will act as a very slowly varying frictional force. Its effect will be merely to displace the phase of the electron relative to the radiofrequency acceleration so that on each cycle the electron may receive sufficient energy to compensate for the radiation losses.

In attacking the equations of motion, it will be fruitful to investigate those orbits (a) which lie in the median plane and (b) for which the radius is constant. These will be defined as the equilibrium orbits and will represent the zeroth approximation to the general motion. Setting $r=a$ and $z=0$ into the equations, one obtains,

$$m=m_0(1+K^2t^2)^{\frac{1}{2}},$$

$$\theta=\int^t\omega_0dt+(a^2H_0-L)\frac{2\pi\Omega}{V_0Nc},$$

$$\omega_0=\frac{c}{a}\frac{Kt}{(1+K^2t^2)^{\frac{1}{2}}},$$

where

$$K=aeH_0\Omega/m_0c^2.$$

Since for the equilibrium orbit, the electron velocity is $a\dot{\theta}$, the radiofrequency may be expressed as,

$$\omega_0=\dot{\theta}=V/a=c\beta/a.$$

It will now be assumed that the actual orbits of the electron differ from the equilibrium orbits by only small quantities. Thus, let,

$$r=a+\lambda\rho,$$

$$m=m_0(1+K^2t^2)^{\frac{1}{2}}+\lambda\mu,$$

$$z=\lambda\zeta,$$

$$\theta=\int^t\omega_0dt+(a^2H_0-L)\frac{2\pi\Omega}{V_0Nc}+\lambda\varphi,$$

$$\omega_0=\frac{c}{a}\frac{Kt}{(1+K^2t^2)^{\frac{1}{2}}},$$

where λ is a parameter of smallness and ρ, μ, φ, and ζ are functions of the time.

These values for r, m, z, and θ are substituted in the equations of motion (10), (11), (12), and (13). The zeroth-order terms are automatically satisfied and all terms in λ^2 and higher are neglected since only an approximation through first order is desired.

$$\frac{d\dot{\rho}}{dt}+\frac{K^2t}{1+K^2t^2}\dot{\rho}+\frac{c^2}{a^2}\frac{(1-n)K^2t^2}{(1+K^2t^2)}\rho-\frac{c^2\mu}{m_0a(1+K^2t^2)^{\frac{1}{2}}}=0, \quad (14)$$

$$\rho+\frac{a^2}{c}\frac{(1+K^2t^2)^{\frac{1}{2}}}{Kt}\dot{\varphi}-\frac{a\mu}{m_0K^2t^2(1+K^2t^2)^{\frac{1}{2}}}=0, \quad (15)$$

$$\dot{\mu}-\frac{eNV_0Kt}{2\pi ac(1+K^2t^2)^{\frac{1}{2}}}\varphi-\frac{\mu}{t(1+K^2t^2)}=0, \quad (16)$$

$$\frac{d\dot{\zeta}}{dt}+\frac{K^2t}{1+K^2t^2}\dot{\zeta}+\frac{c^2nK^2t^2}{a^2(1+K^2t^2)}\zeta=0. \quad (17)$$

The straightforward solution of these equations is still very difficult although perhaps not impossible. It will, however, be possible to obtain a rather simple solution which holds to a high order of approximation except in the immediate neighborhood of $t=0$. According to our equations $t=0$ represents $m=m_0$ and consequently a zero initial injection energy. It is, however, planned to inject at, say, $\frac{1}{2}$ Mev and at this, or higher energies, t is much greater than the critical region just referred to. (This point will be discussed later.)

The method of making the approximation lies in the realization that the magnetic field is changing very slowly indeed compared with the

orbital motion of the electrons. Let us suppose that at a time $t=T$, the magnetic field is frozen. The values of r, m, z, and θ in this case are, to first order of approximation,

$$r=a+\lambda\rho_0,$$

$$m=m_0(1+K^2T^2)^{\frac{1}{2}}+\lambda\mu_0,$$

$$z=\lambda\zeta_0,$$

$$\theta=\omega_0 t+\lambda\varphi_0,$$

$$\omega_0=\frac{c}{a}\frac{KT}{(1+K^2T^2)^{\frac{1}{2}}}.$$

Since the magnetic field is frozen, the betatron terms $a^2H_0\Omega$ and $L\Omega$ of course vanish. The equations for ρ_0, μ_0, ζ_0 and φ_0 may be obtained by the method used earlier and are,

$$\frac{d\dot{\rho}_0}{dt}+\omega_0^2(1-n)\rho_0-\frac{c^2\mu_0}{m_0a(1+K^2T^2)^{\frac{1}{2}}}=0, \quad (18)$$

$$\rho_0+\frac{a}{\omega_0}\dot{\varphi}_0-\frac{a\mu_0}{m_0K^2T^2(1+K^2T^2)^{\frac{1}{2}}}=0, \quad (19)$$

$$\dot{\mu}_0-\frac{eNV_0\omega_0}{2\pi c^2}\varphi_0=0, \quad (20)$$

$$\frac{d\dot{\zeta}_0}{dt}+n\omega_0^2\zeta_0=0. \quad (21)$$

Since in these equations ω_0 and T are constants, it is readily possible to integrate them exactly. The results are as follows where the C_S and B_S are integration constants and where ω_1 and ω_2 are the positive roots of the equation.

$$\omega^4-\left[(1-n)\omega_0^2-\frac{\alpha}{(1+K^2T^2)^{\frac{1}{2}}}\right]\omega^2+\frac{\alpha\omega_0^2(K^2T^2+n)}{(K^2T^2+1)^{\frac{1}{2}}}=0,$$

where $\alpha=eNV_0/2\pi a^2m_0$.

$$\rho_0=C_1\cos(\omega_1t+B_1)+C_2\cos(\omega_2t+B_2),$$

$$\mu_0=\frac{m_0a\alpha}{c^2(1-n)}C_1\cos(\omega_1t+B_1)+\frac{m_0(1-n)}{a}\frac{K^2T^2}{(1+K^2T^2)^{\frac{1}{2}}}C_2\cos(\omega_2t+B_2),$$

$$\varphi_0=-\frac{C_1}{a(1-n)^{\frac{1}{2}}}\sin(\omega_1t+B_1)-\frac{c(1-n)^{\frac{1}{2}}}{a^2\alpha^{\frac{1}{2}}}\frac{KT(K^2T^2+n)^{\frac{1}{2}}}{(K^2T^2+1)^{\frac{1}{2}}}C_2\sin(\omega_2t+B_2),$$

$$\zeta_0=C_3\cos(\omega_3t+B_3),$$

where $\omega_3=n^{\frac{1}{2}}\omega_0$.

This solution for the case of the constant magnetic field is very interesting and contains in it many of the essential features of the motion. The coordinates r, m, and z oscillate harmonically around their average values, namely, a $m_0(1+K^2T^2)^{\frac{1}{2}}$ and zero, respectively. The motion of θ consists of a uniform increase with the time upon which is superimposed a small harmonic oscillation. The average value of the electron mass divided by m_0 will be defined as $f=(1+K^2T^2)^{\frac{1}{2}}$. The equation defining ω_1 and ω_2 is, therefore,

$$\omega^4-\left[(1-n)\omega_0^2-\frac{\alpha}{f^3}\right]\omega^2+\frac{\alpha\omega_0^2(f^2-1+n)}{f^3}=0,$$

and has the solution,

$$\omega^2=\frac{(1-n)\omega_0^2}{2}-\frac{\alpha}{2f^3}\pm\left[\left(\frac{(1-n)\omega_0^2}{2}-\frac{\alpha}{2f^3}\right)^2-\frac{\alpha\omega_0^2(f^2-1+n)}{f^3}\right]^{\frac{1}{2}}. \quad (22)$$

The numerical order of magnitude of the quantities involved in the above equation may be readily estimated for the two limiting cases $f=2$; that is, the time of injection, and $f=200$, the time when the electron will have acquired approximately 100 Mev. Let $a=100$ cm and $n=\frac{1}{2}$. (n determines the fall off law of the static magnetic field.) Let the radiofrequency potential and the number of gaps N be such that $V_0N=3000$ volts $=10$ e.s.u.

Quantity	$f=2$	$f=200$
$\frac{(1-n)\omega_0^2}{2}$	1.7×10^{16}	2.2×10^{16}
$\frac{\alpha}{2f^3}$	5.3×10^{12}	5.3×10^{8}
$\frac{\alpha\omega_0^2(f^2-1+n)}{f^3}$	2.5×10^{30}	3.8×10^{28}

A study of these figures shows that ω_1 and ω_2 may be expressed as,

$$\omega_1=(1-n)^{\frac{1}{2}}\omega_0, \tag{23}$$

$$\omega_2=\frac{\alpha^{\frac{1}{2}}(f^2-1+n)^{\frac{1}{2}}}{(1-n)^{\frac{1}{2}}f^{\frac{1}{2}}}, \tag{24}$$

with an accuracy equal to one part in a thousand when $f=2$ and far better for $f=200$.

The description of the electron motion in the constant magnetic field may now be completed.

1. The average mass of the electron is fm_0.

2. The principal frequency is that associated with the uniform increase of the azimuthal angle θ. It is

$$\omega_0=\frac{c}{a}\frac{(f^2-1)^{\frac{1}{2}}}{f}.$$

3. The electron oscillates in the z direction with a constant amplitude (determined by the initial conditions) and with a circular frequency $n^{\frac{1}{2}}\omega_0$. Evidently this motion is stable only if $n>0$.

4. The radial distance r is equal to a constant plus the sum of two harmonic terms. The first of these has a frequency $\omega_1=(1-n)^{\frac{1}{2}}\omega_0$ which is independent of the accelerating electric field. It will be spoken of as the radial frequency. Clearly this motion will be stable provided $n<1$.

5. The second harmonic term has a frequency

$$\omega_2=\frac{\alpha^{\frac{1}{2}}}{(1-n)^{\frac{1}{2}}}\frac{(f^2-1+n)^{\frac{1}{2}}}{f^{\frac{1}{2}}}.$$

This will be called the frequency of the phase oscillation (phase of θ relative to the radio-frequency field). It is proportional to the square root of the accelerating potential and, for large energies, inversely to the square root of the electron energy. By substituting the numerical constants $a=100$ cm, $n=\frac{1}{2}$, and $V_0N=10$ e.s.u. one finds that ω_2/ω_0 varies from 1/30 to 1/330 as f increases from 2 to 200.

6. The amplitudes of oscillation of r, θ, and m are interrelated for both of the harmonic oscillations ω_1 and ω_2 but otherwise are constant and are determined by the initial conditions.

The nature of the solution for the case where the magnetic field increases slowly may be inferred from the solutions just obtained for the frozen field problem. It is to be expected that the amplitudes C_1, C_2, and C_3 will be slowly varying functions of the time. The frequencies ω_0, ω_1, ω_2, and ω_3 are functions of f, and hence will depend upon the time. These changes will be brought about by the fact that Eqs. (14)–(17) differ from (18)–(21). The differences are of two sorts, (a) the coefficients of the dependent variables and their derivatives are functions of the time in the first group of equations while they are constants in the second group. (b) Equation (14) has the extra term

$$\frac{K^2t}{1+K^2t^2}\dot{\rho},$$

Eq. (16) the extra term

$$-\frac{\mu}{t(1+K^2t^2)},$$

and Eq. (17) the term

$$\frac{K^2t}{1+K^2t^2}\dot{\zeta}.$$

It is to be expected that the influence of these extra terms will be small and will contribute to the slow time variation of the amplitudes and frequencies. It will be convenient to divide the various terms of Eq. (14) through (17) into principal terms and extra terms, the latter being those which have just been defined.

It is now assumed that the solution of Eqs. (14)–(17) may be written in the following form:

$$\rho=D_1\cos\left(\int^t\omega_1dt+B_1\right)+D_2\cos\left(\int^t\omega_2dt+B_2\right),$$

$$\mu=D_3\cos\left(\int^t\omega_1dt+B_1\right)+E_3\sin\left(\int^t\omega_1dt+B_1\right),$$

$$+D_4\cos\left(\int^t\omega_2dt+B_2\right)+E_4\sin\left(\int^t\omega_2dt+B_2\right),$$

$$\varphi = D_5 \sin\left(\int^t \omega_1 dt + B_1\right) + E_5 \cos\left(\int^t \omega_1 dt + B_1\right) + D_6 \sin\left(\int^t \omega_2 dt + B_2\right) + E_6 \cos\left(\int^t \omega_2 dt + B_2\right),$$

$$\zeta = D_7 \cos\left(\int^t \omega_3 dt + B_3\right).$$

It is understood that the above expressions constitute a solution of the equations of motion subject to the following conditions.

1. B_1, B_2, and B_3 are integration constants.

2. D_1, D_2, D_3, D_4, D_5, D_6, and D_7 are slowly varying functions of the time. Thus when they occur in the principal terms of the differential equations, D_i and $\dot{D}_i$ are to be retained but $d\dot{D}_i/dt$ is to be neglected. In the case of the extra terms (whose influence is assumed to be small), D_i will be retained, but $\dot{D}_i$ and $d\dot{D}_i/dt$ are discarded.

3. E_3, E_4, E_5, and E_6 are small, slowly varying, functions of the time. In the principal terms E_i is retained but $\dot{E}_i$ and $d\dot{E}_i/dt$ are not. In the extra terms, E_i, as well as its derivatives, will be neglected.

4. ω_1 and ω_2 are assumed to have the form given by Eqs. (23) and (24) rather than by the more exact relation (22). This means that in any of the equations, a term involving α is to be neglected with respect to a term involving ω_0^2. This last assumption is merely a matter of convenience. It would be quite possible to carry through the work using the exact relation (22), but the anticipated changes from this procedure would amount to only one part in a thousand even for $f=2$.

The above conditions governing the solution of the equations of motion may appear to limit the validity of the results. Actually this is not the case. The basic ideas behind them are very clear and are, (a) an exact solution for the problem of a constant magnetic field has been found, and (b) in the actual problem the magnetic field changes very slowly indeed compared with the motion of the electron. Consequently, the solution for the actual problem cannot differ greatly from the constant field case and must represent a slow unfolding of that motion.

The complete solution for r, θ, z, and m through the zeroth and first order of approximation will now be given. It will prove convenient to express the frequencies in terms of f, the ratio of the average electron mass to its rest mass.

$$f=(1+K^2t^2)^{\frac{1}{2}}, \quad K=\frac{aeH_0\Omega}{m_0c^2}, \quad \alpha=\frac{eNV_0}{2\pi a^2 m_0}, \quad \omega_0=\frac{c(f^2-1)^{\frac{1}{2}}}{af}, \quad \omega_1=(1-n)^{\frac{1}{2}}\omega_0,$$

$$\omega_2=\frac{\alpha^{\frac{1}{2}}(f^2-1+n)^{\frac{1}{2}}}{(1-n)^{\frac{1}{2}}f^{\frac{1}{2}}}, \quad \omega_3=n^{\frac{1}{2}}\omega_0,$$

A_1, A_2, A_3, B_1, B_2, B_3 are integration constants.

$$r=a+\frac{A_1}{(f^2-1)^{\frac{1}{2}}}\cos\left(\int^t \omega_1 dt + B_1\right)+A_2\left[\frac{f^3}{(f^2-1+n)(f^2-1)^2}\right]^{\frac{1}{2}}\cos\left(\int^t \omega_2 dt + B_2\right),$$

$$\theta=\int^t \omega_0 dt+\frac{2\pi\Omega(a^2H_0-L)}{V_0Nc}-\frac{A_1}{a(1-n)^{\frac{1}{2}}(f^2-1)^{\frac{1}{2}}}\left[\sin\left(\int^t \omega_1 dt + B_1\right)\right.$$

$$\left.-\frac{aKf}{2c(1-n)^{\frac{1}{2}}(f^2-1)}\cos\left(\int^t \omega_1 dt + B_1\right)\right]-\frac{c(1-n)^{\frac{1}{2}}}{a^2\alpha^{\frac{1}{2}}}A_2\left[\frac{f^2-1+n}{f^3}\right]^{\frac{1}{2}}$$

$$\times\left[\sin\left(\int^t \omega_2 dt + B_2\right)+\frac{K(1-n)^{\frac{1}{2}}f^{\frac{1}{2}}(f^2-1)^{\frac{1}{2}}}{4\alpha^{\frac{1}{2}}(f^2-1+n)^{\frac{1}{2}}}\left(\frac{3(1-n)}{f^2}-1\right)\cos\left(\int^t \omega_2 dt + B_2\right)\right],$$

$$z=\frac{A_3}{(f^2-1)^{\frac{1}{4}}}\cos\left(\int^t \omega_3 dt+B_3\right),$$

$$m=fm_0+\frac{m_0a\alpha A_1}{c^2(1-n)(f^2-1)^{\frac{1}{4}}}\left[\cos\left(\int^t \omega_1 dt+B_1\right)+\frac{aK(f^2+1)}{c(1-n)^{\frac{1}{2}}f(f^2-1)}\sin\left(\int^t \omega_1 dt+B_1\right)\right]$$

$$+\frac{m_0(1-n)A_2}{a}\left[\frac{(f^2-1)^2}{(f^2-1+n)f}\right]^{\frac{1}{4}}\left[\cos\left(\int^t \omega_2 dt+B_2\right)+\frac{a^2K\alpha^{\frac{1}{2}}(f^2+n-1)^{\frac{1}{2}}(f^2+1)}{c^2(1-n)^{\frac{1}{2}}f^{\frac{1}{2}}(f^2-1)^{\frac{1}{2}}}\sin\left(\int^t \omega_2 dt+B_2\right)\right].$$

The solution just given is very satisfactory. It shows that the orbits are stable since the amplitude of the oscillations of z and of r and θ for the ω_1 vibration decrease as $1/f^{\frac{1}{2}}$ for large values of f. The amplitude of r and θ for the ω_2 motion (phase oscillation) decreases for large f as $1/f^{\frac{1}{2}}$. The phase differences between the motions (represented earlier by the quantities E_3, E_4, E_5, and E_6) also decrease as f increases. The amplitude of the oscillations in the electron mass for the vibration ω_2 will increase as $f^{\frac{1}{2}}$. This does nor represent any instability in the electron orbits, however, and merely gives rise to a slight spread in the final electron energies.

The expressions for r, θ, z, and m have been derived for the case of a uniformly increasing magnetic field. The whole point of the derivation, however, was that the magnetic field changes so slowly that the motion may be represented by slow changes in the constant magnetic field orbits. The particular manner in which the magnetic field changes is immaterial provided the rate of change is small enough. The expressions for r, θ, z, m, ω_0, ω_1, ω_2, and ω_3 given above may be readily modified for a sinusoidally changing magnetic field by making the following changes only.

(1) Replace

$$f=(1+K^2t^2)^{\frac{1}{2}} \text{ by } f=\left(1+\frac{K^2\sin^2\Omega t}{\Omega^2}\right)^{\frac{1}{2}}.$$

(2) Replace the constant phase angle of the equilibrium orbit,

$$\frac{2\pi\Omega}{V_0Nc}(a^2H_0-L), \text{ by } \frac{2\pi\Omega}{V_0Nc}(a^2H_0-L)\cos\Omega t.$$

(3) Wherever K occurs explicitly in the expressions for θ and m, replace it by $K\cos\Omega t$. (This is *not* to be construed as any change in the definition of K itself, however.)

The physical meaning of the constants K and α may be visualized in a number of ways. If the final mass attained by the electron at the end of the magnetic quarter cycle is m^*, then $K=\Omega[(m^*/m_0)^2-1]^{\frac{1}{2}}$. A second method of interpreting K consists in calculating the increase in the average electron energy per revolution divided by its rest mass. It may be readily shown that this quantity,

$$\frac{2\pi}{\omega_0E_0}\left\langle\frac{dE}{dt}\right\rangle_{\text{Av}} \text{ is equal to } \frac{2\pi a}{c}K\cos\Omega t.$$

The magnetic field has been assumed to increase very slowly and hence the numerical values chosen for any actual case must be such that $K\ll c/(2\pi a\cos\Omega t)$. The constant α is related to the radiofrequency potential. If the electron should make one revolution in such a manner as to pick up the maximum amount of energy from the radiofrequency field, the phase angle would necessarily be 90 degrees. The energy it would obtain, divided by the rest energy, would be

$$\frac{(\Delta E)_{\max}}{E_0}=\frac{eNV_0}{m_0c^2}.$$

This quantity is, however, equal to

$$\frac{2\pi a^2}{c^2}\alpha=\frac{2\pi(f^2-1)\alpha}{f^2\omega_0^2}.$$

$$\alpha=\frac{f^2\omega_0^2}{2\pi(f^2-1)}\frac{(\Delta E)_{\max}}{E_0}.$$

If $NV_0=3000$ volts, then

$$\frac{(\Delta E)_{\max}}{E_0}\cong\frac{3}{500} \text{ and } \frac{\alpha}{\omega_0^2}=\frac{3f^2\times10^{-3}}{\pi(f^2-1)}.$$

It is therefore clear that the approximation which has been used, namely, one in which α

TABLE I. Numerical example.

t	No. of turns	$\omega_0/2\pi$	f	Equilibrium phase	z or r amplitude due to ω_2 or ω_1	r amp. due to ω_2	θ amp. due to ω_2	m amp. due to ω_2	ω_2/ω_0
1.57×10^{-5}	0	41.4	2	28.3°	1.0 cm	1.32 cm	20°	$0.010\ m_0$	1/30
2.56×10^{-5}	425	45.1	3	28.3°	0.78	0.88	18.4°	$0.012\ m_0$	1/39
4.44×10^{-5}	1,278	46.8	5	28.3°	0.59	0.57	16.4°	$0.014\ m_0$	1/51
9.00×10^{-5}	3,410	47.5	10	28.3°	0.42	0.33	13.8°	$0.016\ m_0$	1/73
1.81×10^{-4}	7,660	47.7	20	28.2°	0.29	0.20	11.5°	$0.020\ m_0$	1/103
5.60×10^{-4}	16,230	47.8	40	28.0°	0.21	0.12	9.8°	$0.023\ m_0$	1/146
2.01×10^{-3}	42,500	47.8	100	26.6°	0.13	0.06	7.8°	$0.029\ m_0$	1/230
4.16×10^{-3}	198,000	47.8	298	0.0°	0.08	0.03	5.9°	$0.039\ m_0$	1/400

may be neglected in comparison to ω_0^2, will be very good except in the region where f is close to unity. Even for $f=1.05$, corresponding to an electron energy of 25 kev, $\alpha/\omega_0^2=1.02\times10^{-2}$.

It may be of interest to construct a numerical example which will further bring out the order of magnitude of the quantities involved. We shall choose a sinusoidally varying magnetic field with an Ω corresponding to 60 cycles/sec. Let $a=100$ cm, $H_0=5000$ gauss, $V_0N=3000$ volts, $n=\frac{1}{2}$, and let the injection voltage correspond to $\frac{1}{2}$ Mev or $f=2$. The derived constants become, $K=1.105\times10^5$, $\alpha=8.43\times10^{13}$. Let the integration constants be chosen so that the initial amplitude of the z oscillation is 1 cm, the initial amplitude of the radial motion (that is, the ω_1 motion) is 1 cm while the initial amplitude of the phase oscillation is 20 degrees. These conditions mean that

$$A_1=A_3=3^{\frac{1}{2}} \quad \text{and} \quad A_2=\frac{\pi}{9}\frac{a^2\alpha^{\frac{1}{2}}\sqrt{2}}{c}\left[\frac{8}{3.5}\right]^{\frac{1}{2}}.$$

Let $B_1=B_2=B_3=0$.

The quantity, L, depends upon the flux of the magnetic field inside the equilibrium orbit, $r=a$, and will be a function of the magnet design. For this numerical example we will assume that the cross section of the iron has the form

where the return magnetic circuit is inside the electron orbits. One may estimate that the return flux in the iron has twice the value of the flux in the air gap at the pole faces and that, moreover, the equilibrium orbit lies midway in the air gap. If the radial extent of the pole pieces is 100 cm$\pm$7 cm the problem is determined and one finds that $L=-10^7$.

In Table I the first column gives the time, beginning with the injection time $t=1.57\times10^{-5}$ second and extending to the end of a quarter-cycle of the magnetic field, that is, $t=1/240$. The second column lists the number of turns the electron has made since injection. The third column is the radiofrequency in megacycles, while the fourth gives the ratio of the average mass of the electron to its rest mass. The fifth column shows the phase of the equilibrium orbit, namely

$$\frac{2\pi\Omega}{V_0Nc}(a^2H_0-L)\cos\Omega t,$$

expressed in degrees.

The sixth column gives an amplitude in centimeters which is that, either of the z oscillation, or, of that r oscillation which is due to the radial motion (that is, to ω_1). The seventh, eighth, and ninth columns list the amplitudes of r, θ, and m which arise from the phase oscillation ω_2. The last column gives the ratio of the phase oscillation frequency to the orbital frequency ω_0. The ratio of the frequency of the z oscillation as well as that of the radial vibration to the orbital frequency is, of course, constant and equal to $n^{\frac{1}{2}}=(1-n)^{\frac{1}{2}}=1/\sqrt{2}$ for the case $n=\frac{1}{2}$.

The total displacement of the electron in the radial direction will be equal to the sum of the two radial amplitudes and for the numerical example just given has a maximum value of 2.32 cm at injection, which decreases to 0.11 cm at the conclusion of the magnetic quarter cycle. The position of the electron relative to the radio-

frequency, that is, the phase, oscillates in the above example between 48.3° and 8.3° at the time of injection, decreasing to an oscillation between +5.9° and −5.9° at the conclusion. This extreme value of the phase angle, namely 48.3°, seems rather large since it has been assumed that the sine of the phase angle can be replaced by the angle itself in the equations of motion. It is not believed that this constitutes any essential limitation on the validity of the predicted motion however. The reasons for this belief will appear in the following general discussion of the accuracy of the solution which has been obtained.

1. The solution of the equations of motion which has been given is correct through zeroth and first order of approximation but neglects second and higher terms. (The fact that it becomes invalid for very small values of t will be discussed later.)

2. Throughout the discussion the decrease in the amplitudes of the r, θ, and z vibrations has been spoken of as a damping. This is not a proper description since the energy of these vibrations is not disappearing although the amplitudes do grow smaller. For example, if the motion is allowed to continue through the second quarter cycle of the magnetic field, the motion is strictly reversible and the amplitudes of the vibrations will increase as the energy of the electrons decreases. The situation may be visualized in a very direct fashion for the case of the z vibration. Here, the mass of the electron is growing with time but also the restoring force grows at almost precisely the same rate so that, for large values of f, the frequency ω_3 is independent of f. This motion is at right angles to the other (r and θ) motions and its energy is conserved. Thus at the points where $\dot{z}=0$, the potential energy $=\frac{1}{2}Kz^2=$constant. Since the force constant K is proportional to f, the amplitude of the motion will be inversely proportional to $f^{\frac{1}{2}}$. This is precisely the result obtained earlier when f is large. It shows that the decrease in the amplitude cannot be attributed to a damping process but rather is merely a consequence of the simultaneous increase in the mass and in the restoring force constant. The situation for the other vibrations, ω_1 and ω_2, is more complicated but the mechanism by which the amplitudes are decreased appears to be of the same general nature.

3. The phase angle $(\theta-\int^t\omega_0 dt)$ has been assumed to be sufficiently small so that the sine of the phase may be replaced by the phase itself. This may not always be the case as has been illustrated in the numerical example. A study of the motion for the frozen magnetic field indicates that the phase oscillation (that is, the ω_2 oscillation) for large amplitudes bears the same relationship to the motion for small amplitudes that ordinary pendulum motion for large amplitudes bears to simple harmonic motion. Thus it is expected that, in the case of the slowly growing magnetic field, the period of the oscillation will be larger for those electrons with large phase amplitudes but that this circumstance should have no essential influence upon the stability of the orbits. The stability depends upon the growth of the electron mass as has been explained above.

4. There do exist some mechanisms affecting the orbits which have not been included in the analysis. Among these are, (a) the scattering of electrons by gas molecules, (b) space charge, and (c) radiation damping. The first two of these effects will reduce the final yield of high energy electrons. The third, radiation damping, will tend to increase the equilibrium phase angle during the latter portion of the magnetic quarter cycle. This would only become important if it became so large that the phase angle approached 90 degrees. The magnitude of the equilibrium phase angle may of course be reduced by using a higher value of the radiofrequency potential V_0.

5. The zeroth order, or equilibrium orbit, solution is valid for all values of t but the first-order approximation breaks down when t is sufficiently small; that is, for low values of the injection energy. This comes about in two ways: (a) the quadratic equation (22) which determines ω_1 and ω_2 can no longer be well approximated by the simpler relations (23) and (24); (b) The so-called extra terms in the equations of motion no longer have a small influence upon the motion as compared with the principal terms. One manifestation of this latter effect will be that the amplitudes E_3 to E_6 will not be small compared with the amplitudes D_3 to D_6, when taken in respective pairs. From both of these tests one

may estimate that for the numerical example the solution which has been given will be good to one part in a thousand for an injection energy of $\frac{1}{2}$ Mev or $f=2$. It will be good to around 1 percent for an injection energy of 25 kev or $f=1.05$.

The first-order equations of motion resemble in many respects the differential equations defining Bessel functions although they are more complex. When the Bessel equation is treated by the methods used here, one obtains the standard asymptotic form for the function. The argument of the function is the angle θ counting from an initial time when the electron was at rest. At $f=1.05$, $\theta=136$ (using the constants of the numerical example), and for such a large value of the argument the asymptotic expressions for the Bessel functions are not in error by more than 1 percent.

6. The estimates which have just been made apply only to the zeroth- and first-order approximations and are not an indication of the magnitude of the second- and higher order approximations. In general, the ratio of second- to first-order terms is roughly equal to the ratio of first-to zeroth-order terms. In the numerical example the first-order terms were of the order of one or two percent of the zeroth-order quantities so it would seem that the first-order approximation is adequate. There is an exception to the general rule, however, in the case where there exist commensurable relationships between the various fundamental frequencies of the system. Secular changes may then set in, and the amplitudes may slowly build up to large values. For example, the second-order terms have been examined, and it is found that one, and only one, divergent situation may occur. The condition for this is that $2\omega_3-\omega_1=\omega_0[2(n)^{\frac{1}{2}}-(1-n)^{\frac{1}{2}}]=0$. Thus a magnetic fall off with $n=\frac{1}{3}$ must be avoided. It is expected that still higher order approximations will reveal other combinations of the frequencies which would lead to unstable orbits. However, the rate at which the amplitude of the oscillation builds up becomes progressively slower for the higher orders (if the initial amplitudes of oscillation are about 1 cm, the number of turns required for the catastrophe to develop is of the order of a^{p-1}, where a is the radius of the orbit in centimeters and p is the order of approximation for which the frequencies interact) so that eventually a commensurability between the frequencies becomes harmless. The phenomenon of instability due to commensurable relationships between frequencies is not confined to the synchrotron but exists as well in the betatron, although there the situation is somewhat simpler since the phase oscillation ω_2 is absent.

7. The synchrotron which has been considered in this paper is one in which the radiofrequency field is frequency modulated. It is, however, obvious that by the time the electrons have obtained 2 Mev or more of kinetic energy the radiofrequency has become nearly constant. From this point onward the equations and their solution would apply equally well to a synchrotron without frequency modulation or to the combination betatron-synchrotron type of accelerator.

PHYSICAL REVIEW VOLUME 70, NUMBERS 1 AND 2 JULY 1 AND 15, 1946

Compressional Viscosity and Sound Absorption in Water at Different Temperatures

FRANCIS E. FOX AND GEORGE D. ROCK
The Catholic University of America, Washington, D. C.

(Received March 18, 1946)

The temperature dependence of the coefficient of absorption ($2\alpha\nu^{-2}$) of ultrasonic waves in water was measured from 0°C to 33°C. Values range from 137×10^{-17} at 0°C to 40×10^{-17} at 33°C. In particular at 4°C where the sound propagation is isothermal the value 101×10^{-17} is found, and is to be compared with a shear viscosity contribution of 30×10^{-17}. Therefore the excess cannot be caused by the slowness of energy exchange between the internal and external degrees of freedom. The excess absorption is used to calculate the value of a new coefficient of compressional viscosity k, which is found to be 0.052 poise at 4°C and 0.026 poise at 20°C. A general discussion of the origin of sound absorption in liquids is included, with particular applications to recent measurements.

INTRODUCTION

MEASUREMENTS of the absorption coefficient of ultrasonic waves in polyatomic liquids[1-3] have established the fact that the absorption varies as the square of the frequency (ν) from about 2 to 100 megacycles, but is in all cases larger than can be explained by viscosity alone. The effect of heat conduction is usually negligible against that of viscosity; in water the ratio is less than 1 to 100. It is useful to designate the measured intensity absorption coefficient by 2α, the viscosity contribution by $2\alpha_v$ and denote $2(\alpha-\alpha_v)$ by $2\alpha'$, the unexplained part of the absorption. In water at 20°C $2\alpha\nu^{-2}$ is 48×10^{-17} as compared with 16.3×10^{-17} for $2\alpha_v\nu^{-2}$. In some liquids of low viscosity, e.g., benzene, α is many times α_v while in high viscosity liquids α_v accounts for the greater part of α.

The experimental facts are thus, in broad outline, the same as those found in many polyatomic gases where the experimental absorption coefficients are larger than those calculated from viscosity data. As is well known, the work of Herzfeld and Rice,[4] Bourgin,[5] and Kneser[6] has been successful in explaining not only the magnitudes of the measured absorption coefficient, but the dependence upon frequency, as well as the change in the velocity of sound with frequency. The basic assumption in the explanation is that on the average a finite time is required for the conversion of translational energy into rotational or vibrational energy within the molecule. When this time is not small compared to the period of the sound wave the result is an increase in absorption as well as an increase in the sound velocity. One would naturally seek the origin of $2\alpha'$ in liquids in the same process, although here one would expect that the relaxation times would be much smaller because of the greater density of liquids. Herzfeld[7] has shown that the fact that $2\alpha'\nu^{-2}$ is a constant up to 80 megacycles, within the experimental accuracy of 10 percent, is not incompatible with this explanation in the cases of benzene, carbon tetrachloride, and methyl alcohol. But in water the internal specific heat is too small to account for the observed value of $2\alpha'\nu^{-2}=32\times10^{-17}$ since $2\alpha'\nu^{-2}$ has not changed by *more* than 10 percent in this range.

Herzfeld, following a suggestion of Dr. Hubbard, points out that if $2\alpha'\nu^{-2}$ is not zero in water at 4°C its origin must be sought in phenomena not connected with the specific heat. This comes about as follows. Consider, for a liquid like benzene, an adiabatic cycle in which the period is larger than the relaxation time and the volume changes as a square wave. The adiabatic compression is accompanied by an increase in temperature ΔT. If on the average a finite time is needed for the internal degrees of

[1] F. E. Fox and G. D. Rock, J. Acous. Soc. Am. **12**, 505 (1941).
[2] A. Lindberg, Physik. Zeits. **41**, 457 (1940).
[3] J. L. Hunter, J. Acous. Soc. Am. **13**, 36 (1941).
[4] K. F. Herzfeld and F. O. Rice, Phys. Rev. **31**, 691 (1928).
[5] D. G. Bourgin, Nature **122**, 133 (1928); Phil. Mag. **7**, 821 (1929); Phys. Rev. **34**, 521 (1929); Phys. Rev. **42**, 721 (1932); **50**, 355 (1936); J. Acous Soc. Am. **4**, 108 (1932); **5**, 57 (1934).
[6] H. O. Kneser, Ann. d. Physik **11**, 761, 777 (1931); **16**, 347 (1933).
[7] K. F. Herzfeld, J. Acous. Soc. Am. **13**, 33 (1941).

freedom to take up their share of the increased heat energy, the initial ΔT right after the compression is determined by the fact that the increased heat energy is taken up only by the external degrees of freedom. ΔT then decreases as the internal modes gradually take up their share. Upon rarefaction the internal energy is not immediately released by the internal degrees of freedom and the initial temperature drop is determined by the effective specific heat due to the external degrees of freedom. The temperature then gradually increases to its equilibrium temperature for the rarefaction only after equilibrium has been attained between internal and external energies. The result is a hysteresis in which a portion of the energy is trapped in each cycle and remains in the fluid to increase the equilibrium temperature T. It is clear that this process does not occur if there is no change in temperature during compression. But the temperature change is a function of the coefficient of thermal expansion and if this is zero there is no change in temperature.

The temperature change in an adiabatic compression* is

$$dT = a(Tv/C_p)dp,$$

where a is the coefficient of thermal expansion, v is the specific volume, T is the absolute temperature, C_p is the specific heat at constant pressure, and dp is the change in pressure. At 4°C in water $a=0$ and $dT/dp=0$. In this case the distinction between adiabatic and isothermal compression vanishes, the compression is always isothermal so that there is no temperature wave. Since there is no change in temperature there can be no effect due to a delay of energy distribution among the internal and external degrees of freedom contributing to the specific heat.

* In the usual notation

$$TdS = dQ = dU + pdv = dH - vdp,$$
$$dH = (\partial H/\partial T)_p dT + (\partial H/\partial p)_T dp,$$
$$TdS = C_p dT + [(\partial H/\partial p)_T - v]dp,$$
$$(\partial H/\partial p)_T = v - T(\partial v/\partial T)_p = v - vTa,$$
$$TdS = C_p dT - vTadp.$$

In adiabatic change

$$dS = 0,$$
$$C_p dT = vTadp,$$
$$dT/dp = (Tv/C_p)a.$$

EXPERIMENTAL METHOD

The experimental method used to measure the absorption coefficient in water as function of the temperature follows closely the work described in detail in a previous article.[1] Only a brief summary of this together with a short description of the apparatus used will be given here.

(a) Sound Source and Tank

The sound source is an electrically driven X cut quartz crystal 1-inch square having a fundamental response frequency of 3.24 megacycles. This was driven at its 5th harmonic, the frequency actually used being 17.125 megacycles. At this frequency the intensity falls to e^{-1} in less than 10 centimeters at room temperature. The source is cemented over an opening in a brass plate which is bolted over an opening in one end of a rectangular tank. The tank, $3\times1\times1$ feet has plate-glass sides and bottom, and hard-rubber ends. The crystal was driven by a frequency stabilized oscillator capable of delivering from 300 to 50 watts in the range from 1 to 50 megacycles. In it a master oscillator operates at from 1 to 2 megacycles and its output frequency is doubled successively and finally fed into a power amplifier at the required frequency. A link coupled LC circuit tuned to resonance at 17.125 megacycles transferred the power to the quartz crystal which was connected across the condenser in this circuit. The power used to drive the crystal was continually monitored by means of the current indicator of an absorption type wave meter placed near the crystal and adjusted to nearly full scale deflection. This proved to be very sensitive to small changes in the power being supplied to the crystal and detected changes that were far too small to be detected by a change in acoustic output as indicated by the deflection of the bead used to measure the sound intensity. The constancy of the wave meter indicator was taken as ample assurance that the acoustic output of the crystal remained constant during an absorption measurement.

(b) Sound Detector

The sound intensity was determined by measuring the radiation pressure on a sphere placed

in the sound beam, and suspended by a bifilar suspension of single strands of Nylon thread attached to a support that could be moved parallel to the sound beam. The sphere, a plastic bead, has a diameter of 1.25 centimeters and a

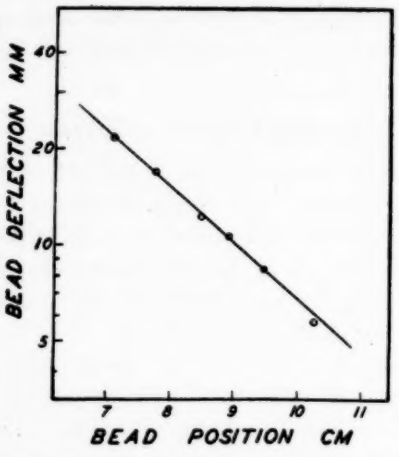

FIG. 1. Semi-log plot of the deflection of the bead as a function of its distance from the sound source. Data used are a set of measurements made at 0°C.

suspension approximately 180 centimeters long. A deflection of one centimeter corresponds to a sound intensity of approximately 0.018 watt per square centimeter. In the present work the deflection of the bead was measured with a traveling telescope mounted on an optical bench parallel to the length of the tank. The telescope is mounted on a micrometer screw, and this unit could be moved along the graduated scale of the optical bench. To determine the deflection at any position along the sound beam, the telescope is moved until a reference point on the bead coincides with the cross hairs, first in the deflected position and then in the undeflected position. The deflection is then the difference of the micrometer readings. No attempt was made to measure the deflection to better than 0.1 millimeter since the stability of the bead in the undeflected position was such that successive readings varied as much as 0.5 millimeter. Care was taken to eliminate the effect of mass flow of water along the sound beam by inserting a thin microfilm of collodion a few millimeters in front of the bead at each deflected reading. For all deflections used the intensity was kept below 0.04 watt per square centimeter. This corresponds to a deflection of about 25 millimeters. The necessity of this precaution has been pointed out before, i.e., that for larger intensities the measured absorption increases with the intensity.

(c) Temperature Adjustment and Control

Several considerations made it apparent that it would not be necessary to provide elaborate means for maintaining a constant temperature. The first of these is the large thermal inertia of the water in the tank (over 70 kg). Preliminary observations showed that many deflections readings could be taken before the temperature changed by as much as 1°C even when making measurements near the freezing point. Secondly, the coefficient of expansion is very small in the neighborhood of 4°C. For the range 3.5°C to 4.5°C the maximum value is less than 5 percent of the coefficient of expansion at 25°C. In addition the change in the coefficient of viscosity per degree Centigrade is much less than 10 percent so that within an experimental accuracy of 10 percent this would not be significant. The preliminary measurements at 4°C indicated that $2\alpha\nu^{-2}$ was considerably greater than $2\alpha_v\nu^{-2}$ so that $2\alpha'$ is not zero but is several times larger than $2\alpha_v$. It was then decided to measure from 0°C to room temperature at approximately 5°C intervals. The procedure was as follows. The absorption was measured at room temperature and then the water was cooled by adding clean ice until the desired temperature was reached, where 2α was again measured. The water was

TABLE I. Temperature dependence of absorption coefficients in water.

Temp. °C	$2\alpha\nu^{-2}\times10^{17}$	$2\alpha_v\nu^{-2}\times10^{17}$*	$2\alpha'\nu^{-2}\times10^{17}$
0	137	34.2	103
4	101	28.7	72
5	95	27.5	67
10	73	22.7	50
15	58	19.1	39
20	48	16.3	32
25	43	14.0	29
30	41	12.3	29
33	40	11.0	29
40		9.7	
50		8.0	
60		6.7	
70		5.8	
80		5.1	
85		4.9	

* Calculated using data from *International Critical Tables* for density (3, 25) and viscosity (5, 10); the sound velocity is from C. R. Randall, Bur. Stand. J. Research 8, 79 (1932).

then heated by an electric heater to the next temperature, where 2α was again measured. The final temperature in each set of measurements was around 20°C. The temperature was actually maintained constant within several tenths of a degree for the 0°C and 4°C measurements in the following manner. For the 4°C measurements the water was not stirred after it had been cooled approximately to 4°C by adding ice, but an ice layer an inch or so thick was allowed to float on the surface. After equilibrium was reached, the water from the bottom of the tank to the ice remained within several tenths of a degree at 4°C. The temperature was read at the position of the sound beam before and after each determination of 2α. To secure the 0°C temperature a layer of ice was weighted down on the bottom of the tank under a fine wire screen, and a layer of ice was allowed to float on the surface. After stirring the water remained very close to 0°C. In these instances a cylindrical tube was used to protect the suspension from contact with the floating ice.

(d) Procedure for Determining the Absorption Coefficient

The deflections of the bead were measured at various positions along the sound beam, making sure that the bead was always centered in the beam. These deflections were then plotted on semi-log graph paper against the deflected position of the bead. A straight line was drawn through the set of points obtained at each temperature, and 2α was calculated from the slope of this line. This is illustrated by Fig. 1 in which the data for 0°C are used. The lines of best fit were drawn by two different individuals for each set of readings, and in all cases agreed within 10 percent.

RESULTS

The experimental results are given in Fig. 2. Here the points are measured values of $2\alpha\nu^{-2}$ plotted against Centigrade temperature. Table I gives $2\alpha\nu^{-2}$ as read from the smooth curve A drawn through the points of Fig. 2. Table I also gives $2\alpha_v\nu^{-2}$. The highest temperature used in the measurements was 33°C but $2\alpha_v\nu^{-2}$ is given for higher temperatures at 10°C intervals over the range where velocity measurements are available. In Fig. 2 these are given by curve B. Table I includes values of $2\alpha'\nu^{-2}=2(\alpha-\alpha_v)\nu^{-2}$ the unexplained part of the absorption coefficient and in Fig. 2 curve C is plotted from these data.

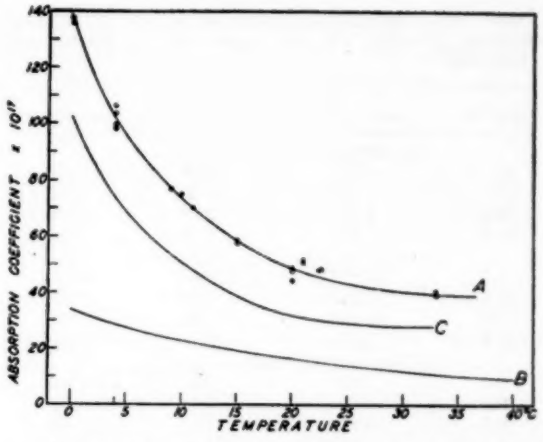

FIG. 2. The absorption coefficients as a function of temperature. Points are measured values of $2\alpha\nu^{-2}$. Curve A is that used to obtain the values of $2\alpha\nu^{-2}$ given in Table I. Curve B is the plot of the calculated shear viscosity contribution $2\alpha_v\nu^{-2}$ given in Table I. Curve C is the plot of the excess absorption $2\alpha'\nu^{-2}=2(\alpha-\alpha_v)\nu^{-2}$ from the values of Table I. Thus $C=A-B$.

DISCUSSION OF SOUND ABSORPTION IN LIQUIDS

It follows from the experimental results available at present, and from theoretical considerations, that the sound absorption is made up of at least four terms:

$$2\alpha=2\alpha_v+2\alpha_H+2\alpha_c+2\alpha_x. \qquad (1)$$

α_v is caused by viscosity[8]; α_H is due to heat conduction[9]; however, this term is usually so small in liquids that it can be neglected. α_c is caused by the slowness of energy exchange between internal and external degrees of freedom. It exists in gases and there is no reason to suspect its absence in liquids, although no direct experimental proof for its existence is available. α_x is the absorption of unknown origin, not connected with viscosity or the internal degrees of freedom, which has been discovered in water. It will be discussed later.

The quantity α', used before, is

$$\alpha'=\alpha_c+\alpha_x.$$

[8] G. G. Stokes, Camb. Trans. Phil. Soc. **8**, 287 (1845); Math. Phys. Pap. **1**, 75 (1880).
[9] G. Kirchoff, Pogg. Ann. **134**, 177 (1868).

TABLE II. Temperature dependence of absorption coefficients (a) olive oil; (b) castor oil; (c) linseed oil; (d) benzene.

Temp. °C	$2\alpha\nu^{-2}\times10^{17}$	$2\alpha_v\nu^{-2}\times10^{17}$	$2\alpha'\nu^{-2}\times10^{17}$
	(a) olive oil,[a] 3.16 megacycles		
9	3780	2560	1220
21.7	2680	1490	1190
36.4	1190	890	300
54.5	890	530	360
	(b) castor oil,[a] 3.16 megacycles		
12.2	36400	29800	6600
18.6	21800	17900	3900
27.0	10400	9700	700
37.0	7400	5200	2200
	(c) linseed oil,[a] 3.16 megacycles		
0.1	2580	1280	1300
10.5	1810	980	830
20.5	1150	750	400
36.2	790	530	260
	(d) benzene,[b] 2.93 megacycles		
7.2	1320	*	
23.0	1440		
47.5	1540		
63.0	1640		
73.5	1700		

* $2\alpha_v\nu^{-2}\times10^{17}=16.7$ at 20°C.
[a] Calculated from data of J. L. Hunter, J. Acous. Soc. Am. 13, 36 (1941).
[b] From data of J. Quinn, Doctoral Dissertation, Catholic University of America (1946).

A discussion of the available experimental results shows the following:

For water $2\alpha'\nu^{-2}=2\alpha_s\nu^{-2}$ is at room temperature 32×10^{-17}, i.e., about $2\times2\alpha_v\nu^{-2}$ and decreases with increasing T; this decrease is by a factor 3.2 between 0°C and 30°C, and neither the immediate neighborhood of the melting point nor 4°C show any peculiarity.

For benzene[10] $2\alpha'\nu^{-2}$ is 1400×10^{-17} or about 100 times $2\alpha_v\nu^{-2}$. It is possible to explain the value of $2\alpha'\nu^{-2}$ by identifying it with $2\alpha_c\nu^{-2}$ and ascribing to the relaxation time a reasonable value. Because of the fact that $2\alpha'\nu^{-2}$ is so much larger than $2\alpha_v\nu^{-2}$, the temperature coefficient of $2\alpha\nu^{-2}$ is that of $2\alpha'\nu^{-2}$. The absorption coefficient is found to increase linearly with T between +7°C and 70°C, with no peculiarity as one approaches the melting point which lies at 5.4°C. The expression $2\alpha\nu^{-2}V$, where V is the sound velocity, turns out to be temperature independent in this range.

For liquids with high viscosity,[3] namely castor oil, olive oil, and linseed oil, $2\alpha_v\nu^{-2}$ is larger than $2\alpha'\nu^{-2}$ and the temperature dependence is approximately that of viscosity. Although the measurements are said to be not more accurate than 30 percent and the difference $2(\alpha-\alpha_v)\nu^{-2}=2\alpha'\nu^{-2}$ is nowhere larger than this, one can still tentatively calculate it from Hunter's measurements. The results are given in Table II,* together with data on benzene. Although, as mentioned above, the possible error is frequently larger than the difference $2\alpha'\nu^{-2}$, the results are in general so consistent that the general conclusions seem reliable. The absolute value of $2\alpha'\nu^{-2}$ lies for these liquids at room temperature, between 6600×10^{-17} and 200×10^{-17}, that is, it is of the same order of magnitude as in benzene, although the viscosity of castor oil at 20°C is 1000 times that of benzene. This means that $2\alpha'\nu^{-2}$ is not in general dependent on the viscosity.

Furthermore, $2\alpha'\nu^{-2}$ decreases with increasing temperature, as in water, while it increases in benzene.

Unfortunately, no data are available at present to separate, for liquids like benzene or the highly viscous liquids, α' into the terms α_c and α_s. The former is given by

$$\frac{2\alpha_c}{\nu^2}=\frac{4\pi^2}{V}\left\{\frac{C'\Delta}{C_p(C_p-\Delta)}\right\}\tau=\frac{4\pi^2}{V}\epsilon\tau, \qquad (2)$$

where C' is the internal specific heat, $\Delta=C_p-C_v$, and τ is the relaxation time. In gases τ has been found[11-13] to decrease in some cases with increasing temperature (proportional to an expression $e^{-Q/RT}$); for other gases it is constant. In liquids, it might in some cases even increase

TABLE III. Values of ϵ for benzene.

Temp. °C	5	20	50
C'[a]	9.66	10.73	12.57
C_p liquid[b]	31.6	32.0	33.9
Δ[c]	9.5	9.73	9.9
ϵ	0.132	0.146	0.153

[a] Calculated from the frequencies given by R. C. Lord and D. H. Andrews, J. Phys. Chem. 41, 149 (1937).
[b] J. S. Burlew, J. Am. Chem. Soc. 62, 696 (1940).
[c] Calculated from the expansion given in reference b and the compressibilities D. Tyrer, J. Chem. Soc. 103, 1675, (1913).

[10] J. Quinn, Doctoral Dissertation, Catholic University of America (1946).

* We express our thanks to Brother John Quinn for making this calculation.

[11] L. Landan and E. Teller, Physik. Zeits. Sowjetunion 10, 34 (1936).
[12] A. Eucken and L. Küchler, Zeits. f. tech. Physik 19, 66 (1938).
[13] L. Kuchler, Zeits. f. physik. Chemie (B) 41, 199 (1938).

with T, because of the expansion of the liquid. For benzene the values of ϵ are given in Table III. ϵ goes up by about 15 percent between 5°C and 50°C and this might very well be compensated by a slight decrease in τ.

Perhaps a possible method might be the measurement of the absorption and of its temperature coefficient in benzene vapor; although the absolute value of the relaxation time τ will be completely different in vapor and liquid, the heat of activation might be the same. If therefore one found a similar temperature coefficient for $2\alpha'\nu^{-2}$ in benzene vapor and liquid benzene one might conclude that the mechanism is in both cases the same, namely slowness of energy exchange between internal and external degrees of freedom. Of course, the thermal expansion of the liquid might destroy this argument.

For large molecules like castor oil, one should expect that

$$\lim (C'/C_v) \sim 1.$$

Then inserting the value of Δ

$$2\alpha_c V\nu^{-2} = d\pi^2 TUa^2(C_p\beta)^{-1}\tau, \qquad (3)$$

where U is the mole volume, a the expansion coefficient, and β the compressibility. With increasing temperature, C_p, β, and Ta^2 increase, but not sufficient data are available to judge whether (3) increases or decreases.

From the theoretical standpoint, Tisza[14] has called attention to the fact that from general considerations of isotropy the stress p_{xx} is

$$p_{xx} = p_{\text{stat}} - \tfrac{2}{3}\eta\left(\frac{\partial u}{\partial x}+\frac{\partial v}{\partial y}+\frac{\partial w}{\partial z}\right) + 2\eta\left(\frac{\partial u}{\partial x}\right)+k\left(\frac{\partial u}{\partial x}+\frac{\partial v}{\partial y}+\frac{\partial w}{\partial z}\right).$$

Tisza defines p_{stat} as the pressure which would result from an adiabatic compression from the equilibrium state. We will instead define it as the hydrostatic pressure which would exist in the liquid at rest at the same density and temperature; u, v, w are the three components of the velocity $\mathbf{v}$, η is the usual coefficient of viscosity, and k a new constant.

$$\text{div } \mathbf{v} = \partial u/\partial x+\partial v/\partial y+\partial w/\partial z$$

is, as can be seen from the equation of continuity, the relative change of density for a given part of the gas, so that

$$k(\partial u/\partial x+\partial v/\partial y+\partial w/\partial z)$$

is a compressional friction. For monatomic gases one can prove that k is zero and Stokes[8] has given reasons that this should generally be the case. If one sets $k=0$, one gets the Stokes[8] formula for $2\alpha_v\nu^{-2}$.

Tisza pointed out that any absorption in excess of the classical value could be interpreted[15] as caused by a term of the form

$$k(\partial u/\partial x+\partial v/\partial y+\partial w/\partial z).$$

In the case of polyatomic gases, there exists only

$$(k \text{ div } \mathbf{v})_{\text{adiabatic}}.$$

The experimental measurements on water described in this paper prove, as Professor E. Teller has pointed out, the existence of a term

$$(k \text{ div } \mathbf{v})_{\text{isothermal}},$$

with a value of k at 4°C given by

$$k = 4/3(2\alpha'\eta/2\alpha_v) = 3.34\eta = 0.0524 \text{ poise}.$$

At 20°C k has decreased to 0.026 poise.[15] They say nothing about the origin of k. However, the decrease with increasing temperature is not inconsistent with the idea that a compression changes the degree of order the molecules have in the liquid, and that this change in order has a finite relaxation time (Debye[16]). One should expect that the amount of order decreases with increasing temperature.

The authors wish to express their gratitude to Professor Karl Herzfeld for many helpful discussions.

[14] L. Tisza, Phys. Rev. 61, 531 (1942).

[15] See also Eugene Tsung Hsu, J. Acous. Soc. Am. 17, 127 (1945).

[16] H. O. Kneser, Physik. Zeits. 39, 800 (1938).

PHYSICAL REVIEW VOLUME 70, NUMBERS 1 AND 2 JULY 1 AND 15, 1946

Schwarzschild Interior Solution in an Isotropic Coordinate System

MAX WYMAN
University of Alberta, Edmonton, Alberta, Canada
(Received April 3, 1946)

The relativistic equations for the case of a sphere of perfect fluid of constant density are solved when an isotropic coordinate system is used. It is again found that a sphere of given density has upper bounds on its mass and radius but that these upper bounds are smaller than those given by the ordinary Schwarzschild solution.

INTRODUCTION

IN determining the gravitational potentials for a spherical mass by means of relativity theory it is customary to use a coordinate system for which the line element takes the form

$$ds^2=e^{\nu}dt^2-e^{\lambda}dr^2-r^2d\theta^2-r^2\sin^2\theta d\phi^2, \quad (1)$$

where ν, λ are functions of r alone. If we denote by m the gravitational mass of the body as measured by its external gravitational field, it is well known that the Schwarzschild exterior solution is

$$e^{\nu}=e^{-\lambda}=1-2m/r. \quad (2)$$

If the density of the sphere is ρ and the radius is a then it is also well known[1] that the interior solution is

$$e^{\nu}=\tfrac{1}{4}[3h(a)-h(r)]^2,\ e^{-\lambda}=[h(r)]^2, \quad (3)$$

where $h(r)=(1-r^2/R^2)^{\frac{1}{2}}$ and $R^2=3/8\pi\rho$. The gravitational potentials (3) are valid everywhere inside the sphere. This solution is based on the following physical assumptions: (1) the density is constant; (2) the pressure is zero at the surface of the sphere and is finite and positive inside the sphere; (3) the matter comprises a perfect fluid at rest; (4) the gravitational potentials of the exterior and interior solutions are continuous at the boundary of the sphere; (5) de^{ν}/dr is continuous at the boundary.

When one uses an isotropic coordinate system[2] the line element takes the form

$$ds^2=e^{\nu}dt^2-e^{\mu}(dr^2+r^2d\theta^2+r^2\sin^2\theta d\phi^2) \quad (4)$$

and the corresponding exterior solution is known to be

$$e^{\nu}=[q-m/r]^2/q^2,\ e^{\mu}=q^4, \quad (5)$$

where $q=(1+m/2r)$. However as far as the author knows the corresponding interior solution has never been derived. It is the object of this paper to obtain this solution on the same physical bases as given above.

I. SOLUTION OF THE FIELD EQUATIONS

Since the matter in the sphere comprises a a perfect fluid at rest, the components of the energy-momentum tensor T_j^i satisfy the following equations: $T_1^1=T_2^2=T_3^3=-p$, $T_j^i=0$, $i\neq j$, where p is the proper pressure of the fluid. Since the matter is also of constant proper density we have $T_4^4=\rho=$constant. For the line element (4) the field equations imply:[3]

$$8\pi p=e^{-\mu}\left(\frac{\mu'^2}{4}+\frac{\mu'\nu'}{2}+\frac{\mu'+\nu'}{r}\right), \quad (1.1)$$

$$8\pi p=e^{-\mu}\left(\frac{\mu''+\nu''}{2}+\frac{\nu'^2}{4}+\frac{\mu'+\nu'}{2r}\right), \quad (1.2)$$

$$8\pi\rho=e^{-\mu}\left(\mu''+\frac{\mu'^2}{4}+\frac{2\mu'}{r}\right). \quad (1.3)$$

In the above equations the prime notation means differentiation with respect to r. If we substitute

$$\mu=4\log w-2\log r,\ x=\log r, \quad (1.4)$$

Eq. (1.3) becomes

$$d^2w/dx^2=\tfrac{1}{4}w-2\pi\rho w^5. \quad (1.5)$$

This can be integrated to give

$$\left(\frac{dw}{dx}\right)^2=\frac{w^2}{4}-2\frac{\pi\rho}{3}w^6+k. \quad (1.6)$$

[1] R. C. Tolman, *Relativity, Thermodynamics and Cosmology* (Clarendon Press, Oxford, 1934), pp. 245–247.
[2] A. S. Eddington, *Mathematical Theory of Relativity* (Cambridge University Press. New York, 1923), pp. 93–95.
[3] R. C. Tolman, reference 1, pp. 242–243.

In order to avoid a singularity at the origin it is not difficult to show that $k=0$. An infinite singularity in this case implies the pressure would be infinite at the origin. Taking $k=0$ we can integrate (1.6) to obtain

$$w=[R/\cosh(x+c)]^{\frac{1}{2}}, \tag{1.7}$$

where $R^2=3/8\pi\rho$ and "c" is an arbitrary constant. The corresponding solution for μ is given by

$$e^{\mu}=4R^2/(e^c r^2+e^{-c})^2. \tag{1.8}$$

In order to determine ν, we note that the equality of (1.1) and (1.2) implies

$$\nu''+\nu'^2/2-\nu'/r-\mu'\nu'+\mu''-\mu'^2/2-\mu'/r=0. \tag{1.9}$$

By use of (1.8) Eq. (1.9) can be reduced to

$$\nu''/\nu'+\nu'/2-1/r-\mu'=0. \tag{1.10}$$

This can be integrated to give

$$e^{\nu}=\left\{\frac{Ar^2+B}{e^c r^2+e^{-c}}\right\}^2, \tag{1.11}$$

where A, B are both arbitrary constants.

Thus, three arbitrary constants remain in our solution which are evaluated by means of the boundary conditions.

II. THE BOUNDARY CONDITIONS

By means of (1.1), (1.8) (1.11) the pressure is determined by

$$8\pi p=[A(e^{-2c}-2r^2)+B(e^{2c}r^2-2)]/R^2(Ar^2+B). \tag{2.1}$$

Thus $p=0$ at $r=a$ implies

$$A(e^{-2c}-2a^2)+B(e^{2c}a^2-2)=0. \tag{2.2}$$

Further if we let $v=(1-m/2a)(1+m/2a)$, then the continuity of e^{ν}, e^{μ} at $r=a$ implies

$$Aa^2+B=(e^c a^2+e^{-c}), \tag{2.3}$$

$$2R=(1+m/2a)^2(e^c a^2+e^{-c}). \tag{2.4}$$

Solving (2.2), (2.3) for A, B, we obtain

$$A=v(2-e^{2c}a^2)/(e^{-c}-a^2e^c), \tag{2.5}$$

$$B=v(e^{-2c}-2a^2)/(e^{-c}-a^2e^c). \tag{2.6}$$

Since the pressure at $r=0$ is given by

$$(p)_{r=0}=3a^2/8\pi R^2(e^{-2c}-2a^2), \tag{2.7}$$

and since this pressure is positive, we must have

$$e^{-c}-e^c a^2>0. \tag{2.8}$$

Equation (2.4) can be written in the form

$$e^c a^2+e^{-c}=2R/(1+x)^2, \tag{2.9}$$

where $x=m/2a$. By squaring both sides of (2.9) and subtracting $4a^2$ we obtain

$$(e^{-c}-e^c a^2)^2=4R^2(1-y(1+x)^4)/(1+x)^4, \tag{2.10}$$

where $y=a^2/R^2$. Taking the positive square root of both sides we have, because of (2.8), that

$$e^{-c}-e^c a^2=2R[1-y(1+x)^4]^{\frac{1}{2}}/(1+x)^2. \tag{2.11}$$

The final boundary condition to be satisfied is the continuity of de^{ν}/dr at $r=a$. This leads to the equation

$$2a^2(Ae^{-c}-Be^c)/(e^c a^2+e^{-c})^2=2x/(1+x)^2; \tag{2.12}$$

by means of (2.5), (2.6), (2.9), (2.11) this last equation can be put into the form

$$y/[1-y(1+x)^4]^{\frac{1}{2}}=4x/(1+x)^5(1-x). \tag{2.13}$$

Solving this for y we obtain

$$y=4x/(1+x)^6. \tag{2.14}$$

Equation (2.14) represents the determination of the mass "m" in terms of the density ρ and radius a of the sphere. If x is small we have as an approximate equation $y=4x$. This implies $m=4\pi\rho a^3/3$, which is of course the ordinary Newtonian expression. Physically we require that m be uniquely determined if a and ρ are specified. This means that x must be a single valued function of y. By finding the maximum value of y we find that this condition implies $x\leqslant 0.2$, $y\leqslant 0.27$. This means $m\leqslant 0.4a$, $a^2\leqslant 0.27R^2$.

Hence we find, as was found in the Schwarzschild solution, that a sphere of given density has an upper bound on its size and mass. More will be said on this point in the conclusion of this paper.

Because it is not easy to express x in terms of y we find it better to consider m and a as the known constants for the sphere. We can then explicitly express all other constants in terms of these two. The density ρ is given by (2.14) to be

$$\rho=\frac{3m}{4\pi a^3(1+m/2a)^6}. \tag{2.15}$$

From (2.9), (2.11), (2.14) we find $e^c=(m/2a^3)^{\frac{1}{2}}$. Similarly the values of A and B can be found to be

$$A=(m/2a^3)^{\frac{1}{2}}(4a-m)/(2a+m), \quad (2.16)$$

$$B=(2a^3/m)^{\frac{1}{2}}(2a-2m)/(2a+m). \quad (2.17)$$

As our final solution for the gravitational potentials we obtain

$$e^{\mu}=(1+m/2a)^6/(1+mr^2/2a^3)^2, \quad (2.18)$$

$$e^{\nu}=[2a-2m+m(4a-m)r^2/2a^3]^2/[(2a+m)(1+mr^2/2a^3)]^2. \quad (2.19)$$

III. CONCLUSION

In the Schwarzschild solution it was found[4] that a sphere of given density is bounded in mass and size by $m\leqslant 4a/9$, $a^2\leqslant 8R^2/9$. In our solution these bounds are smaller and are given by $m\leqslant 0.4a$, $a^2\leqslant 0.27R^2$. Thus an observer using an isotropic coordinate system would find smaller upper bounds than an observer using a coordinate system in which the line element takes the form (1). This shows that these upper bounds are definitely a property of the coordinate system used by the observer, and it is conceivable that coordinate systems may exist in which these upper bounds may be infinite.

Having obtained the interior solution it is easy to show that the complete solution is mathematically equivalent to the Schwarzschild solution. It is already known that the transformation

$$\bar{r}=(1+m/2r)^2r, \; r\geqslant a$$

takes the isotropic exterior solution into the Schwarzschild exterior solution. The transformation

$$\bar{r}=(1+m/2a)^3r/(1+mr^2/2a^3), \; 0\leqslant r\leqslant a$$

does the same for the interior solution. Moreover the two transformations piece together continuously at the boundary $r=a$.

[4] A. S. Eddington, reference 2, p. 170.

PHYSICAL REVIEW VOLUME 70, NUMBERS 1 AND 2 JULY 1 AND 15, 1946

Forced Vibrations of Piezoelectric Crystals

H. EKSTEIN
Armour Research Foundation, Chicago, Illinois
(Received March 6, 1946)

The vibrations of anisotropic bodies under the influence of sinusoidally variable volume forces and boundary stresses are investigated. The displacement components are represented as sums of a system of "zero-order" solutions which solve approximately the free-vibration problem. By using Betti's theorem, the problem is reduced to a system of inhomogeneous linear equations which, for the free-body case, further reduces to the homogeneous system derived in an earlier paper (reference 2). If the external forces are piezoelectric, the forces are no longer given explicitly because the electrical field distribution is known only if Maxwell's equations are solved simultaneously. However, if the pertinent piezoelectric constants are small, the field can be calculated approximately as if the crystal were not vibrating. The solutions can then be obtained by the above method, and the electric reaction of the crystal upon the driving system can be determined. As an example, forced vibrations of thin quartz plates between parallel electrodes are discussed.

I. INTRODUCTION

THE rigorous solution of vibration problems meets such great mathematical difficulties that even in comparatively simple cases only approximation methods can be used. The analogy with scalar vibration problems of the Schrödinger type suggests that the solution U_i might be represented as a linear combination of "zero-order" functions $u_i^{(m)}$. This method is straightforward if the $u_i^{(m)}$ satisfy the boundary conditions of the problem. But in most cases, the convenient system $u_i^{(m)}$ does not satisfy the

given boundary conditions. In this case, the sum

$$U_i = A_m u_i^{(m)}$$

cannot be differentiated term by term after being inserted in the differential equation of the problem. In the following, the self-adjoint property of the differential operator, as stated by Betti's theorem, is used to avoid this difficulty. It is then only necessary to assume that an infinite series involving $u_i^{(m)}$ may be integrated term by term, a condition which imposes fewer restrictions upon the series. In this manner, the coefficients A_m can be calculated after a secular equation has been solved. The usual methods of perturbation theory can be used to obtain approximate solutions.

The piezoelectric excitation of vibrations presents a more complicated problem. The stress depends upon the electric field which in turn depends upon the strain. It would be necessary to solve Maxwell's equations simultaneously with the elastic equations. The following approximation method can be used when the piezoelectric constants are small, as in most cases: the electric field is put equal to the external field (in absence of the crystal) so that the problem reduces to the case of given surface and volume stresses. Once this problem is solved, e.g., by the perturbation method described above, the polarization can be expressed in terms of the known strains. With this value of the polarization, the electric field equations are integrated again. As a result, one obtains the electric reaction of the crystal upon the driving system. Successive higher approximations can be obtained by inserting the improved values of the electric field into the elastic equation, etc.

It is convenient to represent the reaction of the crystal upon the driving system by an equivalent electric network. It will be shown that this is possible if the network contains a series of parallel resonant circuits and a series of resonant circuits which are coupled inductively and capacitatively to the parallel circuits. The values of the circuit elements can be expressed completely in terms of the crystal constants. This equivalence will be discussed for a particular case.

Very little is known about the energy dissipation in crystals. Although Voigt has developed a formal theory of friction, in which the frictional stresses are proportional to the rate of change of the strains, experiments have shown that the process is more complicated. In the case of quartz, e.g., the friction depends mainly upon the minute surface irregularities[1] rather than upon volume constants. Under these conditions, it seems preferable to renounce an introduction of damping in the general equations and to insert simply a damping constant into the final formulas, or to insert a resistance into each resonant circuit of the equivalent electrical network.

II. FORCED VIBRATIONS WITH GIVEN EXTERNAL FORCES

In this section the forced vibrations of a nonpiezoelectric crystal, driven by sinusoidally variable volume forces and boundary stresses, are treated. Only cartesian coordinates are used, so that we do not need to distinguish between covariant and contravariant tensors.

In the steady state, all mechanical quantities have a time-part $\exp(i\omega t)$ where $\nu = \omega/2\pi$ is the frequency of the driving forces. In the following, this time-part will be omitted. Let U_i be the displacement components, and

$$S_{ij} = \frac{1}{2}\left(\frac{\partial U_i}{\partial x_j} + \frac{\partial U_j}{\partial x_i}\right) \tag{1}$$

the strain tensor. With the usual convention on summation, the stress tensor is

$$T_{ij} = -c_{ijkl} S_{kl} = -c_{ijkl}\partial U_k/\partial x_l, \tag{2}$$

where

$$c_{ijkl} = c_{jkl} = c_{jilk} = c_{ijlk} = c_{klij}. \tag{3}$$

The dynamical equations are:

$$f_i^{(e)} + \rho\omega^2 U_i = \frac{\partial T_{ij}}{\partial x_j} = -c_{ijkl}\frac{\partial^2 U_k}{\partial x_j \partial x_l}, \tag{4}$$

where $f_i^{(e)}$ are the components of the volume force. If $\varphi_i^{(e)}$ are the components of the boundary stresses, then the boundary conditions are:

$$T_{ij} n_j = -n_j c_{ijkl}\partial U_k/\partial x_l = \varphi_i^{(e)} \tag{5}$$

where n_j are the components of the normal to the surface, directed inward. The solution U_i is now represented as a linear combination of

[1] K. S. Van Dyke, Proc. I.R.E. 23, 386 (1935).

functions $u_i^{(m)}$.

$$U_i = A_m u_i^{(m)}, \tag{6}$$

where in general the number of functions $u_i^{(m)}$ will be infinite. It is not required that $u_i^{(m)}$ satisfy any specific boundary conditions. Practically, one will choose solutions of a reasonably similar but sufficiently simple problem for $u_i^{(m)}$.

We multiply Eq. (4) by $u_i^{(n)}$, sum over the index i, and integrate over the crystal volume:

$$\int u_i^{(n)}(f_i^{(e)} + \rho\omega^2 U_i)dv = -\int u_i^{(n)} c_{ijkl} \frac{\partial^2 U_k}{\partial x_j \partial x_l} dv. \tag{7}$$

Through integration by parts, the second member becomes

$$-\int u_i^{(n)} c_{ijkl} \frac{\partial^2 U_k}{\partial x_j \partial x_l} dv = \int u_i^{(n)} n_j c_{ijkl} \frac{\partial U_k}{\partial x_l} ds + \int c_{ijkl} \frac{\partial u_i^{(n)}}{\partial x_j} \frac{\partial U_k}{\partial x_l} dv, \tag{8}$$

the first integral on the right-hand side being extended over the surface.

The second integral of the second member of Eq. (8) does not change when the functions $u_i^{(n)}$ and U_i are interchanged, on account of the symmetry of c_{ijkl}. Therefore

$$\begin{aligned} -\int c_{ijkl} \frac{\partial u_i^{(n)}}{\partial x_j} \frac{\partial U_k}{\partial x_l} dv &= \int u_i^{(n)} c_{ijkl} \frac{\partial^2 U_k}{\partial x_j \partial x_l} dv + \int u_i^{(n)} n_j c_{ijkl} \frac{\partial U_k}{\partial x_l} ds \\ &= \int U_i c_{ijkl} \frac{\partial^2 u_k^{(n)}}{\partial x_j \partial x_l} dv + \int U_i n_j c_{ijkl} \frac{\partial u_k^{(n)}}{\partial x_l} ds. \end{aligned} \tag{9}$$

Equation (9) expresses Betti's theorem.

Equation (7) may now be written

$$\int u_i^{(n)}(f_i^{(e)} + \rho\omega^2 U_i)dv + \int U_i c_{ijkl} \frac{\partial^2 u_k^{(n)}}{\partial x_j \partial x_l} dv + \int U_i n_j c_{ijkl} \frac{\partial u_k^{(n)}}{\partial x_l} ds + \int u_i^{(n)} \varphi_i^{(e)} ds = 0. \tag{10}$$

In the last integral Eq. (5) has been used.

We substitute Eq. (6) for U_i and assume that the integration can be carried out term by term. If we define

$$N_{nm} = N_{mn} = \int u_i^{(n)} u_i^{(m)} dv, \tag{11}$$

$$-H_{nm} = -H_{mn} = \int u_i^{(m)} c_{ijkl} \frac{\partial^2 u_k^{(n)}}{\partial x_j \partial x_l} dv + \int u_i^{(m)} n_j c_{ijkl} \frac{\partial u_k^{(n)}}{\partial x_l} ds, \tag{12}$$

$$F_n = \int f_i^{(e)} u_i^{(n)} dv + \int \varphi_i^{(e)} u_i^{(n)} ds, \tag{13}$$

then Eqs. (10) and (6) yield

$$A_m(\rho\omega^2 N_{mn} - H_{mn}) + F_n = 0. \tag{14}$$

The fact that $H_{mn} = H_{nm}$ in Eq. (12) results from Betti's theorem (Eq. (9)).

In the case of free vibrations, $F_n = 0$, and Eq. (14) becomes a homogeneous system of linear equations which has non-vanishing solutions only for certain characteristic values of $\rho\omega^2$. This case has been discussed in a previous paper.[2]

Let us suppose that the functions $u_i^{(m)}$ are exact solutions of the free problem where $f_i^{(e)} = \varphi_i^{(e)} = 0$. Then it can be proved that the "non-orthogonality" integrals N_{nm} vanish for $n \neq m$.[3] The non-diagonal elements H_{nm} also

[2] H. Ekstein, Phys. Rev. 66, 108 (1944). Further referred to as I.

[3] A. E. H. Love, *Mathematical Theory of Elasticity* (Dover Publications, New York, 1944), p. 180. This is not necessarily true for degenerate solutions but it can be so postulated.

vanish in this case, because by Eq. (4) (for $f_i^{(e)}=0$) the volume integral in Eq. (12) becomes proportional to N_{nm} and, therefore, vanishes, while the surface integral in Eq. (12) vanishes in virtue of Eq. (5) (for $\varphi_i^{(e)}=0$). Then Eq. (14) reduces to

$$A_n(\rho\omega^2 N_{nn}-H_{nn})+F_n=0, \tag{15}$$

or

$$A_n=-\frac{F_n}{\rho\omega^2 N_{nn}-H_{nn}}. \tag{16}$$

By Eq. (6) we have

$$U_i=\frac{-F_n u_i^{(n)}}{\rho\omega^2 N_{nn}-H_{nn}}, \tag{17}$$

which is, of course, equal to the solution of the analogous scalar problem. If we want to take into account the effect of energy dissipation, we simply add an imaginary term to the denominator:

$$U_i=\frac{-F_n u_i^{(n)}}{\rho\omega^2 N_{nn}-H_{nn}+i\eta_n}, \tag{18}$$

where η_n may be a function of the driving frequency, but not necessarily proportional to it. In any case, when the dissipation is small, only one term of the series (18) will be important, *viz.* the term for which

$$\rho\omega^2\cong H_{nn}/N_{nn}. \tag{19}$$

On the other hand, if the functions $u_i^{(n)}$ are not exact solutions of the "free" problem under consideration, but solutions of a similar but simpler problem, then the above statements are, in general, true approximately, except when several $u_i^{(n)}$ are degenerate. One case of this particular type was discussed in I.

III. PIEZOELECTRIC EXCITATION OF MECHANICAL VIBRATIONS AND REACTION UPON THE DRIVING SYSTEM

When a piezoelectric crystal is placed between two electrodes with sinusoidally variable potential difference, it is excited to mechanical vibrations. It will be assumed that the crystal is otherwise free from mechanical forces. According to Voigt, the general equations of piezoelectricity are

$$-T_{ij}=c_{ijkl}S_{kl}-e_{ijk}E_k, \tag{20}$$

$$P_i=e_{kli}S_{kl}+\kappa_{ik}E_k. \tag{21}$$

In these equations, E_k are the components of the electric field intensity, e_{ijk} the piezoelectric constants, κ_{ik} the (clamped) susceptibilities, and P_i the components of the electric polarization.

We consider again the steady state, where all variables have a time-dependent factor exp $(i\omega t)$ which will be omitted in the following equations.

The dynamical equations are again

$$\rho\omega^2 U_i=\partial T_{ij}/\partial x_j, \tag{4a}$$

as in Eq. (4) in absence of external mechanical forces, and the boundary conditions are

$$T_{ij}n_j=0. \tag{5a}$$

These equations do not yet fully determine the problem, because the field intensity is in turn dependent upon the strains.

In the absence of true charges, we have

$$\frac{\partial D_i}{\partial x_i}=\frac{\partial(E_i+4\pi P_i)}{\partial x_i}=0, \tag{22}$$

and

$$\text{curl }\mathbf{E}=-\frac{1}{c}\frac{\partial \mathbf{B}}{\partial t}. \tag{23}$$

We shall consider only comparatively low frequencies so that the second member in Eq. (23) may be disregarded. We then have the equation of the static field

$$\partial E_i/\partial x_j-\partial E_j/\partial x_i=0, \tag{24}$$

and the field intensity can be represented as a potential gradient:

$$-E_i=\partial V/\partial x_i. \tag{25}$$

On the conducting electrodes

$$V=\text{constant}, \tag{26}$$

$$E_t=0, \tag{27}$$

$$D_n=4\pi q, \tag{28}$$

where q is the surface charge density, D_n the normal component of the displacement, and E_t the tangential component of the field intensity.

According to the method discussed in the introduction, we first calculate the field as if the crystal were absent, i.e., we integrate the electrostatic problem defined by Eqs. (22), (24) to (26) as if P_i were zero. In this manner, we obtain a field distribution described by the function E_{oi}.

TABLE I. Comparison of notation.

Voigt	x	y	z	x_x	y_y	z_z	y_z	x_z	x_y
This paper	x_1	x_2	x_3	S_{11}	S_{22}	S_{33}	$2S_{23}$	$2S_{13}$	$2S_{12}$
Voigt	X_x	Y_y	Z_z	Y_z	X_z	X_y	u	v	w
This paper	T_{11}	T_{22}	T_{33}	T_{23}	T_{13}	T_{21}	U_1	U_2	U_3

TABLE II. Correlation of subscripts.

Voigt	1	2	3	4	5	6
This paper	11	22	33	23 or 32	13 or 31	12 or 21

Inserting this into Eqs. (2) and (4a) and taking into account the definition of S_{kl} (Eq. (1)) we obtain

$$-e_{ijk}\frac{\partial E_{ok}}{\partial x_j}+\rho\omega^2 U_i=-c_{ijkl}\frac{\partial^2 U_k}{\partial x_j \partial x_l}, \tag{29}$$

and by Eq. (5a)

$$n_j c_{ijkl}\frac{\partial U_k}{\partial x_l}=n_j e_{ijk}E_{ok}. \tag{30}$$

Equations (29) and (30) are analogous to Eqs. (4) and (5) which can be solved by the method discussed in Section II. Let the solution thus obtained be U_{oi}. If this is inserted into Eq. (21) we obtain

$$P_{1i}=e_{kli}\frac{\partial U_{ok}}{\partial x_l}+\kappa_{ik}E_{1k} \tag{31}$$

as a first approximation for the polarization. E_{1k} are here the components of the field intensity in first approximation, which can be determined by integrating the electrostatic Eqs. (25) to (27) together with Eq. (31). When this is done, Eq. (28) yields the first approximation of the charge density, i.e., the reaction of the crystal upon the driving system.

This method follows closely the one which Voigt uses for the static problems of piezoelectricity. The same method has been used by Cady[4] for a particular vibration problem in piezoelectricity.

It seems necessary to establish the correspondence between the abridged notation used in this paper and Voigt's notation (Table I).

In order to correlate the constants c_{ijkl} used here with the constants c_{mn} used by Voigt, it suffices to correlate each pair of subscripts (ij) and (kl) with one of Voigt's subscripts n and m, respectively. Table II gives this correlation. e.g., our constant $c_{1282}=c_{1223}$ equals Voigt's constant $c_{64}=c_{46}$. The physical definitions are identical with those of Voigt, e.g., the stresses are positive when they are compressive.

The piezoelectric constants e_{ijk} must satisfy the following symmetry requirements:

$$e_{ijk}=e_{jik}, \quad e_{iik}=e_{kki}, \tag{32}$$

if they are to agree with Voigt's piezoelectric constants e_{nm}. The correlation between our constants e_{ijk} and Voigt's e_{nm} is found by replacing the first pair of subscripts (ij) by Voigt's corresponding subscript n according to Table II; the third subscript k of our notation is identical with Voigt's second subscript m, e.g.,

$$e_{123}=e_{63}, \quad e_{232}=e_{42}.$$

IV. THIN QUARTZ PLATES OF THE Y_θ TYPE

The general method will be applied to the case of thin rectangular quartz plates which have one of their major edges parallel to the crystallographic twofold axis. The AT and BT crystals on which most of the experimental work concerning coupling of modes has been done, belong to this type. The crystals under consideration have metal coating on both major surfaces but otherwise they are free. The weight of this metal will be disregarded.

In this section the explicit notation of Voigt will be used rather than the abridged notation of the preceding sections. The edges will be assumed to be parallel to the x, y, z direction and to have the lengths $2a$, $2b$, $2c$, respectively, and the thickness $2b$ to be small as compared to either $2a$ or $2c$. The origin of the system of reference is at the center of the plate.

The first step is to select the zero-order modes. Of course, this selection is largely arbitrary, but the nature of the problem suggests the convenient choice. As pointed out by Atanasoff and Hart[5] the vibrational spectrum of thin plates becomes simple as the lateral dimensions tend toward infinity. The complex spectrum actually found

[4] W. G. Cady, Physics **7**, 237 (1936).

[5] F. V. Atanasoff and P. F. Hart, Phys. Rev. **59**, 85 (1941).

on thin plates can be attributed to the existence of the small lateral surfaces. It is logical, therefore, to consider as zero-order functions those which satisfy the *volume equations of free vibrations* (*Eq. (4) with* $f_i^{(e)}=0$) *and the boundary conditions* (5) *of free vibrations on the major, but not on the lateral surfaces.* These zero-order functions will be closer to exact solutions as the lateral surfaces are smaller in comparison to the major ones.

It has been shown in a previous paper[6] that, if the solution is assumed under the form

$$u,\ v,\ w=\left.\begin{matrix}\cos\alpha x\\ \sin\alpha x\end{matrix}\right\}f(y), \tag{33}$$

it is possible to satisfy the above-mentioned requirements with elementary functions of y. Furthermore, it is possible to satisfy approximately the boundary conditions of free vibrations on the lateral boundary, by convenient choice of α.

One particular type of zero-order mode was treated explicitly in (II), namely,

$$u_t=\begin{cases}\cos\dfrac{m\pi}{2a}x\sin\dfrac{n\pi}{2b}y+\cdots & (m\text{ odd},\ n\text{ odd})\\ \sin\dfrac{m\pi}{2a}x\sin\dfrac{n\pi}{2b}y+\cdots & (m\text{ even},\ n\text{ odd})\end{cases} \tag{34}$$

and the components v and w are proportional to b/a. The frequency belonging to this mode is

$$\nu_t=\frac{1}{2}\left(\frac{c_{66}}{\rho}\right)^{\frac{1}{2}}\left[\left(\frac{n}{2b}\right)^2+k\left(\frac{m}{2a}\right)^2\right]^{\frac{1}{2}}. \tag{35}$$

If a tends towards infinity, this "thickness shear mode" becomes identical with the thickness-shear solution for an infinite plate

$$u=\sin\frac{n\pi}{2b}y,\qquad v=w=0 \qquad \text{with } \nu=\frac{1}{2}\left(\frac{c_{66}}{\rho}\right)^{\frac{1}{2}}\frac{n}{2b}. \tag{36}$$

From the equations given in (II) the existence of other types of zero-order modes of the form (33) could be inferred. For these "lateral" modes the frequency is mainly determined by the dimensions a and c, and the wave number α is of the order of magnitude of the inverse thickness $1/2b$.

We shall apply the method developed above to this case. If the presence of the crystal is disregarded, the electric field between the two plane-parallel electrodes is

$$E_{oy}=-V/2b,\quad E_{ox}=E_{oz}=0, \tag{37}$$

disregarding, as usual, the small curvature of the lines of force in the neighborhood of the lateral edges.

According to Eq. (29) the dynamical equation is that of the free body:

$$\rho\omega^2U_i=-c_{ijkl}\frac{\partial^2U_k}{\partial x_j\partial x_l}. \tag{38}$$

On the major surfaces, we have $n_1=n_3=0$ and $n_2=\mp1$ for $y=\pm b$, so that Eq. (30) becomes:

$$-n_jc_{ijkl}\frac{\partial U_k}{\partial x_l}=\pm e_{i22}E_{oy}. \tag{39}$$

As the subscript i runs from 1 to 3, Voigt's corresponding subscript n takes the values 6, 2, and 4, so that the piezoelectric constants in Eq. (39) are e_{62}, e_{22}, and e_{42}. But according to Voigt, the constants e_{22} and e_{24} vanish, since the x axis coincides with a twofold axis. Therefore, we have

$$\begin{aligned}-n_jc_{ijkl}\frac{\partial U_k}{\partial x_l}&=\pm e_{62}E_{oy},\\ -n_jc_{2jkl}\frac{\partial U_k}{\partial x_l}&=-n_jc_{3jkl}\frac{\partial U_k}{\partial x_l}=0.\end{aligned} \tag{40}$$

If we introduce the symbols $\varphi_i^{(e)}$ of Eq. (5) for the first members of Eq. (39), we obtain

$$\varphi_1^{(e)}=\pm e_{62}E_{oy},\quad \varphi_2^{(e)}=\varphi_3^{(e)}=0. \tag{41}$$

The quantities F_n defined by Eq. (13) are:

$$F_p=e_{62}E_{oy}\int[u_p(b)-u_p(-b)]dxdz, \tag{42}$$

where p stands for one of the zero-order modes. According to the discussion in Section 2, only those zero-order modes whose frequencies are near the driving frequency $\omega/2\pi$, will be of importance. We shall discuss here the case where

[6] H. Ekstein, Phys. Rev. **68**, 11 (1945). Further referred to as II.

one of the high frequency shear modes is excited, i.e., when ν is close to one of the values given by Eq. (35). When the index p in Eq. (42) refers to one of the "lateral" modes, then the quantity α in Eq. (33) is of the order of $1/b$ so that u changes its sign many times between $x=-a$ and $x=+a$. Therefore, most of the integral (42) will cancel out, and these quantities F_p will be very small. The "lateral" modes are only slightly "driven" by the exciting field. These values F_p will be disregarded.

In general, F_p vanishes for each mode u_p which is an even function of y or an uneven function of x or z, as can be seen from Eq. (42). Therefore, the thickness-shear modes u_l with m even, according to Eq. (34), are not "driven."

For the thickness modes with m and n odd, we find by Eqs. (34) and (42):

$$F_p=e_{62}E_{oy}2\cdot 2c\int_{-a}^{+a}\cos\frac{m\pi}{2a}x\,dx=\frac{16}{m\pi}cae_{62}E_{oy}. \quad (43)$$

If all the zero-order functions are chosen, the coefficients of Eq. (14) are known. After solving for A_p, the solution appears under the form (6):

$$U_i=A_pu_i^{(p)}.$$

We now have to calculate the charge q on the electrodes by Eq. (31). The quantities U_{ok} there are identical with the approximate solution used here. Because of the linear character of all the equations, we can determine separately the contribution to q of the applied voltage V and those of the zero-order modes $u_i^{(p)}$.

The contribution of the voltage V alone, disregarding the crystal motion, to the surface charge density is the same as for a non-piezoelectric crystal plate in a condenser:

$$q_v=(1+4\pi\kappa_{22})\frac{V}{8\pi b} \quad (44)$$

on the plane $y=b$ and the opposite at $y=-b$. The total charge due to the applied voltage is

$$Q_v=\int q\,dx\,dz=\epsilon_{22}\frac{ac}{2\pi b}V, \quad (45)$$

where

$$\epsilon_{22}=1+4\pi\kappa_{22} \quad (46)$$

is the dielectric constant of the plate in the y direction.

The separate contribution of each zero-order mode is determined by putting $V=0$ on both electrodes. The "lateral" modes will give a negligible contribution to the charge Q because the integration over x cancels most of the half-waves against each other, just as for the excitation.

For the thickness modes, the displacements are slowly variable functions of x. We may expect, therefore, that the x and z-derivatives of the electric field will also be small. In the following, all terms proportional to b/a will be disregarded when they are in addition to terms of the order of unity. Under these conditions, we can write for Eqs. (22) and (24):

$$\operatorname{div}\mathbf{D}=\partial D_y/\partial y=0, \quad (47)$$

$$\partial E_z/\partial y=0, \quad (48)$$

$$\partial E_x/\partial y=0, \quad (49)$$

so that D_y, E_z, and E_x are constant. Since, by Eq. (27) E_z and E_x vanish at the boundaries, they must vanish everywhere.

From Eqs. (31) and (47) we obtain

$$\frac{\partial D_y}{\partial y}=\frac{\partial}{\partial y}\left[4\pi e_{kl2}\frac{\partial u_k^{(p)}}{\partial x_l}+(1+4\pi\kappa_{22})E_y\right]=0 \quad (50)$$

for the contribution of one single zero-order mode of the shear type. From Eq. (34) it is clear that of the derivatives $\partial u_k/\partial x_l$ only $\partial u/\partial y$ is large; all others are smaller by a factor of order b/a and can be omitted. Integrating Eq. (50) we have:

$$D_y=4\pi e_{62}\frac{\partial u^{(p)}}{\partial y}+\epsilon_{22}E_y=\phi(x,z), \quad (51)$$

where ϕ is a function of x and z only. We integrate Eq. (51) over the thickness remembering that

$$-V=\int E_y dy=0$$

for this calculation:

$$4\pi e_{62}[u^{(p)}(b)-u^{(p)}(-b)]=2b\phi. \quad (52)$$

Eliminating ϕ from Eqs. (51) and (52) and

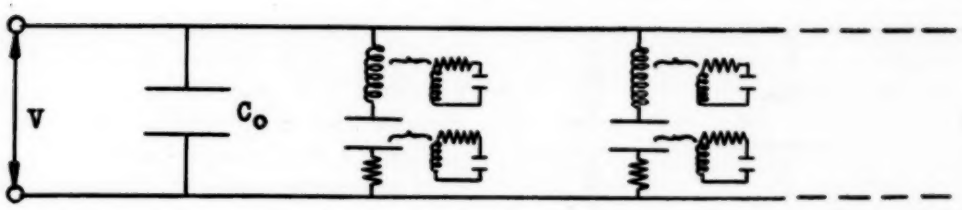

FIG. 1. Equivalent network.

inserting D_y into Eq. (28) we have

$$Q^{(p)}=\int q^{(p)}dxdz$$

$$=-\frac{4\pi e_{62}}{4\pi 2b}\int[u^{(p)}(b)-u^{(p)}(-b)]dxdz. \quad (53)$$

The minus sign in the third member is caused by the fact that at the electrode $y=b$, the normal n has the $(-y)$ direction.

Inserting the functions $u^{(p)}$ from Eq. (34) into Eq. (53) we can carry out the integration:

$$Q^{(p)}=-\frac{8ace_{62}}{m\pi b} \quad (m \text{ odd}),$$
$$Q^{(p)}=0 \quad (m \text{ even}). \quad (54)$$

The total charge will be the sum of Q_v and of the contribution of each mode, $Q^{(p)}$, multiplied by their respective coefficients A_p:

$$Q=\frac{ac\epsilon_{22}V}{2\pi b}-\sum_p A_p\frac{8ace_{62}}{m\pi b}. \quad (55)$$

The subscript p stands for any combination of odd integers m and n. The current flowing through the crystal is

$$I=i\omega Q=i\omega\left(\frac{ac\epsilon_{22}V}{2\pi b}-\sum A_p\frac{8ace_{62}}{m\pi b}\right). \quad (56)$$

V. ELECTRIC NETWORK ANALOGY

In most cases of piezoelectric excitation, the reaction of the crystal upon the input voltage is measured. Therefore, it seems convenient to substitute for the crystal an analogous electric network.

However, the representation of crystal vibrations by equivalent networks has played a role in the recent research which is not limited to the case of electric excitation. Giebe and Scheibe,[7] and Giebe and Blechschmidt[8] used a semi-empirical equivalence to derive vibrational frequencies which could not be calculated. They replaced the crystal by a number of coupled linear oscillators to which they attributed certain characteristic frequencies and coupling constants which were partly surmised and partly determined empirically.

Lack[9] found that the variation of resonant frequencies of a quartz crystal subjected to temperature change can be represented qualitatively if it is assumed that the crystal is equivalent to a system of two coupled resonant circuits, one of which is being driven by an external force. A great number of papers dealing with crystal vibrations have used this empirical analogy, but none of them has derived the equivalent network from the equations of elasticity.

The following network analogy is based upon the approximate solution of the piezoelectric equations.

The individual terms of Eq. (56) can be considered as partial currents flowing through impedances which are all connected in parallel.

The first term

$$i\omega\frac{ac\epsilon_{22}V}{2\pi b}$$

is equivalent to the current through a condenser of capacity

$$C_0=ac\epsilon_{22}/2\pi b \quad (57)$$

which is the static capacity of the quartz plate.

The other terms are equivalent to partial

[7] E. Giebe and A. Scheibe, Ann. d. Physik [5] **9**, 93 (1931).
[8] E. Giebe and E. Blechschmidt, Ann. d. Physik **18**, 417 (1933).
[9] F. R. Lack, Bell Sys. Tech. J. **8**, 515 (1929).

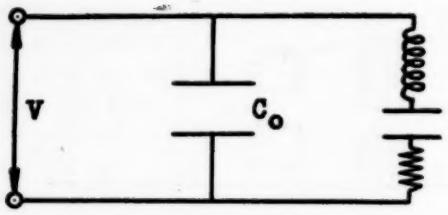

FIG. 2. Simplified equivalent circuit.

currents I_p flowing through a number of parallel branches, each of which represents an uncoupled thickness mode.

It follows that

$$i\omega A_p \frac{e_{26} 8ac}{m\pi b} = I_p \tag{58}$$

if m refers to any parallel branch.

The general network representing the crystal has the equation

$$\sum_p I_p i\left(\omega M_{pq} - \frac{1}{\omega C_{pq}}\right) - V_q = 0. \tag{59}$$

We take $V_q = V$ for all subscripts referring to thickness modes (m odd) and $V_q = 0$ for all other equivalent meshes. In Eq. (59) M_{pq} is the mutual inductance and C_{pq} the mutual capacitance of two meshes.

In particular

$$M_{qq} = L_q, \quad C_{qq} = C_q, \tag{60}$$

are the self-inductance and the capacity of a single mesh. If the Eqs. (15) which determine the values A_p are to be identical with Eq. (59) then it follows from Eqs. (43) and (58) that

$$\begin{aligned} \rho N_{pq}/\gamma = M_{pq}; \quad L_q = \rho N_{qq}/\gamma, \\ H_{pq}/\gamma = 1/C_{pq}; \quad 1/C_q = H_{qq}/\gamma, \end{aligned} \tag{61}$$

where

$$\gamma = 8e_{26}ac/m\pi b. \tag{62}$$

If energy dissipation is to be taken into account, each mesh can be assigned a resistance R_p. As pointed out in the introduction; these resistance values are not determined by crystal constants, but mainly by small irregularities variable from one crystal to another.

Figure 1 illustrates the network.

If a suitable analytical form for the lateral zero-order modes were known then Eqs. (61) in conjunction with the definitions (11) and (12) would allow a determination of the reactive components of the equivalent network. As this is not the case, we limit ourselves to a qualitative discussion.

If the exciting frequency ω is close to the natural frequency of one of the thickness modes so that

$$\rho\omega^2 \cong H_{qq}/N_{qq} = \rho/L_q C_q$$

then the other parallel branches will offer a very high impedance and can be disregarded.

In general, one or several lateral zero-order modes will have values H_{qq}/N_{qq} which are close to $\rho\omega^2$. This corresponds to a state where one or several coupled circuits are tuned to the parallel branch which is at near-resonance. In this case, even small values of the corresponding constants H_{pq} and N_{pq} will give rise to a considerable effective coupling. The resonance curve will exhibit the familiar "double-hump" shape.

However, it will be possible to find crystal dimensions such that the quasi-degeneracy described above does not appear. In this case, the coupled circuits may be disregarded, and the whole equivalent system reduces to the well-known simplified circuit (Fig. 2).

If it is desired, as in most practical applications, to have a resonator with the least possible energy dissipation, then the crystal dimensions will be chosen so as to avoid the coupling as far as possible. This circumstance was empirically recognized by Sykes[10] who also measured a number of desirable crystal dimensions.

[10] R. A. Sykes, Bell Sys. Tech. J. **23**, 52 (1944).

Letters to the Editor

PROMPT publication of brief reports of important discoveries in physics may be secured by addressing them to this department. The closing date for this department is the third of the month. Because of the late closing date for the section no proof can be shown to authors. The Board of Editors does not hold itself responsible for the opinions expressed by the correspondents. Communications should not in general exceed 600 words in length.

Capture Cross Sections for Slow Neutrons. II. Small Capture Cross Sections

C. O. MUEHLHAUSE AND M. GOLDHABER
Department of Physics, University of Illinois, Urbana, Illinois
March 21, 1942*

IN a previous paper Coltman and Goldhaber[1,2] have described a method for measuring capture cross sections for slow neutrons. It consisted in measuring the reduction in slow neutron intensity inside a cylindrical cavity when a mixture of an element and graphite powder was introduced. The slow neutrons were detected with a BF_3 ionization chamber connected to a linear amplifier. The arrangement was calibrated with the help of boron carbide, assuming the capture cross section of boron to be 600×10^{-24} cm². It was also found necessary to correct for the scattering of the slow neutrons, as the arrangement was sensitive to a change in scattering cross section. The scattering correction was found to be approximately linear and equal to −6 percent for 1000 g of graphite added. Though this leads to only a small correction in most cases, it becomes very important for capture cross sections $<10^{-25}$ cm², as comparatively large amounts of the elements have then to be used to obtain an appreciable absorption. In fact, it may be desirable in these cases to use the pure element, or a compound, instead of the graphite mixture. It therefore becomes essential to know the scattering cross section of the element or compound very accurately in order to be able to make the scattering correction. Such a procedure is possible and in this way it has been found that of a large number of elements investigated, three had very small capture cross sections, *viz.*, Be, Si, and Bi[2]. However, the error due to the scattering correction was fairly large in these observations, and therefore it seemed worth while to improve the arrangement so that the scattering correction should be less important.

It is obvious that the scattering correction depends very sensitively on the particular geometrical arrangement adopted, and by small alterations, it was found possible to make the scattering correction positive instead of negative, and also to obtain an arrangement where it was practically zero in the range under investigation. The alteration of the arrangement shown in reference 1, Fig. 1, consisted essentially in replacing the paraffin top above the sample can by cadmium.

With this arrangement, we have investigated a few elements with small capture cross sections for slow neutrons. Table I shows our results. In the last column R represents the ratio of the counting rate relative to the empty can. Rows 1 to 3 demonstrate how close to zero the scattering correction becomes in the new arrangement. Row 4 indicates how sensitive the arrangement is to capture of slow neutrons. The 0.045 g of B "add on the average" to each carbon atom a capture cross section of 2.3×10^{-25} cm², and give a reduction of 2.5 percent in the counting rate. If we use the result of Frisch, v. Halban, and Koch,[3] that the capture cross section of carbon for slow neutrons is $<10^{-26}$ cm², we find rows 5–8 indicate that the capture cross sections of Be, O, F, Si, and Bi are smaller than, or of the order of 10^{-25} cm².

TABLE I. Data on capture cross sections for slow neutrons.

	Element	Grams of element	Moles of element or compound	R
1	Empty can	—	—	1.000
2	C	1300	108	1.005 ±0.001
3	C	2200	183	0.991 ±0.003
4	C+B	1300 − C 0.045 − B	108 − C 4.2×10^{-3} − B	0.975 ±0.004
5	BeO	1027	41.0	1.018 ±0.003*
6	BeF_2	2405	51.0	1.004 ±0.002*
7	SiO_2	1039	17.3	0.997 ±0.002
8	Bi	4012 (mixed with 1411 g C)	19.2	1.006 ±0.005

* In the values given for R in rows 5 and 6, we have already allowed for a small contribution (~0.002) due to photo-neutrons produced in the Be by the γ-rays of the Ra-α-Be source. These contributions were measured with the help of a Ra source of similar intensity.

We believe it would be stretching our method beyond its limit of validity if we were to use these results to calculate the capture cross sections of these elements in the manner described in the previous paper.[1] This would be meaningful only as long as we can assume that any difference in scattering, with respect to angular dependence, as well as energy dependence, between the elements or compounds investigated on the one hand, and carbon on the other hand, will have a negligible effect on the value of R. Such effects, which would be due to molecular interference effects for thermal neutrons, were probably negligible for the case of the larger capture cross sections investigated previously,[1] but may not be so in the present case. A different attack on the problem of the magnitude of the very small capture cross sections for thermal neutrons is therefore advisable.

BeO was investigated with particular care, and in many different arrangements with negative, "zero", and positive scattering corrections.[2] In each arrangement we could calculate an "apparent capture cross section" $<10^{-24}$ cm². Be, or BeO, may therefore prove useful as a "slowing down" medium for neutrons.

* This letter was received for publication on the date indicated but was voluntarily withheld from publication until the end of the war.
[1] J. W. Coltman and M. Goldhaber, publication postponed.
[2] J. W. Coltman, Ph.D. thesis, University of Illinois, May, 1941.
[3] O. R. Frisch, H. v. Halban, and J. Koch, Proc. Danske Videnske Sels. 15, 10 (1938).

New Photographic Emulsions Showing Improved Tracks of Ionizing Particles

PIERRE DEMERS
National Research Council Laboratory, Montreal, Province of Quebec, Canada
December 28, 1945

THE tracks of protons and of heavier particles can be recorded in photographic emulsions. In Eastman α emulsion, the tracks show up as rows of grains about 0.8μ in diameter, the distance between the centers of consecutive grains being about 1.5–2μ for an α-particle or a proton near the end of its range, and larger for a fast proton.

New emulsions have been prepared, in which the grains, as seen under the microscope after development, appear to have a diameter of 0.2μ or smaller, and in which the distance between the centers of consecutive grains may have the following small values: 0.1–0.2μ at the beginning of the tracks of a heavy fission fragment; 0.2–0.3μ for an α-particle or at the end of a proton track; 0.5μ at the beginning of a 7–8 Mev proton track. The stopping power is about 1800.

A typical emulsion was prepared by the simultaneous dropwise addition of 30 cc of a 0.6-g/cc solution of silver nitrate, and of 30 cc of an equivalent solution of potassium bromide, to 75 cc of a well-stirred 6 percent gelatine solution kept at 40–50°C. During the operation, the volumes of the two reacting solutions which have been poured are kept constantly equal. The operation lasts 30 minutes. This gives a concentrated emulsion similar to the Lippmann type, which contains after washing and drying, about 80 percent of silver bromide in the form of grains less than 0.2μ diameter. Concentrations as high as 92 to 95 percent can be obtained directly by a like procedure. Slightly larger grains result from operating a room temperature or from slower stirring. A mixture of halides can be used. Grains are finer, and silver bromide concentration is higher than in most commercial emulsions.

A smaller grain size, a lower silver bromide concentration, and a weaker development will tend to render visible exclusively the tracks of heavy fission fragments; by controlling these factors, it is possible to bring out the α-rays too, or to bring out the protons as well.

Complete fission tracks show clearly the ionization maximum at the center, and in certain emulsions the maximum at the very end of the tracks too. Range measurements of ThC′ α-particles in one case indicated a standard deviation of 2 percent, which is about three times that obtained in air, and half that obtained in an Eastman α-emulsion. Proton tracks of a few 100 kev can be clearly recognized, as the end of a proton track may show as many as 2 or 3 grains per mm of air equivalent; the beginning of the long proton tracks is also very clear; the beginning of a 7–8 Mev proton may show 1 grain per mm of air equivalent, in which case each developed grain corresponds to an energy loss of 5 kev.

Such a high sensitivity leads one to believe that electrons in the equivalent of their last few centimeters of air render developable grains spaced in the emulsion by only a few millimeters of air equivalent, but no unquestionable tracks of electrons have yet been seen. Mesotrons near the end of their path should leave visible tracks.

β- and γ-rays will fog these plates; but proton tracks have been seen on a plate fogged by 100 r units of γ-rays, and fission tracks on a plate fogged by several hundred r units of γ-rays.

These emulsions are not very sensitive to visible light, but their small gelatine contents may render them of some use in the Schumann region. A chromic acid treatment, as is well known, removes from the silver bromide grains the sensitivity specks which enhance the sensitivity of the grains toward light. Such a treatment was observed to decrease or to remove the sensitivity to the tracks. It therefore appears that the sensitivity specks that enhance the sensitivity to light also enhance the sensitivity to the tracks.

A more complete report will be sent to the *Canadian Journal of Research*.

This work was carried on between June and December, 1945.

The Advance of the Perihelion of Mercury

F. W. WARBURTON
University of Kentucky, Lexington, Kentucky
March 2, 1946

ANY action of one body on another after the finite time required for propagation from the first body to the second body has more concrete physical meaning than an assumed instantaneous action at a distance, since the latter does not conform to any known method such as wave motion or ballistic transfer. Transfer at finite speed can occur by means of wave motion or be ballistic even when it may not yet be known which of these modes of propagation is the proper one.

In the development of the reciprocal energy and force formulas of one charge on another,[1] magnetic force is considered as the variation in electrostatic force due to the ratio of the (relative) velocity of the charges to the propagation speed c. Gravitational attraction of one atom on another is very much smaller than their magnetic forces, and as has been suggested may very well be caused by further modification of electromagnetic forces. Such an explanation would be entirely in keeping with the mass-energy relation obtained from the coefficient of the acceleration term in the reciprocal force formula. The question at once arises, that if mass is a measure of internal electrostatic energy, why not also a function of internal magnetic energy. These two suggested developments point to higher power terms in the $1/c$ expansion. Coupled with the finite propagation discussed above, it should not be surprising that gravitational force be found to follow the reciprocal formula, reducing to Newton's gravitational law for small velocities.

The theories of Ampère, Weber, and Riemann went a long way in the direction of a pure relativistic description of nature. They were not carried far enough, however, to describe adequately the transverse propagation of light. Also, the best value in 1890 for the advance of the perihelion of mercury, 38″ per century, gave approximately

$\alpha=5/3$ in the combination of the Weber and Riemann formulas in the hands of Tisserand[2] and Lévy,[3] $W=\alpha W_R+(1-\alpha)W_W$. The Ritz[4] theory and O'Rahilly's[5] preference $\lambda=3$ ($=4A-1$, corresponding to $A=1$ in the reciprocal force) failed to account for Mercury's advance because of the lack of certain acceleration terms. The reciprocal energy formula,[1] however, with the preferred value $A=1$ (and hence with $B=-\frac{1}{2}$), namely

$$W=(ee'/r)(1+u^2/c^2-(\mathbf{u}\cdot\mathbf{r})^2/2c^2r^2+\cdots), \qquad (1)$$

when applied to gravitation, predicts closely the advance of the perihelion of mercury. Using the value 14.4″ per century given by Tisserand for the Weber formula[2] and twice that for the Riemann energy,[3] and setting $\alpha=2$, which reduces Lévy's expression to Eq. (1), one finds for the advance of the perihelion of Mercury the value 43.2″ per century. The observational advance[6] is listed as 43.5″ per century, while the value predicted by the partially relativistic theory of Einstein is given as 42.9″ per century. A recheck using more recent values of the measured quantities gives the advance of the perihelion of Mercury as 43.0″ per century, both on the standard relativity basis and on the basis of the reciprocal force formula. The observed advance of the perihelion of the planets thus does not distinguish between Einstein relativity and an electrical theory conforming the Newtonian relativity.

[1] F. W. Warburton, Phys. Rev. **69**, 40 (1946).
[2] M. F. Tisserand, Comptes rendus **110**, 313 (1890); *Celesti Mechanigne*, Vol. 4, pp. 502, 507.
[3] M. Lévy, Comptes rendus **110**, 545 (1890).
[4] W. Ritz, Ann. de Chemie et de Physique **13**, 145 ff (1908). Ges. Werke-Œuvres, p. 421.
[5] Alfred O'Rahilly, *Electromagnetics*, pp. 588, 616, 544.
[6] R. C. Tolman, *Relativity, Thermodynamics and Cosmology*, p. 209.

Energy-Angle Distribution of Betatron Target Radiation†

L. I. Schiff*
University of California, Los Alamos, New Mexico
July 2, 1946

An approximate expression for the energy-angle distribution of the bremsstrahlung produced by fast electrons in a thin target has been given by Sommerfeld.[1] This is obtained by integration of the Bethe-Heitler formula over the angular coordinates of the outgoing electron, and is valid with neglect of screening when the energy of the incident electron is large in comparison with its rest energy. It is not applicable when the target is of the thickness used in betatrons, since the electron beam is spread out by multiple scattering in the target.

According to Williams[2] the normalized distribution in angle θ per unit solid angle of electrons of energy E after penetrating a thickness t of target containing N atoms of nuclear charge Ze per unit volume is:

$$(1/2\pi\theta_0^2)\exp(-\theta^2/2\theta_0^2), \quad \theta_0=(9.2Ze^2/E)(Nt)^{\frac{1}{2}}\equiv(\beta t)^{\frac{1}{2}};$$

the numerical coefficient 9.2 is nearly constant for heavy metal targets such as tungsten having thicknesses of the order of a tenth millimeter. The angular spread of the x-rays due to just the radiation process is of order mc^2/E. For tungsten, θ_0 is large compared to mc^2/E if $t\gg10^{-4}$ cm; this is usually the case.

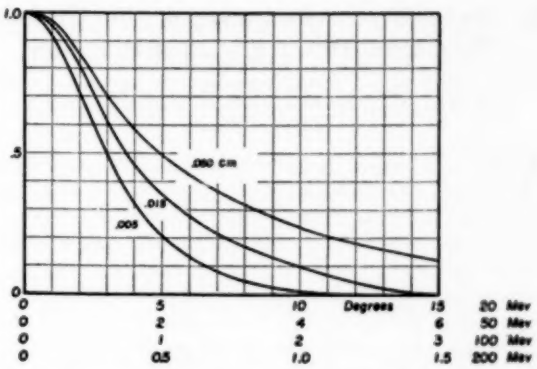

FIG. 1. Ratio of radiation intensity at angle θ to the intensity at $\theta=0$ for three thicknesses of tungsten target.

Since electrons are radiating at all values of t from zero to the total target thickness x, Williams' formula must be integrated over t to give the effective electron angular distribution per unit solid angle:

$$(1/2\pi\beta)[-Ei(-\theta^2/2\beta x)].$$

This assumes single traversal of the target, and is valid so long as the target is thin enough so that there is not excessive straggling of the electrons; for tungsten this corresponds to $x\lesssim0.05$ cm. The energy-angle distribution of the x-rays is now obtained by combining this electron distribution with Sommerfeld's formula. For angles somewhat larger than mc^2/E this means simply that the angular distribution of the x-rays is the same as that of the electrons, and the energy spectrum is that obtained by integrating the Bethe-Heitler formula over the directions of both the outgoing electron and the quantum.[3] For small angles, however, the divergence in the electron distribution makes it necessary to carry through the combination in detail. This is readily done for $\theta=0$; in the absence of screening, the energy distribution is still the integrated spectrum, and this is a good approximation when screening is included.

The result is that to good approximation the energy distribution at all angles is that usually associated with the total radiation. The ratio of intensity at an angle θ somewhat larger than mc^2/E to the intensity at $\theta=0$ is per unit solid angle:

$$[-Ei(-\theta^2/2\beta x)]/[\ln(2\beta xE^2/m^2c^4)-0.5772].$$

Since β is proportional to $1/E^2$, the denominator is independent of E and curves for different energies differ only by a scale factor that is inversely proportional to E. Curves for three thicknesses of tungsten target are shown in Fig. 1; they are in good agreement with measurements reported by D. W. Kerst (private communication). Thanks are due T/5 C. B. Gass for help with the numerical computations.

* Now returned to the University of Pennsylvania from leave of absence.
† Submitted for clearance March 19, 1946.
[1] A. Sommerfeld, *Atombau und Spektrallinien* (Vieweg, Braunschweig, 1939), Vol. 2, p. 551.
[2] E. J. Williams, Phys. Rev. **58**, 292 (1940).
[3] W. Heitler, *Quantum Theory of Radiation* (Oxford, 1936), p. 170.

The Probability of Excitation of the Nucleus ^{206}Pb in the α-Disintegration of Polonium

N. FEATHER
Department of Natural Philosophy, Edinburgh, Scotland
June 1, 1946

A FULL account has recently been published[1] of work already briefly reported[2] which would indicate the presence of 12 lines of feeble intensity, hitherto unobserved, in the α-particle spectrum of polonium. The spectrum was obtained using the Princeton cyclotron magnet to produce "semicircular" focusing and was found to cover an energy range of 1.6 Mev on the low energy side of the main line. This spectrum extended over 10 cm on the photographic plate used as detecting instrument. Adequate resolution was therefore available for the study of even complicated fine structure, and conditions would have been perfect for exact determinations of energy if it had been possible to employ sources of considerably greater strength than those actually used ($\frac{1}{10}$ to $\frac{1}{3}$ mC). On account of this limitation in source strength, however, it was necessary in the experiments in question to fix the positions of the lines and to deduce relative intensities by microscopic examination of the plates and the counting of single α-particle tracks.

In discussing the α-particle spectra which he obtained in this way, Chang makes the natural assumption that the fine structure observed is nuclear in origin, and he points out fully how this assumption introduces considerable difficulties when taken in relation to the accepted theory of α-disintegration. He discusses also the measure of concordance between his results, as he interprets them, and the information available regarding the γ-rays of polonium. Although he notes an apparent discrepancy here, he concludes "In general we may say that, as far as energy and intensity are concerned, these γ-ray lines are compatible with the α-particle groups" (page 73). It is the purpose of this note to examine this conclusion in respect of the intensities; as concerns the energies it is obviously unexceptionable.

It may be recalled that in 1931 Curie and Joliot, having failed to identify the high energy γ-rays of polonium by the ionization method, using sources of 8–10 mC strength,[3] succeeded in detecting this radiation and investigating its absorption in lead only when a source of 100 mC strength was employed.[4] Bothe and Becker had previously reported the radiation,[5] and had examined its properties using a point counter as detector,[6] and somewhat later Webster[7] published the results of an investigation in which a pressure ionization chamber was used in a similar study. In 1935 Bothe[8] obtained the "natural" β-particle spectrum in a spectrograph of high collecting power (using a 30 mC source), and in the following year the "excited" spectrum of the photoelectrons produced in lead by the γ-rays.[9] The absorption experiments indicated the presence of a softer and a harder component in the radiation, and on the basis of the natural and excited spectrum results the latter component was shown to consist of two main "lines" of quantum energies 0.80 and 1.07 Mev. It is in respect of these lines that existing information regarding intensities is most complete. Calibrating his pressure chamber with the 2.62 Mev γ-rays from thorium C″, Webster deduced $(12\pm1)\times10^{-6}$ for their combined intensity, per atom disintegrating, and Bothe and Becker concluded in effect that, on the basis of equal members of disintegrations, the intensity of these radiations as measured by their counter was 6.6×10^{-6} of that of the γ-rays of a sealed radium source. The two estimates are generally concordant, and taking count of the difficulties of standardization we may say that the absolute intensity of the combined radiations is $(10\pm4)\times10^{-6}$ quantum per disintegration. On the other hand Chang has concluded that the excitation of the nuclear states of ^{206}Pb of more than 0.80-Mev energy of excitation, due to the emission of polonium α-particles of less than the normal energy, is 2.3×10^{-4} per disintegration, with a possible error of 50 percent.

It would appear that, in spite of his quoted remark, there is a very real discrepancy here which can only be resolved if the γ-rays in question are internally converted to a high degree, or if de-excitation of the nucleus takes place in multiple cascade—or by the emission of radiation other than γ-rays. Bothe's experiments,[8] however, dispose of the first possibility: it can be calculated, on the basis of the data in the original paper, that the intensity of the natural photoelectron lines is in no case greater than 10^{-7} per atom disintegrating. We are led, therefore, to examine the possibility of cascade emission.

If we accept Chang's intensities, the average energy of excitation of the residual nucleus in the polonium disintegration is 445 ev. Taking 10^5 ev as a reasonable mean energy for the cascade γ-rays (reasonable, that is, on the basis of the nuclear levels revealed by the fine structure spectrum), we obtain a hypothetical "soft" γ-ray intensity of 4.45 quanta per thousand disintegrations. Such a component of the γ-radiation could not well have been missed in the early investigations—particularly in those of Curie and Joliot.[3] It would appear, therefore, that if Chang's intensities are correct some entirely new effect is in question.

There are other reasons for coming to the same conclusion. In a paper shortly to be published, Broda and the writer will show that the 4.2 minute β-activity, previously attributed to ^{204}Tl, in reality belongs to ^{206}Tl. The disintegration in this case, therefore (giving rise to β-particles of maximum energy 1.7 Mev, but no γ-rays) results in the same residual nucleus as does the disintegration of polonium. It would seem that there must be something distinctly peculiar in the nuclear level system if there are 12 states energetically capable of being excited in the β-disintegration which are not appreciably excited. Qualitatively one would say that excitation of the residual nucleus is a more frequent feature of β-disintegration than of α-disintegration.

It may be remarked in conclusion, that even if Chang's intensities do not eventually prove to be correct large values of the spin change in the α-disintegration are still required to account for the intensities of the less-hard γ-rays (quantum energy 0.2 to 0.43 Mev) reported by Bothe and Becker and Webster. Unless the 0.8-Mev state is the first excited state of the ^{206}Pb nucleus, lower states

are required to account for these radiations, and the excitations of these states appear abnormally small. It may be that there is some connection between this conclusion and the observation of Waldman and Collins[10] that a metastable level of 1.6 minutes half-value period and about 0.3-Mev energy of excitation can be excited by the action of high energy x-rays on lead.

[1] W. Y. Chang, Phys. Rev. **69**, 60 (1946).
[2] W. Y. Chang, Phys. Rev. **67**, 267 (1945).
[3] I. Curie and F. Joliot, J. de Phys. et rad. **2**, 20 (1931).
[4] F. Joliot, Comptes rendus **193**, 1415 (1931).
[5] W. Bothe and H. Becker, Zeits. f. Physik **66**, 289 (1930).
[6] W. Bothe and H. Becker, Zeits. f. Physik **66**, 307 (1930).
[7] H. C. Webster, Proc. Roy. Soc. **A136**, 428 (1932).
[8] W. Bothe, Zeits. f. Physik **96**, 607 (1935).
[9] W. Bothe, Zeits. f. Physik **100**, 273 (1936).
[10] B. Waldman and G. B. Collins, Phys. Rev. **57**, 338 (1940).

High Energy Carbon Nuclei

CORNELIUS TOBIAS* AND EMILIO SEGRÈ
Radiation Laboratory, Department of Physics, University of California, Berkeley, California
May 28, 1946

$C^{12(++++++)}$ AND other nuclei having approximately the same e/m ratio as deuterons can be accelerated in the cyclotron under similar conditions to those required for the deuteron beam.[1] Their kinetic energy will be greater in the ratio of their mass to the mass of the deuteron. By using them, new types of nuclear reactions might be detected, namely, ones involving higher excitation energies than hitherto known. CO_2 was the most satisfactory source of carbon ions. A shallow ionization chamber was used to identify the beam, and to measure its specific ionization and range. Precise measurements cannot be made until the intensity can be increased with the help of a specially built ion source. The Gamow theory of penetration of nuclear barriers has been applied for the case of light bombarding nuclei. Penetration of most nuclei by s waves can be expected even at lower energies than now reached (96 Mev for carbon), although the maximum cross section will be reached only at considerably higher energies, where the contribution of higher incident angular momenta becomes important. The electric moment induced in the bombarding particles at the approach of a nucleus may lead to the splitting off of alpha-particles before the potential barrier can be penetrated. The tracks due to the 96-Mev carbon particles accelerated in the 60″ cyclotron were recorded in photographic emulsions. Their grain density, track length, and the total number of grains have been measured and plotted in relation to the specific ionization and the air equivalent range. Some of the microphotographs taken show elastic collisions with various nuclei. A few cases that may represent inelastic collisions were observed. Two star-shaped inelastic collisions were found and analyzed.

* Abstract of thesis submitted by Cornelius Tobias to the faculty of the University of California in partial fulfillment of the requirements for the degree of Doctor of Philosophy in 1942, and not published because of the war.

[1] L. W. Alvarez, Phys. Rev. **58**, 192 (1940).

Assignment of Mass to 46-Hr. Samarium and 9.2-Hr. Europium by a Mass Spectrograph

RICHARD J. HAYDEN AND MARK G. INGHRAM
Metallurgical Laboratory, University of Chicago, Chicago, Illinois
June 24, 1946

A NITRIC acid solution of Sm_2O_3 was irradiated by slow neutrons to produce the 46-hr. samarium activity reported in Seaborg's table.[1] Part of this irradiated sample was placed on the filament source of a mass spectrograph. By operation of the spectrograph the samarium isotopes were separated according to mass on a photographic plate. After removal from the spectrograph, this plate was placed face to face with another photographic plate. With the passage of time the particles emitted from the active isotopes on the first plate gave rise to a developable image on the second plate. After both plates were developed, the original plate showed the normal spectrum of samarium (Sm^+ and SmO^+) while the second plate showed only two lines. These corresponded to masses 153 and 169 on the original plate. Because of the emission of the form SmO^+, the activity at mass 169 was ascribed to the same isotope as was the activity at mass 153. A decay curve of a second portion of the irradiated samarium solution showed that more than 95 percent of the activity was caused by the isotope with 46-hour half-life. Thus we may conclude that the mass of 46-hr. samarium is 153.

A nitric acid solution of Eu_2O_3 was irradiated by slow neutrons to produce the 9.2-hr. europium activity reported in Seaborg's table.[1] The same mass spectrograph technique was applied to this sample as to the samarium sample. In this case the second photographic plate showed a single line corresponding to mass 152 on the original plate. A decay curve of a portion of the irradiated europium solution showed that more than 95 percent of the activity was caused by an isotope with 9.2-hr. half-life. Thus we may conclude that the mass of 9.2-hr. europium is 152.

[1] G. T. Seaborg, Rev. Mod. Phys. **16**, 1 (1944).

Activation of Ag (225 d.) by Resonance Neutrons

M. GOLDHABER*
The Argonne Laboratory, University of Chicago, Chicago, Illinois
June 25, 1946

BY activation of Ag in the Argonne heavy water pile it is shown that the Cd filtered neutrons activating the long period of Ag (225 d.) are strongly absorbed in both Ag and Au. As this is also the case for the resonance neutrons leading to Ag^{110} (22 sec.) but not for those leading to Ag^{108} (2.3 min.),[1] it is plausible to assign Ag (225 d.) to an isomeric state of Ag^{110}. Mass assignment of isomers through identification of neutron resonance groups may be a useful method in other cases and is now being applied to Ir.

* On leave of absence from the University of Illinois.

[1] A. A. Yalow and M. Goldhaber, Phys. Rev. **68**, 99(A) (1945).

Binding Energy of Polyelectrons

AADNE ORE
Sloane Physics Laboratory, Yale University, New Haven, Connecticut
June 10, 1946

THE question as to the existence of groups of electrons and positrons having temporary stability has recently been raised by J. A. Wheeler,[1] who shows that clusters of the form $++$ and $++-$ are stable with respect to decay into their elementary constituents. With regard to more complex structures no definite judgment could be reached.

Wheeler found, as a first approximation, the upper limit of -9.93 ev for the ground state energy of the hypothetic "electromeson" or "polyelectron" composed of two electrons and two positrons. A binding energy of 9.93 ev is, however, about 3.6 ev below the energy $me^4/2\hbar^2$ necessary to prevent disintegration into two systems each of which contains one electron and one positron.

The variational function in Wheeler's calculation is, aside from a difference in notation and in the values of the parameters, the ground state function employed by H. Margenau and W. A. Tyrrell in their variational calculations of the binding energy of the alpha-particle,[2] in which orthogonal Hermite functions were used to approximate the state of the particle.

The symmetry considerations in the alpha-particle problem may be transferred unaltered to the case of the four-component polyelectron in question.

If we choose the notation of Margenau and Tyrrell the Hamiltonian of the polyelectron may be written

$$H=-\frac{\hbar^2}{2m}(2\nabla_1^2+\nabla_2^2+\nabla_3^2)+2^{-\frac{1}{2}}e^2\left(\frac{1}{\rho_2}+\frac{1}{\rho_3}-\Sigma\frac{2}{|\boldsymbol{\rho}_1\pm\boldsymbol{\rho}_2\pm\boldsymbol{\rho}_3|}\right).$$

The summation extends over four different terms indicated by the double signs. In this form the Hamiltonian does not include the center of mass term. The relative coordinates are the scalar components along the Cartesian axes of the vectors

$$\boldsymbol{\rho}_1=(\tfrac{1}{2})^{\frac{1}{2}}(\mathbf{r}_1+\mathbf{r}_2-\mathbf{r}_a-\mathbf{r}_b),\quad \boldsymbol{\rho}_2=(\tfrac{1}{2})^{\frac{1}{2}}(\mathbf{r}_1-\mathbf{r}_2),\quad \boldsymbol{\rho}_3=(\tfrac{1}{2})^{\frac{1}{2}}(\mathbf{r}_a-\mathbf{r}_b).$$

The ground state harmonic oscillator function which yields the energy value presented by Wheeler then takes the form

$$\psi_0=\text{const.}\cdot\exp-\tfrac{1}{2}[p\rho_1^2+q(\rho_2^2+\rho_3^2)],\quad p=1.134q.$$

It follows from the form of the Hamiltonian above that functions of odd degree of excitation do not combine with the ground-state function. Nor do the two doubly excited functions combine when p and q are given the values which minimize H_{00}.

The total second-order perturbation energy resulting from the eight quadruply excited functions comes out to be roughly 0.9 ev of which 0.65 ev originates from the third and fourth functions in the enumeration of reference 2.

The three first sextuply excited functions add altogether about 0.1 ev.

While there is no clear indication of convergence at this stage, the small magnitude of the contributions from these orthogonal functions suggests with reasonable assurance that this structure is not stable against disintegration into two bielectrons.

This conclusion is perhaps somewhat strengthened by the following consideration. If the binding energy of the bielectron $(+-)$ is computed variationally with the use of the analog of our ψ_0 there results a binding energy of 5.75 ev, i.e., 85 percent of the true value of 6.77 ev. The calculations on light nuclei show that ψ_0 represents a better approximation to the lowest state of the four-particle system than to that of the two-particle system. If, then, we assume the value of 9.93 ev to represent 85 percent of the true energy of the cluster, we arrive at a limit of 11.7 ev, which is still 1.8 ev below stability.

For these reasons the preceding perturbation calculations were not extended by more refined variational methods.

It might seem that while Hermite functions are adapted to the alpha-particle problem with its short range forces, the Coulomb potentials in polyelectrons require more hydrogenlike functions. To investigate this point, we choose a new set of coordinates, replacing $\boldsymbol{\rho}_1$, $\boldsymbol{\rho}_2$ and $\boldsymbol{\rho}_3$ by

$$\mathbf{s}=(\tfrac{1}{2})^{\frac{1}{2}}(\mathbf{r}_1+\mathbf{r}_2-\mathbf{r}_a-\mathbf{r}_b),\quad \mathbf{t}=(\tfrac{1}{2})^{\frac{1}{2}}(\mathbf{r}_1-\mathbf{r}_2-\mathbf{r}_a+\mathbf{r}_b)$$
$$\text{and}\quad \mathbf{u}=(\tfrac{1}{2})^{\frac{1}{2}}(\mathbf{r}_1-\mathbf{r}_2+\mathbf{r}_a-\mathbf{r}_b).$$

The symmetry in identical particles leads to functions symmetric and of even degree in the t and u coordinates. When we take this fact into account we may write the proper Hamiltonian for the calculation of matrix elements in the form

$$H=-\frac{\hbar^2}{m}[\Delta_s^2+2\Delta_t^2]+2^{\frac{1}{2}}e^2\left[\frac{1}{|\mathbf{u}-\mathbf{t}|}-\frac{2}{|\mathbf{t}-\mathbf{s}|}\right].$$

Let us consider functions of the kind

$$\psi_i=\text{const.}\ (s\cdot t\cdot u)^i\exp-\tfrac{1}{2}[\alpha s+\beta(t+u)],$$

and take for α and β the values that minimize the respective H_{ii}. $i=0$ yields in this way a binding energy of 9.5 ev, that is, *less* than the ground-state oscillator function. $i=\frac{1}{2}$ however, yields 10.0 ev for $\alpha=1.5505\beta$, $\beta=0.81888\cdot me^2/\hbar^2$. This energy value is 73.8 percent of the minimum binding energy required for stability. With five functions in linear combination, $i=1/2,\ 3/2,\ \cdots,\ 9/2$, and the same α and β which minimize H_{ij}, this percentage is increased to about 75 percent.

This is in fact below the value of 10.3 ev or 76 percent which we may get variationally by combining the ground-state harmonic oscillator function with the rather effective fourth quadruply excited function. Changes in the values of the parameters have been found to have very little effect on this result for the binding energy.

Although the evidence here presented against the stability of the polyelectron composed of two electrons and two positrons is not conclusive in a strict mathematical sense, it counsels against the assumption that clusters of this (or even of higher) complexity can be formed.

[1] J. A. Wheeler, Ann. New York Acad. Sci. to be published. The bielectron has also been discussed by A. E. Ruark, cf. Phys. Rev. **68**, 278 (1945).
[2] H. Margenau and W. A. Tyrrell, Jr., Phys. Rev. **54**, 422 (1938).

Particle Accelerators as Mass Analyzers

PAUL B. WEISZ
Socony-Vacuum Oil Company, Inc., Research and Development Laboratories, Paulsboro, New Jersey
June 14, 1946

THE appropriate resonance condition for many of the known particle accelerating machines contains the factor e/m. If a mixture of particles of different masses is injected, the resulting beam should be mass selective. One may speculate on new mass-spectrographic apparatus on this basis. A mass spectrographic apparatus employing this principle would be designed for high beam intensity and mass selectivity rather than high particle velocity, and the dimensions and limitations of such a modified accelerator would differ from those of the familiar high velocity accelerator. The mass constituents of the resulting beam could be "scanned" by changing another parameter in the resonance condition. For example, for a mass analyzer based on the cyclotron principle of operation, governed by the resonance condition $f=eH/2\pi m$, H or f might be varied.

Since it is very desirable to do away with the necessity of having a magnet, a modification of the linear accelerator principle is particularly interesting. Hartman and Smith[1] have briefly described the mass selective properties of the familiar linear accelerator consisting of successive alternately phased cylindrical electrodes and operation with a continuous ion beam. For a given accelerator with ten gaps they have calculated an intensity reduction of the emerging beam of roughly 60 percent when the initial beam consisted of masses of $1.5\,M_0$ as compared to a beam of masses M_0, the latter mass satisfying the resonance condition for maximum acceleration. They have, furthermore, pointed out that no clean mass separation is possible because of the unhindered passage of a portion of ions of masses $M<M_0$ and of certain "harmonic masses" $M=(2m-1)^2M_0$. However, upon dismissing the usual considerations relating to the attainment of high particle velocity, in favor of those pertaining to mass discriminating ability of the system, it appears that useful variations of the familiar accelerator design may result. Recently, W. E. Stephens described[2] work on a mass spectrograph utilizing the velocity modulation of a pulsed beam of mixed ions after traversing a single accelerating field, and measurement of resulting arrival times. An extension of this principle to the use of successive and phased accelerating fields leads to such a system. A pulsed ion beam initially accelerated by a voltage E_1 could be made to travel through a series of n gaps in such a manner that for a given mass M_0 the ion pulses arrive at all gaps at zero phase. In contrast to the usual type accelerator, ions of mass M_0 would now be subject to no additional acceleration. However, dE/dt would be a maximum rather than a minimum at the time of their arrival at the gaps. A frequency of period T would be applied to the gaps of equal spacing S, such that $T=S/v_0$, and the travel time to the first gap may also be made equal to T. An ion with mass differing from M_0 by $\pm\Delta M/M_0$ will experience a phase-shift in arrival time at gap 1 corresponding to a fraction K_1 of a cycle equal to $\mp(\Delta M/M_0)^{\frac{1}{2}}$. These ions will receive an additional acceleration of $\mp E_0 \sin 2\pi K_1$, and thus the resulting arrival times will be shifted in phase by ever increasing amounts at subsequent gaps. At gap n the arrival time will be (as a fraction of T)

$$k_n=\left(\sum_1^{n-1} K_r\right)+\left(1+\frac{E_0}{E_1}\sin 2\pi K_{n-1}\right)^{-\frac{1}{2}}.$$

For the condition: Initial accelerating field $E_1=1.00$ kev, and r-f voltage on electrodes $=1.00\sin\omega t$ kev, where ω satisfies the resonance condition for ions of mass M_0, we find the following: Ions of mass M_0 emerge with a final velocity of 1.00 kev. For a mass smaller than M by 2 percent, the velocity dispersion after initial 1-kev acceleration, i.e., at the time of arrival at gap 1, is 1 percent. The additional acceleration in the first gap is 0.07 kev; the arrival time at gap 2 is shifted by 4.4 percent, the resulting additional acceleration is 0.26 kev; the arrival time at gap 3 is shifted by 17.4 percent, the additional acceleration is 0.89 kev. Thus after 3 gaps the ions with 2 percent smaller mass emerge with an energy of about 2.2 kev, as compared to 1.0 kev for ions of mass M_0. Ions of 2 percent larger mass are rejected by the third gap. Differentiation of the 1.0-kev beam component in the process of detection would now be relatively simple. With a gap-to-gap distance of 30 cm, the above example would require a frequency range of 4.75 mc to 0.475 mc for masses from 1 to 100.

A device of this nature might therefore be designed to increase the velocity dispersion in existing types of mass analyzers. Passage of "harmonic masses" other than M_0 is possible whenever $M=M_0(m/2)^2$, for all integer m for which M becomes integer. However, the use of a pulsating beam and a method of detection which involves the arrival time of the ions, such as Stephens' method, eliminate any ambiguity introduced by "harmonic masses."

[1] P. L. Hartman and L. P. Smith, Rev. Sci. Inst. **10**, 223 (1939).
[2] W. E. Stephens, paper presented before American Physical Society, Cambridge, Massachusetts, April 26, 1946.

Dispersion of the Velocity of Sound in Normal and Para-Hydrogen

J. ELMER RHODES, JR.
Rowland Physical Laboratory, Johns Hopkins University, Baltimore, Maryland
June 18, 1946

CONTINUATION of the study of ultrasonic waves in this laboratory has confirmed the dispersion of sound in hydrogen reported by Stewart, Stewart, and Hubbard.[1] In the range of frequency-to-pressure ratio from one to sixty megacycles per atmosphere and at temperatures of 195°, 273°, and 297° absolute we have observed dispersion curves that can be identified with the failure of the rotational specific heat to follow the sound wave. Relaxation times for the transitions of rotational quantum numbers 0–2 and 2–4 for para-hydrogen and 0–2, 1–3, and 2–4 for ortho-para-hydrogen mixtures are being measured.

[1] E. S. Stewart, J. L. Stewart, and J. C. Hubbard, Phys. Rev. **68**, 231 (1945).

The Electrical Conductivity of Rapidly Frozen Solutions of Sodium in Liquid Ammonia*

H. A. Boorse, D. B. Cook, R. B. Pontius, and M. W. Zemansky
Department of Physics, Columbia University, New York, New York
June 28, 1946

IN a recent note to *The Physical Review*, Ogg[1] reported a large decrease in electrical resistance accompanying the rapid freezing of an approximately one-molar solution of sodium in liquid ammonia, and also the production of a persistent current, as in the classical Kammerlingh Onnes experiment, in a rapidly frozen ring of solution. The purpose of the present note is to report an unsuccessful attempt to repeat these experiments. It is not our intention to maintain that the effect does not exist, but rather to point out that the conditions under which the effect may be obtained are obscure.

In all the experiments to be described, the solute was extremely pure distilled sodium obtained in thin-walled glass ampoules from the General Electric Vapor Lamp Company. These contained about 0.6 g of sodium which was dissolved in anhydrous liquid ammonia (99.95 percent) to make an approximately one-molar solution. Care was exercised to avoid contamination with moisture, but no attempt was made to measure the concentration of the solution with great accuracy because of the change in concentration always taking place due to evaporation of ammonia. For all the experiments the concentration, however, was within the range of 0.5–2 molar in which two liquid phases separate out on slow cooling. The magnetic field for the production of persistent currents was produced by an electromagnet capable of providing a field up to 1200 oersteds at a pole separation of 9 cm, the latter being sufficient to allow a Dewar flask to be inserted. Liquid nitrogen was used as a refrigerant for rapid freezing of the solutions.

In the first experiments a closed system was used. The glass ampoule containing the sodium was crushed by a magnetically operated hammer and the resulting solution was forced into a glass tube one of whose vertical arms ($\frac{3}{32}$" bore, $\frac{3}{64}$" wall thickness, 6" length) was equipped with four sealed-in leads for resistance measurements by the potentiometer method. At the bottom of the tube was a glass ring of $\frac{3}{16}$" bore, $\frac{1}{32}$" wall thickness, and a $1\frac{1}{4}$" mean diameter. It was found impossible with this apparatus to prevent separation of the liquid column and cracking upon freezing, so that no resistance measurements were obtained. After freezing the solution in the ring while in a field of 1200 oersteds, and then removing the magnet and bringing a sensitive compass needle near the Dewar flask, no persistent current was detected, although the compass needle gave an unmistakable response to a field as low as 0.05 oersted. Four trials were made, in two of which the Dewar flask was removed momentarily so that the compass needle could be brought even closer to the ring.

The closed system proved to be cumbersome and difficult to manipulate, and upon advice that the original effects were obtained by making the solutions in open vessels, surrounded by a refrigerant at −33°C, the latter technique

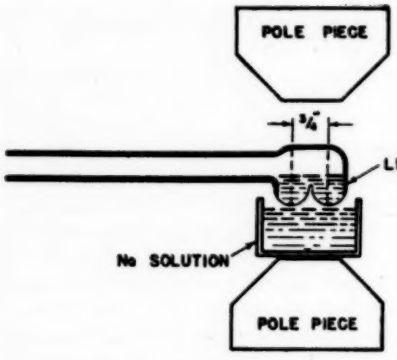

FIG. 1.

was adopted. Contamination was minimized by capping the vessels and using a slight overpressure of ammonia vapor or precooled dry nitrogen.

Further attempts to measure the resistance of a column of liquid in a capillary before and after freezing led to results that were not reproducible. Cracking of the column led to the conclusion that a different apparatus would be necessary for this type of measurement, so that it was thought best to concentrate on attempts to detect a persistent current, using smaller and thinner rings to obtain more rapid freezing.

Experiments were then tried by preparing the solution in a tube, attached to the bottom of which was a walled disk of diameter $\frac{3}{4}$", total thickness 40 mils, and a wall thickness of about 10 mils. Seven trials were made with this apparatus: in every case the solutions were of a deep blue color upon freezing in the magnetic field. No persistent currents were observed.

A special glass tube was then constructed in the shape of a pipe, as shown in Fig. 1, and the bulb filled with liquid nitrogen. The magnet was turned to give a vertical field, and a shallow dish of solution was placed on one of the pole pieces. Upon dipping the bulb into the solution a circular film was frozen immediately on the exterior of the bottom wall in the presence of the field. The "pipe" was then quickly removed from the field to a compass needle capable of reacting to a field of 0.02 oersted. It took about a second to bring the ring of film near the needle, and throughout six trials, no persistent current was detected. The frozen solution was always deep blue in color, and became bronze-colored only after the test with the compass needle was over.

On the assumption that the structure or composition of the film frozen on a glass wall might have properties different from a thin lamina formed between glass plates, new cells were constructed similar to those used by Dr. Ogg. These were constructed with two microscope cover glasses 10 mils thick and $\frac{3}{4}$ in. in diameter, separated by a circular mica spacer at the center. Adhesion of the cover glasses to the mica was secured by using a small amount of apiezon stopcock grease. A narrow glass tweezers was used to hold the cover glasses. Upon being dipped into the solution, the annulus was filled by capillary action.

The spacers varied in thickness from 2 mils to 8 mils. Extremely rapid freezing was possible by dipping the cell directly into liquid nitrogen situated in the magnetic field,

and the frozen solution always appeared dark blue when first formed. The rings of frozen solution were tested for persistent currents by removing them from the magnetic field and bringing them up quickly to a compass needle immersed in liquid nitrogen. The compass needle was enclosed in a brass case with a glass top which was tight enough to prevent liquid nitrogen from entering. The sensitivity of 0.02 oersted was found to be unaffected by immersion in the liquid nitrogen. The solution into which the cells were dipped was kept free of moisture with a stream of precooled nitrogen, and its concentration was kept approximately at one molar by adding fresh liquid ammonia from time to time as the volume of solution decreased by evaporation. Twenty-four trials were made with fields ranging from a few oersteds to 1000; in no case was there any indication of a persistent current.

* Publication assisted by the Ernest Kempton Adams Fund of Physical Research of Columbia University.
[1] R. A. Ogg, Jr., Phys. Rev. **69**, 243 (1946).

Superconductivity in Solid Metal-Ammonia Solutions

RICHARD A. OGG, JR.
Department of Chemistry, Stanford University, California
July 1, 1946

THROUGH the courtesy of Drs. Boorse *et al.*, their concurrently appearing communication was submitted to the author before publication. The implications of such a report make it advisable to publish at this time the experimental details which lack of space caused to be omitted from the previous communication.[1]

The conductivity cell was U-shaped, constructed of Pyrex capillary tubing some 10 cm in length and 0.2 mm in bore, with flanged ends sealed to relatively large reservoir vessels, the latter containing strip platinum electrodes. The sodium-ammonia solutions were prepared directly in the cell, while the latter was immersed in a bath of liquid ammonia. Resistances were measured with a direct current bridge. After calibration, estimates of concentration could be made from the measured resistance at −33°C.

In typical experiments, measured resistances at −33°C were of the order of 10,000 ohms. On *slow* cooling to temperatures slightly above the melting point (some −80°C) the resistance *increased* by a factor of some three to five. Behavior on rapid immersion of the cell in liquid oxygen was distinctly erratic, but the typical result consisted of a rapid resistance decrease to some few hundred ohms, followed by a sudden breaking of the circuit, as shrinkage caused fracture of the column. On then immersing the cell in a pre-cooled pentane bath at some −95°C, expansion usually caused reclosing of the circuit, with a fairly constant resistance of the order of 10 to 50 ohms. Further slow temperature rise caused practically no change until the melting point was reached, when the resistance suddenly rose to values of the order of 30,000–50,000 ohms. In a few cases the systems remained conducting at liquid oxygen temperature, with practically no change in the (relatively small) resistance between −180°C and the melting point. Such behavior, the variability of the lowest obtainable resistances, and the obvious difficulties with mechanical breakage strongly suggest that even the small residual resistances found were largely caused by poor contacts. Such large resistance changes were observed only with solutions in the concentration range characterized by liquid-liquid phase separation. It must be observed that the phenomenon is of the nature of a *discontinuity* at the melting point of the rapidly frozen solid solution, and is not to be confused with the exponential temperature dependence of the resistance of a solid semiconductor.

Cells for study of persistent currents were constructed (afresh for each trial) of thin circular microscope cover glasses, separated by a small center spacer of extremely thin mica, fastened with vaseline. Each cell was attached to a glass rod handle. The cell was dipped into a sodium-ammonia solution (in the concentration range characterized by liquid-liquid phase separation) at −33°C, and allowed to fill by surface tension. It was then plunged rapidly into a Dewar vessel containing liquid oxygen, situated in a magnetic field of strength up to 1500 gauss. The cell was quickly transferred to another liquid oxygen bath containing a fixed search coil attached to a semi-ballistic galvanometer. Any residual magnetic moment was detected by "flipping" of the ring sample in the vicinity of the coil. Fields of the order of 0.05 gauss were detectable. Nearly two hundred trials, with differing concentrations and field strengths, yielded negative results. However, in seven cases unmistakable galvanometer deflections were observed, indicating rather rapidly decaying fields of the order of one or two gauss at the first measurement, but remaining of measurable magnitude for periods of one or two minutes. Since the decay constant of a current in a closed circuit is the ratio of the resistance to the self-inductance (the latter estimated from the cell geometry), it is apparent that this degree of persistence indicates a resistance of the order of 10^{-13} ohm or smaller. In view of the fact that the liquid samples possessed resistances of the order of a thousand ohms, the solids in question may fairly be said to be superconducting.

The very large proportion of negative results seems to be in accord with expectations from the obvious contact difficulties encountered in the resistance studies. The solids probably crack into a micro mosaic pattern, and it would appear to be a very rare accident that the residual contact resistances are sufficiently small to allow an appreciably persistent current.

[1] R. A. Ogg, Jr., Phys. Rev. **69**, 243 (1946). See also April 1 and 15, 1946 issue, for erratum.

Note on the Problem of Uniform Rotation

NATHAN ROSEN
University of North Carolina, Chapel Hill, North Carolina
June 18, 1946

RECENTLY, in an article with the above title,[1] E. L. Hill considered the problem of determining the velocity as a function of position for a fluid rotating with constant angular velocity, according to relativity theory. However, his method of calculation appears questionable

since it makes use of a Lorentz transformation in going over to an accelerated frame of reference. It therefore seems desirable to try a different method.

One way of solving the problem is first to generalize the definition of angular velocity in relativity theory and then to use that definition to get the motion of the fluid directly in an inertial coordinate system. In classical mechanics the angular velocity of a fluid is given by

$$\omega=\tfrac{1}{2}\nabla\times\mathbf{v},$$

where $\mathbf{v}$ is the velocity vector. In general relativity theory, the obvious generalization is to define angular velocity as an antisymmetric tensor

$$\omega_{ik}=\frac{1}{2}\left(\frac{\partial u_i}{\partial x^k}-\frac{\partial u_k}{\partial x^i}\right), \quad (i, k=1, 2, 3, 4),$$

where u_i is the covariant velocity vector, the contravariant vector for a moving point being given by

$$u^i=dx^i/d\tau,$$

with $d\tau$ the proper-time element.

Consider a Galilean coordinate system with coordinates $x^1=x$, $x^2=y$, $x^3=z$, $x^4=ct$, so that the metric is taken as -1, -1, -1, $+1$, and $d\tau=(1-\beta^2)^{\frac{1}{2}}dt$ $(\beta=v/c)$. For small velocities one finds that ω_{23}, ω_{31}, ω_{12} reduce to the classical expressions for the x, y, z components of ω, while ω_{41}, ω_{42}, ω_{43} are proportional to the components of acceleration. If we take $v=v(R)$, with $R^2=x^2+y^2$, and

$$v_x=-vy/R, \quad v_y=vx/R, \quad v_z=0,$$

calculate ω_{ik} and set

$$\omega_{12}=\omega=\text{const.},$$

we find

$$v(R)=\frac{\omega R}{(1+\omega^2R^2/c^2)^{\frac{1}{2}}}.$$

This velocity v is in general different from that obtained by Hill, although it has nearly the same behavior for small and large values of R.

This question will be treated more fully in a forthcoming paper.

[1] E. L. Hill, Phys. Rev. 69, 488 (1946).

Solar and Lunar Effects on Cosmic Rays

M. KIDNAPILLAI
Department of Mathematics, Ceylon Technical College, Colombo, Ceylon, India
AND
A. W. MAILVAGANAM
Department of Physics, University of Ceylon, Colombo, Ceylon, India
April 25, 1946

DUPERIER[1] has from a harmonic analysis of the hourly records made in London, reported a semidiurnal variation of cosmic-ray intensity of amplitude 0.18 percent and nearly in opposite phase to the semidiurnal oscillation of the barometer. He explains this variation in terms of the finite lifetime of mesons and the up-and-down motion of the meson-producing layer in the atmosphere, caused by the semidiurnal solar atmospheric tides; and using certain calculations of atmospheric oscillations[2] he showed that one could entirely account in this manner for the observed semidiurnal variation of cosmic-ray intensity.

Independently of Duperier, one of us[3] has applied the theory of forced oscillations, magnified by resonance, of the earth's atmosphere with a period of 12 hours as worked out by Pekeris[2] to the oscillation of the meson-producing layer in the atmosphere and obtained, taking into account the finite lifetime of mesons, for the amplitude of the semidiurnal variation of the meson intensity 0.14 percent. This is in fair agreement with the value deduced by Duperier from his harmonic analysis of the London records.

We have continued our calculations with a view to seeing to what extent the tide-producing properties of the moon affect the meson intensity as observed at the earth's surface. For this purpose we have used with slight modifications, the theory of atmospheric tides developed by Pekeris.[2] We also use the stratification of the atmosphere employed by him. It is, of course, to be expected that the lunar effect will be smaller than the solar effect, in view of the fact that the atmosphere has free periods of oscillation, *viz.* 10.5 and 12 hr., neither of which is sufficiently close to 12 hr. 25 min. which is the semiperiod of the motion of the moon round the earth.

It can be shown that, when the period of forced oscillation of the atmosphere is 12 hr. 25 min. (mean solar time), the atmosphere oscillates like an ocean of depth of 7.04 km. Assuming that the moon moves in the equatorial plane, the semidiurnal component of the tidal potential Ω at a place on the equator is

$$-2.63\times10^4\cos(\sigma t+2\varphi+\epsilon)$$

where $2\pi/\sigma$ and φ are the period of oscillation and the longitude of the place, respectively, and ϵ is a constant. The amplitude of the lunar semidiurnal pressure variation at the equator is taken to be 72 microbars. Substituting these values of Ω and p in Eq. (47) of Pekeris,[2] the constant B/A is calculated. In the case of forced oscillations the vertical velocity in the region (0–1) of the atmosphere is given by the equation

$$w=-\frac{\gamma H}{2(n+1)x^n}\left\{A\left[J_n(x)-\frac{\gamma x}{0.8n-2}J_{n+1}(x)\right]+B\left[Y_n(x)-\frac{\gamma x}{0.8n-2}Y_{n+1}(x)\right]\right\}-\frac{i\sigma\Omega}{g}.$$

Since B/A is known, we obtain the values of A and B by means of this equation. In the region (1–2) χ satisfies the differential equation,

$$\frac{d^2\chi}{dy^2}+\frac{1}{h_1}\frac{d\chi}{dy}+\frac{\gamma-1}{\gamma}\frac{\chi}{h_1H}=0.$$

The solution of this equation is

$$\chi=C\exp(-y/2h_1)\cos\frac{Vy}{2h_1}+D\exp(-y/2h_1)\sin\frac{Vy}{2h_1},$$

where

$$V=\left|\left(1-\frac{8h_1}{7H}\right)^{\frac{1}{2}}\right|.$$

We have also

$$w=\gamma H \exp(-y/2h_1)\left\{C\left[\left(\frac{h_1}{H}-\frac{1}{2}\right)\cos\frac{Vy}{2h_1}+\frac{V}{2}\sin\frac{Vy}{2h_1}\right]+D\left[\left(\frac{h_1}{H}-\frac{1}{2}\right)\sin\frac{Vy}{2h_1}-\frac{V}{2}\cos\frac{Vy}{2h_1}\right]\right\}-\frac{i\sigma\Omega}{g}.$$

$$i\sigma\frac{p}{\rho_0}=\frac{1}{2}gH\left[(C+VD)\exp(-y/2h_1)\cos\frac{Vy}{2h_1}+(D-VC)\exp(-y/2h_1)\sin\frac{Vy}{2h_1}\right]-i\sigma\Omega.$$

The continuity of χ and w gives us C and D. By substituting the appropriate value of y, we find the pressure variation at 16 km, which is taken to be the bottom of the meson-producing layer. If p_0 is the pressure at 16 km when the atmosphere is in equilibrium, and $p+p_0$ the pressure when it is disturbed, and if h is the displacement of the isobar, on which the pressure is p_0, from the equilibrium position, then considering the equilibrium of the layer between 16 km and $16+h$ km, $p=g\rho_0 h$, i.e., $h=p/g\rho_0$, neglecting the variation of density ρ_0 in the layer.

We thus find that h varies harmonically with an amplitude of 101.3 cm. Taking the mean free path (decay) of mesons to be 8.5 km,[4] we obtain in the usual way for the amplitude of the semidiurnal variation in meson intensity at the earth's surface due to lunar effects 0.012 percent, the amplitude decreasing with increasing latitude. This may be compared with the result reported recently by Duperier,[5] who obtains from his records (0.023 ± 0.011) percent for the lunar semidiurnal amplitude of the cosmic-ray intensity variation.

We hope to publish elsewhere in the near future a more comprehensive theory of solar and lunar effects on cosmic rays.

[1] A. Duperier, Proc. Phys. Soc. **57**, 464 (1945).
[2] C. L. Pekeris, Proc. Roy. Soc. **A158**, 650 (1937).
[3] A. W. Mailvaganam, Proc. Phys. Soc. to appear shortly.
[4] B. Rossi, H. V. N. Hilberry and J. B. Hoag, Phys. Rev. **56**, 837 (1939).
[5] A. Duperier, Nature **157**, 296 (1946).

Removal of the Electron Beam from the Betatron*

L. S. SKAGGS
Tumor Clinic, Michael Reese Hospital, Chicago, Illinois
AND
G. M. ALMY, D. W. KERST, AND L. H. LANZL
Physics Department, University of Illinois, Urbana, Illinois
June 30, 1946

THE electron beam has been extracted from the University of Illinois 22-Mev betatron by means of a simple laminated iron channel. The iron structure is about 10 cm long and 0.7 cm high with a 1.75-mm by 5-mm channel in the edge facing the orbit. It is placed just outside the point where the magnetic field decreases as $1/r$ and a few centimeters outside of the equilibrium orbit. At the entrance end the channel is tangent to the orbits so that electrons entering it proceed in approximately a straight line to the other end where they emerge in a very weak magnetic field.

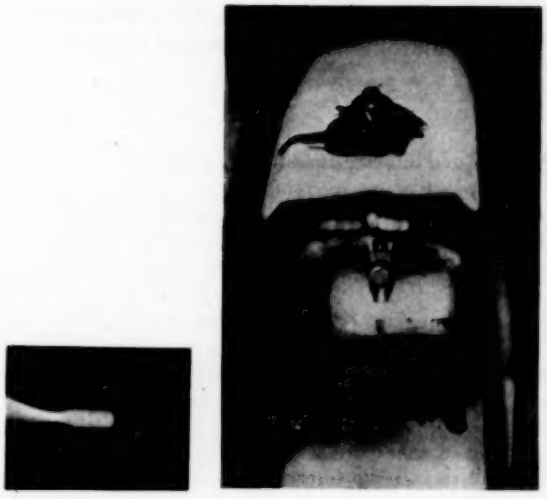

FIG. 1. FIG. 2.

When an electron orbit is expanded into the region where the field falls off faster than $1/r$, the radial focusing forces disappear and the orbits spiral outward automatically. Spirals having a pitch of 1 mm to 5 mm have been observed. Electrons can be caused to enter the channel by the spiralling action. They are forced out to the spiralling region by the orbit expander.

An injector above the plane of the orbit was used so that the outward motion of the electrons was not obstructed. Tests with injectors placed inside the equilibrium orbit show that this type of injection should also be suitable.

A short time after the extraction scheme began to operate, the glass window 2 cm beyond the exit of the channel showed a sharp brown image of the channel with slight spreading of the beam. Multiple scattering in the $\frac{1}{16}$" glass window spread the beam beyond. At one meter from the channel an ionization yield of over 100 r per minute was obtained.

When 4 inches of Pressdwood were used to absorb the beam, the ionization intensity dropped to about 1 percent, indicating that the x-ray intensity is very small. Photographic effects behind various thicknesses of Pressdwood gave ranges in agreement with the electrical calibration of the betatron's energy. The abrupt drop of photographic density at the end of the range is good evidence that the effects are caused by electrons.

Figure 1 shows the beam cross section as it emerges from the glass window and passes through a photographic film. The rectangular end is about the size of the channel and the fan-shaped end is composed of electrons not quite captured in the channel.

Figure 2 shows the window of the porcelain vacuum tube. The end of the iron channel is visible and the dark spot produced by the beam penetrating the glass can be seen at the inside edge of the window.

* This work was in part supported by the U. S. Navy, Office of Research and Inventions.

An Electrostatic Generating Voltmeter for Measurement of Very Small e.m.f.'s

S. A. SCHERBATSKOY AND R. E. FEARON
Tulsa, Oklahoma
July 3, 1946

NEW and hitherto unrealized potentialities of vibrating reed capacitative commutators (electrostatic generating voltmeters) for the stable measurement of very small electromotive forces have been explored and offer outstanding advantages in measurement of ionization currents. Low parasitic capacity (order of 10 micro-microfarads) is secured, making quick responses possible with high valued resistors coupling the source of current. Minimum detectible current (parasitic capacity×rate of drift of zero) is 10^{-19} ampere or better, and can easily be improved further.

Amplifier tubes are employed coupled with negative feedback to increase further the energy of the generated signal. The extreme stability of the contact potential of pure gold with respect to pure gold, or of graphite with respect to graphite, is made use of by employing a null system for the measurements using the generating voltmeter composed of these materials as a null indicator. Electrical performance superior to that of the Hoffman electrometer is secured with nearly complete immunity to mechanical and thermal abuse. Long term zero stability allows comparable absolute measurements to be done in resistance coupled systems as well as in rate of drift arrangements.

These engineering developments which began in the oil industry in 1938 were brought to the Metallurgical Laboratory in 1942 in a high state of perfection after extensive industrial applications in all major U. S. oilfields. We understand Messrs. Harry Palevsky, Robert K. Swank, and Raymond Grenchik, are about to report improvements which they have contributed in this field, beyond the developments outlined here. The writers and Messrs. Thos. Gilmartin and Gilbert Swift have a paper in preparation. This paper would have been available for presentation at the June meeting of the American Physical Society had notice of declassification been received in time.

On the Positive Particles Appearing Near Beta-Ray Emitters

LLOYD SMITH AND GERHART GROETZINGER*
Ohio State University, Columbus, Ohio
June 29, 1946

A SERIES of investigators have found in cloud chambers a number of tracks of light positively charged particles originating in or near natural and artificial beta-ray emitters.[1] Sources which have been investigated for the production of these particles are Ra(B+C), RaE, Th(C+C′+C″), UX, AcC, and P^{32}. The particles have been found in all cases, and to approximately the same extent. The rate of occurrence is about 1×10^{-2} per decay electron, far too great to be accounted for by the pair production by the gamma- and beta-rays from the source.

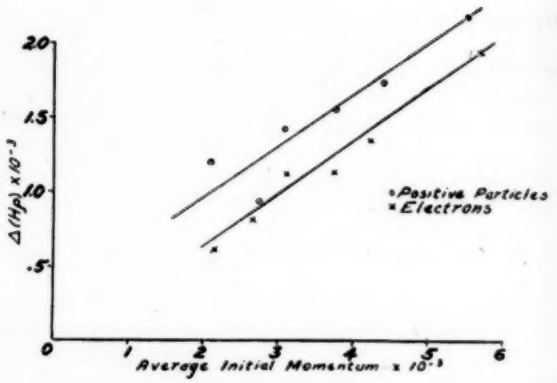

FIG. 1. Momentum loss vs. momentum for the positive particle and electrons.

The tracks still occur when the source is surrounded by enough material to absorb all positrons of the energies indicated by the curvature measurements. The momentum spectra do not resemble the characteristic beta-decay spectrum; for the same maximum momentum, the average momentum is much lower. It is apparent from the properties of these particles that the phenomenon is quite distinct from branching, i.e., the alternative decay of an isotope by the emission of a positron (e.g., Cu^{64}, As^{74}). The apparent penetrating power and the apparent absence of annihilation radiation, which should occur if the particles are positrons, led Bradt, Heine, and Scherrer[1] to suggest that the particles have a mass considerably less than that of the electron.

This suggestion seemed to us to be inconsistent with a part of the experimental facts. We have performed experiments in which the behavior of the positive particles could be studied more directly. For this purpose we used a cloud chamber in which a P^{32} source was mounted at the end of a short aluminum channel which led into the chamber. A metal foil of 0.06 g/cm² thickness was stretched across the center of the chamber, 10 cm from the source. With this arrangement, the loss of momentum of positive particles which traverse the foil could be compared with the loss of momentum of decay electrons which penetrate the foil, allowing a determination of the actual penetrating power of the particles.

In 1300 pictures there appeared 11,000 electron tracks. A total of 107 positive particles, with $H\rho$ up to 6000 gauss-cm, were observed, of which 34 penetrated the foil. 48 electron tracks covering the same range of initial momentum were selected for comparison. Figure 1 shows for each type of particle six points which represent the average momentum losses for six intervals of initial momentum. The initial momentum ascribed to each point is the average of the initial momenta of the five to ten particles in the interval.

The electron points exhibit the effect found by a number of observers, namely, that the momentum loss increases with increasing momentum, at a rate greater than that predicted for ionization and radiation losses. The positive particles show a similar behavior. By comparing the two

sets of points, it can be seen that the positive particles are certainly not more penetrating than electrons. It follows that they must be secondaries of a more penetrating radiation coming from the source. The rate of decrease of the number of positive particles with increasing thickness of material surrounding the source[1] gives, then, an indication of the rate of absorption of the primary radiation. Unfortunately, the data of different observers are not in sufficiently good agreement to warrant a quantitative estimate, but the absorption rate is certainly greater than that for 0.5-Mev gamma-rays.

In addition to the positive tracks originating near the source, six of the tracks which appeared to start or end in the wall of the chamber far from the source, or in the foil, could be definitely attributed to positive particles starting in the wall or in the foil. They were apparently produced by a non-ionizing radiation, but the number is too great by several orders of magnitude to be caused by pair production by the bremsstrahlung from the source.

The fact that the positive particles seem to lose momentum at a consistently higher rate than electrons of the same momentum, as seen from Fig. 1, might indicate that they are not positrons, but have a higher mass. This would be in agreement with the fact that they are apparently not accompanied by an annihilation radiation.

* Now at the Institute for Nuclear Studies, University of Chicago.
[1] A résumé of experiments concerning this question and a good bibliography are contained in an article by Bradt, Heine, and Scherrer, Helv. Phys. Acta **16**, 491 (1943).

Superconductivity of Lead at 3-Cm Wave-Length*

F. Bitter, J. B. Garrison, J. Halpern, E. Maxwell, J. C. Slater, and C. F. Squire
Research Laboratory of Electronics, Massachusetts Institute of Technology, Cambridge, Massachusetts
July 1, 1946

IT is known that superconductivity exists not only in the range of direct currents, but up to ultra-high frequencies. H. London[1] has reported measurements on Sn at a wave-length of 20.5 cm in which the resistivity, though it did not drop instantly to zero at the temperature of transition, nevertheless underwent a striking decrease, falling a few degrees below the transition temperature to much smaller values than were found immediately above the transition. On the other hand, no indications of superconductivity have been found in the study of infrared reflectivity. There must be a range of frequencies between these values, then, in which superconductivity ceases to make itself felt. To explore this possibility, we have been investigating the superconductivity of Pb at a wave-length of approximately 3.2 cm, using modern microwave techniques. We have so far achieved preliminary results, which indicate that the phenomenon is similar to that observed by London at 20.5 cm.

Our experiment has been to measure the Q of a resonant cavity of Pb, as a function of temperature, through the transition point. The resistance of a cavity is similar to that of a series resonant circuit, in which Q can be written in the form $(L/C)^{\frac{1}{2}}/R$, where R is the series resistance, L and C being inductance and capacity. The series resistance in the microwave region, with a conductivity σ and skin depth δ, which is proportional to $1/(\sigma\omega)^{\frac{1}{2}}$, may be computed by taking a surface layer of depth δ, and computing its resistance as in direct currents. Thus R is proportional to $1/\sigma\delta$, so that Q is proportional to $(L/C)^{\frac{1}{2}}(\sigma/\omega)^{\frac{1}{2}}$. Since L/C is independent of frequency and conductivity, we see that a fixed frequency Q is proportional to the square root of the conductivity. Thus as the temperature is decreased, and the conductivity rises, Q should increase, and it should theoretically become infinite in the superconducting state.

The most successful cavity which we have used has been of rectangular shape, like a section of wave guide terminated by plungers of a half-wave-length apart. It has been fed by an iris from a wave guide. It was made by hobbing two half-sections, the joint being parallel to the lines of flow of the current, and the two pieces soldered together along the joint. The Q was measured by conventional standing wave techniques, both by measuring standing wave ratio as a function of frequency through the resonance, and by sweeping the local oscillator frequency through the resonance and observing the reflected power from the cavity as a function of frequency on a scope. The apparatus was unusual only in that provisions had to be made to measure very high Q's, of the order of a million. This demands an oscillator whose frequency can be very accurately stabilized and adjusted. This was achieved by stabilizing a 2K25 reflex oscillator with a stabilizing cavity, in the manner worked out in the Radiation Laboratory by R. V. Pound,[2] beating the resulting signal with the output of a signal generator capable of working from a few kilocycles to a few megacycles, and taking the beat note output of a crystal. This output has a frequency equal to that of the reflex oscillator (which is set close to the frequency of the resonance to be investigated) plus the frequency of the signal generator, and can then be regulated by the frequency control on the signal generator, which can be set and read to a few kilocycles. By this means, good resonance curves can be obtained with very high Q values. In the cavity which has been used so far, the coupling through the iris was such that the external or window Q, which we may call Q_{ext} (the Q which the cavity would have if it had no losses, but were loaded by a matched load in the output), was of the order of 10^5. If the unloaded Q is Q_0, the standing wave ratio in voltage on resonance is Q_0/Q_{ext}. Since measurements of standing wave ratio in voltage can conveniently be made for values from about 1/50 to 50, this allows us to make fairly accurate measurement of Q_0 in the range from 2000 to 5×10^6.

The refrigeration was accomplished by the helium refrigerator described by Collins in an accompanying note. This refrigerator is still somewhat experimental, and as a result of the combined difficulties of the low temperature and the electrical techniques, only two partly successful runs have been made so far. The net result, however, is that there is unquestionably a very large increase of Q in the temperature range immediately below the transition

point, though we do not yet have accurate measurements of the exact values. The best indications which we so far have suggest that a cavity with Q_0 of the order of 2000 at room temperature has a value of the order of 7000 at 30°K, whereas at 4°K the value is of the order of magnitude of 10^8, a large part of the increase apparently coming over a narrow temperature range. This would indicate conductivity at 4°K of 10^8 times as great as at room temperature, and a skin depth of the order of 50A. Further measurements are in progress, with the aim of getting more reliable measurements, finding whether the residual resistance indicates a true bulk resistivity of the Pb or comes from some extraneous source, and comparing with results on other materials. Later in the program, other wavelengths will probably be investigated as well.

The refrigerator, as has been mentioned, was developed by Professor S. C. Collins of the Department of Mechanical Engineering at the Institute. He has actively assisted in the low temperature part of the project, and we are greatly indebted to him for his assistance. We are also indebted to Dr. W. E. Henry for assistance with the temperature measurement.

* This paper is based in whole or in part on work done for the Office of Scientific Research and Development under Contract OEMsr-262 with the Massachusetts Institute of Technology.

[1] H. London, Proc. Roy. Soc. **176A**, 522 (1940).

[2] See forthcoming paper in Rev. Sci. Inst.

A Helium Cryostat

S. C. Collins

Department of Mechanical Engineering, Massachusetts Institute of Technology, Cambridge, Massachusetts

July 1, 1946

A HELIUM cryostat, constructed at the Massachusetts Institute of Technology on an AAF contract,* has been assembled and tested with the cooperation of personnel of the Research Laboratory of Electronics and the use of its facilities. This machine provides an experimental chamber which can be cooled to very low temperatures, that of liquid helium and below. The refrigeration is produced by the adiabatic expansion of helium within a well-insulated inclosure. A 10-hp compressor circulates gaseous helium in a closed cycle. A counter flow heat exchanger makes possible the compression of the helium at room temperature and its subsequent expansion at very low temperatures with almost no loss of refrigeration.

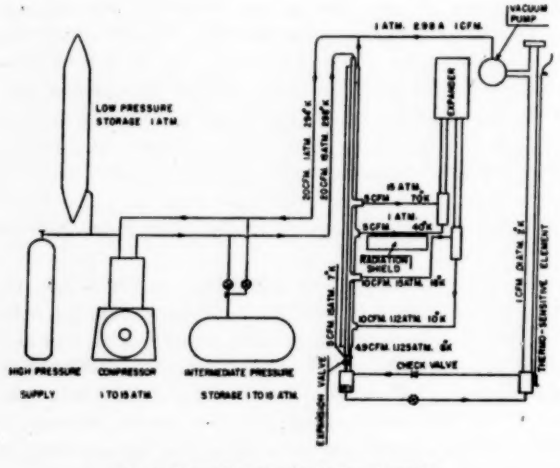

FIG. 1. Flow diagram for helium liquefier.

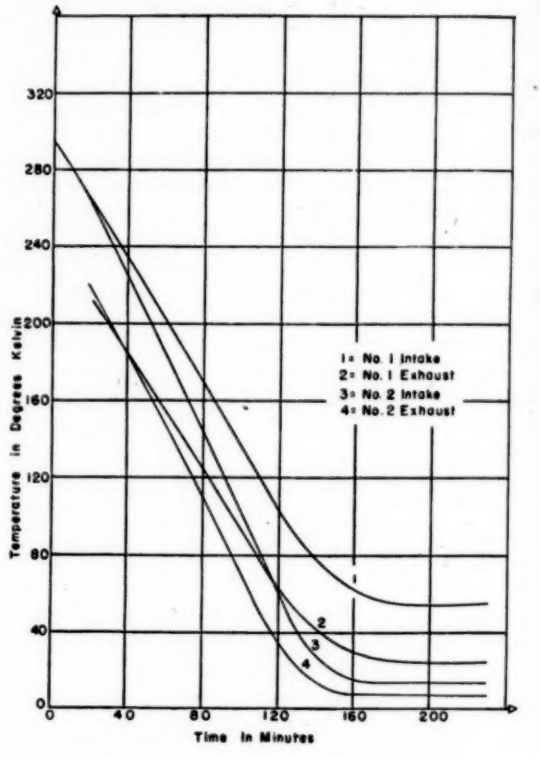

FIG. 2. Performance characteristics of helium liquefier.

Accessories to the cryostat are the compressor, already mentioned, water-cooled after-cooler, oil separator, liquid air-cooled charcoal traps to remove gaseous impurities, 1-atmos. gas holders, and instruments for temperature measurements. The last item includes thermocouples, constant volume gas thermometer, hydrogen vapor pressure thermometer, and helium vapor pressure thermometer.

The flow diagram of the complete assembly is shown in Fig. 1. The outermost shell is the vacuum case. Next is the radiation shield which is attached to the inner wall of the vacuum case. Immediately inside the inner wall of the vacuum case is the heat exchanger, one channel of which is a helix of one-quarter inch finned brass tubing. The helix occupies the annular space between two thin-walled stainless steel cones. The annular space constitutes the second channel of the heat exchanger. Compressed helium flows in the tube, expanded helium in the annulus. The two expansion cylinders and their connections to the heat exchanger appear in the center of the drawing.

A fair amount of experience in operating the machine has been gained. One has reasonable assurance of success

in the attainment of liquid helium temperature level on each attempt.

Figure 2 gives the time rate of cooling. Note that approximately two hours are required to reach the liquid air level (80°K), three hours for liquid hydrogen (20°K) and four hours for liquid helium (4°K). In going from 20°K to 4.2°, the boiling point of helium, a large quantity of gaseous helium accumulates in the experimental chamber. Since the gas must be cooled from room temperature it represents a sizable refrigerative effort on the part of the unit.

* W33-038ac-13866.

Proceedings of the American Physical Society

Minutes of the Meeting at Chicago, June 20–22, 1946

THE 272nd meeting of the American Physical Society was held at Chicago in the buildings of the University of Chicago on Thursday, Friday, and Saturday, June 20–22, 1946. There were 585 registrants, and about a thousand people present in Mandel Hall at the session of Thursday morning. While the registration did not match the two previous meetings nor the largest of the Washington meetings of old, this was by far the largest meeting ever held away from the Atlantic seaboard, and its disadvantage with respect to the few just mentioned is fully explicable by the greater spacing of the centers of physics in the Midwest. Incidentally it was much the largest summer meeting of our history. The Secretary thanks A. J. Dempster, A. E. Shaw, Miss Alberta Jeffrey (secretary of the Department of Physics), and her colleagues for their assistance with the local arrangements.

This will be long remembered as the great nuclear-physics meeting at which a large amount of the work done under the famed "Manhattan Project" was finally brought to light. It is understood that the clearance authorities were laudably assiduous in carrying through with great dispatch the complicated process in the short available time—too short indeed for many who for one good reason or another were unable to prepare in time, and whose contributions may appear at later meetings. A certain number of nuclear-physics papers also came from other than Project sources, and three and a half of the sessions were filled with contributed papers from other fields of physics. There were 97 contributed papers altogether: the abstracts follow.

The programme was enriched with eight invited papers mostly from the Project: the titles and the speakers are given hereinafter. Even the speech of Mr. Seaborg was well attended, though an emergency required it to be given on short notice twenty-four hours before the time allotted. Attention is drawn to the list of scientists on whose work was based the survey by H. H. Goldsmith: this list, not available when the Bulletin was issued, is printed *infra* after the title of the paper.

The dinner of the Society was held on Thursday evening at the Hotel Shoreland, with an attendance of 300. The after-dinner programme consisted almost wholly of the address by A. H. Compton "Physics Research and the Release of Nuclear Energy."

The Council met on Friday afternoon, and elected nine candidates to Fellowship and one hundred and sixteen to Membership: their names are appended.

Elected to Fellowship: W. N. Arnquist, T. B. Brown, H. H. Goldsmith, Victor Hicks, P. E. Lloyd, W. H. Pielemeier, D. H. Rank, M. M. Shapiro, and O. C. Simpson.

Elected to Membership: Edward F. Allen, Frank L. Allen, Mark E. Amdursky, Lowell O. Anderson, Alan Andrew, Joseph Ballam, E. Bleuler, J. W. Bond, William Brauner, Willard E. Buck, William Irving Burg, Alan C. Byers, Paul A. Caldwell, Hans M. Cassel, T. S. Chambers, Richard S. Christian, James Stacy Coles, Kenneth C. Crumrine, Robert B. Duffield, Edgar Everhart, Hubert H. Evinger, Arnold Feldman, Rogers B. Finch, Sister Germaine Fogarty, S.L., Judson Cull French, Ernesto E. Galloni, Clifford S. Garner, Norman E. Gibbs, Homer T. Gittings, Jr., Donald Arthur Glaser, Harold Goldberg, Nicholas E. Golovin, Eugene Paul Gross, P. C. Gugelot, Anatole M. Gurewitsch, Edwin E. Hahn, Jr., Norman S. Hall, Jr., Martin D. Herbst, Melvin A. Herlin, O. Huber, George Gaynor Hyde, Jack Howard Irving, Julius L. Jackson, Nithipat Jalichandra, Sidney Kaufman, George P. Kerr, Jr., George P. Kirkpatrick, Wilfred Konneker, John Herbert Ladd, Arthur E. Laemmel, Simon Larach, Albert H. Lasday, James L. Lauer, Norman T. Lavoo, Lawrence Lee, Sam Legvold, John J. Lentz, Abraham Sidney Levenson, Paul Luger, Paul Thomas Masley, James J. McGlynn, John Armin McIntyre, Howard Oldford McMahon, W. Lathrop Meaker, H. Medicus, William Ralph Mercer, R. C. Meyer, Louis Milgrom, Carlton W. Miller, Herbert I. Miller, Horace L. Newkirk, Robert H. Noble, Arthur S. Nowick, Russell S. Ohl, Benjamin J. Patton, Martin A. Paul, William Perl, Melvin A. Preston, Samuel J. Raff, Milton A. Rothman, Sylvan Rubin, Matthew Sands, Marcello Damy de Souza Santos, Arthur

R. Sayer, Carl Wilhelm Scheerer, Carleton H. Schlesman, Boyd J. Sevold, G. B. Shook, Edmund G. Shower, Sheldon I. Sixfin, Jack H. Smith, Stanley C. Snowden, Bernard I. Spinrad, R. Steffen, Wilbur A. Strauser, Murray Strasberg, Gustaf Strömberg, Nathan Sugarman, M. A. Treuhaft, F. Villars, Hermann Waffler, Robert M. Walker, Roger W. Wallace, Robert L. Wathen, H. R. Wei, David West, Roy V. Wiegand, William Leslie Wilcock, Alfred Wiora, Carl S. Woodward, Harvey Robert Worthington, Jr., Louis F. Wouters, Arianna Wright, J. R. Wright, Greta Yee-Tak Yu, and W. Zunti.

The Council approved changes in the By-Laws of the Division of High Polymer Physics desired by the Division: (the text of these will be made known by the Division). K. K. Darrow and L. N. Ridenour were appointed representatives of the Society on the Council of the A.A.A.S.

The following Resolution had been submitted to the Council by mail ballot:

"The Council of the American Physical Society, being convinced that the national welfare and even the national security depend on the progress and diffusion of scientific knowledge, go on record as affirming that the restoration of freedom of scientific research and publication as it existed before the war is an urgent national necessity. The healthy condition of our science and technology, which was such a great national asset during the war years, will be greatly impaired if the freedom of science is not restored in the immediate future."

Favorable ballots were received from a large majority of the Council, and no unfavorable ballot from any member. This resolution is accordingly to be taken as expressing the sentiment of the Council of the American Physical Society on the important issue involved.

Four alterations in the By-Laws of the Society had likewise been submitted to the Council by a mail ballot, and commanded a large majority. These alterations were submitted to a Business Meeting of the Society convoked on Thursday for the purpose, and were adopted. The By-Laws as hereby amended will be printed in the next Membership List of the Society.

By action of the membership and of the Nominating Committee, the following people were nominated as candidates for the offices and terms which are indicated: *President* 1947, L. A. DuBridge; *Vice President* 1947, G. P. Harnwell, F. W. Loomis, J. R. Oppenheimer, I. I. Rabi; *Secretary* 1947, K. K. Darrow; *Treasurer* 1947, G. B. Pegram; *Editor* 1947–49, J. T. Tate; *Councillors* 1947–1950, D. W. Kerst, P. M. Morse, J. R. Oppenheimer, W. Shockley; *Members of Board of Editors* 1947–49, H. A. Bethe, L. N. Ridenour, W. H. Zachariasen.

The Society has lost through death the following Members: Malcolm C. Hylan (University of Colorado), Howard C. Latham (Navy, lost in action), J. F. Thovert (died in "Resistance" in France some time ago), Max Wehrli (University of Basel); also Louis Slotin (Los Alamos), a candidate for Fellowship.

KARL K. DARROW, *Secretary*
American Physical Society
Columbia University
New York 27, New York

Invited Papers

Elementary Pile Theory. E. FERMI, *University of Chicago.*

The Small Enriched Reactor at Los Alamos. R. R. CHRISTY, *University of Chicago.*

Theory of Nuclear Reactions. GREGORY BREIT, *University of Wisconsin.*

A Critical Survey of Neutron Cross Sections. H. H. GOLDSMITH, *Metallurgical Laboratory:* reporting and collating the work of the following: *from the Metallurgical-Argonne Laboratories:* Messrs. H. L. Anderson, Dancoff, Dempster, Feld, Fermi, Hughes, Langsdorf, Lichtenberger, J. Marshall, L. Marshall, Seren, Snell, Sturm, Szilard, Wattenberg, Weil, and Zinn; *from the Clinton Laboratories:* Messrs. Bernstein, Borst, Sawyer, and Wollan; *from the Los Alamos Laboratory:* Messrs. Barschall, Frisch, Linenberger, Manley, Segrè, Taschek, Williams, and R. R. Wilson; *from Cornell-Los Alamos:* Messrs. E. E. Anderson, Bacher, Baker, Holloway, Lavatelli, McDaniel, and Sutton; *from Columbia:* Messrs. Dunning, Havens, Rainwater, and Wu; and *from Illinois:* Messrs. Coltman, Goldhaber, and Muehlhause.

Problems and Plans of Nucleonics Research. FARRINGTON DANIELS, *Metallurgical Laboratory.*

Neutron Spectroscopy. J. R. DUNNING, *Columbia University.*

The Transuranium Elements. G. T. SEABORG, *University of California.*

Introduction to the Theoretical Papers from Princeton. E. P. WIGNER, *Princeton University.*

Physics Research and Release of Nuclear Energy. A. H. COMPTON, *Washington University.*

ABSTRACTS OF CONTRIBUTED PAPERS

A1. Nomographic Charts for Nuclear Reactions. J. L. McKibben, *Los Alamos Laboratory.*—Use of artificial neutron sources made it convenient to have charts as described and displayed here. In the general reaction with energy Q, mass M_1 with kinetic energy E_1 strikes M_2 at rest producing M_3 at laboratory angle θ with kinetic energy $E_3 = C^2$. The vectoral velocity of M_3 in the laboratory system $[C(2/M)^{\frac{1}{2}}]$ is equal to the vectoral velocity of M_3 in the c.g. system $[B(2/M)^{\frac{1}{2}}]$ plus the vectoral velocity of the c.g. system $[A(2/M)^{\frac{1}{2}}]$. As B/A and B depend only upon M_1, M_2, M_3, M_4, E_1, and Q and not upon the angles, a series of semicircles are drawn with radii B and whose centers are displaced from the origin by distance A. About the origin a series of semicircles of radii C are drawn and through the origin a set of radial lines are drawn to demark angles. The two sets of semicircles are labeled with the appropriate energies. A triple intersection designates a set of values.

$$A=\left[\frac{M_1M_3}{(M_1+M_2)^2}\right]^{\frac{1}{2}}(E_1)^{\frac{1}{2}};$$

$$B=\left[\frac{M_2M_4}{(M_1+M_2)(M_3+M_4)}\right]^{\frac{1}{2}}\left[E_1+\frac{M_1+M_2}{M_2}Q\right]^{\frac{1}{2}}.$$

A2. Thick Target Yields with Deuteron-Proton Reactions. Edgar C. Barker,* *Metallurgical Laboratory.*—A study of the thick target yields for the deuteron-proton reactions of 29 isotopes of elements from sodium to bismuth was made with 6.7-Mev deuterons from the Chicago cyclotron. These yields were examined as a function of the atomic number of the parent nucleus so that yields for other isotopes could be predicted without actual bombardment. After normalizing the experimental yields to a parent abundance of 100 percent and a half-life of one hour, the data were empirically linearized. The yields were thus found to have a trend-like variation with atomic number, expressible as

$$Y=\frac{41IZ^{-0.736Z^{1/3}}}{t_h},$$

where Y is the yield in millicuries per microampere-hour bombardment, I is the abundance of the parent isotope in percent, Z is the atomic number of the parent nucleus, and t_h is the half-life of the product isotope in hours. The total variation in Y extends over a factor of 10^5 from Na to Bi; individual yields depart from the trend by as much as a factor of eight.

* Now at Clinton Laboratories.

A3. Cross Section of D(*d*,*n*) He³ Reaction.[1] J. H. Manley, J. H. Coon, and E. R. Graves, *Los Alamos Laboratory.*—The total neutron yield from a thick heavy ice target has been measured at four bombarding energies from 100 to 300 kev by comparison of the activity induced in a large tank of $MnSO_4$ solution surrounding the source with the activity induced by a standard Ra–Be source. The results are summarized in Table I.

Table I.

Neutron energy (kev)	Thick target yield neutrons/deuteron	Cross section (10^{-26} cm²)
119	1.1×10^{-7}	2.5
171	2.3×10^{-7}	3.7
220	3.6×10^{-7}	5.1
294	7.1×10^{-7}	8.4

[1] Work done at Metallurgical Laboratory.

A4. Cross section of D(*d*,*p*) H³ Reaction.[1] A. C. Graves, E. R. Graves, J. H. Coon, and J. H. Manley, *Los Alamos Laboratory.*—The total proton yield from a thick heavy ice target has been measured for four bombarding voltages between 100 and 300 kev by counting protons emerging from the target chamber at three angles. The results are summarized in Table I.

Table I.

Neutron energy kev	Thick target yield protons/deuterons $\times10^7$	Cross section (10^{-26} cm²)
122	0.78	2.6
171	1.7	3.3
219	3.0	3.9
300	5.5	5.2

[1] Work done at the Metallurgical Laboratory.

A5. The Yield Function and Angular Distribution of the D+D Neutrons. W. E. Bennett, C. E. Mandeville, and H. T. Richards,* *Rice Institute.*—The thin target yield of neutrons from the D+D reaction has been measured for deuteron energies 0.5 to 1.8 mv. The neutron yield in the forward direction increases smoothly throughout this interval, but the yield at 80° to the bombarding beam remains almost level. Values of A in the expression $(1+A\cos^2\theta)$ representing the angular distribution of the neutrons in the c.g. system are calculated from the yield data and plotted as a function of voltage. A is found to increase from 1.8 at 0.5 mv deuteron energy to 3.4 at 1.8 mv.

* Now at the University of Wisconsin.

A6. Disintegrations of Neon and Argon by *d*-*d* Neutrons. E. R. Graves and J. H. Coon, *Los Alamos Laboratory.*—An investigation has been made of reactions in argon, krypton, and neon induced by 2.5-Mev neutrons from a *d*-*d* source. Pulses from a gas filled ionization chamber passed through a linear amplifier into an oscilloscope and were recorded photographically. A calibration of pulse height *vs.* energy was made using recoils from a thin heavy paraffin radiator which was removable. The neutron flux from the *d*-*d* source was known from previous work so that cross sections could be determined. An n,α reaction occurred in spectroscopic argon with a cross section of about 10^{-28} cm². The Q value for the reaction was measured to be +1.8 Mev. An upper limit of $(1/30)\times10^{-28}$ cm² may be placed on the cross section for any exoergic reaction in Kr. Measurements of the $Ne^{20}(n,\alpha)O^{17}$ gave $Q=-0.6$ Mev and $\sigma\approx.005\times10^{-24}$ cm².

A7. Reaction Constants of $Li^7(p,n)Be^7$. HAROLD ARGO, ARTHUR HEMMENDINGER, HOWARD KRATZ, ROLLAND PERRY, RUBBY SHERR, RICHARD TASCHEK, AND DUDLEY WILLIAMS, *Los Alamos Laboratory*.—This reaction has been previously studied at Wisconsin by Benedict, Blair, Hanson, and McKibben who established that the neutrons were mono-energetic and studied the general properties leading to its extensive use at Los Alamos as a variable energy source of fast neutrons, but did not accurately determine the cross sections. The reaction cross section of $Li^7(p,n)Be^7$ has been determined at several proton energies by measuring the total neutron flux in a standard Ra–Be source calibrated manganese bath. By intercalibrating the Be^7 43-day γ activity with bath activity, the measurements were extended from 1.90 to 2.50 Mev in 50 kev intervals, target thickness being measured chemically. The angular distribution of the neutrons from this reaction has been measured as a function of proton energy in 50-kev intervals using a counter whose response is independent of neutron energy; it is found that the center of gravity distribution is not mono-tonic in any of the coefficients required to fit the data. Slides of the results will be shown.

A8. Gamma-Rays from Tungsten. W. M. SCHWARZ, *Indiana University* AND M. L. POOL, *Ohio State University*.—A low resolution beta-ray spectrometer has been employed to study the gamma-rays of tungsten. Tungsten bombarded with deuterons was placed below Th or U foils of sufficient thickness to stop the highest energy beta-rays. Electrons photoelectrically produced in the thorium by the tungsten gamma-rays are measured by the spectrometer using a G–M counter and a scale of 4. The spectrometer calibration was checked with the annihilation radiation from copper positrons. Lines were observed at electron energies of 570 kev and 370 kev. These lines are quite weak but have been checked several times. Other peaks seem to be present but have not yet been satisfactorily checked. Assuming that these peaks are K electrons, we have evidence of a gamma-ray of about 680 kev and one of 480 kev. The first may be the gamma-ray suggested by Sullivan.[1]

[1] W. H. Sullivan, Phys. Rev. 68, 277 (1945).

A9. On the Positive Particles Emitted by Radioactive Electron Sources. LLOYD SMITH AND GERHART GROETZINGER, *Ohio State University*.—A series of investigators have found in cloud chambers a number of tracks of light positively charged particles originating in natural and artificial beta-ray emitters. The rate of occurrence of these particles is about 1×10^{-3} per electron, far too great to be accounted for by pair production by the beta- and gamma-radiation from the source. The tracks still occur when the source is surrounded by enough material to absorb all positrons of the energies indicated by curvature measurements. The momentum spectra do not resemble the characteristic beta-decay spectra; for the same maximum momentum, the average momentum is much lower. The apparent penetrating power led Bradt, Heine, and Scherrer[1] to suggest that they have a mass considerably smaller than that of the electron. To gain information concerning the nature and origin of the positive particles, we have performed cloud-chamber experiments in which a number of the particles were found to come from the neighborhood of a P^{32} source and to traverse a metal foil placed in the chamber 10 cm from the source. The decrease in momentum of 34 particles passing through the foil showed that they are not more penetrating than electrons of the same momentum. For this reason they must be of secondary origin, being created by a more penetrating radiation from the source.

[1] Bradt, Heine, and Scherrer, Helv. Phys. Acta 16, 491 (1943).

A10. Distribution of Neutrons in the Atmosphere. H. M. AGNEW, W. C. BRIGHT, AND D. K. FROMAN, *Los Alamos Laboratory*.—A B-29 airplane has been used to carry counters filled with BF_3 enriched in B^{10} to an altitude of 30,000 feet above sea level. Experiments in progress will be extended to 45,000 feet. The tail compartment contained a bare counter, one completely covered with 0.030″ CD, and one covered with 2.54 cm of B_4C. All hydrogenous material within 25 feet of these counters was removed. The radar room contained a counter completely covered with a 5 cm of paraffin surrounded by a layer of 0.030″ C. The counting rate in all counters varied according to $\exp(-0.083P)$ where P is the pressure in cm of Hg at altitudes above 7000 feet. A constant Cd ratio of 2.2 was obtained. The data above are uncorrected for counts not caused by neutrons. The high biases used should make the corrections small, and the corrections will be determined by using counters filled with normal BF_3. A definite cloud effect has been noted and further investigation is planned. Repeat counts taken during flight show that the amount of gasoline carried by the plane does not affect the counting rates.

E1. Production of Low Energy Neutrons by Filtering Through Graphite. HERBERT L. ANDERSON, ENRICO FERMI, AND LEONA MARSHALL, *Argonne Laboratory*.—Neutrons of energy much lower than thermal were produced by filtering a beam of thermal neutrons through a block of graphite 23 cm long. In such a block, Bragg scattering removes the neutrons whose wave-length is less than the largest Bragg wave-length in graphite, 6.69 Angstroms. Measurement of the boron absorption of the filtered neutrons showed that they had an effective wave-length of 7.15 angstroms which corresponds to neutron temperatures around 18° Kelvin. The cross section of graphite for the filtered neutrons is 0.70×10^{-24} cm². That a part of this is due to the incoherence due to thermal agitation of the atoms of the crystal was demonstrated by heating the crystal and observing the increase in this cross section. The filtered neutrons were used to show interference effects in other substances such as Be, Bi, and S. In water the fourfold increase in the scattering cross section of hydrogen due to chemical binding was observed.

E2. The Bragg Reflection of Neutrons by a Single Crystal. W. H. ZINN, *Argonne Laboratory*.—The intense beam of neutrons which can be obtained from a chain reacting pile has been used to study the diffraction of

neutrons by a crystal. It is found that a neutron beam can be so collimated so that the angular width is of the order of 10′ and that a rocking curve obtained with a single crystal of calcite has the expected width. $CaCO_3$, LiF, and other crystals have been used to construct a single crystal monochromator for the study of resonance neutron absorption. The instrument, which is very similar to an x-ray spectrometer, will be described. The spectrum of the neutrons from the reactor has been determined and the effect of 2nd and higher order reflections investigated.

E3. Studies of Neutron Resonances with a Crystal Spectrometer. WILLIAM J. STURM AND SOLOMON TURKEL, *Argonne Laboratory.*—Using the neutron crystal spectrometer described in the previous paper, measurements have been made of total cross sections as a function of neutron energy for a number of elements. The method involving measurement of the transmission of a sample of the element in the reflected beam has been used in the region between .04 and 65. ev. At energies lower than .04 ev the high order Bragg reflections contribute greater than 5 percent of the total observed effect, while the upper limit of the usable energy range is set by size of the glancing angle allowed by the present collimators. Strong resonances were observed in Cd at .182 ev; in Gd at ~.03 ev; in Sm at .096 ev; in Eu at .465 ev; in Rh at 1.28 ev; in Ir at .635 ev, 1.35 ev, and 6.1 ev. The strong absorption of thermal neutrons in Dy was shown to have a negative energy level. It has been possible to analyze some of the resonance levels at low energy with the help of the Breit-Wigner one-level formula, and to assign values to the constants in this expression.

E4. Reflection of Neutrons on Mirrors. E. FERMI AND W. H. ZINN.—The fact that neutrons are scattered by atoms leads one to expect that various materials will have an index of refraction n for neutrons. $n-1$ is positive or negative and of the order of 10^{-6}. When $n<1$ one might expect total reflection for angles of a few minutes. The phenomenon is analogous to the reflection of x-rays, since they have wave-length and scattering cross section comparable to those of thermal neutrons. The total reflection of neutrons has actually been observed as follows. A very narrow beam of thermal neutrons from the heavy water pile of the Argonne Laboratory was obtained by collimating it with two slits one millimeter wide and placed 5 meters apart. This beam was allowed to fall on polished surfaces of various materials with a very small and adjustable angle of incidence. The search for the reflected beam was carried out with BF_3-filled proportional counters with an entrance slit 2 millimeters wide and placed at a distance of 4.7 meters from the second collimating slit. Reflection was observed very intensively for angles of incidence up to 10′ and for mirrors of graphite, glass, aluminum, beryllium, copper, zinc, nickel, and iron.

E5. Phase of Neutron Scattering. E. FERMI AND L. MARSHALL, *Argonne Laboratory.*—A neutron wave may be scattered with a change in phase of either 0° or 180°. By studying the intensities of the orders of Bragg reflection for neutrons, one can compare the phase of neutron scattering of the different nuclei which compose a crystal. A beam of thermal neutrons from the Argonne heavy water pile was monochromatized by Bragg reflection from the 100 face of CaF_2. From a second crystal in the mono-energic beam Bragg reflections of various orders were obtained. The form factors were calculated from the positions and scattering cross sections of the atoms in the unit cell, and were compared with the observed variation of intensities of orders in several crystals. From the fact that carbon totally reflects neutrons, found by Fermi and Zinn, it follows that the phase change for carbon is 180°. The present investigation shows that O, Ca, Fe, S, Pb, F, and tentatively C scatter with the same phase shift, and that the phase shift for Mn is opposite. Consequently, the phase shift for the group may be tentively identified as 180°, and that for Mn tentatively identified as 0°.

E6. Diffraction Phenomena in Angular Distribution of Fast Neutrons Scattered by Pb-Nuclei. E. AMALDI, *Rome University,* D. BOCCIARELLI, AND G. C. TRABACCHI, *Istituto di Sanità Pubblica.* (To be presented by G. C. Wick).—Fast neutrons from a Li+D (800 kv) source were detected with the 9.9 min. activity induced in a small, Cd-shielded, Cu cylinder placed 80 cm from the Li-target. The direct neutron beam was cut off by a long thin paraffin cylinder. Hollow, barrel-shaped scatterers were used, such that the scattering angle θ was the same for all points of the scatterer. Scatterers were built for the angles: $\theta=20$, 25, 30, 35, 40, 50, 60, 70, 80 degrees, with weights varying from 20 to 300 kg. The indefinition of θ due to finite thickness of the scatterers was from 2° to 4°; the indefinition due to finite dimensions of source and detector was 2°. Variations of source intensity were checked with another Cu detector placed on the opposite side. The angular distribution found exhibits a strong forward maximum, and a small secondary maximum at an angle between 35° and 40°. These data are supplemented with an evaluation of scattering intensity at $\theta=0°$ from the total scattering cross section (5.10^{-24} cm²) by means of an optical theorem. The forward maximum is found to be at least 40 times the minimum. These features are believed to be connected with diffraction of neutron waves by the edge of the nucleus, as pointed out by Bethe and Placzek.

E7. An Application of the Fokker-Planck Equation to the Energy Spectrum of Thermal Neutrons. G. C. WICK, *Notre Dame University.*—An equation of the Fokker-Planck type, first used by Rayleigh to study the thermal equilibrium of a *heavy* particle with a gas of *light* molecules, can also be applied to the opposite case of a *light* particle in equilibrium with a gas of *heavy* molecules, because in one collision the energy change of the particle is small. This equation has been applied to the slowing down of neutrons (below the Cd absorption limit) in paraffin, which is assimilated to a gas of free CH_2 groups (Arley). Using calculated cross sections, one is led to the equation:

$$\frac{\partial F}{\partial t}=\frac{1}{\theta}\frac{\partial^2}{\partial y^2}(yF)+\frac{\partial}{\partial y}[(y-3/2)F]-\frac{1}{\tau}F,$$

where y is the energy in units kT, F is the distribution function, θ is a "relaxation time" ($\theta \sim 10\mu$ sec) and τ is the mean lifetime of a neutron in paraffin. The equation may be applied to study deviations from the Maxwellian distribution, and to time processes.

E8. Energy of Delayed Neutrons from U^{235} Fissions. MERLE BURGY, L. A. PARDUE, H. B. WILLARD, AND E. O. WOLLAN, *Clinton Laboratories.*—A study of delayed neutron energies from U^{235} fission products has been made by measuring recoil proton tracks in a hydrogen-filled cloud chamber. A sample of uranium was irradiated in a graphite pile by means of a pneumatic tube, and brought to the cloud chamber for observation. Five different times of irradiation and decay were used so as to give different proportions of the five delayed neutron activities studied. From composite neutron energy distribution curves, the curves for the separate activities have been obtained. The average energies lie in the region from 0.2–0.8 Mv. There is no simple relation between energy and half-life.

E9. Angular Distribution of *n-d* Scattering for 2.5-Mev Neutrons. J. H. COON, R. W. DAVIS, AND H. H. BARSCHALL, *Los Alamos, New Mexico.*—The angular distribution of the scattering by deuterium of 2.5-Mev *d-d* neutrons was measured by analyzing the distribution in energy of recoiling deuterons. A thin layer of heavy paraffin was mounted in a krypton filled ionization chamber. The ionization pulses due to recoiling deuterons were amplified, and recorded photographically. In the center of mass system the differential cross section appears constant for the scattering of neutrons through angles between 70° and 110°. It rises gradually for angles greater than 110° to a peak value for backward scattering of more than twice the cross section at 110°. The excess over isotropic scattering in the peak contains approximately fourteen percent of the scattered neutrons. The measurements do not extend below 70°. The neutron-proton scattering observed under similar conditions showed a slight rise of the differential cross section from a scattering angle of 75° to 180°.

E10. The Neutron Absorbing Isotopes in Samarium and Gadolinium. R. E. LAPP, J. R. VANHORN, AND A. J. DEMPSTER, *Metallurgical Laboratory.*—The large absorption for slow neutron in samarium was found to be due to the isotope at mass 149, and in gadolinium to the isotopes at masses 155 and 157, the cross section for 157 being about three times that for 155. Mass spectra were made with the double focusing mass spectrograph using a spark with nickel tubes packed with oxide as electrodes. Mass spectra of normal samples were compared photometrically with those of samples in which this isotope abundances had been altered by long exposure to slow neutrons. In the altered gadolinium the abundance of mass 157 was less than 155 in place of greater, and 156 was greater than 160 in place of less. In samarium the abundance of mass 149 was reduced to be nearly as weak as 148, and mass 150 was correspondingly increased.

U1. Instrument Lubricant Having a Low Hardy Coefficient. S. BLOOMENTHAL, *Automatic Electric Company.*—At the last Chicago meeting of the A.P.S. a moderate Hardy friction coefficient was reported for glass surfaces lubricated with Elgin M 56a watch oil. Recently M 56b oil, for which the makers claim increased oiliness, has been introduced as a general purpose watch and instrument lubricant. Measurement of the Hardy coefficient by the inclination method for glass on glass lubricated with M 56b oil gives about 0.09 for 100-g. load, a value appreciably less than that reported for M 56a oil. This value compares favorably with coefficients obtained with the automatic inclination apparatus for other high grade instrument lubricants. The influence of adsorbed polar molecule concentration upon static friction between solid surfaces, evident in H. Dunken's report on wartime experiments in Germany with an inclination balance, will be discussed.

U2. Dislocation Theory of the Creep of Metals. A. S. NOWICK AND E. S. MACHLIN, *Aircraft Engine Research Laboratory* (Introduced by A. R. Bobrowsky).—An equation for the steady-state rate of creep of pure annealed polycrystalline metals is derived through dislocation theory and Eyring's theory of rate processes. The present analysis differs from that of Kauzmann[1] in that it is the generation of dislocations rather than a flow mechanism which is shown to be the rate-determining process. A specific mechanism for the generation process is presented. From it the heat and entropy of activation of the generation process are expressible in an approximate form in terms of physical constants of the material. In addition, the lowering under stress of the potential-energy barrier, which yields the stress-dependent term, is given in terms of constants of the material and a "back-stress" term. The latter depends on the stress field about a dislocation and on the distribution of dislocations in the material.

The creep equation thus obtained is found to be in good agreement with data, both in the dependence of creep rate on stress and temperature and in the dependence of the heat and entropy of activation on the physical constants of the material.

[1] W. Kauzmann, Trans. A. I. M. E. **143**, 57 (1941).

U3. The Energy of Impurity Levels in Semi-Conductors. B. SERIN, *University of Pennsylvania.*—The field for an electron in an insulating crystal containing an impurity atom is estimated, assuming that the general nature of the band states of the crystal is unaffected by the foreign atom. The field for an electron due to a donator impurity is attractive and gives a bound electron state below the conduction band. This case can be treated in an analogous way to Tibbs' calculation* of the energy levels of an F-center. The field caused by an acceptor impurity is repulsive over most of the crystal and results in the splitting off of states from the top of the normally full band. The calculation for the acceptor case is done using the variation method with trial functions expressing the physical nature of the impurity states. The latter calculation is applied to semi-conducting silicon.

* S. R. Tibbs, Trans. Faraday Soc. **35**, 1471 (1939).

U4. Atomic Polarizabilities and the Local Field in Alkali-Halide Crystals. W. SHOCKLEY, *Bell Telephone Laboratories.*—The use of polarizability values deduced from the refraction of ions in solution and from theory gives 10 to 20 percent errors in n^2 when applied to alkali-halide crystals. These discrepancies have been attributed to distortion of the ions and failure of the Lorenz-Lorentz field.[1] Assuming a constant polarizability for each ion and using $A4\pi P/3$ with $A=0$, $\frac{1}{2}$, 1, $\frac{3}{2}$, the set of atomic polarizabilities giving a least square fit with experimental molecular polarizabilities extrapolated to long wave-lengths was determined for each A. The best fit occurred for $A=1$, the sums of the squared deviations for the four A values being 1.5, 0.10, 0.033, 0.054, indicating no significant failure of the Lorenz-Lorentz formula. For $A=1$, predicted and observed n^2 values are within 3 percent with an average error of 1 percent. The value of the atomic polarizabilities in A^3 for the $A=1$ case (first number) differ in a systematic way from Pauling's theoretical values[1] (second number)—Li 0.045, 0.03; Na 0.28, 0.179; K 1.13, 0.83; Rb 1.79, 1.40; Cs 2.85, 2.42; F 0.86, 1.04; Cl 2.92, 3.66; Br 4.12, 4.77; I 6.41, 7.10.

[1] See Mott and Gurney, "Electronic Processes in Ionic Crystals," for a discussion of these difficulties.

U5. Electrostatic Potentials and Fields in Ionic Lattices. J. M. RICHARDSON AND W. SHOCKLEY, *Bell Telephone Laboratories.*—Computations of the electrostatic potential and its derivatives have been carried out for an elementary charge distribution consisting of positive point charges on the corners of a simple cubic lattice embedded in a compensating uniform distribution of negative charge. For ionic crystals whose symmetry is cubic, or tetragonal or orthorhombic with certain restricted axial ratios, the charge distribution for point ions can be obtained by superimposing the elementary charge distribution considered. Thus from the elementary potential and its derivatives the Madelung's energy and local fields can be computed for a wide variety of crystals. Values are not needed except at restricted points in the unit cell. Those chosen were $l/4$, $m/4$, $n/4$ with l, m, n integers; because of the symmetry only 10 points need be computed. The Ewald method of calculation was employed using several systems of checks for internal consistency. The local field results have been used in computing the refraction indices of some crystals for which the Clausius-Mosotti formula is invalid.

U6. High Temperature Anelastic Effects in Polycrystalline Aluminum. T'ING-SUI KÊ, *University of Chicago.*—The sudden drop of temperature coefficient of elastic modulus (dG/dT) of certain metals at high temperatures has often been reported in the literature and vaguely attributed to a sudden change in strength. The rigidity of fine-grained 99.991 percent aluminum wires was determined using a dynamic torsional method from room temperature up to 450°C. The wire was first annealed at 450°C for five hours to eliminate effects of cold work and to give a stable grain size. A sudden drop in dG/dT was observed around 200°C. This drop was not observed in single crystal aluminum wires. The behavior of polycrystalline aluminum can be interpreted as due to viscous slip along crystal boundaries. The grain boundaries apparently behave in a viscous manner with the viscosity decreasing with temperature, as first suggested by Rosenhain in 1912. The temperature at which the elastic modulus curve changes slope corresponds to the temperature at which the relaxation time associated with the slip is comparable to the period of torsional vibration. This picture is supported by measurements of internal friction and elastic after-effects, which are related phenomena resulting from anelasticity, a property by virtue of which strain lags behind stress in the conventionally elastic range.*

* C. Zener and J. H. Hollomon, J. App. Phys. 17, 69 (1946).

U7. The Photo-Diode and Photo-Peak Characteristics in Germanium.* S. BENZER, *Purdue University.*—Two photo-sensitive types of characteristic may be observed in particular germanium crystals when contacted with a metal point. In the photodiode, the current saturates as the voltage is raised, the saturation current being sensitive to illumination and temperature. The photocurrent is linear with intensity and independent of voltage, identifying it as a primary photocurrent. Visible and near infrared light are effective, with threshold ~1.5 microns and maximum response ~1.3 microns, at which latter wavelength the order of unit quantum efficiency may be obtained. The sensitivity to white light is several milliamperes per lumen. The variation of saturation current with temperature is exponential, with an activation energy of ~0.8 ev. In the photopeak, the current-voltage curve is triple-valued, there being a voltage peak followed by a region of negative resistance which becomes positive again at higher currents. Illumination or increased temperature causes the voltage peak to be reduced, and, at sufficiently high temperature or level of illumination, the peak is eliminated. This behavior is entirely reversible, making it useful in the design of a trigger photo-cell.

* This work was part of a research program carried out under Contract OEMsr-362 between the Purdue Research Foundation and the Office of Scientific Research and Development. Based on NDRC Reports, November 1, 1944 and October 31, 1945.

U8. Investigation of Oxidation of Copper by Use of Radioactive Cu Tracer.[1] J. BARDEEN, W. H. BRATTAIN, AND W. SHOCKLEY, *Bell Telephone Laboratories.*—A very thin layer of radioactive copper was electrolytically deposited on a copper blank. The surface was then oxidized at 1000°C for 18 minutes, giving an oxide layer with a thickness of 1.25×10^{-2} cm. After quenching, successive layers of the oxide were removed chemically, and the Cu activity in each layer was measured. The observed diffusion of radioactive Cu in the oxide layer agrees quantitatively with a theory based on the following assumptions: (a) The oxide grows by diffusion of vacant Cu^+ sites from the outer surface of the oxide inward to the metal. (b) The concentration of vacant sites at the outer surface is independent of the oxide thickness, and drops linearly from this constant value to zero at the metal boundary. (c) Accompanying the inward flow of vacant sites, there

is a flow of positive electron holes to maintain electrical neutrality. (d) Tagged Cu^+ ions diffuse only by motion into vacant sites. This gives a fairly direct confirmation of the theory of oxidation first suggested by Wagner.

[1] The radioactive copper and the activity measurements were made in 1939 with help of J. Steigman of Columbia University.

U9. Magneto-Resistance and Domain Theory. R. M. BOZORTH, *Bell Telephone Laboratories.*—Changes of electrical resistivity with magnetization and tension have been studied in some iron-nickel alloys. A particularly simple application of domain theory can be made to the permalloys containing more than 81 percent nickel. Since the magnetostriction of these alloys is negative, tension aligns the domains at right angles to the axis of tension. If an increasing magnetic field is then applied, the domains rotate toward parallelism with the axis, and at a certain field strength will be restored to their original orientations (or to orientations differing from them by 180°). This field strength can be calculated satisfactorily by domain theory. Changes in resistivity at saturation in longitudinal and transverse fields have been measured for alloys containing 40 to 100 percent nickel, and these are compared with the changes due to tension.

U10. Magnetic Domain Patterns on Silicon-Iron Crystals. H. J. WILLIAMS, *Bell Telephone Laboratories.*—Magnetic powder patterns of several new types have been observed in carefully purified single crystals of iron-silicon alloys containing 3.8 percent silicon. Surfaces were parallel to (100), (110), and (211) planes. When a (100) surface was carefully polished mechanically in the usual way, "maze" patterns were found, like those reported by Kaya[1] and by McKeehan and Elmore.[2] When electrolytically polished as suggested by Elmore,[3] the same surface showed lines running along [110] directions and then curving together in pairs to form points (like dagger blades). Near saturation this pattern disappeared and the usual series of lines formed perpendicular to the applied field, as observed by Bitter.[4] On (110) surfaces magnetized in a [110] direction, intricate figures appeared in rows about 0.1 mm apart. As the magnetization increased, these figures grew in size and changed again to the usual series of line segments perpendicular to the field. Still other patterns were observed on the (211) surfaces. Fields were applied either parallel or perpendicular to the surface examined. The colloid used was magnetite, kindly supplied by Dr. Elmore.

[1] Zeits. Physik **89**, 796 (1934).
[2] Phys. Rev. **46**, 226 (1934).
[3] Phys. Rev. **51**, 982 (1937).
[4] Phys. Rev. **41**, 507 (1932).

U11. Contact Potential Difference in Crystal Rectifiers. W. E. MEYERHOF, *University of Pennsylvania.*—The crystal rectifiers considered here are mainly silicon-metal point contact rectifiers. The rectification ability of these contacts depends strongly on the difference in work function of the semiconductor and metal. This contact potential difference has been measured in two different ways: (a) by the variation of the d.c. contact resistance as a function of the temperature,[1] and (b) by the Kelvin method[2] where the semiconductor and metal are not in contact. Although offhand one would expect a correlation between the two measurements, no such correlation exists. This is probably caused by layers on the semiconductor and metal which undergo changes on forming a contact.

[1] W. E. Stephens, B. Serin, and W. E. Meyerhof, Phys. Rev. **69**, 42 (1946); Erratum: Phys. Rev. **69**, 245 (1946).
[2] W. E. Meyerhof and P. H. Miller, Jr., Rev. Sci. Inst. **17**, 15 (1946).

U12. Positive Ions from Thoriated Tungsten. G. A. JARVIS, *University of Wisconsin.*—When thoriated tungsten is heated above 2600°K, appreciable reduction of thorium dioxide occurs, accompanied by the emission of singly charged positive ions of thorium monoxide, thorium, and tungsten. After the filament has been operated at a high temperature for sufficient time to reduce a large portion of the thorium dioxide, it is found that the temperature dependence of the positive thorium ion emission is similar to that for positive ions from pure metals. By employing a magnetic analyzer simultaneous measurements of the emission of thorium and tungsten positive ions as a function of filament temperatures have been made and approximate values of the work functions determined from the slopes of the Richardson plots. When a thoriated tungsten filament is held at a temperature around 2000°K reduced thorium gradually accumulates on the surface. The growth of this surface layer is investigated by raising the filament temperature after known activating periods and measuring the momentary flash current of thorium ions.

F1. Thresholds for Slow Neutron Induced Reactions. L. I. SCHIFF, *University of Pennsylvania.*—It is pointed out that the threshold energy for a particular mode of disintegration of a compound nucleus formed by capture of a slow neutron may be determined experimentally under some circumstances. This corresponds to the determination of the greatest negative energy with which a neutron can be captured and produce the reaction. Negative neutron energies may be obtained by bombarding with deuterons and selecting those cases in which the outgoing proton carries off more energy than the bombarding energy minus the binding energy of the deuteron. The greatest proton energy observed is simply connected with the negative neutron energy threshold. If more than one mode of decay of the compound nucleus can occur, a particular one could be selected by coincidence with energetic protons. This latter procedure should be effective with slow neutron fissionable nuclei. In this case, Volkoff's treatment* of the Oppenheimer-Phillips process indicates that sufficiently large energy transfers to the outgoing proton are not so improbable as to make this effect impossible to observe.

* G. M. Volkoff, Phys. Rev. **57**, 866 (1940).

F2. Radiative Capture Cross Sections For Fast Neutrons. D. J. HUGHES, *Argonne Laboratory.*—For neutron energies higher than some hundreds of kilovolts resonance phenomena are not expected to occur because the spacing

of nuclear levels is less than their width. As a result the (n,γ) cross sections for fast neutrons might vary regularly with atomic weight. The radioactive capture cross sections for fast neutrons of about thirty isotopes of stable elements have been measured by using fast neutrons from the chain-reacting pile of the Argonne Laboratory as the neutron source and measuring the resulting beta-activity. The main results are: (1) The cross sections do not vary at random from isotope to isotope as do the thermal values but follow a smooth curve within experimental error. (2) The cross section for atomic weight (A) less than 100 decrease very rapidly with decreasing A, from about 10^{-1} barn (1 barn $=10^{-24}$ cm^2) at $A=100$ to about 10^{-4} b at $A=15$. (3) The cross section seems to remain roughly constant above $A=100$ except for Pb and Bi which fall abnormally low. (4) There is evidence that in the case of isomers the isomeric branching ratio is the same at high energy as at thermal.

F3. On the Existence of a Resonance Absorption of Neutrons in Graphite. S. BERNSTEIN, *Clinton Laboratories.*—The purpose of the experiment was to determine whether or not an appreciable resonance absorption exists in graphite. A Ra-Be photo-source was surrounded by an 11″ radius graphite sphere. The sphere was surrounded by a 4″ thick spherical graphite shell. The graphite shell was surrounded by a minimum of 13″ of paraffin. The total number of neutrons emitted by the source was determined from the total number of neutrons absorbed as thermals in the graphite and paraffin for the following three cases: sphere, shell, and paraffin in place; sphere removed, shell and paraffin in place; sphere and shell removed. The difference between these numbers is a measure of the number of neutrons absorbed in the graphite resonance region. The results indicate that if a resonance absorption exists in graphite, then at most 5 percent of all neutrons passing through such a level would be absorbed by the 11″ graphite sphere.

F4. Total Cross Sections of Various Materials For Indium Resonance Neutrons. JOHN MARSHALL, *Argonne Laboratory.*—Measurements were made, using cadmium filtered, boron carbide collimated neutrons from a 2″ hole leading to the interior of the Argonne pile, of the total atomic cross sections of various substances for indium resonance neutrons. The collimation was such that no neutron scattered by more than about 6° was registered by the indium foil detector. The detector was shielded from thermal neutrons by thick cadmium and from stray epi cadmium neutrons by thick shields of boron carbide. Background measurements were made by inserting an indium filter in the beam. The observed cross sections in units of 10^{-24} cm^2 were: C–4.84, Be–6.10; D_2O–10.30, H_2O–44.4, Al–1.46, BeO–10.1, Pb–11.39, BF_3–107, F (in C_7F_{16})–3.7. In all cases but that of boron, the total cross section should be due almost entirely to scattering. Assuming the indium resonance energy to be 1.44 electron volts and the scattering cross section of boron to be 2, the cross section of boron for neutrons of 2200 meters per second velocity (kT at 293°K) is 710×10^{-24} cm^2.

F5. The Slow Neutron Cross Sections of Indium, Gold, Silver, Antimony, Lithium and Mercury as Measured with a Neutron Beam Spectrometer. WILLIAM W. HAVENS, JR. AND JAMES RAINWATER, *Columbia University.*—The variations of the slow neutron transmissions of In, Au, Ag, Sb, Li, and Hg have been investigated as a function of the time of flight of the incident neutrons for a 5.4 meter path with a neutron beam spectrometer (1). A method of analysis is developed for determining $E_0=\sigma_0\Gamma^2$ for resonances above 1 ev based on the experimental transmission curves and the Breit-Wigner theory. The positions of the levels located, listed in order of importance for each element, are: In, (1.44 ± 0.04) ev; Au, (4.8 ± 0.2) ev; Ag, (5.11 ± 0.2) ev, (13.7 ± 1) ev, and (43 ± 5) ev; Sb, (6.3 ± 0.4) ev, (19.2 ± 1.0) ev, and indications of other unresolved levels in the region of 50 to 500 ev; Li, only a $1/v$ cross section; Hg, a negative level at $(-2.0\pm0.2$ ev) and indications of unresolved positive levels above 25 ev. In the thermal region, the Ag, Sb and Li cross-section curves can be resolved into the sum of a constant term and a $1/v$ term. If E is the neutron energy in ev, these are:

$$\text{Ag: } [(9.05\pm0.10)E^{-\frac{1}{2}}+(6.6\pm0.5)]\times10^{-24} \text{ cm}^2/\text{atom}$$
$$\text{Sb: } [(0.64\pm0.02)E^{-\frac{1}{2}}+(4.2\pm0.3)]\times10^{-24} \text{ cm}^2/\text{atom}$$
$$\text{Li: } [(11.5\pm0.2)E^{-\frac{1}{2}}+(1.7\pm0.2)]\times10^{-24} \text{ cm}^2/\text{atom}$$

LiF was used in the Li measurements and a value 2.5×10^{-24} cm^2/atom has been deducted for the F. The Hg cross section below 5 ev was well matched by the relation $(64\pm3)E^{-\frac{1}{2}}(1+E/2.0)^{-2}\times10^{-24}$ cm^2/atom.

F6. Neutron Beam Spectrometer Studies of Boron, Cadmium, and the Energy Distribution from Paraffin. JAMES RAINWATER AND WILLIAM W. HAVENS, JR., *Columbia University.*—A slow neutron velocity selector has been developed for use with the Columbia University cyclotron. By the method of arc modulation, neutron production is usually confined to intervals of (10–200) microseconds out of a (1000–10,000)-microsecond cycle. Neutrons slowed down in paraffin are detected by BF_3 proportional counters. Excellent collimation is obtained by using an extensive B_4C and Cd collimating system. Experiments were conducted principally at a 5.4-meter source detector distance. A special selector system counts all the neutrons detected and also selectively counts those detected in an adjustable timed interval after the cyclotron burst. The slow neutron energy distributions from paraffin "source" slabs were shown to be of a modified Maxwellian form with an asymmetrical high-energy "tail." Data for the resonance absorption by Cd were well matched by a one-level Breit-Wigner formula having $E_0=(0.180\pm0.008)$ ev, $\Gamma=(0.112\pm0.006)$ ev, $\sigma_0=(7{,}800\pm800)\times10^{-24}$ cm^2/atom. The results of measurements with several boron filters over the range of 0.01 ev to over 100 ev were well matched by the $1/v$ relation, $\sigma_B=(118\pm4)E^{-\frac{1}{2}}\times10^{-24}$ cm^2/atom.

F7. Fissionability Studies. L. B. BORST AND J. J. FLOYD, *Clinton Laboratories.*—A special photographic emulsion has been developed of low general sensitivity. Fission fragments record as tracks in this emulsion, whereas

alpha-particles and protons do not record as tracks, but only produce general fog. The selective sensitivity of these plates to fission fragments has been used as a basis for determining the thermal fissionability of several nuclear species. The photographic plate in contact with a deposit of the substance under investigation was exposed to a strong thermal neutron source. The developed plate was examined with a microscope for fission tracks. Reasonable estimates have been made of the size of the sample and the area examined. The following values constitute probable upper limits to the thermal fission cross sections of the substances indicated:

$Pb^{204} < 1.7 \times 10^{-28}$ cm²
$Pb^{206} < 1.1 \times 10^{-28}$ cm²
$Pb^{207} < 1.1 \times 10^{-28}$ cm²
$Pb^{208} < 5 \times 10^{-30}$ cm²
$Bi^{209} < 2.5 \times 10^{-30}$ cm²
$Po^{210} < 10^{-28}$ cm².

F8. Diffraction of Neutrons and Neutron Absorption Spectra. L. B. BORST, A. J. ULRICH, C. L. OSBORNE, AND B. HASBROUCK, *Monsanto Chemical Company, Clinton Laboratories.*—A crystal spectrometer has been constructed for the diffraction of neutrons. A collimated beam of neutrons from a chain reacting graphite-uranium pile impinged upon a large crystal. The diffracted beam passed through a second collimator and boron counter. Crystals used have been calcite, lithium fluoride and quartz. Greater intensities were obtained by using the reflected beam from a quartz crystal of variable curvature. Angular resolutions of less than four minutes have frequently been used. The crystal spectrometer has been used as a velocity selector to study the neutron absorption spectra of several elements of large thermal cross section. The low lying resonance levels may be accurately fit by a Breit-Wigner formula of the following form:

$$\sigma\sqrt{E} = \sigma_0\sqrt{E_0}/1+\left(\frac{E-E_0}{\Gamma}\right)^2$$

where σ = total cross section at neutron energy E(cm²): σ_0 = total cross section at resonance: E_0 = resonance energy (ev): Γ = resonance width (half-width at half-maximum) (ev). Values of these quantities will be given for several nuclei.

V1. A Mechanical Synthesizer for Gas Diffraction Patterns. H. J. YEARIAN, *Purdue University*, AND W. M. BARSS, *National Research Council of Canada.*—Molecular structure investigations by electron diffraction require the evaluation of sums of the type

$$\Sigma A_{ij} \sin (sr_{ij})/sr_{ij}$$

where s is the scattering variable, r_{ij} the distance between the i'th and j'th atom of the molecule and A_{ij} the product of their scattering amplitudes which must in general be considered a function of s. A mechanical calculator has been built to facilitate this evaluation. The coefficients A_{ij} are plotted against a logarithmic scale of s extending around a cylindrical drum. A standard curve of sin s/s is also plotted against log s on a similar drum coaxial with and adjacent to the first. Adjustable stops permit rapid selection of a relative displacement of the drums by log r_{ij} so that abscissa s on the A drum coincides with sr_{ij} on the sin s/s drum. The multiplication of the corresponding ordinates is accomplished by setting on them cross hairs whose positions are controlled by logarithmic cams. The relative rotation of the cams gives the product desired.

V2. Electron Diffraction Study of C Cl_2NO_2. W. M. BARSS, *National Research Council of Canada*, AND H. J. YEARIAN, *Purdue University.*—Electron diffraction patterns of gaseous C Cl_2NO_2 with a flat background obtained by using a rotating shutter in a focussing type camera have been evaluated photometrically. These patterns of nine distinct maxima and eight minima give an improved radial distribution analysis and may be compared with synthesized patterns with confidence. A reasonable range of all parameters has been considered. The best agreement is with a model C−Cl = 1.75±.01A, Cl−C−Cl $\angle$ = 110.8° ±2°, N−O = 1.21A, O−N−O $\angle$ = 127° and C−N = 1.59 ±.04A, with free rotation of the nitro group. The large increase in the C−N bond over the usual values seems necessary and may be partially justified by dipole moment measurements.

V3. Calculation of the Higher Energy Levels of the Asymmetric Rotor by Means of the Correspondence Principle. GILBERT W. KING, *Arthur D. Little, Inc.*—According to the old quantum theory, the energy of a rotor with three distinct reciprocal moments, $a \geqslant b \geqslant c$, depends[1] on elliptic integrals. The linear transformation of the rotational energy, $2E(a,b,c) = (a-c)E(\varkappa)+(a+c)J(J+1)$, reduces the difficult part of the calculation to a problem in one parameter, $\varkappa = (2b-a\mp c)/a-c$. The application of the correspondence principle to the hypothetical rotor of energy $E(\varkappa)$ and "moments" 1, $\varkappa-1$ leads to a simple expression for the integral, $\lambda = \Lambda_0(\alpha,\beta)$ where $\lambda = K/J(J+1)$, K being the internal quantum number of the doubly degenerate level at one of the limiting symmetric rotors, and $\Lambda_0(\alpha,B)$ is Heuman's canonical form of the complete elliptic integral of the third kind, with parameters given by cos $2\beta = E(\varkappa)/J(J+1) = \eta$ and sin α = cot β tan $(\cos^{-1} 2\varkappa)$. Heuman has tabulated $\Lambda_0(\alpha,\beta)$ for $\alpha,\beta = 0°$ [1°] 90°, but this table is not of direct value since it gives the quantum number in terms of the energy and asymmetry. We have "inverted" this table to give β (i.e. the energy) in terms of λ and $\varkappa$ directly. This table gives excellent approximations to the energy of the asymmetric rotor at $J \sim 12$ except near the singularities of the integral, $\eta \sim \varkappa$, especially $\sim \pm 1 (\eta \gtrless \varkappa)$. For these regions further calculation of $E(\varkappa)$ by the new quantum theory is necessary in order to obtain sufficient accuracy.

[1] P. Epstein, Phys. Zeits. **20**, 289 (1919); F. Reiche, Phys. Zeits. **19**, 394 (1918); F. Lutgemeier, Zeits. f. Physik **38**, 251 (1926); E. E. Witmer, Proc. Nat. Acad. Sci. **12**, 602 (1926).

V4. Expected Absorption in the Microwave Region by Water Vapor and Similar Molecules. R. M. HAINER AND GILBERT W. KING, *Arthur D. Little, Inc.*, AND PAUL C. CROSS, *Brown University.*—The absorption of microwaves

by molecular rotation is dependent on a permanent dipole, most commonly found in asymmetric rotors. Here the spacing of energy levels is complex, and the existence of permitted transitions in the region accessible to present-day equipment is accidental. To predict microwave absorption, it is necessary to determine all possible transitions between asymmetric-rotor levels about one wave number apart. Since very weak lines can be detected, the calculations are carried to high levels ($J\sim12$) where the population is still appreciable.

Since the transition probabilities of the asymmetric rotor cannot be approximated by the symmetric-rotor values, and since "forbidden" lines can be detected, it is necessary to calculate the true values. Exact values of the energies and transition probabilities of H_2O were calculated and the position and intensity of absorption in the microwave region determined. These values were compared with interpolation from basic tables[1] for the asymmetric rotor previously published. A study of the deviations allow the use of the tables to predict the microwave absorption of gases with one moment of inertia small, and has been done for D_2O, HDO, H_2S, D_2S, H_2Se, D_2Se.

[1] G. W. King, R. M. Hainer, and P. C. Cross, J. Chem. Phys. 11, 27 (1943) and 12, 210 (1944).

V5. The Infra-Red Spectrum of Heavy Water. FRED P. DICKEY AND HARALD H. NIELSEN, *Ohio State University.*—The rotation-vibration bands ν_2 and ν_3 of D_2O have been measured and an analysis of the rotational structure has been carried out for low values of J. In order to assist in the analysis, a method of determining tentative term values, similar to that used by Nielsen[1] in the case of H_2O has been used. Also the intensities of lines of a rigid asymetric rotator, as tabulated by Cross, Hanier and King,[2] have been used. And a plot of the spectrum using the experimentally determined term values and corresponding intensities, as determined from the above tabulation, has been made and compared with the measured spectrum. The frequency ν_2 is found to be 1178.3 cm^{-1}. The frequency ν_3 is found to be 2787.2 cm^{-1}. For the state ν_2 the effective moments of inertia are $I_A=1.685\times10^{-40}$ g cm^2, $I_B=3.807\times10^{-40}$ g cm^2, $I_C=5.775\times10^{-40}$ g cm^2. For the state ν_3 the effective moments of inertia are $I_A=1.877\times10^{-40}$ g cm^2, $I_B=3.857\times10^{-40}$ g cm^2, $I_C=5.718\times10^{-40}$ g cm^2.

[1] Harald H. Nielsen, Phys. Rev. 59, 565 (1941).
[2] P. C. Cross, R. M. Hanier, and G. W. King, J. Chem. Phys. 12, 210 (1944).

V6. Resolution and Pressure Broadening of the Ammonia Spectrum Near One-cm Wave-Length. CHARLES HARD TOWNES, *Bell Telephone Laboratories.*—Twelve lines of the ammonia inversion spectrum[1] were resolved and examined at pressures less than one-mm Hg. The shape of the $J=3$, $K=3$ line was examined in detail at two pressures and agrees well with theory[2] if the frequency of collisions is 17×10^7/sec. at one-mm Hg pressure.

J	K	*Frequency in Megacycles*
1	1	23,693
2	2	23,722
3	3	23,870
4	4	24,137
5	5	24,529
6	6	25,046
2	1	23,097
3	2	22,840
7	6	22,927
8	7	23,231
9	8	23,656
10	9	24,202

[1] Cleeton and Williams, Phys. Rev. 45, 235 (1934).
[2] Van Vleck and Weisskopf, Rev. Mod. Phys. 17, 227 (1945).

V7. The Inversion Spectrum of Ammonia. WILLIAM E. GOOD, *Westinghouse Research Laboratories and University of Pittsburgh.*—The strong absorption band[1] of NH_3 at 0.8 cm^{-1} has been resolved into 28 sharp, widely separated lines. The necessary high resolution was obtained by using a continuous wave source. The gas sample is held in a section of wave guide two and one-half meters long, which is arranged in a balanced system with two crystal detectors. At a pressure of about 0.1-mm Hg it is possible to observe each fine structure line on an oscilloscope by synchronizing the horizontal sweep of the oscilloscope with the frequency sweep of the oscillator tube. Identification of the lines is accomplished by using a calibrated absorption type wavemeter. Each line can be associated with the molecule being a definite rotational state. The centrifugal distortion caused by being in a particular rotational state slightly affects the inversion frequency. An expression which identifies each of these lines with the rotation quantum numbers will be given. The observed intensity of the lines agrees well with the population of the various rotational levels for thermal equilibrium at 300°K. As the pressure of the NH_3 is reduced, the lines are observed to become sharper and at a pressure of about 10^{-2} mm Hg a hyperfine structure is resolved. A Stark effect shift is also observed when a d.c. field is applied to the gas.

[1] C. E. Cleeton and N. H. Williams, Phys. Rev. 45, 234 (1934).

V8. Dissociation of $SiCl_4$ by Electron Bombardment. R. H. VOUGHT, *University of Pennsylvania.*—An ordinary relative abundance mass spectrometer was used to study the processes resulting from electron bombardment of silicon tetrachloride. This substance is well suited to this type of analysis because the negative ions produced provide checks on the dissociation energies of the molecular fragments in addition to those provided by positive ions. A consistent interpretation of the processes involved in positive and negative ion production confirms the values of heats of dissociation estimated from thermochemical and spectroscopic data. The dissociation processes are somewhat different from those observed in CCl_4;[1] ionization of the parent molecule contributes a much larger fraction of the total. The ionization energy of $SiCl_2$ was measured directly from residual molecules produced by dissociation of the $SiCl_4$. It is also noted that where more than one process is energetically possible, the one producing the greatest number of dissociation products seems to be the most probable.

[1] Baker and Tate, Phys. Rev. 53, 683A (1938).

V9. The Continuous Absorption Coefficient of the Negative Hydrogen Ion. S. CHANDRASEKHAR, *University of Chicago.*—The absorption cross sections of the negative hydrogen ion for radiation of various wave lengths and

arising from the bound-free and the free-free transitions have been evaluated with some care. It is shown, for example, that the cross sections for the bound-free transitions are most reliably evaluated in terms of the matrix elements of the momentum operator, while the evaluation of the cross sections for the free-free transitions require a careful consideration of the distortion of the plane wave representation for the electrons generally adopted. It is further shown that the derived cross sections are in very good agreement with the demands of astrophysical observations.

V10. Variations of the Viscosity of Polyatomic Gases with Frequency. W. P. MASON, *Bell Telephone Laboratories.*—A method for measuring the viscosity of gases and liquids has been devised which consists in measuring the resistance and mass loading applied to a torsionally vibrating crystal by a viscous medium. By using a long thin torsional crystal placed in a long thin tube, the coupling can be eliminated to modes of motions that tend to set up compression waves. Applying the method to helium, dry air, nitrogen, oxygen, and hydrogen, the viscosity measured was independent of frequency and pressure. When water vapor was present in the air, the loading over a pressure cycle showed a hysteresis effect indicating that more water molecules were adsorbed during the increasing pressure cycle than came off during the decreasing phase. When measurements were made for carbon dioxide, methane and nitrous oxide indications were obtained that the viscosity varied with frequency. For carbon dioxide the total variation of viscosity was 100 to 1. This variation in viscosity appears to be connected with the production of excited states in the polyatomic molecules. The mechanism of exchange of momentum appears to be a force acting at the moment of generation or decay of an excited state.

V11. Optical Microwave Detector. P. H. MILLER, JR. AND B. GOODMAN, *University of Pennsylvania.*—The possibility of using electro-optical or magneto-optical effects at microwave frequencies for the detection of microwave power has been investigated. A proposed device utilizing a Kerr cell placed in the region of a resonant cavity in which the oscillating electric field is strongest will be described. The oscillating electric field is used to modulate the intensity of plane polarized light passing successively through a Kerr cell to which a large bias voltage has been applied and an analyser. If the light is monochromatic the intensity modulation will generate side bands which can be measured in any convenient interferometer. With the proposed design, now under construction, a sensitivity of 10^{-7} watt appears feasible. Possible improvements in technique which may permit a sensitivity of 10^{-12} will be discussed.

V12. A Simple Instrument for Measuring the Rheological Properties of Elastic Fluids. H. GOLDBERG AND O. SANDVIK, *Kodak Research Laboratories.*—An instrument will be demonstrated with which the shear modulus of gels may be measured easily. The gel is placed in the annular space formed by two concentric cylinders, one of which is oscillated mechanically at frequencies ranging from 10 to 6000 cycles per minute. After the resonance frequency and maximum amplitude of the system have been observed, the elastic constants of the system may be calculated quickly or read directly on a calibrated dial. A modified model of this apparatus will be described. It allows measurements to be taken while the sample is being sheared at various rates. It is possible in this way to follow any changes of shear modulus which may take place as stress is applied or removed. Typical results showing cases of work hardening and work softening will be shown. If a photographic recording device is attached to the instrument, rapid variations of elastic constants occurring within a few seconds may be followed.

V13. A Suggestion Concerning Fundamental Particles. JOHN R. PLATT, *University of Chicago.*—Let a particle be thought of as the standing wave of a scalar, ϕ, formed by an isotropic distribution of plane waves of frequency, f, and velocity, c, all in phase at a single point. Let the energy be hf, mass hf/c^2, with interactions represented by the appearance of sum and difference frequencies. To describe two particles many wave-lengths apart in the same field requires an interference frequency c/d, energy change empirically $\pm\alpha/2\pi hc/d$ (coulomb); with an additional "exchange" energy bhc/d (gravity) for particles of the same frequency. A Lorentz transformation on a single particle leads to an amplitude factor identifiable with the Schrödinger ψ-function. A quantum may be identified with a running wave having no back wave. In one dimension it may be transformed into the sum of symmetric and antisymmetric standing waves. The interference frequency required to describe two particles in a field reaches an upper limit as d approaches λ. Possibly compound nuclei may be describable in this system as standing waves with many poles; charge, spin, and so on, being represented by symmetries or phases or other properties of the wave system.

R1. Manufacture of Carbon 14 in the Chain-Reacting Pile. L. D. NORRIS, A. H. SNELL, E. P. MEINERS, JR., AND L. SLOTIN, *Clinton Laboratories.*—Using the reaction $N^{14}(n, p)C^{14}$, carbon 14 can be manufactured in a chain-reacting pile in three ways; batch processing of irradiated solid nitrogenous material, continuous extraction from some kind of an emanating nitrogenous substance, and continuous extraction from a liquid such as ammonium nitrate solution. A "factory" of the latter type has been in use at Clinton Laboratories. The solution is circulated through the pile with a glass centrifugal pump, and the active carbon is carried out, mostly as CO_2, with the other gases resulting from radiation decomposition of the liquid. The carbon is precipitated from the gas stream as barium carbonate. The isotopic concentration is about 5 percent C^{14}; two early samples analyzed 3.3 percent C^{14} with the mass spectrometer. The rate of production and the amount made so far cannot be stated here. Plans are now being made under which the material will be made available for general use in the near future.

R2. Mass Spectrometric Observation of Radioactive C^{14}. MARK G. INGHRAM, *Metallurgical Laboratory.*—A sample containing radioactive C^{14} prepared by the reaction $N^{14}(n, p)C^{14}$ was studied with a Nier type mass spectrometer. The sample was obtained from Dr. Snell of the Clinton Laboratories in the form of $BaCO_3$. Analysis was accomplished using the CO_2 evolved, by heating the $BaCO_3$ in quartz to 1100°C. The usual technique of liberating the CO_2 by addition of acid was not used for the following reasons: (1) Measurement showed that the first one hundredth of the sample evolved by heating was not characteristic of the carbon isotopes in the sample. (2) In handling small quantities of CO_2, the solubility of CO_2 in the acid is important. (3) The heating technique removes the problem of traping out unwanted vapors. Curves obtained in the mass 42 through 48 positions showed a peak in the mass 46 position 9.3 times larger than that obtained for normal CO_2. This peak must be owing either to O^{18} or C^{14}. Measurement of the O^{18} concentration showed this to be normal. Thus the mass of radioactive carbon is 14 in agreement with radioactivity predictions. Computation of the carbon abundances gave 95.61 percent, 1.04 percent, and 3.35 percent for the C^{12}, C^{13}, and C^{14}, respectively. Correlation of this data with the specific beta-activity of the sample gives a value for the half-life of C^{14}.

R3. A Mass Spectrograph for the Study of Fission Product Mixtures. LLOYD G. LEWIS AND RICHARD J. HAYDEN, *Metallurgical Laboratory.*—A mass spectrograph with 60° magnetic deflection giving 2.5 mass despersion for one percent change in mass was developed for studies of radioactive isotopes formed in fission. The geometry of the ion accelerating electrodes and of the magnetic analyzer was chosen so that a maximum fraction of the ions formed by the source would reach the collector. It was possible to collect one ion for each 40 ions formed. An ion source using thermal emission of positive ions was found to possess several advantages for this work. Source efficiencies for conversion of atoms to ions was very high for several elements (16 percent in the case of La) and the character of the emission was dependent on the chemistry of the elements. This emission data makes it possible to identify not only the mass number of an isotope but also, in many cases, the element to which it belongs. The positions of the radioactive isotopes on the spectrograph plate may be located by means of a Geiger counter or by means of a "radio-autograph" of the spectrograph plate. This instrument and technique has been used primarily for the study of isotopes or rare earth elements.

R4. Assignments of Mass to Fission Isotopes by Mass Spectrograph. RICHARD J. HAYDEN AND LLOYD G. LEWIS, *Metallurgical Laboratory.*—The methods described in the previous paper were applied to specific fission product isotopes. The masses of the radioactive chains containing the following fission activities: 55-day strontium, 30-year strontium, 57-day Yttrium, 1-year ruthenium, 35-year cesium, 40-hour lanthanum, 28-day cerium, 14-day praseodymium, 275-day cerium, 1–2 year illinium, long-lived samarium, and 2–3 year europium were found to be 89, 90, 91, 106, 137, 140, 141, 143, 144, 147, 151, and 155, respectively. The identification of the element was made by means of characteristic ion emission of the element in the case of some of the rare earth fission products. In other cases chemical methods were adequate. Methods were developed for applying the mass spectrograph to elements which are not emitted as ions from a filament.

R5. Chemical Isolation of Two of the Delayed Neutron Activities; Resolution of Delayed Neutron Periods. A. H. SNELL, J. S. LEVINGER, R. G. WILKINSON, E. P. MEINERS, AND M. B. SAMPSON, *Metallurgical Laboratory.*—Work subsequent to that of Snell, Nedzel, and Ibser (Smyth Report, Appendix 3) has improved the resolution of the shorter delayed neutron periods, and shown that the decay starting 0.32 second after the stop of saturation activation follows the equation

$$I = C\{0.4e^{-1.6t} + 0.5e^{-0.38t} + 1.1e^{-0.16t} + 1.0e^{-0.031t} + 0.14e^{-0.013t}\},$$

with t in seconds. Data were taken with short irradiations and with rapidly flowing uranyl nitrate solution. The corresponding half-lives are 0.44, 1.8, 4.3, 22, and 56 seconds. The 22-second activity has been found to follow the chemistry of iodine, and the 56-second activity that of bromine. Inasmuch as like periods have been found[1] in the beta-activities of Br^{87} and I^{137}, it is possible within the present evidence that delayed neutrons are emitted by the nuclei Kr^{87} and Xe^{137}.

[1] Strassman and Hahn, Naturwiss. 28, 817 (1940); Seelman-Eggebert and Born, Naturwiss. 31, 59 and 86 (1943).

R6. Mo^{93} and Cb^{94} from Columbium. D. N. KUNDU AND M. L. POOL, *Ohio State University.*—Metallic columbium in the form of thin foils and rods were subjected to 5-Mev proton and 10-Mev deuteron bombardment. A 6.70±0.05 hr Mo activity was produced by proton bombardment. The chemistry consisted of a bisulfate fusion of the Cb, solution in tartaric acid, separation of Mo as MoS_3, solution of the sulfide in NaOH and NaS, and two precipitations of nickel sulfide away from the Mo. The activity is assigned to Mo^{93} which is also confirmed by two new reactions $Cb^{93}(d, 2n)$ and $Zr^{90}(\alpha, n)$. The characteristic radiations are 1.6-Mev gamma-rays and 0.3-, 0.7-Mev β-particles. No soft electrons or x-rays are emitted, the decay taking place by positron emission. By bombarding a number of thin foils shielded on all sides except the front and of such thickness that the deuterons were completely stopped by the first foil, it was found on a comparison of the 6.6-min. activity in the different foils that, in addition to the (n, γ) reaction, the $Cb^{93}(d, p)Cb^{94}$ reaction also takes place. In the bottom foils the half-life of 2.5 days because of the reaction $Cb^{93}(n, \alpha)Y^{90}$ was also observed.

R7. The Decay of Cb^{94} (6.6 min). M. GOLDHABER* AND W. J. STURM, *Argonne Laboratory.*—In the studies of the activation of Cb by thermal neutrons an activity of very low intensity decaying with a half-life time of 6.6 min. was found. A direct determination of the capture cross

section of Cb leads one to expect an activation cross section about 150 times larger than previously reported. In calculating the activation cross section, it had been assumed that β-rays are emitted by the 6.6 min. Cb^{94}. We now find that this isotope, produced by exposure of very pure Cb_2O_5 to slow neutrons from the Argonne heavy water pile, emits mainly x-radiation with an absorption coefficient of 10 cm^2/g Al. Because of the low efficiency of the normally used Geiger counters for CbK x-rays, the big discrepancy between the activation and capture cross section can be qualitatively understood.

* On leave from The University of Illinois.

R8. Mass Assignments of Some Radioactive Isotopes of Pd and Ir. WILFRED RALL, *Metallurgical Laboratory.*—Mass assignments of the following activities produced in Pd and Ir by slow neutron absorption have been made by the mass spectrograph: Pd^{109} (13 hr), Ir^{192} (60 d), Ir^{194} (19 hr). The Pd and Ir ions were produced by a high frequency spark and were analyzed in a new double focusing mass spectrograph. Mass lines of radioactive isotopes were identified by placing the emulsion of an unexposed plate in contact with that of the undeveloped collecting plate immediately after removal from the spectrograph. When developed after sufficient exposure to the beta-particles, the transfer plate showed the active masses while the collecting plate showed inactive masses as well. Approximately 10^8 beta disintegrations are required to produce a line on the plates used compared to 10^7–10^8 Pd^+ ions of 12,000-volt energy. To obtain maximum intensity, all collimating slits were removed and the source slit was opened to .6 mm resulting in a resolution of about 100. The ratio of atoms consumed in the spark to singly charged ions collected was then found to be 5×10^7.

R9. Radioactive Isotopes in the Osmium Region. LEON J. GOODMAN AND M. L. POOL, *The Ohio State University.*—A γ emitting 99-day period and a 1.5-Mev β emitting 30 hour period have been found by Re$(d, 2n)$ and placed as isomers at Os^{185}·Os^{191} produced by $(n, 2n)$ and (n, γ) has been verified. The activity was also produced by Os(d, p) and Ir(d, α). The half-life is $31.8\pm.2$ hours and the β energy is 0.87 Mev. No evidence of the 17-day period has been found unless its branching ratio is less than 1/300 compared to Os^{191}. A new activity was made in Ir by $(n, 2n)$ and (γ, n) and placed at Ir^{190}. The period is 9.4 days, the β energies are 0.96 and .091 Mev, and the γ-ray is 0.26 Mev. Isomers at Ir^{192} are made by $(n, 2n)$, (d, p), (n, γ), and (γ, n). One has a period of 19.0 hours, β of 2.05 Mev, and γ of 1.6, 0.43, and 0.19 Mev. The other has a period of 68 days, β of 0.59 Mev, and γ of 0.46 Mev. Re^{186} has a half-life of $92.8\pm.1$ hours and a β of 1.14 Mev. Re^{188} has a half-life of $18.9\pm.1$ hours and a β of 2.07 Mev. Chemical separations of Os, Re, and Ir were carried out.

R10. Nuclear Electric Quadrupole Moment and the Radiofrequency Spectra of Homonuclear Diatomic Molecules. BERNARD T. FELD, *Massachusetts Institute of Technology.*—The molecular beam magnetic resonance spectrum for a homonuclear diatomic molecule has been calculated as a superposition of spectra already calculated[1] for heteronuclear molecules. The electric quadrupole term in the Hamiltonian for homonuclear diatomic molecules of total nuclear spin $\mathbf{I}=\mathbf{i}_1+\mathbf{i}_2$, where $i_1^2=i_2^2=i^2$, reduces to the case of heteronuclear molecules of spin I and electric quadrupole interaction energy αe^2qQ. $\alpha(I, i)$ is calculated for all I's, corresponding to $i=1$ through 9/2. The final spectrum is a superposition of the spectra for $I=1, \cdots, 2i$ with a suitable weighing factor for the spectrum for each I. These factors are calculated for weak and strong oscillating fields. In addition, the natural widths of the lines are taken into account. Kusch, Millman, and Rabi have reported the spectra of Na_2 and K_2.[2] From these experiments values of e^2qQ for Na_{23} and K_{39} of $\sim6\times10^{-22}$ and 2×10^{-22} ergs, respectively, are deduced.

[1] B. T. Feld and W. E. Lamb, Jr., Phys. Rev. **67**, 15 (1945).
[2] P. Kusch, S. Millman, and I. I. Rabi, Phys. Rev. **55**, 1176 (1939)

R11. The Measurement of Nuclear Spin, Magnetic Moment, and Hyperfine Structure Separation by a Microwave Frequency-Modulation Method.* ARTHUR ROBERTS, YARDLEY BEERS, AND A. G. HILL, *Massachusetts Institute of Technology.*—The h.f.s. separation of the $^2S_{\frac{1}{2}}$ ground-state levels of the single isotope Cs^{133} has a transition frequency of 9192.6 Mc/sec.[1] Since the spin of Cs^{133} is 7/2, the weak field Zeeman pattern consists of 15 lines, 8π- and 7σ-components. Monatomic Cs vapor in a resonant cavity will then be expected to change the resonant cavity frequency because of the permeability change near transition resonances. The Zeeman transition frequencies can be modulated by varying the magnetic field. We have observed 14 of the 15 lines (the center line cannot be modulated by weak fields) by introducing a few micrograms of Cs vapor at 4×10^{-3} mm pressure into the frequency-controlling resonant cavity of a stabilized oscillator near 9192.6 Mc/sec., and observing the 30-c.p.s. component of the audio-signal detected by an f-m receiver when a weak external magnetic field in the cavity is modulated at 30 c.p.s. The observed frequency deviations, line shape, line width, line separation, and r-f power limitation are in reasonable agreement with theoretical expectation. The scope of the method will be discussed.

* This paper is based in whole or in part on work done for the Office of Scientific Research and Development under Contract OEMsr-262 with the Massachusetts Institute of Technology.
[1] S. Millman and P. Kusch, Phys. Rev. **60**, 91 (1941).

W1. Cold-Cathode Gas Tubes as Noise Generators.* STANLEY RUTHBERG, *Purdue University.*—Several types of cold-cathode gas tubes have been examined as noise generators, namely, glow tube, mercury arc with mercury-pool electrodes, corona-discharge monode. The discharges obtained in a glow tube were found to be similar in noise behavior to those of hot-cathode gas tubes. Noise amplitude spectra were obtained from .05 to 5 megacycles for the glow discharge. The oscillations and noise characteristics are affected by a magnetic field transverse to the discharge in such a way as to suppress the oscillations and to increase the high frequency noise, usually. As high as

60 volts peak-to-peak noise was found in the glow tube. The mercury arc, although it gave primarily oscillations, was not stable enough for quantitative measurements. The corona monode produced steep pulses rather than the grassy appearance of the noise from the glow tube. In general the glow tube is the best generator of "good" noise of the three types of tubes.

* This paper is based on work done for OSRD under contract OEMsr-411 with the President and Fellows of Harvard College.

W2. Noise and Oscillations in Hot-Cathode Arcs.* J. D. COBINE AND C. J. GALLAGHER, *General Electric Company.*—Gas discharges generate oscillations superimposed on random noise of several megacycles band width. Positive ions oscillate in two distinct regions of the discharge, i.e., the plasma and the potential minimum at the cathode. The disturbances produced by the ion motions appear as voltage variations between the electrodes. Oscillations generated in the plasma are usually below 400 kc/sec., while "cathode" oscillations are about 700 kc/sec. As the discharge current is increased, the amplitude of the plasma oscillation increases while its frequency decreases. The random noise also depends on current, increasing rapidly as the Townsend discharge changes into an arc. After arc conditions are fully established, the noise changes slightly with current. Probe studies show that the noise voltage between probe and cathode increases rapidly as space charge conditions change to permit acceleration of electrons to the probe. When the probe collects positive ions, the noise as viewed on an oscilloscope is coarse, i.e., lacking in high frequency components. An explanation of the noise generation may be found in the random fluctuations of space charge at the electrodes. Calculations based on this theory give voltage fluctuations of the observed order of magnitude.

* This work was done in whole or in part under Contract OEMsr-411 between the President and Fellows of Harvard College and the Office of Scientific Research and Development, which assumes no responsibility for the accuracy of the statements contained herein.

W3. Effect of Magnetic Field on Noise and Oscillations in Hot-Cathode Arcs.* C. J. GALLAGHER AND J. D. COBINE, *General Electric Company.*—The voltage disturbances discussed in the previous abstract are markedly affected by a magnetic field transverse to the normal flow of current. The normal plasma oscillations can be suppressed and the noise level above 1 Mc/sec. greatly increased. The oscillations appear to be transmitted to the electrodes by electrons whose velocity is modulated by the plasma ion oscillations as they travel directly from cathode to anode. The effect of the magnetic field is to remove these electrons from the current reaching the anode. A critical value of magnetic field will suppress the oscillations and reduce the noise to a minimum. As the magnetic field is further increased the high frequency noise level increases. The high frequency noise level also increases if the pressure decreases, or if a lighter gas is used. The noise level is independent of the plasma volume. The effect of the magnetic field is to build up a region of high ion density in a narrow region near the electron source. Plasma oscillations with continuous spectrum are generated in this region of high density and high density gradient.

* This work was done in whole or in part under Contract OEMsr-411 between the President and Fellows of Harvard College and the Office of Scientific Research and Development, which assumes no responsibility for the accuracy of the statements contained herein.

W4. Electrical Contact Noise. M. H. GREENBLATT, P. H. MILLER, JR., AND L. I. SCHIFF, *University of Pennsylvania.*—A theory of the low frequency noise observed in biased electrical contacts involving semiconductors will be described which is based on the diffusion of impurities between the bulk of the semiconductor and the interface region where large electric fields exist. Experiments which indicate that the noise power is inversely proportional to the frequency at which it is measured are extended to determine the frequency characteristics at temperatures above and below room temperature and the dependence on impurity concentration. Preliminary results indicate agreement between theory and experiment on the following points. The noise power (1) is inversely proportional to frequency at low frequencies and falls off more rapidly than this at higher frequencies, (2) is proportional to the square of the back bias current, and (3) is nearly independent of temperature.

W5. Contour Fringes and Asymmetries of Electron Microscope Objectives. JAMES HILLIER AND EDWARD G. RAMBERG, *RCA Laboratories.*—Experimental data have indicated that a practical limit to the resolving power of the magnetic electron microscope has been imposed by departures from axial symmetry of the objective lens field. Contour fringes in images taken near focus provide a sensitive criterion of such asymmetries. These fringes have been investigated experimentally. It has been found that they can be interpreted on the basis of ordinary Fresnel diffraction if the phase relations between the interfering waves are properly accounted for. Calculations of the effects of physical asymmetries in the pole pieces indicate the necessity for a very high degree of perfection in machining and magnetic materials. Since this is scarcely attainable with existing methods and materials a procedure for compensating asymmetries was devised. A new pole piece system incorporating means for such compensation is described and some of the improved results obtained are shown.

W6. Mechanical-Electronic Control System. ROBERT HOFSTADTER, *Norden Laboratories Corporation.*—A mechanical-electronic system has been developed for control of position and motion of massive bodies. For such bodies, large time lags exist and high accelerations are unobtainable or undesirable. The usual type of control manually selects a variable rate of motion until the desired position is nearly reached. The rate of motion is then decreased until the body is brought to rest in the correct position. The developed system attempts to bring the body automatically to the correct position, independently of many parameters, so that the decay of positional error is approximately exponential. This is achieved by balancing the positional error against a signal, approximately proportional to the

rate of change of positional error, derived by condenser-resistor differentiation of positional error. Balancing is brought about by the circuit, which controls a servo that varies the actual error rate. To allow for delay of the body in assuming the desired rate, an anticipatory signal is taken from the servo motion through a condenser. Controlled transitions between widely different positions are facilitated by gradually introducing changes of position-equivalent voltage by a resistor-condenser combination. Results will be given of an application to altitude control of massive aircraft.

W7. Microsecond Phosphorescent Decay Periods of X-Ray Fluorescent Screens. FITZ-HUGH MARSHALL, *Westinghouse Research Laboratories.*—Many highly developed wartime electronic devices can now be applied advantageously in other fields. The following experiment is offered especially as a suggestive example. Microsecond square-wave x-ray pulses, repeated a thousand times a second, were produced by operating an x-ray tube directly from a radar pulser. Various x-ray fluorescent screen materials were irradiated with the pulsed x-rays, and the light emitted by them was measured by a photo-multiplier tube connected to a DuMont 248 oscilloscope, on the trace of which accurate time markers can be added. This oscilloscope was used as a synchroscope, to trigger the pulser and to sweep the cathode-ray beam for a selected short time starting a microsecond before the x-ray pulse. Photographs of the oscilloscope screen permit accurate measurement of the build-up of fluorescent intensity during the x-ray pulse and of the phosphorescent decay. $CaWO_4$ (radiographic intensifying screens) and $BaSO_4$ with 5 percent $PbSO_4$ have exponential responses with time constants of 5.8 and 0.7 microseconds, respectively, for decay to $1/e$th intensity. Patterson *B* (fluoroscopic) and *D* (photofluorographic) screens, of mixed compositions, reveal assorted superimposed decay curves, some possibly hyperbolic.

W8. High Particle Density in Cosmic-Ray Air Showers. MARIO IONA, JR., *The University of Denver.**—The investigations of the University of Chicago group on the particle density of cosmic-ray air showers were continued, using two Carnegie Model "*C*" ionization chambers. The use of these stable instruments permitted recording of coincidences of bursts over a longer period of time so that showers of very high particle density could be studied. It was found that the majority of very large bursts with several hundred particles passing through an unshielded (1.25-cm iron wall thickness) spherical ionization chamber of about 0.1 m^2 cross-sectional area gave rise to a burst coincidence recorded in two ionization chambers separated by a distance of 1 m between centers. This demonstrates the existence of large atmospheric showers of very high particle density extending over an area of at least 1 m^2. The boundary of the high density region, however, seems to be rather sharply defined, since in several cases a very marked difference was noted in the size of the individual bursts recorded in each chamber. In some cases there was no observable increase in ionization recorded in one chamber while in the other chamber a burst of ionization was recorded corresponding to several hundred or even thousand particles of average ionization.

* Work done at the University of Chicago. This paper is placed on the Saturday programme at the author's request.

W9. Radiation Resistance of Loaded Antennas.[1] RICHARD C. RAYMOND AND WAYNE WEBB, *Department of Physics, The Pennsylvania State College.*—Driving point impedances for antennas with numerous forms of metallic and dielectric loading arrangements have been examined experimentally. Low loss dielectric materials of dielectric constant up to 22.4 were used as sheaths to load cylindrical stub antennas. The resistances at resonance are compared with resistances calculated by the Poynting vector method for assumed current distributions in the antennas. The current distributions in selected cases are being checked experimentally. For a given current distribution, the resonant resistance is a function only of the length of the antenna in wave-lengths. Measured points for all loaded antennas studied were found to fall between the curves for uniform and for sinusoidal distribution.

[1] This paper is based on work done for the Army Air Forces under contract W33-038ac7677.

W10. On the Irradiation of Microorganisms with Variable Sensitivity. I. OPATOWSKI, *The University of Chicago.*—The ordinary processes of life (e.g., growth) cause sometime changes in sensitivity of the microorganism to radiation. This must be taken into account in evaluating the effect of radiation. The present paper develops a method to calculate such change of sensitivity from ordinary types of experiments. The theory is based on a probabilistic approach as applied e.g., by I. A. Crowther.[1] Known methods to estimate the so-called "sensitive volume" i.e., the size of the aggregate of molecules through which the radiation produces the observed effect are extended to the present case of variable sensitivity and applied to some experiments with x-rays recently discussed by N. Koyenuma.[2] The paper will appear in the September 1946 issue of the *Bulletin of Mathematical Biophysics.*

[1] I. A. Crowther, Proc. Roy. Soc. London **100B**, 390–404 (1926).
[2] N. Koyenuma, Zeits. f. Physik **120**, 185–211 (1943).

W11. Unipolar Magnetic Charges (Poles). FELIX EHRENHAFT, *New York City.*—Aime Cotton[1] has arrived at the same values for the unipolar magnetic charges, north or south, using convincing photomicrographs by Pierre Tauzin.[2] The author has presented such charges repeatedly to the A.P.S. and has published them.[3] Further methods of measuring these charges will be given. No difficulties are encountered when these charges are introduced into the system of physics, because the theory of magnetism has from the mathematical point of view according to Coulomb, Biot-Savart, Ampere, etc., already taken into account the existence of these unipolar magnetic poles. Hertz clearly predicted the existence of these charges; J. Stefan, P. Curie searched for them. Maxwell's equations were enlarged in this respect by O. Heaviside. Now, their existence is experimentally shown. The author will show that the recognition of unipolar magnetic charges

offers a promising approach to the study of the particles of modern physics, mass spectroscopy etc. The interpretation of the helical movement of matter occurring in the homogeneous magnetic field without the influence of light, the helical movement of matter in the homogeneous beam of light without external magnetic fields (photophoresis), and the movements caused by the simultaneous action of fields and light pose problems. It is necessary to make some clarifications pertaining to previous bulletins,[4] which will be done in an abstract entitled "Rotational Movements of Matter in the Homogeneous Fields of Magnets or of Radiation."

[1] Aime Cotton, Ann. de physique **20**, 228 and 557 (1945).
[2] Pierre Tauzin, Cahiers de physique, Societe francaise de physique, No. 15, 76, 1943; No. 19, 2, 1944.
[3] Felix Ehrenhaft, J. Frank. Inst., **233**, 248 (1942).
[4] Felix Ehrenhaft, Phys. Rev. **69**, 52 and 260 (1946), St. Louis Meeting, Nov. 30, 1945, and New York Meeting, Jan. 29, 1946, respectively.

S1. Pile Kinetics*. L. W. NORDHEIM, *Clinton Laboratories.*—A pile will run steadily at an arbitrary level if it is just critical. For a pile not at equilibrium, equations of motion can be set up that contain as variables the pile power, the number of delayed neutron emitters and, in case it is of importance, also the pile temperature. The coefficients will depend on the average lifetime of the neutrons in the pile, the fractions and periods of delayed neutrons, temperature coefficients of reactivity, and similar quantities. For a definite "excess reactivity," which may be positive or negative, the power level will change exponentially with time with periods determined by the so-called "inhour" relation. For control and safety problems the transient behavior of the pile under reactivity changes has to be investigated. A number of limiting cases can be solved explicitly. A general method for the solution of the pile equations is available for small deviations from a steady state. In this case a pile impedance can be defined in close analogy to electric circuit theory.

* The development of the fundamental ideas of pile kinetics are due to the efforts of many authors, particularly E. P. Wigner, S. Fermi, J. A. Wheeler, R. Christy, and J. Schwinger.

S2. Pile Perturbation Theory. HARRY SOODAK, *Clinton Laboratories.*—The determination of the critical size and of the neutron distribution in a pile constitutes a characteristic value problem. Exact solutions are obtainable only for simple geometries and uniform pile structures. Other cases can be treated by perturbation theory in analogy to the Raleigh-Schroedinger method. The simplest case concerns the effect of localized absorbers. Their effect on critical size in simple piles turns out to be proportional to the square of the neutron density at the considered position which, suitably normalized, can be used as a statistical weight factor for irregular distributions. In the next approximation the distortion of the neutron distribution can also be evaluated. Other problems that can be treated are composite piles with parts of different properites, irregularities of shape of the pile, and the periods of non-critical piles. A systematic scheme for non-homogeneous piles involves the introduction of adjoint equation and solution for the neutron distribution in the pile.

S3. Calculation of Critical Size of Heterogeneous Slow Neutron Chain Reactors. A. M. WEINBERG, *Clinton Laboratories.*—The critical size of a large slow neutron chain reacting system is determined by the multiplication constant k, (average number of neutrons produced per neutron absorbed), and the migration length, (essentially the r.m.s. distance a neutron travels from birth as a fast neutron to death as a slow neutron). The multiplication constant is the product of $\eta\epsilon pf$.* The calculation of f, the thermal utilization in a heterogeneous arrangement is usually based on the following assumptions: (*a*) Wigner-Seitz cellular approximation is valid; (*b*) production of slow neutrons in moderator is constant over cell; and (*c*) first-order diffusion theory is applicable. The last assumption is incorrect, as stressed by Placzeck, because the dimensions of the lumps are not large compared to the mean free path of the neutrons and the absorption in the lumps is not negligible compared to the scattering. The breakdown of diffusion theory implies that the angular distribution of neutron velocity vectors around a point must be represented by more than the first two spherical harmonics. It is found that the neutron density in the moderator is higher than computed by first-order theory. This leads to a lowering of the first-order thermal utilization.

* For notation see H. D. Smyth, *Atomic Energy for Military Purposes* (Princeton University Press, Princeton, New Jersey, 1945) and Rev. Mod. Phys. **17**, 351 (1945).

S4. Theory of Pile Control Rods. R. SCALETTAR AND L. W. NORDHEIM, *Clinton Laboratories.*—A control rod absorbs neutrons and increases the leakage of neutrons from the pile through the depression of the neutron density in its vicinity. To determine the effect of controls on critical conditions for a pile the absorber may be considered, as in the electrical analog, to produce a singularity in neutron density at its position. The strength of such a singularity is determined by the boundary conditions which must be satisfied at the surface of the black or non-black absorber and the order of the singularity is determined by the geometry of the problem. The general solution of the pile equations can then be expressed by a sum of a regular solution plus the solution containing the proper singularities and this total solution can be adjusted to satisfy the boundary conditions. By this means the effect of control rods of various sizes and positions on pile reactivity and neutron distributions and the effects of mutual control rod shading have been investigated both by a thermal and by a two-group theory.

S5. Radiation from Fission Products. KATHARINE WAY, *Metallurgical Laboratory* AND E. P. WIGNER, *Princeton University.*—A fissioning nucleus can divide into any of about twenty pairs of product nuclei. Each product nucleus is in general unstable and goes through several radioactive β-transitions before it reaches stability. Each transition, of course, has its own peculiar radiations and lifetime. The radioactivity which follows a number of fissions is thus made up of a number of individual activities of many periods and energies. The energy emitted per second per fission at time t after a fission is given by

$$\int_0^{\lambda_{max}} \lambda n(\lambda,t)E(\lambda)d\lambda,$$

where $n(\lambda,t)$ is the number of nuclei of decay constant λ existing at the time t after a fission. Evaluation of this expression gives, for times greater than one day, the result

$$\text{Mev/sec./fission} \approx 3.75t^{-1.2}+96t^{-1.4},$$

where t is measured in seconds. For shorter times a curve is given. This is the total energy emitted including that carried by neutrinos. Agreement with experimental results is fairly good. Handy rules of thumb giving correct values within a factor of two for times between 10 sec. and 100 days are:

$$\beta+\gamma\text{Mev/sec./fission} = 2.66t^{-1.2},$$
$$\gamma\text{Mev/sec./fission} = 1.26t^{-1.2}.$$

The total disintegration energy per fission turns out to be $\approx 22\pm 3$ Mev.

S6. Refraction and Diffraction of Neutrons by Crystals. M. L. GOLDBERGER, *University of Chicago* AND FREDERICK SEITZ, *Carnegie Institute of Technology.*—The refraction and diffraction of neutrons by crystalline matter is discussed theoretically on the basis of a generalization of a method first used by Fermi. In the present treatment it is assumed that the nuclei of which the matter is composed both scatter and absorb neutrons; however, the approximations used are valid only when the "phase shift" of the wave functions by the nuclei is small. This condition is satisfied for a large number of nuclei in cases in which thermal neutrons are being considered. In the region of long wave-length, the medium behaves like an optical medium characterized by a refractive index n and an extinction coefficient κ which are related to the cross sections σ_s^p and σ_a^p for scattering and absorption, respectively, by means of the equations

$$n = 1+n_0\pm\Sigma_p\pm\frac{2\pi}{k^2}\left(\frac{\sigma p_s}{4\pi}\right)^{\frac{1}{2}}, \qquad \kappa = n_0\Sigma_p\frac{\sigma p_a}{2k}.$$

Here n_0 is the number of atoms or molecules per unit volume, k is the wave number of the neutron, and p is summed over all atoms of the constituent molecules. The sign appearing before each term in the first summation is related to the sign of the "phase shift" for the corresponding nucleus. It is shown that these equations are valid whenever Bragg's condition is not satisfied. The problem of neutron diffraction is treated by a method closely related to that used in the dynamical theory of x-ray diffraction and the results obtained bear a very close relation to those for x-rays.

X1. Short Range Alphas in Natural Radioactivity. S. M. DANCOFF, *University of Illinois.*—We have considered to what extent the fine structure of the alpha-rays emanating from naturally radioactive nuclei can be theoretically understood. We are concerned here only with rays whose energy is less than would correspond to a transition between ground states of the parent and daughter nuclei. Of various methods whereby such an alpha-particle can suffer energy loss the most interesting and important appears to be the excitation of the residual nucleus after the alpha-particle has been ejected. This takes place by the mechanism of electrostatic interaction between the alpha-particle and the nuclear matter. The probability for exciting nuclear dipole transitions in this manner has been estimated to be of the order of unity if the transition energy is about 100 kev. Quadrupole transitions will also be strongly excited.

X2. Crystal Structure Studies of Plutonium and Neptunium Compounds. W. H. ZACHARIASEN, *Metallurgical Laboratory.*—The crystal structures of thirty-two plutonium compounds and of thirteen neptunium compounds have been determined. Most of these compounds were identified by means of the x-ray diffraction method, and crystal chemical considerations at a time when plutonium or neptunium were available in too small amounts to permit the use of microchemical methods of analysis. The crystal radii of plutonium and neptunium have been determined for the various normal valence states and for subnormal valence states observed in such compounds with metallic-type binding as PuO and NpO. The crystal structure results for normal-valence compounds have shown that electrons go into the 5*f*-shell, thus confirming the old hypothesis of a new rare earth series being started towards the end of periodic system. In the series of ions $(UO_2)^{+2}$, $(NpO_2)^{+2}$, $(PuO_2)^{+2}$ or Th^{+4}, U^{+4}, Np^{+4}, Pu^{+4}, or U^{+3}, Np^{+3}, Pu^{+3} there is a contraction in size with increasing atomic number analogous to the lanthanide contraction.

X3. X-Ray Long Spacing Diffraction from Lauryl Amine Hydrochloride and Sodium Laurate.* RICHARD W. MATTOON, *University of Chicago.*—Sodium or potassium soaps of saturated fatty acids usually have a long spacing (d_l) nearly twice the length (l) of the molecule ($d_l = 2l \sin\beta$, β near 90°), corresponding to their head-to-head and tail-to-tail arrangement. For potassium laurate, $l \approx 16$A and $d_l = 31.3\pm 0.2$A, measured in a vacuum camera.[1] Further for lauryl amine hydrochloride $l \approx 18$A and $d_l = 35.4\pm 0.3$A (assuming the innermost strong diffraction to be order 1). An 8.4 percent aqueous solution of sodium laurate at 30°C is a clear liquid solution which gives a very broad, weak band. Cooled to 15°C it becomes an opaque, white gel, giving a sharp diffraction pattern with $d_l = 31.8\pm 0.2$A (order 1 strong, 2 weak, 3 medium). For anhydrous sodium laurate $d_l = 31.6\pm 0.2$A (order 1 strong, 2 weak, 3 medium). The gel formation is a large structural change at the same over-all concentration. These measurements suggest that this particular gel is composed of long, thin fibers head-to-head and tail-to-tail with no water in the head-to-head interface. The fibers may form an entangling meshwork with water entrapped *between* the fibers.

* Done in connection with Government Research on Synthetic Rubber, Office of Rubber Reserve, Reconstruction Finance Corporation.

[1] W. D. Harkins, R. W. Mattoon, and M. L. Corrin, J. Am. Chem. Soc. **68**, 220 (1946).

X4. A Null Method for the Comparison of Two Ion Currents in a Mass Spectrometer. ALFRED O. NIER, EDWARD P. NEY,* AND MARK G. INGHRAM,** *University of Minnesota.*—Isotope abundance ratios are ordinarily determined in a mass spectrometer by employing a single

ion collector and alternately measuring one isotopic current and then the other; since the currents may be drifting in magnitude, sufficient readings are taken so that a reliable ratio is obtained. If two ion collectors are employed and if the more abundant isotope is measured by means of an inverse feedback amplifier, whereas the rarer isotope is measured simultaneously by a conventional electrometer tube amplifier, a measurable fraction of the output signal of the inverse feedback amplifier may be used to balance out the input signal owing to the rarer isotope. The electrometer tube is then used merely as a null indicating instrument. The balance point is independent of ion intensity so that the method may even be used to accurately compare currents which are pulsating in magnitude. A second inverse feedback amplifier may take the place of the electrometer tube amplifier. The method lends itself to automatic recording.

* Now at the University of Virginia.
** Now at the University of Chicago.

X5. The Dynamic Condenser Electrometer.* HARRY PALEVSKY, ROBERT K. SWANK, AND RAYMOND GRENCHIK, *Metallurgical Laboratory.*—Dynamic condenser electrometers are characterized by the fact that mechanical energy is used to move the impressed charge in an electrostatic field. Mechanical energy is thereby transformed into electrical energy; i.e., an a.c. signal, which is a measure of the impressed charge. An associated vacuum tube circuit is usually used to measure the generated a.c. signal. With proper design the sensitivity is limited by the termal agitation noise in the input circuit. Zero-drift is dependent only upon the change in contact potential of the condenser surfaces. Since the signal into the amplifier is an alternating voltage it may be amplified to any required power level with a stable a.c. amplifier. The possibility of stable amplification is important since it permits the use of a fairly insensitive indicating meter having a short period of response. Neither changes in amplifier gain or variations in power supply voltages contribute to the zero-drift. The construction of the dynamic condenser requires careful work, but once it is assembled and sealed from the atmosphere, it is extremely rugged and does not require any further adjustments. The condenser itself is not sensitive to electromagnetic disturbances. Data of performance will be given.

X6. Control Equipment for 2.5-Mev Van de Graaff Giving an Ion Beam Constant to ±1.5 kev. J. L. MCKIBBEN, and D. H. FRISCH,* J. M. HUSH,** *Los Alamos Laboratory.*—A degenerative control system having above characteristics will be described. The system used is about 15 times better than was previously possible by regulating the charging current on the belt because use was made of a variable corona leak[1] to the high potential electrode. The improvement resulted as the ions formed by the corona could cross the high voltage gap in 1/150 second rather than $\frac{1}{10}$ second required by the belt. The leakage current can be varied from 50 to 150 microamperes by varying the potential on 4 needles projecting about $\frac{1}{4}$" through $\frac{1}{2}$" holes by means of a H & K 257 B pentode. The grid potential is controlled by an amplifier connected to a pair of pick-up plates on the electrostatic analyser similar to that used by Hanson.[2] The design of the focused analyser will be discussed. The 40-kv supply for the analyzer is powered by a specially regulated 400-cycle generator. Constancy of voltage has been checked by measurement on Li(p, n) near threshold, and by an amplifier capacity coupled to the high potential electrode.

* Now at Massachusetts Institute of Technology.
** Now at Commonwealth Engineering Company, Dayton, Ohio.
[1] R. M. Ashby and A. O. Hanson, Rev. Sci. Inst. 13, 128L (1942).
[2] A. O. Hanson, Rev. Sci. Inst. 15, 57 (1944).

X7. A Precision Alpha-Proportional Counter.* JOHN A. SIMPSON, JR., *Metallurgical Laboratory.*—An instrument is described which will detect and record the alpha-disintegration rate of prepared radioactive samples even though soft beta-radiation up to 2×10^3 disintegrations per minute may also be present. The resolution losses because of the detector, electronic amplifier, scaler and recorder total 0.8 percent with an alpha-counting rate of 10^3 counts per minute. The instrument employs a proportional counter through which 99 percent CH_4 at one atmosphere slowly flows. The proportional counting region is approximately 300 volts in length with 0.5 percent change in counting rate in an interval of 200 volts. Thin radioactive samples deposited on metal disks up to 2.5 cm in diameter are easily inserted into the counter volume by means of a special gas lock. The counter detects 0.50 of the disintegrations from a thin radioactive sample. A linear amplifier with a band extending from 5×10^3 c.p.s. to 10^6 c.p.s. is used with a gain of 180 to amplify the alpha-pulses. The counter background can be maintained at about 14 counts per hour. A high vacuum, low geometry attachment provides reductions in geometry down to at least 10^{-4} of the sample counting rate. Some theory of gas flow proportional counters is presented along with details of the instrument construction.

* This work was done under the Manhattan District Engineers contract with the University of Chicago, 1943.

X8. An A.C. Operated Mattauch Type Mass Spectrograph. A. E. SHAW AND W. RALL, *Metallurgical Laboratory.*—A mass spectrograph for chemical analysis of solid samples has been developed. The Mattauch arrangement of a 31°50′ electric deflection followed by a 90° deflection in a magnetic field was used in order to obtain a large mass range in focus on one plate. The accelerating and deflecting voltages and the current for the electromagnet were obtained from stabilized rectifier circuits connected to the 60 cycle a.c. supply. The electromagnet with 100 milliamperes gave a field of 18,800 gauss across a $\frac{1}{4}$" gap. During the introduction of the plate or insertion of new electrodes a gate valve was closed to isolate the spectrograph from the pumping system. In this way different samples could be examined rapidly. The ion source was energized by a compact Tesla transformer wound on lucite cylinders. One exposure covered a mass range from any mass M up to a mass $8M$. Examples of the resolution with nickel ions will be shown.

Z1. Split Anode Magnetrons for the 100-800 Megacycle Range. J. P. BLEWETT, D. A. WILBUR, AND L. D. ROBERTS, *General Electric Company.*—The conventional split anode magnetron has found a rather limited application because of a variety of undesirable operation characteristics. At high frequencies cathode back heating and anode dissipation have limited the range of operation to low powers. At low frequencies, electrons escape from the anode structure and again introduce severe limitations in power. These magnetron properties have been studied and new shielding procedures have been evolved for low frequency operation which permit operation of small glass-enclosed magnetrons at power levels up to and above one kilowatt over the frequency range from 100 to 400 megacycles. Anode temperatures are controlled by liquid cooling. Over the frequency range from 350 to 800 megacycles, a liquid cooled structure, in which an internal loop is mounted in parallel with the external tank circuit, is capable of generating 150 watts or more. Procedures will be described for shielding, external tuning over wide frequency ranges, and coupling-out power.

Z2. New Magnetron Designs for Continuous Operation in the Decimeter Wave Range. D. A. WILBUR, *General Electric Company.*—At the high frequency end of the range of the split anode magnetrons described in the preceding abstract, severe limitations are introduced by cathode back heating. To remove this limitation, two new structures have been devised, in which multi-gap operation is attained without sacrificing the easily tunable external tank circuit characteristic of the split anode magnetron. In one structure, only two of the segments of the multi-gap type of magnetron are developed. The remaining segments are replaced by a single electrode known as a "neutrode" which is maintained at zero r-f potential. A second structure includes a multiplicity of electrodes mounted internally on a conducting helix. Tubes of these two types have been operated at efficiencies up to 70 percent in the frequency range between 500 and 1500 megacycles. The tuning range of a single tube can be as high as 1.5:1. Both designs involve liquid cooling. Output power levels up to and above one kilowatt have been attained.

Z3. A 10-Kilowatt Magnetron with Water-Cooled Cathode. R. V. LANGMUIR AND R. B. NELSON, *General Electric Company.*—A high power magnetron oscillator, originally developed for radar jamming, has several unusual features. It is a simple split-anode magnetron, and its performance demonstrates that this type of oscillator is just as efficient as the now common multiple-anode magnetron. The output is over 10 kw, C.W. at 60 percent efficiency. Experimental tubes were built to cover several frequency ranges, the most work being done on a model tuning from 560 to 625 megacycles to cover the German AI radar band. The cathode operates by secondary emission. Since it receives about $\frac{1}{3}$ of the total power dissipated in the tube, it is water-cooled. Several materials were tried for the secondary-emission surface; of these a magnesium alloy was found to be the best.

Z4. Methods of Tuning Multiple-Cavity Magnetrons. R. B. NELSON, *Research Laboratory, General Electric Company.*—Several methods have been developed for tuning multiple-cavity magnetron oscillators over wide frequency ranges. The most successful of these involves simultaneous variation of both the inductance and capacity of all the resonant cavities by a single tuning motion. Tuning ranges of better than 1.4:1 have been obtained with good efficiency throughout. As an example, a magnetron is described which tunes from 760 mc to 1160 mc, delivering over 2 kilowatts C.W. at any frequency setting.

Z5. Neutron Spectra. H. T. RICHARDS, LYDA SPECK, AND I. H. PERLMAN, *Los Alamos Laboratory.*—Recoil protons in photographic emulsions have been used to record the neutron spectra of Po-B and Po-Be. The photographic emulsions have been calibrated with monochromatic neutrons from the $Li^7(p, n)Be^7$ reaction and the D-D reaction. The use of thick (200-micron) emulsions unbacked by glass is described. The inferred neutron spectrum for Po-B shows a broad maximum at 2.5 Mev and extrapolates to 0 at about 6 Mev on the high energy side. No group structure is found. The inferred neutron spectrum for Po-Be shows a maximum between 2 and 3 Mev but has an average energy of more than 4 Mev. The high energy end extends beyond 10 Mev. Some group structure may be present, but the large intensities of neutrons with energy less than 2 Mev which earlier workers report is not corroborated.

Z6. Neutrons from $C^{12}+D$. W. E. BENNETT AND H. T. RICHARDS, *Los Alamos Laboratory.*—Recoil protons in a cloud chamber have been used to measure the energy spectrum of the neutrons from $C^{12}+H^2$. The neutrons are found to be monochromatic when produced by 2-Mev deuterons. An accurate Q value of -0.27 ± 0.02 Mev is computed from the range of the recoil protons. This Q value gives a more accurate mass for N^{13} namely, 13.00990 ±0.00005. A geometry correction for cloud chambers is computed for the arrangement in which the neutron source is at finite distance from the chamber.

Z7. The Neutron-Proton and Neutron-Carbon Scattering Cross Sections for Fast Neutrons. C. L. BAILEY, WILLIAM E. BENNETT, T. BERGSTRAHL, RICHARD G. NUCHOLLS, H. T. RICHARDS, AND J. H. WILLIAMS, *Los Alamos Laboratory.*—The good geometry scattering of fast neutrons from cyclohexane and carbon as a function of energy in the range from 350 kev to 6 Mev has been observed. The results have been analyzed to determine the neutron-proton and neutron-carbon total cross sections. The former follows a smooth curve which may be described in terms of a potential well theory. The latter exhibits a resonance in the neighborhood of 4 Mev.

Z8. Isotopic Constitution of Tellurium and Tungsten. DUDLEY WILLIAMS AND PHILIP YUSTER, *Los Alamos Laboratory.*—Relative isotopic abundances for tellurium and tungsten have been redetermined by means of a mass spectrograph utilizing electrical methods of detection.

The TeF_3^+ and TeF_3^+ ions from tellurium hexafluoride and W^+ ions from tungsten hexacarbonyl were used in the analysis. The results obtained are:

Tellurium								
Isotope	130	128	126	125	124	123	122	120
Relative abundance	100	92.3	54.2	20.2	13.3	2.47	7.05	0.26

Tungsten					
Isotope	186	184	183	182	180
Relative abundance	92.7	100	47.0	86.2	0.44

On the basis of existing data on packing fractions, the above data give chemical atomic weights of 127.64 for tellurium and 183.88 for tungsten.

SP1. The Isotopic Composition of Tungsten, Silicon and Boron.* MARK G. INGHRAM, *University of Chicago*—The normal isotopic constitutions of tungsten, silicon, and boron have been determined by a Nier-type gaseous mass spectrometer. The gases used in the investigations were WF_6, SiF_4, BF_3, and $BO(CH_3)_3$. Five isotopes of tungsten were observed at masses 180, 182, 183, 184, and 186 with abundances of 0.122 percent, 25.77 percent, 14.24 percent, 30.68 percent, and 29.17 percent, respectively. Three isotopes of silicon were observed at masses 28.29, and 30 with abundances of 92.28 percent, 4.67 percent and 3.05 percent, respectively. Two isotopes of boron were observed at masses 10 and 11 with abundances of 18.83 percent and 81.17 percent respectively. Upper limits for the existence of other hypothetical normal isotopes in the immediate neighborhood of the known isotopes are given. The systematic errors of various kinds involved in absolute isotope abundance measurements are discussed and estimates of their magnitude are given.

* To be given at the end of Session Z if time permits.

T1. The Ionosphere as a Measure of Solar Activity. M. LINDEMAN PHILLIPS, *National Bureau of Standards, Washington, D. C.*—Critical frequencies of all regular ionospheric layers vary diurnally, seasonally, with geographic latitude and longitude, and with solar activity so that, for any location and any season, $f^0 = F_1(t) + F_2(t)S$, where f^0 is the critical frequency, F_1 and F_2 functions of (t), the time of day, and S is the sunspot number. For locations where such ionospheric trends are well established, observations of critical frequency may be used to determine an ionospheric "sunspot number." If values of F2-layer critical frequency for hours near local noon are used, since these generally have the most pronounced variation with solar activity, the ionospheric "sunspot number" obtained is considerably closer to its running-average value than is ordinary sunspot number. In addition, it is practically independent of varying atmospheric conditions and personal variation among observers, therefore probably presenting a more precise index of solar activity.

T2. Rotational Movements of Matter in the Homogeneous Fields of Magnets or of Radiation. FELIX EHRENHAFT, *New York City.*—Clarifications of previously published abstracts* are given. From the Lorentz force the electric charge of particles moving in helical paths due to magnetic fields can be calculated. From the dimensions of such a helical path previously reported it is seen, when the superimposed field of 50 gauss alone is taken into account, that the particle should carry 1.7 times 10^{-13} magnetic units of electric charge, or 5.1 times 10^{-3} e.s.u. But such small particles are unable to bear higher charges than 10^{-8} e.s.u. due to their saturation limit.** Calculating with the Lorentz force values about 10^5 times higher than the charges the particles can carry are found. The rotational movement can therefore not be explained as "magnetic action of electric currents" (Oersted-Lorentz), nor as "electric action of magnetic currents" formulated by the author in formal symmetry with Oersted, nor as "electric action of magnetic currents" defined by Poincare and called "Hertz force." Seemingly we are confronted with a new force which is capable of causing matter to move in helical paths at a velocity of 10^{10} times slower than the velocity of light in weak magnetic fields.

* Felix Ehrenhaft, Phys. Rev. **69**, 52 and 260 (1946), St. Louis Meeting, Nov. 30, 1945 and New York Meeting, Jan. 24, 1946, respectively.
** Satiendra Nat Ray, Ann. d. Physik **77**, 99 (1925).

T3. A High Level Electronic Noise Source.* J. D. COBINE AND C. J. GALLAGHER, *Research Laboratory, General Electric Company.*—A noise source which is capable of generating a continuous noise spectrum from the very low audio range to beyond 5 Mc/sec. has been built in the form of a gas discharge tube with cylindrical electrode structure. The tube contains argon at 12 microns and is used in conjunction with an axial magnetic field at about 850 gauss. The arc drop is about 35 volts with a current of 30 ma. The r.m.s. noise voltage spectrum is substantially flat from very low frequency to 1 Mc/sec. at a level of 32 mv/kc$^{\frac{1}{2}}$. From 1 Mc/sec. to 5 Mc/sec. the noise level drops by 18 db. This drop is much less than is found in other tubes, where the decrease may be as much as 30 or 40 db.

* This work was done in whole or in part under Contract OEMsr-411 between the President and Fellows of Harvard College and the Office of Scientific Research and Development, which assumes no responsibility for the accuracy of the statements contained herein.

Author Index to Abstracts of Papers Presented at the Chicago Meeting

Agnew, H. M., W. C. Bright, and D. K. Froman—No. A10
Amaldi, E., D. Bocciarelli, and G. C. Trabacchi—No. E6
Anderson, Herbert L., Enrico Fermi, and Leona Marshall—No. E1
Argo, Harold, Arthur Hemmendinger, Howard Kratz, Rolland Perry, Rubby Sherr, Richard Taschek, and Dudley Williams—No. A7

Bailey, C. L., William E. Bennett, T. Bergstrahl, Richard G. Nucholls, H. T. Richards, and J. H. Williams—No. Z7
Bardeen, J., W. H. Brattain, and W. Shockley—No. U8
Barker, Edgar C.—No. A2
Barschall, H. H.—see Coon, J. H.
Barss, W. M. and H. J. Yearian—No. V2
—— see Yearian, H.J.
Beers, Yardley—see Roberts, Arthur
Bennett, W. E., C. E. Mandeville, and H. T. Richards—No. A5
—— **and H. T. Richards**—No. Z6
Bennett, William E.—see Bailey, C. L.
Benzer, S.—No. U7
Bergstrahl, T.—see Bailey, C. L.
Bernstein, S.—No. F3
Blewett, J. P., D. A. Wilbur, and L. D. Roberts—No. Z1
Bloomenthal, S.—No. U1
Bocciarelli, D.—see Amaldi, E.
Borst, L. B. and J. J. Floyd—No. F7
——, **A. J. Ulrich, C. L. Osborne, and B. Hasbrouck**—No. F8
Bozorth, R. M.—No. U9
Brattain, W. H.—see Bardeen, J.
Bright, W. C.—see Agnew, H. M.
Burgy, Merle, L. A. Pardue, H. B. Willard, and E. O. Wollan—No. E8

Chandrasekhar, S.—No. V9
Cobine, J. D. and C. J. Gallagher—No. W2
—— **and C. J. Gallagher**—No. T3
—— see Gallagher, C. J.
Coon, J. H., R. W. Davis, and H. H. Barschall—No. E9
—— see Manley, J. H.
—— see Graves, A. C.
—— see Graves, E. R.
Cross, Paul C.—see Hainer, R. M.

Dancoff, S. M.—No. X1
Davis, R. W.—see Coon, J. H.
Dempster, A. J.—see Lapp, R. E.
Dickey, Fred P. and Harald H. Nielsen—No. V5

Ehrenhaft, Felix—Nos. T2, W11

Feld, Bernard T.—No. R10
Fermi, E. and L. Marshall—No. E5
—— **and W. H. Zinn**—No. E4
—— see Anderson, Herbert L.
Floyd, J. J.—see Borst, L. B.
Frisch, D. H.—see McKibben, J. L.
Froman, D. K.—see Agnew, H. M.

Gallagher, C. J. and J. D. Cobine—No. W3
—— see Cobine, J. D.
Goldberg, H. and O. Sandvik—No. V12
Goldberger, M. L. and Frederick Seitz—No. S6
Goldhaber, M. and W. J. Sturm—No. R7
Good, William E.—No. V7
Goodman, B.—see Miller, P. H., Jr.
Goodman, Leon J. and M. L. Pool—No. R9
Graves, A. C., E. R. Graves, J. H. Coon, and J. H. Manley—No. A4
Graves, E. R. and J. H. Coon—No. A6
—— see Graves, A. C.
—— see Manley, J. H.
Greenblatt, M. H., P. H. Miller, Jr., and L. I. Schiff—No. W4
Grenchik, Raymond—see Palevsky, Harry
Groetzinger, Gerhart—see Smith, Lloyd

Hainer, R. M., Gilbert W. King, and Paul C. Cross—No. V4
Hasbrouck, B.—see Borst, L. B.
Havens, Jr., William W., and James Rainwater—No. F5
—— see Rainwater, James
Hayden, Richard J. and Lloyd G. Lewis—No. R4
—— see Lewis, Lloyd G.
Hemmendinger, Arthur—see Argo, Harold
Hill, A. G.—see Roberts, Arthur
Hillier, James and Edward G. Ramberg—No. W5
Hofstadter, Robert—No. W6
Hughes, D. J.—No. F2
Hush, J. M.—see McKibben, J. L.

Inghram, Mark G.—Nos. No. R2, SP1
—— see Nier, Alfred O.
Iona, Jr., Mario—No. W8

Jarvis, G. A.—No. U12

Ke, T'ing-Sui—No. U6
King, Gilbert W.—No. V3
—— see Hainer, R. M.
Kratz, Howard—see Argo, Harold
Kundu, D. N. and M. L. Pool—No. R6

Langmuir, R. V. and R. B. Nelson—No. Z3
Lapp, R. E., J. R. VanHorn, and A. J. Dempster—No. E10
Levinger, J. S.—see Snell, A. H.
Lewis, Lloyd G. and Richard J. Hayden—No. R3
Lewis, Lloyd G.—see Hayden, Richard J.

Machlin, E. S.—see Nowick, A. S.
Mandeville, C. E.—see Bennett, W. E.
Manley, J. H., J. H. Coon, and E. R. Graves—No. A3
—— see Graves, A. C.

Marshall, Fitz-Hugh—No. W7
Marshall, John—No. F4
Marshall, Leona—see Anderson, Herbert L.
Marshall, L.—see Fermi, E.
Mason, W. P.—No. V10
Mattoon, Richard W.—No. X3
McKibben, J. L.—No. A1
——, **D. H. Frisch, and J. M. Hush**—No. X6
Meiners, E. P.—see Snell, A. H.
Meiners, E. P., Jr.—see Norris, L. D.
Meyerhof, W. E.—No. U11
Miller, P. H., Jr., and B. Goodman—No. V11
—— see Greenblatt, M. H.

Nelson, R. B.—No. Z4
—— see Langmuir, R. V.
Ney, Edward P.—see Nier, Alfred O.
Nielsen, Harald H.—see Dickey, Fred P.
Nier, Alfred O., Edward P. Ney, and Mark G. Inghram—No. X4
Nordheim, L. W.—No. S1
—— see Scalettar, R.
Norris, L. D., A. H. Snell, E. P. Meiners, Jr., and L. Slotin—No. R1
Nowick, A. S. and E. S. Machlin—No. U2
Nucholls, Richard G.—see Bailey, C. L.

Opatowski, I.—No. W10
Osborne, C. L.—see Borst, L. B.

Palevsky, Harry, Robert K. Swank, and Raymond Grenchik—No. X5
Pardue, L. A.—see Burgy, Merle
Perlman, I. H.—see Richards, H. T.
Perry, Rolland—see Argo, Harold
Phillips, M. Lindeman—No. T1
Platt, John R.—No. V13
Pool, M. L.—see Goodman, Leon J.
—— see Kundu, D. N.
—— see Schwarz, W. M.

Rainwater, James and William W. Havens, Jr.—No. F6
—— see Havens, Jr., William W.
Rall, W.—see Shaw, A. E.
Rall, Wilfrid—No. R8
Ramberg, Edward G.—see Hillier, James
Raymond, Richard C. and Wayne Webb—No. W9
Richards, H. T., Lyda Speck, and I. H. Perlman—No. Z5
—— see Bailey, C. L.
—— see Bennett, W. E.
Richards, H. T.—see Bennett, W. E.
Richardson, J. M. and W. Shockley—No. U5
Roberts, Arthur, Yardley Beers, and A. G. Hill—No. R11
Roberts, L. D.—see Blewett, J. P.
Ruthberg, Stanley—No. W1

Sampson, M. N.—see Snell, A. H.
Sandvik, O.—see Goldberg H.
Scalettar, R. and L. W. Nordheim—No. S4
Schiff, L. I.—No. F1
—— see Greenblatt, M. H.
Schwarz, W. M. and M. L. Pool—No. A8
Seitz, Frederick—see Goldberger, M. L.
Serin, B.—No. U3
Shaw, A. E. and W. Rall—No. X8
Sherr, Rubby—see Argo, Harold
Shockley, W.—No. U4
—— see Bardeen, J.
—— see Richardson, J. M.
Simpson, John A., Jr.—No. X7
Slotin, L.—see Norris, L. D.
Smith, Lloyd and Gerhart Groetzinger—No. A9
Snell, A. H., J. S. Levinger, R. G. Wilkinson, E. P Meiners, and M. N. Sampson—No. R5
—— see Norris, L. D.
Soodak, Harry—No. S2
Speck, Lyda—see Richards, H. T.
Sturm, William J. and Solomon Turkel—No. E3
—— see Goldhaber, M.
Swank, Robert K.—see Palevsky, Harry

Taschek, Richard—see Argo, Harold
Townes, Charles Hard—No. V6
Trabacchi, G. C.—see Amaldi, E.
Turkel, Solomon—see Sturm, William J.

Ulrich, A. J.—see Borst, L. B.

VanHorn, J. R.—see Lapp, R. E.
Vought, R. H.—No. V8

Way, Katherine and E. P. Wigner—No. S5
Webb, Wayne—see Raymond, Richard C.
Weinberg, A. M.—No. S3
Wick, G. C.—No. E7
Wigner, E. P.—see Way, Katherine
Wilbur, D. A.—No. Z2
—— see Blewett, J. P.
Wilkinson, R. G.—see Snell, A. H.
Willard, H. B.—see Burgy, Merle
Williams, Dudley and Philip Yuster—No. Z8
—— see Argo, Harold
Williams, H. J.—No. U10
Williams, J. H.—see Bailey, C. L.
Wollan, E. O.—see Burgy, Merle

Yearian, H. J. and W. M. Barss—No. V1
—— **see Barss, W. M.**
Yuster, Philip—see Williams, Dudley

Zachariasen, W. H.—No. X2
Zinn, W. H.—No. E2
—— see Fermi, E.